

Sheffield Hallam University

Characterisation and behaviour of recycled concrete and bricks as engineered fill.

CHIDIROGLOU, Iordanis.

Available from the Sheffield Hallam University Research Archive (SHURA) at:

<http://shura.shu.ac.uk/19456/>

A Sheffield Hallam University thesis

This thesis is protected by copyright which belongs to the author.

The content must not be changed in any way or sold commercially in any format or medium without the formal permission of the author.

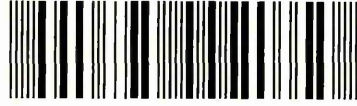
When referring to this work, full bibliographic details including the author, title, awarding institution and date of the thesis must be given.

Please visit <http://shura.shu.ac.uk/19456/> and <http://shura.shu.ac.uk/information.html> for further details about copyright and re-use permissions.

Sheffield S1 1WB

25351

101 895 494 5



Sheffield Hallam University
Learning and IT Services
Adsetts Centre City Campus
Sheffield S1 1WB

REFERENCE

ProQuest Number: 10694337

All rights reserved

INFORMATION TO ALL USERS

The quality of this reproduction is dependent upon the quality of the copy submitted.

In the unlikely event that the author did not send a complete manuscript and there are missing pages, these will be noted. Also, if material had to be removed, a note will indicate the deletion.



ProQuest 10694337

Published by ProQuest LLC (2017). Copyright of the Dissertation is held by the Author.

All rights reserved.

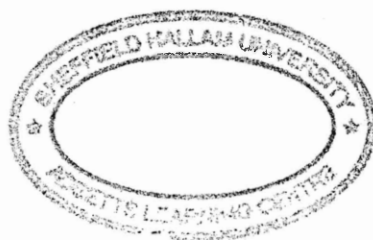
This work is protected against unauthorized copying under Title 17, United States Code
Microform Edition © ProQuest LLC.

ProQuest LLC.
789 East Eisenhower Parkway
P.O. Box 1346
Ann Arbor, MI 48106 – 1346

Characterisation and Behaviour of Recycled Concrete and Bricks as Engineered Fill

Iordanis Chidiroglou

A thesis submitted in partial fulfilment of the requirements of
Sheffield Hallam University
for the degree of Doctor of Philosophy



August 2007

Abstract

Demolition waste materials mainly consist of concrete and bricks and arise from the demolition of existing structures and buildings. Environmental and economical reasons make their recycling necessary but up to date little research has been undertaken to what is perceived as low level reuse of these materials.

This project tries to understand the behavioural characteristics of three types of recycled materials to determine their potential for engineering fill applications. For this purpose their physical and mechanical characteristics have been extensively investigated. Two types of crushed concrete, one obtained straight after demolition and the other further processed to industry specifications, and one type of crushed bricks were tested.

Due to the variable nature of recycled materials large quantities were tested and their grading, particle shape and aggregate crushing and impact values established. In addition, large scale equipment was developed for the determination of their compaction and permeability characteristics.

An extensive large scale shear box test regime was used to determine the shear strength behaviour of the materials. Two different densities and maximum particle sizes were used, and their influence on the shear strength established. The degree of particle breakage was also quantified by sieving the shear box specimens before and after testing.

The comparison of the behaviour of the materials during shearing has shown that the two crushed concrete based materials behave similarly despite the different degrees of processing, but there is difference between them and the crushed brick material. The friction angles of the materials decrease with decreasing density and maximum particle size, with the reduction of the latter affecting the friction angles values more.

The results show that the friction angles reduce with increasing normal stress, the shear-normal stress envelopes exhibit curvature at low normal stresses and the materials exhibit dilatancy at low normal stresses that decreases with increasing normal stress. This behaviour during shearing is similar to the behaviour exhibited by natural granular materials from literature. For all the three types of materials tested, the friction angles fall above the lower limits of strength for rockfill set by Leps (1970), which indicates their suitability for use as engineered fill.

Acknowledgements

The author is indebted to Dr Andy Goodwin, Professor Pritpal Mangat and Dr Liz Laycock for their guidance throughout this research and would also like to thank Dr Finbarr O'Flaherty for his assistance.

Thanks must also be presented to Controlled Demolition Group Ltd for providing Materials A and to Sam Allon (Contracts) Ltd for providing Materials B and C for this research.

The author wishes to thank Stephen, Bob, Geoff, Steven, Paul, John and Les, technical staff of Sheffield Hallam University, for their valuable help in completing the testing for this investigation.

Friends that have been a rock for me since I have arrived in Sheffield and have helped immensely with this research one way or the other includes Belen, Fin, James, Helen, Howard, Mark, Esref, Margaret, Nikos G., George, Mimis and Nikos K. Your love and support will never be forgotten.

Special thanks go to Elena, Aleka, Iliia, Aristidi, Fotula, Antoni, Stella and Petro.

The author is extremely grateful to his grandfather Iliia and grandmother Athanasia for their love, support and encouragement in the past 29 years.

Wish there were words to thank my Family. Forever in your debt.

Candidate's declaration

I hereby declare that no portion of the work referred to in this thesis has been submitted in support of an application for another degree or qualification of this or any other university or other institution of learning. All sources of information have been duly acknowledged.

Candidate

Iordanis Chidioglou – August 2007

Director of studies

Pritpal Mangat – August 2007

CONTENTS

List of Figures	I
List of Tables	V

CHAPTER 1 - INTRODUCTION

1.1 Background to Research	1
1.2 Need and Scope of Research	4
1.3 Thesis Structure	5

CHAPTER 2 - LITERATURE REVIEW

2.1 Introduction	7
2.2 Crushing and Processing of Demolition Waste	7
2.3 Particle Shape Classification	10
2.4 Effects of Material Characteristics on Shear Strength	11
2.4.1 Particle shape	11
2.4.2 Sample Gradation and Maximum Particle Size	13
2.4.3 Confining Pressure	16
2.4.4 Density	18
2.4.5 Particle Crushing	18
2.4.5.1 Factors affecting Particle Crushing	19
2.4.5.2 Particle crushing quantification	20
2.4.6 Relation between permeability and particle crushing	21
2.4.7 Summary	22
2.5 Compaction	22
2.6 Compressibility	
2.6.1 Introduction	23
2.6.2 Effect of Particle Shape	24
2.6.3 Effect of Individual Particle Strength	25
2.6.4 Effect of Material Void Ratio (dry density)	25
2.6.5 Effect of Material Grading	25
2.6.6 Effect of time	26
2.6.7 Effect of Water	26

2.7 Leachate	27
2.8 Recycled aggregates research	28
2.9 Concluding Remarks	29

CHAPTER 3 - RATIONALE FOR EXPERIMENTAL PROGRAMME

3.1 Fundamental Aspects of Experimental Programme	32
3.1.1 Selection of Maximum Particle Size	32
3.1.2. Testing Programme	33
3.1.3 Number of Tests	34
3.2 Physical Properties Testing Series	34
3.2.1 Shape	35
3.2.2 Grading	35
3.2.3 Compaction	36
3.2.4 Aggregate Impact Value (AIV) and Aggregate Crushing Value (ACV)	36
3.2.5 Freezing and Thawing	36
3.3 Main Series Testing (MST)	36
3.3.1 Specimens Moisture Content and Dry Density	37
3.3.2 Permeability	38
3.3.3 Shear Strength Testing	39
3.3.4 Particle Crushing	41

CHAPTER 4 - DESCRIPTION OF TEST EQUIPMENT

4.1 British Standard Tests	42
4.2 Compaction Tests	42
4.3 Climatic Chamber	43
4.4 Permeability	44
4.5 Shear Box	48

CHAPTER 5 - TEST PROCEDURES

5.1 Introduction	50
5.2 Physical Properties Testing Series	
5.2.1 Materials Grading	50
5.2.2 Particle Shape	51

5.2.3 Compaction	52
5.2.4 Resistance to Freezing and Thawing	54
5.3 Main Series testing	
5.3.1 Permeability	55
5.3.2 Particle Crushing	58
5.3.3 Shear Box Testing	58

CHAPTER 6 - TEST MATERIALS

6.1 Introduction	62
6.2 Principles of Acquisition, Transportation, Handling and Storage	62
6.3 Source and Description of Materials	64
6.4 Water absorption and particle density	69
6.5 Particle Shape	
6.5.1 Angularity	69
6.5.2 Flakiness and Elongation Index	71
6.5.3 Angularity Values	72
6.5.4 Complete Shape Description	72
6.6 Compaction	73
6.7 Aggregate Impact and Aggregate Crushing Values	80
6.8 Resistance to Freezing and Thawing	81

CHAPTER 7 - MAIN SERIES TEST RESULTS

7.1 Introduction	83
7.2 Permeability	83
7.3 Shear Box Testing	85
7.3.1 Stress-Strain Behaviour	86
7.3.2 Shear Stress Values	91
7.3.3 Volume Change Behaviour	92
7.3.4 Repeatability of Results	96
7.4 Particle Crushing	97

CHAPTER 8 - DISCUSSION OF RESULTS

8.1 Introduction	100
8.2 Particle shape	100

8.3 Aggregate Impact and Aggregate Crushing Value Tests	
8.3.1 Comparison between Material A, B and C	101
8.3.2 Comparison with Industry Products	102
8.4 Freezing and thawing tests	104
8.5 Permeability	105
8.6 Test Parameters Investigated in Shear Box and Particle Crushing Tests	106
8.7 Particle Crushing	107
8.8 Introduction to Shear Box Testing	109
8.9 Initial Observations on Behaviour during Shearing	110
8.10 Influence of Specimen Density on Behaviour during Shearing	
8.10.1 Influence on stress-strain behaviour	113
8.10.2 Influence on volume change behaviour	114
8.10.3 Influence on shear strength	115
8.10.4 Summary of conclusions	117
8.11 Influence of Maximum Particle Size on Behaviour under Shearing	
8.11.1 Influence on stress-strain behaviour	117
8.11.2 Influence on volume change behaviour	119
8.11.3 Influence on shear strength	120
8.11.4 Summary of conclusions	121
8.12 Influence of Normal Stress on Behaviour under Shearing	
8.12.1 Influence on stress-strain behaviour	122
8.12.2 Influence on volume change behaviour	123
8.12.3 Influence on shear strength	127
8.12.4 Summary of conclusions	129
8.13 Comparison of Friction Angles with AIV and ACV Tests	129
8.14 Comparison with Natural Granular Materials	130
8.15 Engineering Fill Applications	134
8.16 Comparison with other Recycled Aggregates	135

CHAPTER 9 - CONCLUSIONS AND RECOMMENDATIONS

9.1 Introduction	139
9.2 Main Conclusions	139
9.3 Secondary Conclusions	140
9.4 Recommendations	142

References	143
Appendices	159
Appendix A	1
Appendix B	2
Appendix C	7
Appendix D	11
Appendix E	14
Appendix F	29

Publications

LIST OF FIGURES

Chapter 1

Figure 1.1: Construction and Demolition Waste Management in England and Wales: 1999, 2001 and 2003 (Office of the Deputy Prime Minister, 2004)	1
Figure 1.2: Aggregates consumption in Great Britain (British Geological Survey, 2005)	2

Chapter 2

Figure 2.1: Diagram of Possible routes for Demolition Waste to Re-use/ Recycling	8
Figure 2.2: Photographs of (a) Jaw Crusher (courtesy of www.metsominerals.com) and (b) Impact Crusher (courtesy of www.sanger.net)	9
Figure 2.3: Three dimensional shape categories determined by the elongation and flatness ratios (after Rösslein, 1941)	10
Figure 2.4: Chart for determining visually the degree of angularity (after Lees, 1964)	11
Figure 2.5: The effect of particle shape on friction angles (after Cho <i>et al</i> , 2006)	12
Figure 2.6: Effect of grading on shear strength	13
Figure 2.7: Influence of material gradation of friction angles (after Becker <i>et al</i> , 1972)	14
Figure 2.8: Influence of maximum particle size on friction angle of alluvial rockfill (after Varadarajan <i>et al</i> , 2003)	15
Figure 2.9: Influence of maximum particle size on friction angle of quarried rockfill (after Varadarajan <i>et al</i> , 2003)	15
Figure 2.10: Effect of normal stress on friction angles (after Leps, 1970)	17
Figure 2.11: Effect of normal stress on shear stress of granular material	17
Figure 2.12: The effect of relative density on friction angles (after Zeller and Wulliman, 1957)	18
Figure 2.13: Angle of internal friction against breakage factor (after Marachi <i>et al</i> , 1969)	19
Figure 2.14: Breakage Factors (Lade, Yamamuro & Bopp, 1996)	21
Figure 2.15: Compression and decompression indices against particle shape (after Cho <i>et al</i> , 2006)	24

Figure 2.16: Displacement against time for sand (After Houlsby and Psomas, 2001)	26
--	----

Figure 2.17: Volume change behaviour of saturated and unsaturated materials (after Sun <i>et al.</i> , 2004)	27
--	----

Chapter 4

Figure 4.1: The large scale compaction mould	42
Figure 4.2: The climatic chamber and computer control system	43
Figure 4.3: Recorded profile of Temperature against Time for the Freezing cycle	44
Figure 4.4: Schematic of the large scale permeability cell	45
Figure 4.5: Schematic of the Permeability Cell (Plan View)	46
Figure 4.6: Permeability Cell	46
Figure 4.7: The shear box, displacement transducers and computer logging system	48

Chapter 5

Figure 5.1: Behaviour of Materials A, B and C when compacted with 8 % moisture content	54
Figure 5.2: The containers (with material A) in the thawing tank after the freezing cycle	55
Figure 5.3: The permeability cell with the compaction plate	56
Figure 5.4: The shear box apparatus	59
Figure 5.5: The shear box on the floor with Material C compacted in it	60

Chapter 6

Figure 6.1: Material B and C in the laboratory storage bays	63
Figure 6.2: Grading curve for Material A	64
Figure 6.3: Grading curves for Material B and C	65
Figure 6.4: Average grading curves for Material A, B and C	66
Figure 6.5: Wet and dry grading curves	67
Figure 6.6: Shape categories for all the size fractions for Materials A (after Rösslein, 1941)	70
Figure 6.7: Shape categories for all the size fractions for Materials B (after Rösslein, 1941)	70

Figure 6.8: Shape categories for all the size fractions for Materials C (after Rösslein, 1941)	71
Figure 6.9: Compaction Curves for all the types of compaction for Material A	74
Figure 6.10: Variability of compaction results for Material A	75
Figure 6.11: Large scale compaction curves for Material A (1st layer)	76
Figure 6.12: Large scale compaction curves for Material A (2nd layer)	76
Figure 6.13: Large scale compaction curves for Material B (1st layer)	77
Figure 6.14: Large scale compaction curves for Material B (2nd layer)	77
Figure 6.15: Large scale compaction curves for Material C	78
Figure 6.16: Compaction curves for all Materials – 1st Layer	78
Figure 6.17: Compaction curves for all Materials – 2nd Layer	79

Chapter 7

Figure 7.1: Water flow through permeability specimens	83
Figure 7.2: Manometer differences for permeability tests	84
Figure 7.3: Shear Stress against Horizontal Displacement for Material B	86
Figure 7.4: Shear Stress against Horizontal Displacement for Material C	87
Figure 7.5: Stress-Strain behaviour of Material A for SBT1	88
Figure 7.6: Stress-Strain behaviour of Material A for SBT2	88
Figure 7.7: Stress-Strain behaviour of Material A for SBT3	88
Figure 7.8: Stress-Strain behaviour of Material B for SBT1	89
Figure 7.9: Stress-Strain behaviour of Material B for SBT2	89
Figure 7.10: Stress-Strain behaviour of Material B for SBT3	89
Figure 7.11: Stress-Strain behaviour of Material C for SBT1	90
Figure 7.12: Stress-Strain behaviour of Material C for SBT2	90
Figure 7.13: Stress-Strain behaviour of Material C for SBT3	90
Figure 7.14: Volume Behaviour for Material A, SBT1 at 95 kPa	92
Figure 7.15: Volume Change behaviour for Material A, SBT1	93
Figure 7.16: Volume Change behaviour for Material A, SBT2	93
Figure 7.17: Volume Change behaviour for Material A, SBT3	93
Figure 7.18: Volume Change behaviour for Material B, SBT1	94
Figure 7.19: Volume Change behaviour for Material B, SBT2	94
Figure 7.20: Volume Change behaviour for Material B, SBT3	94
Figure 7.21: Volume Change behaviour for Material C, SBT1	95

Figure 7.22: Volume Change behaviour for Material C, SBT2	95
Figure 7.23: Volume Change behaviour for Material C, SBT3	95
Figure 7.24: Grading curves for all the Materials after SBT1	98
Figure 7.25: Grading curves for all the Materials after SBT2	99
Figure 7.26: Grading curves for all the Materials after SBT3	99

Chapter 8

Figure 8.1: Mean stress-strain behaviour curves at 95 kPa normal stress	110
Figure 8.2: Volumetric behaviour for SBT1, 190 and 317 kPa normal stress levels	112
Figure 8.3: Normal against shear strength for SBT1	112
Figure 8.4: Axial strain values at failure for SBT1 and SBT2	113
Figure 8.5: Volumetric strain values at failure for SBT1 and SBT2	114
Figure 8.6: Shear-normal stress curves for SBT1 and SBT2	115
Figure 8.7: Axial strain values at failure for SBT1 and SBT3	118
Figure 8.8: Volumetric strain values at failure for SBT1 and SBT3	119
Figure 8.9: Shear-normal stress curves for SBT1 and SBT3	120
Figure 8.10: Influence of normal stress on axial strain at failure	122
Figure 8.11: Influence of normal stress on volumetric strain at failure	123
Figure 8.12: Possible continuations of the best fit graphs for Materials A, B and C	124
Figure 8.13: Changes in ϵ_v between SBT1 and SBT2 and SBT1 and SBT3	125
Figure 8.14: Friction angle values in relation to normal stress levels	127
Figure 8.15: Shear-normal stress envelopes	130
Figure 8.16: Shear-normal stress envelopes comparison	132
Figure 8.17: Influence of normal stress on friction angles	133
Figure 8.18: Friction angles of Materials and rockfill strength limits (after Leps, 1970)	134

LIST OF TABLES

Chapter 2

Table 2.1: Effect of maximum particle size on friction angles (after Marsal, 1973)_____	16
Table 2.2: Summary of parameters affecting shear strength_____	22

Chapter 3

Table 3.1: Tests included in the Physical Properties Series_____	34
Table 3.2: Tests included in the Main Series_____	37
Table 3.3: Types of shear box tests and variables investigated_____	40
Table 3.4: Number of tests for each of the materials for all different types of tests for all five different normal stresses_____	40

Chapter 4

Table 4.1: Calibration factors and 95% confidence limits_____	49
---	----

Chapter 5

Table 5.1: Mass and particle numbers tested for each of the size fractions for Material A, B and C_____	51
--	----

Chapter 6

Table 6.1: Initial similarities and relations between the three types of materials____	62
Table 6.2: Summary of Grain Size characteristics of test materials_____	66
Table 6.3: Comparison between wet and dry sieving results_____	67
Table 6.4: Variability of grading results for all materials_____	68
Table 6.5: Particle density and water absorption values_____	69
Table 6.6: Values of all the Flakiness and Elongation Indices for all the Materials_____	71
Table 6.7: Summary of F_1 and E_1 values for all the materials_____	72
Table 6.8: Angularity values for all materials (after Lees, 1964)_____	72
Table 6.9: Maximum dry density and corresponding moisture content values____	73
Table 6.10: Variability of dry density results for Material A and B_____	79
Table 6.11: Variability of dry density results for Material C_____	80

Table 6.12: Dry and soaked AIV and SD values for all the materials	81
Table 6.13: Dry and soaked ACV and SD values for all the materials	81
Table 6.14: Results of the particle percentage passing the 5 mm sieve after the weathering process	81
Table 6.15: ACV and AIV for all the materials after the freezing – thawing process	82

Chapter 7

Table 7.1: Values of the Coefficient of Permeability (k) for all the Materials	84
Table 7.2: Specimen parameters for shear box tests	85
Table 7.3: Particle shape for maximum particle size of 37.5 and 28 mm	85
Table 7.4: Mean peak Shear Stress values for all the materials	91
Table 7.5: Mean peak shear stress Standard Deviation values (kPa) for all the types of shear box tests for all the materials	91
Table 7.6: Standard deviation as a percentage of mean peak shear stress values	96
Table 7.7: Upper and lower limits of the envelopes of the volumetric-axial strain curves	97
Table 7.8: Breakage Index, B_i , for SBT1, SBT2 and SBT3	98

Chapter 8

Table 8.1: Flakiness and Elongation Indexes	100
Table 8.2: AIV and ACV results	101
Table 8.3: AIV over ACV ratios	102
Table 8.4: Values for ACV, AIV, F_i and water absorption for Material A, B and C and industry products	102
Table 8.5: Freezing thawing results	104
Table 8.6: ACV and AIV for all the materials before and after the freeze-thaw	104
Table 8.7: Flakiness and Elongation Indexes values for SBT1 and SBT3	107
Table 8.8: Breakage Indices	107
Table 8.9: Reduction in values of B_i between SBT1 and SBT2	108
Table 8.10: Comparison of AIV and ACV tests with particle crushing results	109
Table 8.11: Friction angle values for SBT1 and SBT2	116
Table 8.12: Friction angle values for SBT1 and SBT3	121

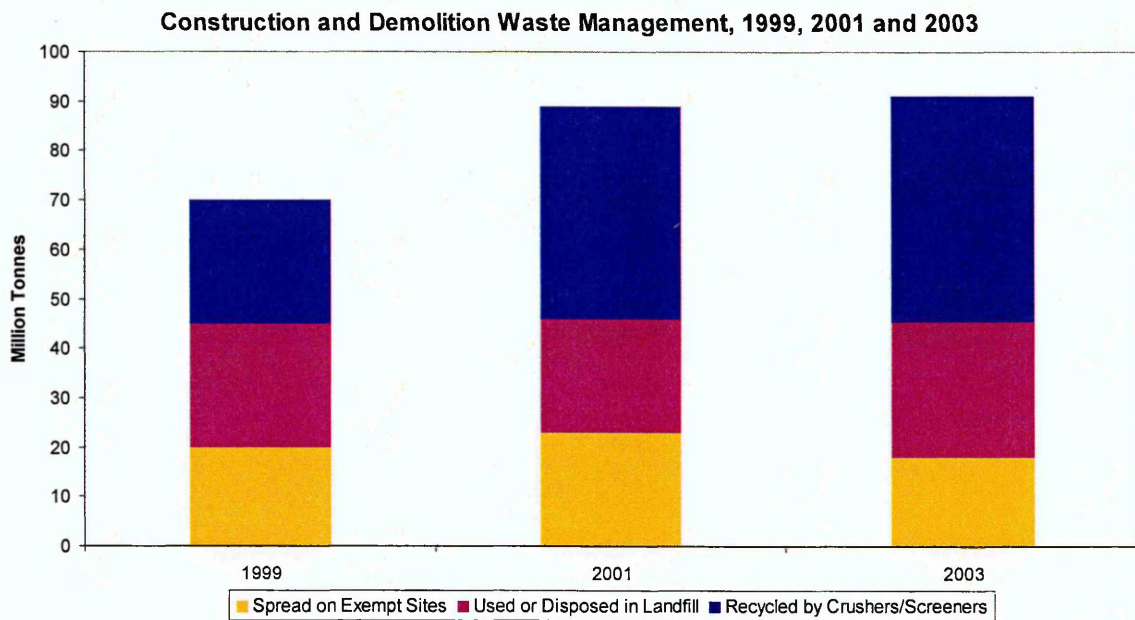
Table 8.13: Point of zero ϵ_v change between SBT1 and SBT2 and SBT1 and SBT3 _____	126
Table 8.14: Comparison of ACV and AIV tests with SBT1 and SBT2 _____	129
Table 8.15: Comparison of ACV and AIV tests with SBT3 _____	130
Table 8.16: Characteristics of the tests compared in Figure 8.15 _____	131
Table 8.17: Characteristics of the Materials compared in Figure 8.16 _____	133
Table 8.18: Comparison of Material A, B, C, DG2 and OG2 _____	136

CHAPTER 1

INTRODUCTION

1.1 Background to Research

Construction and demolition waste arises from the construction, repair, maintenance and demolition of buildings and structures. It includes brick, concrete, topsoil and subsoil and generally contains small quantities of timber, metal and plastics. The annual amount of construction waste was almost 95 million tonnes in 2003 and accounted for about 30% of all the waste produced in England and Wales (Office of the Deputy Prime Minister, 2004). The same research showed that 47% of the construction and demolition waste was recycled either by re-use on site or, after processing, was sold off-site. Reportedly, almost 20% was used for landfill engineering and another 5% was landfilled in 2003 according to the same data (Figure 1.1).



Source: Office of the Deputy Prime Minister: Survey of Arisings and Use of Construction, Demolition and Excavation Waste as Aggregate

Figure 1.1: Construction and Demolition Waste Management in England and Wales: 1999, 2001 and 2003 (Office of the Deputy Prime Minister, 2004)

The UK government faces stringent European targets to reduce the amount of waste landfilled and the European Union, with the co-operation of the national governments, has established a waste strategy (Department of the Environment, Transport & the Regions, 2000) to implement the necessary changes (Office of the Deputy Prime Minister, 2002).

In the year 2003 the UK consumed about 226 million tonnes of aggregates per year (Figure 1.2) to cover its construction needs and it was estimated that the amount of crushed rock aggregates needed in the UK will rise further (by an estimated 20 million tonnes per year) especially with the Olympic Games in London in 2012 and their subsequent construction needs (British Geological Survey, 2005). It was estimated that about 60 of these 226 million tonnes were recycled or secondary aggregates. There are some localised recycling schemes in the UK construction industry based on individual company initiatives but by no means have all the companies across the UK adopted a policy of reusing construction and demolition waste. The environmental problems that arise from the consequential extensive quarrying activities are not just restricted to the quarry areas, as the transportation of the materials causes noise and air pollution problems too.

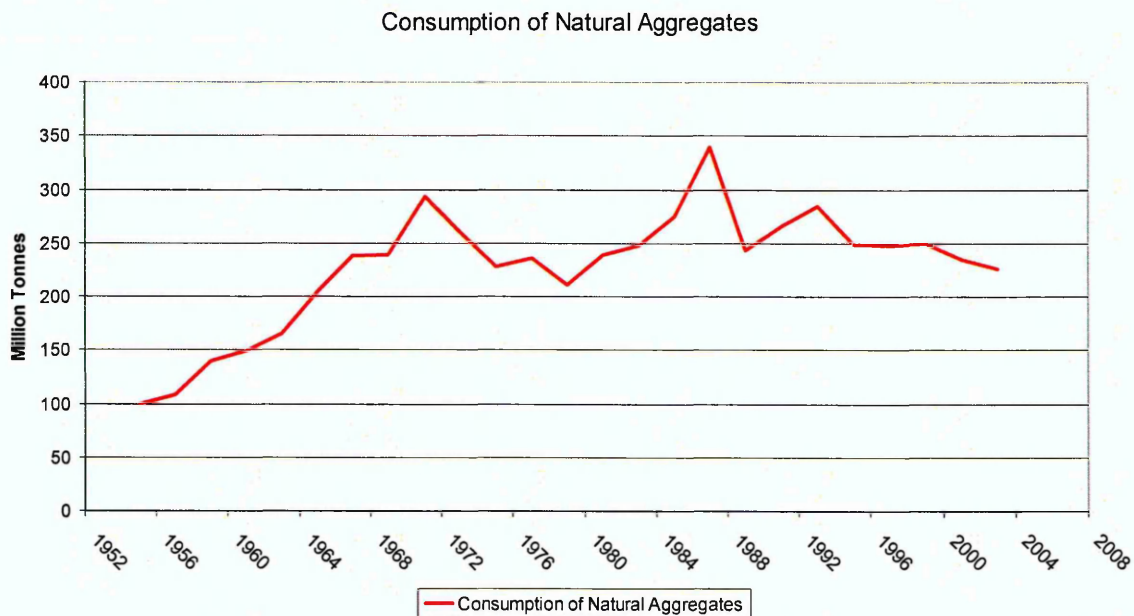


Figure 1.2: Aggregates consumption in Great Britain (British Geological Survey, 2005)

A future increase in the re-use of demolition waste will benefit the environment as well as industry. It is considered that the introduction of the landfill tax (which increased to £15 from £1/tonne/year between 1999 and 2004, HM Treasury, 2004) has led to an annual increase in the cost of disposing of construction and demolition waste to landfill of approximately £15 million per annum. This cost to the industry was compounded by the introduction of the aggregates levy in 2002, the increase in costs of both the haulage of primary aggregates to site and the removal of waste materials to the disposal sites. Given the cost of over-ordering construction materials, it would appear that the reuse of waste materials makes both environmental and economic sense. Construction companies would have to provide a more environmental approach to their projects especially when governments recommend that in construction projects at least 10% of the construction value of the materials used should be dedicated to recycled, re-used and reclaimed materials (Waste & Resources Action Programme, 2005).

Despite the apparent attractions offered by recycling of construction waste, the re-use of these materials has some restraints and disadvantages that have to be taken into consideration in order for their application to construction projects to be effective. The main restraints are the possible unsuitability of the materials for recycling, the distance between the construction site and the recycling plant, the available storage space on site for these materials, noise and dust pollution from crushing equipment, and the cost of cleaning and sorting of the possible contaminants (e.g. wood, plastic, steel reinforcement and electricity and plumbing installations).

On the other hand, the advantage that the re-use or recycling of demolition materials, particularly concrete and bricks, has in comparison with the other types of waste is that there is not a great need to identify and establish a market for the materials since the construction industry is already a major receptor for these materials. The industry also has the full support of the government in developing new technology for recycling and in researching potential uses for these materials. The Department of Trade and Industry established a Sustainable Construction Unit in 2002, and in 2003 the Sustainable Buildings Task Group was set up. The roles of both of these two groups are to encourage more corporate social responsibility and push a sustainable construction initiative.

1.2 Need and Scope of Research

Despite the will and initiatives for recycling and reusing these types of materials, their use can not be accurate and widespread before many technical issues have been addressed:

1. Understanding the behavioural characteristics of recycled concrete and bricks
2. Establishing testing procedures and appropriate engineering specifications
3. Use of combinations of materials (e.g. concrete and bricks)
4. Developing possible new ways of re-using the materials

This research project relates to the first issue. Typical uses of recycled concrete and bricks as fill include filter gravel, sub base for roads and car parks, hardcore and general site cover, and backfill to quarries. It has generally been assumed in practice that the behaviour of such fills would be similar to that of natural aggregates, and therefore accumulated data on the properties of such aggregates has been extrapolated and applied to recycled materials used in industry. There are two areas of concern with this approach though:

- Little research has been undertaken into what is perceived as the low level, non-structural re-use of the materials as bulk fills, though some recent work (Sivakumar *et al*, 2004, Brampton *et al*, 2004, Forth *et al*, 2006, Ghataora *et al*, 2006) indicates that there is increasing interest in this aspect.
- The 1st of June 2004 saw the introduction of the New European Standards for aggregates that are applicable to 'aggregates from natural, recycled and manufactured materials'. Even though these standards address the possible specified use of recycled materials, the main problem is that they do not tackle the non homogeneous nature of some of the materials. In some tests (e.g. Freeze Thaw - EN 1367-1, Particle shape - EN-933-3 and Impact Test Value - EN-1097-2) it is possible to test particles that are not representative of the overall composition of the materials (e.g. small particles in crushed concrete mainly consist of the original aggregates used for the manufacturing of concrete and not of composite concrete based particles).

The fundamental driver behind this research was a desire to confirm or refute these assumptions/problems. Thus the overall aim of the project was to investigate the physical and mechanical properties of crushed bricks and concrete. The limited research on the

subject and the lack of information on the strength and physical properties of recycled materials makes this investigation necessary from the academic point of view, not only for increasing the knowledge on the materials but also for providing a platform for future research.

As it has been mentioned in the previous section of this chapter, the industry is under pressure to recycle more of its waste and use more recycled aggregates for its construction purposes. This investigation aims to provide the industry with the data it needs to safely, and under the guidelines of the existing standards, utilise materials such as crushed concrete and/or bricks in present and future projects.

With these in mind, the specific objectives of this investigation are as follows:

1. To provide a base for future research by investigating the physical and mechanical characteristics of crushed recycled aggregates
2. Provide data on the strength of recycled aggregates so they can be utilised by the industry.
3. Compare the properties of recycled materials with other research on recycled and primary aggregates.
4. Compare the characteristics and performance of different types of recycled materials.

1.3 Thesis Structure

The thesis structure following this introduction is as follows:

- Chapter 2 presents a literature review concentrating on the testing, properties and behaviour of coarse granular materials. The economics and management aspects of the recycling processes fall outside the scope of this research.
- Chapter 3 presents the rationale behind the tests performed in this investigation and describes the aspirations of the testing programme.
- Chapter 4 reports on the test equipment used and the calibration procedures adopted.
- Chapter 5 describes the test procedures followed in this investigation.
- Chapter 6 describes the three material types used in this project, some of their physical characteristics and their transportation to and storage in the laboratory.

- Chapters 7 and 8 respectively present and analyse the factual results of the main testing series.
- Finally, Chapter 9 presents the conclusions from this investigation and provides recommendations for further work.

CHAPTER 2

LITERATURE REVIEW

2.1 Introduction

Past research into the properties of demolition waste for geotechnical engineering purposes has been limited, compared with other areas of geotechnics. In order to devise a testing programme that would produce a valid description of their properties and behaviour, a comprehensive review of the research literature was undertaken. In summary the review presented in this thesis examines:

- The crushing and processing of demolition waste, in order to identify the types of materials that need to be investigated in this project.
- The methods for classifying particle shape
- The effect of different material parameters on shear strength of granular material
- Quantification methods for particle crushing.
- The compaction and compressibility behaviour of coarse granular materials and how they are affected by variations in the material parameters.
- The potential for leachate generation from recycled materials.

2.2 Crushing and Processing of Demolition Waste

In order to be able to identify the types of recycled materials (both concrete and/or bricks) for laboratory testing that are representative of the materials used by industry, it is necessary to investigate:

1. The types of crushing procedures used
2. The amount of processing they might undergo after demolition.

Crushing of demolition waste can take place on site by temporary mobile units, or the materials can be removed from the demolition site, crushed and processed in a fixed site constructed for this purpose.

Due to the nature of the majority of the structures demolished, the material produced typically contains some architectural components other than concrete, so it is necessary to remove them mainly before the crushing takes place. Generally fixtures and fittings such as carpets, windows, doors etc are removed before the demolition takes place, with the large pieces of the utilities components such as cables and pipes removed manually

after crushing. Structures containing reinforced concrete allow simple separation as the steel is easily removed from the concrete since its bond with the concrete is weak after the individual components (columns, beams, and floors) are demolished. Usually a small vibration or sudden movement of the steel rods is enough to “free” the steel from the concrete.

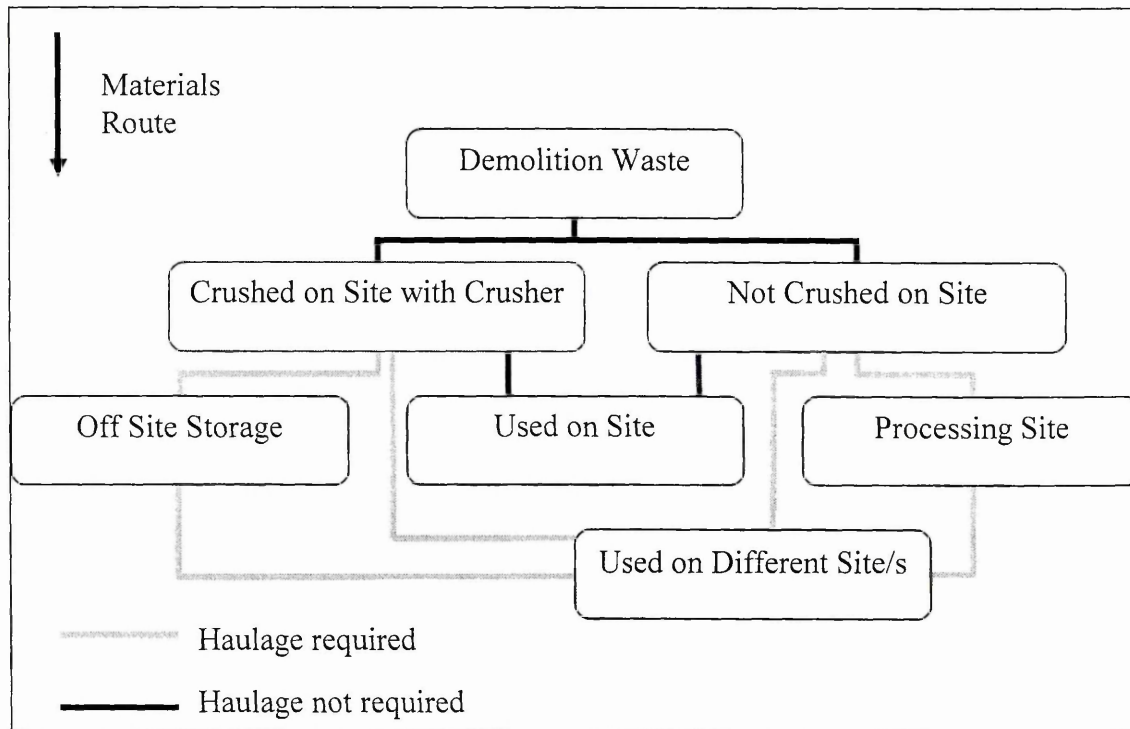


Figure 2.1: Diagram of Possible routes for Demolition Waste to Re-use/ Recycling

The procedures used for the processing of demolition waste vary depending on the intended use and the processing equipment available. Most methods include transportation of the materials from the production area to the reuse site. Depending on the routes followed this can be costly in economic and environmental terms due to charges and air and noise pollution caused by haulage. Figure 2.1 summarises the possible routes for reusing and/or recycling of materials. The reduction of the number or distance of the routes marked with grey lines will benefit the industry and the environment as they will reduce the transportation needs for the utilisation of these materials.

Reducing the distances the materials have to be transported between the points of demolition and the crusher reduces the cost of the whole procedure of crushing and

Reducing the distances the materials have to be transported between the points of demolition and the crusher reduces the cost of the whole procedure of crushing and processing. This has resulted in the development of mobile crushers. The types of mobile crushers vary and the main types used are jaw crushers (Figure 2.2.a), impact crushers (Figure 2.2 b), hammer mills and cone crushers.

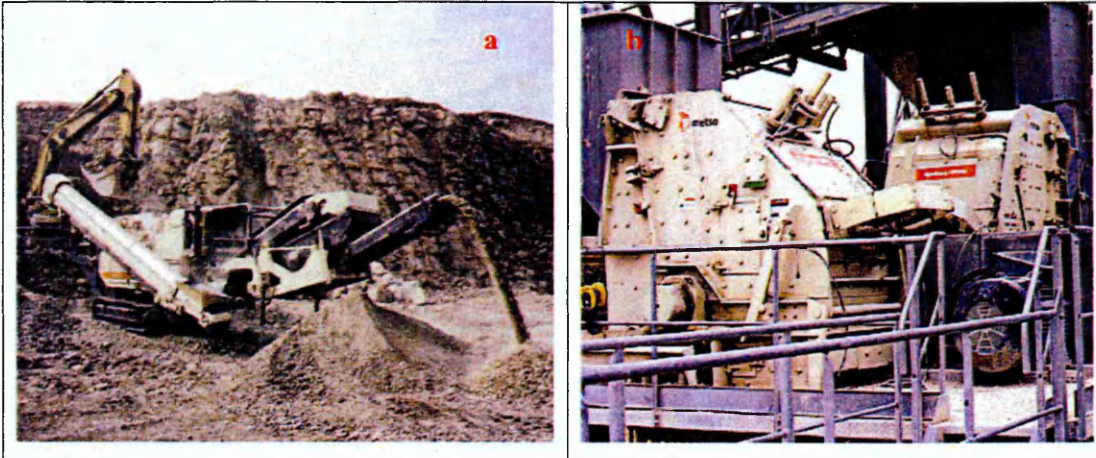


Figure 2.2: Photographs of (a) Jaw Crusher (courtesy of www.metsominerals.com) and (b) Impact Crusher (courtesy of www.sanger.net)

Depending on the intended use of the materials the screens used on the processing sites have different size and shape of aperture, and different types of screens such as vibrating, inclined or horizontal are used depending on different parameters existing on site (headroom, operational area required grading etc.). Screening and sorting devices can also be useful for purposes other than only establishing maximum particle sizes. They are most of the time used for removing undesirable impurities such as plastics, roof and wall hardboards and any other types of wood. In some sites when secondary crushers are employed, screening is used to provide materials with particle size that can be crushed by that specific crusher.

It is therefore clear that there are mainly two types of demolition waste reused by the industry:

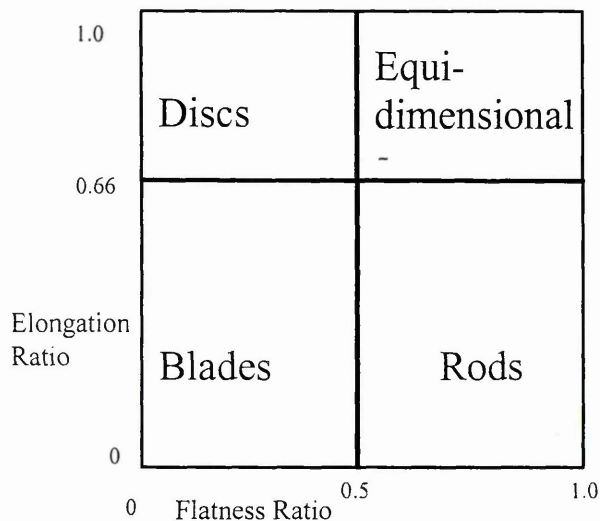
1. Materials that have not been processed further than the original demolition and crushing
2. Materials that have been processed further by crushing to particular specifications

2.3 Particle Shape Classification

Particle shape can be classified by the Elongation and Flatness ratios (after BS 812-105) but numerous other methods also exist for characterising the particle shape of materials.

Bowman *et al* (2001) have used Fourier description analysis and scanning electron microscope photographs to analyse the shape of sands, and his technique would have been quite useful in determining the shape of the smaller particles of the materials. Since, though, the BS methods used do not examine particles below 6.3 mm, it was decided that its use was outside the purpose of this research, since only particles larger than 6.3 mm were tested.. The 3D characterization of coarse particles proposed by Lanaro and Tolppanen (2002) falls within the scope of this investigation and produces accurate shape descriptions but it would have been a time consuming process if a large number of particles were to be studied. In addition to the above, the methods used by O’Fannery and O’Mahony (1999) were reviewed but they were not used for the same reason.

For a more complete description, than the one given by the British Standards, can be given if the methods by Rösslein (1941) and by Lees (1964) are employed. Using a combination of the three dimensional shape categories (Figure 2.3, after Rösslein, 1941) and the chart for visually determining the degree of angularity (Figure 2.4, after Lees, 1964) a complete description of the particles' shape can be presented.



The elongation ratio (q) is the ratio of the intermediate length of the particle over the greater length and the flatness ratio (p), the ratio of the shortest length over the intermediate length.

Figure 2.3: Three dimensional shape categories determined by the elongation and flatness ratios (after Rösslein, 1941)

The categories given in Figure 2.3 can also be described as:

- Discs are the particles that are flaky but not elongated
- Equidimensional the particles that are neither flaky nor elongate
- Rods are the particles that are elongate but not flaky
- Elongate and flaky particles are described as blades (Lees, 1964).

0-99	100-199	200-299	300-399	400-499	500-599	600-699	700-799
800-899	900-999	1000-1099	1100-1199	1200-1299	1300-1399	1400-1499	1500-1599

Note: The numbers indicate the degree of sharp edges appearing on the particles, with the most rounded being zero and most angular being 1599

Figure 2.4: Chart for determining visually the degree of angularity (after Lees, 1964)

2.4 Effects of Material Characteristics on Shear Strength

Various researchers have conducted experiments to investigate the effects of different properties of materials, like shape size and gradation, on their shear strength. The most important characteristics affecting the shear strength are particle shape, gradation, particle size, confining pressure, density and particle crushing. The literature on each is reviewed separately below, as far as possible.

2.4.1. Particle shape

Chen (1948) conducted a series of triaxial tests on various sands and gravels, with density varying from loose to compact, where strength was measured by loading to failure. He found that for all the densities investigated, the strength of the materials increased with increased angularity. Holtz and Gibbs (1956) conducted triaxial tests on two types of materials (quarried rock fragments and rounded river pebbles) with the

same gradation but varying the angularity of the particles. Their work indicated that the angular material had a higher shear strength than the sub-rounded and sub-angular materials. A series of shear box tests were conducted by Pike (1973) on 17 different aggregate samples ranging from fine sand to coarse gravel. Increased angularity generally resulted in increased strength. The conclusions of these tests were also verified by Thom and Brown (1989) who found that increasing angularity increased the shear strength of 18 different materials including crushed rock, sand and gravel, all tested in a dry condition.

Eerola and Ylosjoki (1970) found that the shear strength of materials increased in proportion to the ratio of particle length to thickness (i.e. flakiness). Dunn and Bora (1972) conducted triaxial tests on limestone with particles up to 38 mm, and also found that when flaky particles were present, especially in the range of 25-75% of the sample, the shear strength of the materials increased.

Cho *et al* (2006) found, by examining large amounts of research data, that the critical state friction angle of natural and/or crushed sand reduces as the roundness of particles increases (Figure 2.5). However, Gur *et al* (1978) showed that flaky particles increase the level of deformation of samples at failure.

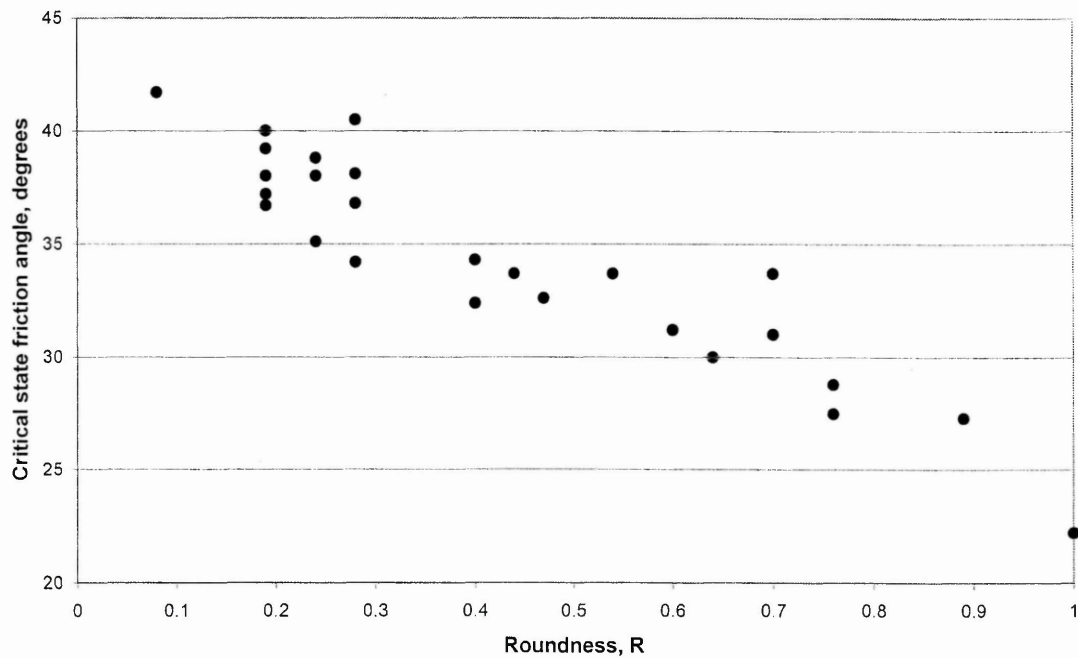


Figure 2.5: The effect of particle shape on friction angles (after Cho *et al*, 2006)

2.4.2. Sample Gradation and Maximum Particle Size

Rico *et al* (1977) tested materials with different gradations, but with the same maximum particle size of 35 mm, and found that a more broadly-graded material gave a higher strength than a narrowly-graded specimen. Marsal (1967) changed the gradation of rockfill material, while keeping the maximum particle size the same, and found that shear strength in triaxial shear increased as the gradation became broader. During testing of Latite Basalt but with two different gradations, Indraratna *et al* (1998), found that the existence of smaller sized particles within the sample increased the shear strength of the material compared with the same material without the presence of these smaller particles. Kirkpatrick (1965) conducted triaxial tests on sand, in which the top and bottom sizes were kept the same and at the same time the mean size was varied. In most of the results the shear strength increased with decreasing mean size. Leslie (1963) increased the mean size of the material and broadened its gradation by keeping the minimum size stable but changing the maximum size of the particles. The results of the triaxial tests showed that the shear strength decreased as the mean size increased.

A graphic representation of approximate grading curves (not utilising their actual results) of these conclusions is given in Figure 2.6. The arrows point in the direction of strength increase. The positions of the curves are independent from maximum particle size values. The x-axis does indicate values of maximum particle sizes.

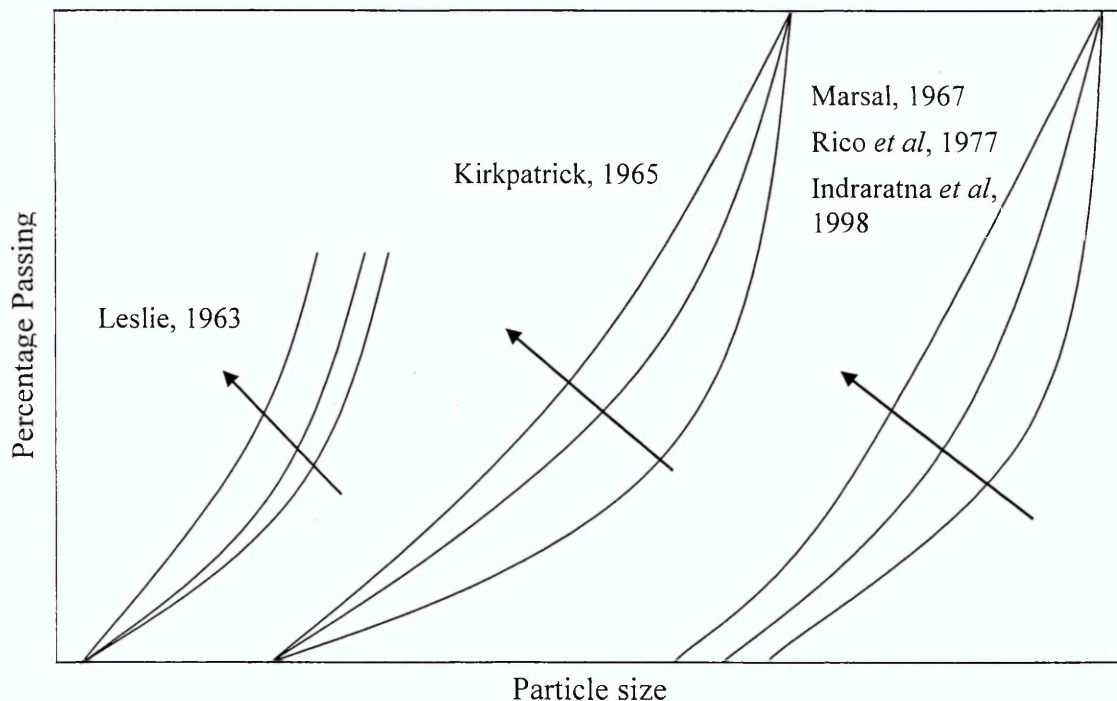


Figure 2.6: Effect of grading on shear strength

Becker *et al* (1972) also found that higher Coefficients of Uniformity produced higher friction angles for a range of normal stresses for similar materials when they were tested in a triaxial cell (Figure 2.7). Klugar (1978) also found that reduced deformation and degradation is related to a broader gradation.

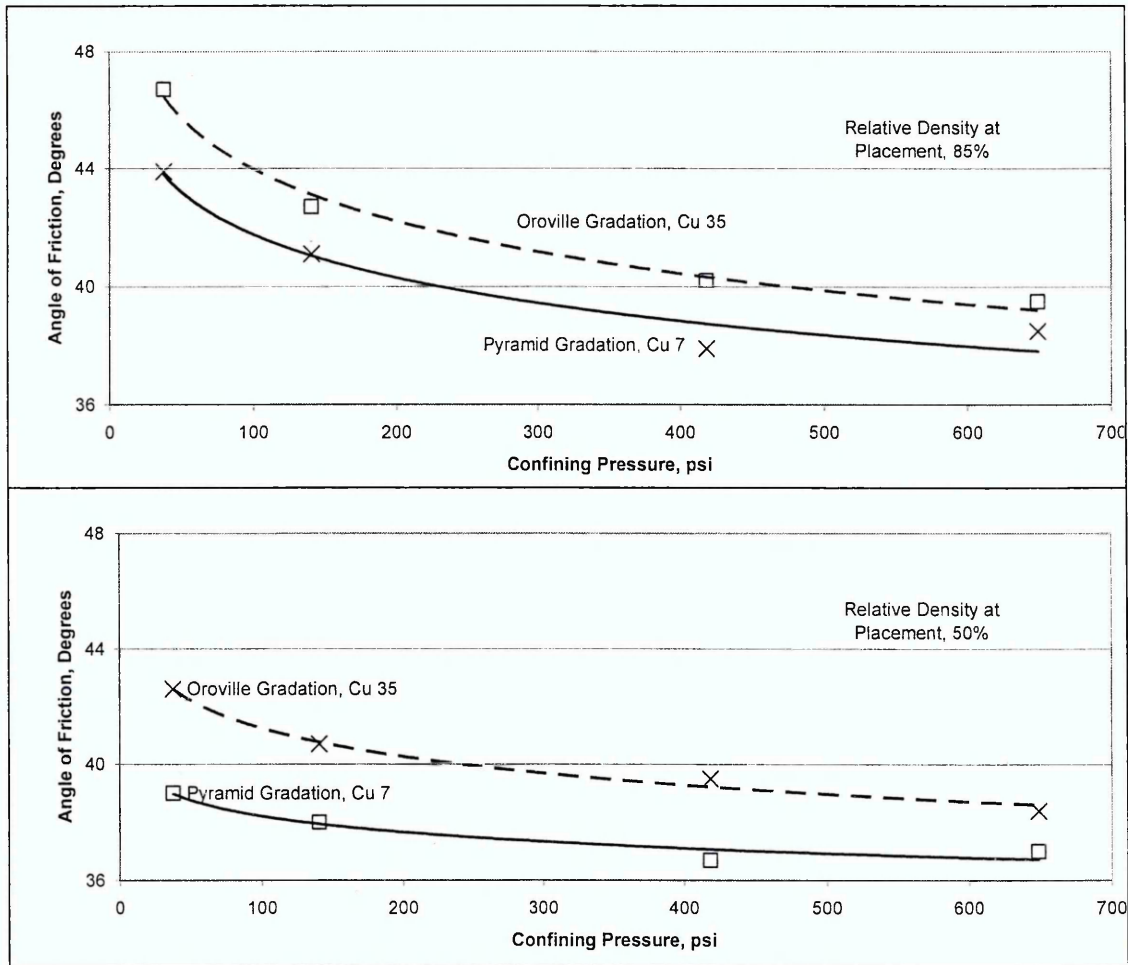


Figure 2.7: Influence of material gradation of friction angles (after Becker *et al*, 1972)

Dunn and Bora (1972) showed that shear strength increases with increased particle size. Tombs (1969) and Charles (1973) found that the shearing resistance angle was not significantly affected by the particle size as it was about 2° bigger for materials of D_{max} 75 mm than for samples of D_{max} of 10mm.

Varadarajan *et al* (2003) tested two different materials by using three different maximum particle sizes (25, 50 and 80 mm) and found that the friction angle of materials increased (Figure 2.8) or decreased (Figure 2.9) depending on the type of material with maximum particle size.

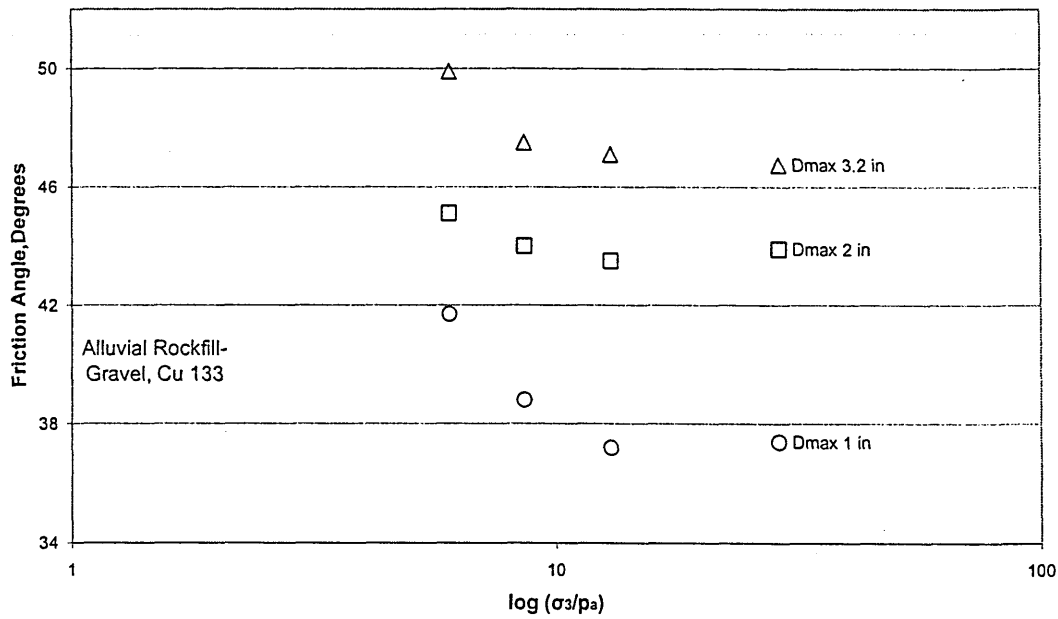


Figure 2.8: Influence of maximum particle size on friction angle of alluvial rockfill (after Varadarajan *et al*, 2003)

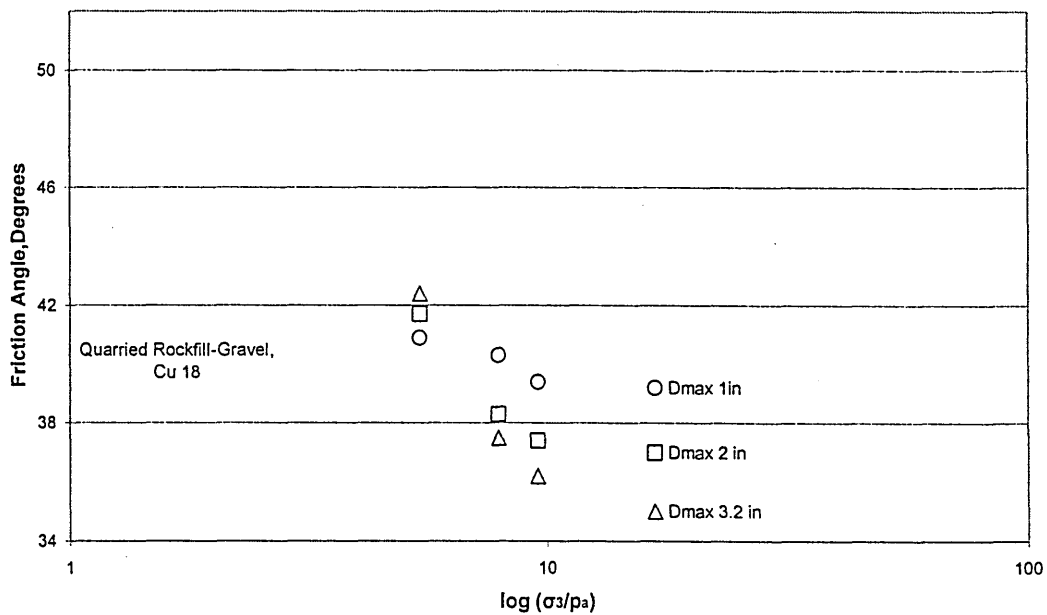


Figure 2.9: Influence of maximum particle size on friction angle of quarried rockfill (after Varadarajan *et al*, 2003)

The results of a series of triaxial tests on sand by Koerner (1970) showed that the strength of the material increased as particle size decreased. Another example is the

tests performed by Marachi *et al* (1969), where he found that samples with maximum particles (D_{max}) of 150 mm had an angle of shear resistance of about 4° smaller than samples with a maximum particle size of 12 mm. Marsal (1973) performed tests on basalt at which he varied the maximum particle size but kept the specimen diameter the same. Table 2.1 shows the effect of this change on friction angle. The influence of maximum particle size on the friction angle appears to be minimal at high confining pressures

Table 2.1: Effect of maximum particle size on friction angles (after Marsal, 1973)

σ_n , MPa	d_{max1}/D	d_{max2}/D	$(\phi_1 - \phi_2) / \phi_2$, %
0.8	0.07	0.18	3
1.6	0.07	0.18	4
3.9	0.07	0.18	0.3

d_{max1} , d_{max2} is the maximum particle sizes, D the diameter of the specimen (1130 mm) and ϕ_1 , ϕ_2 the friction angles for d_{max1} , d_{max2}

Roner (1985) concluded that there are no direct relationships between shear strength and particle size that can be generalised in all types of soils. Other researchers (Holtz & Gibbs, 1956; Vallerga *et al*, 1957) also showed that little relation exists between the particle size and the shear strength of a specific material.

It is therefore quite difficult to rate the influence of maximum particle size and gradation on the shear strength of the materials, since these two parameters are inter-related and are affected by any changes, unless tests are performed when one is kept stable when the other is changed (simpler to perform by keeping the maximum particle size the same)

2.4.3 Confining Pressure

In 1966 Bishop conducted a series of triaxial compression tests under drained conditions on sand and found that the internal friction angle decreased as the confining pressure increased. The same was observed by Leps (1970) as is shown in Figure 2.10, when conducting shear box tests.

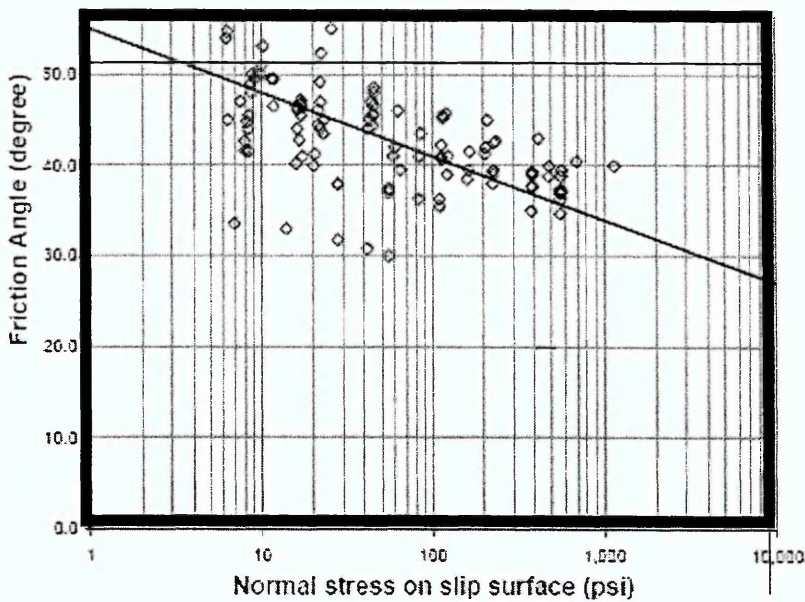


Figure 2.10: Effect of normal stress on friction angles (after Leps, 1970)

Pike (1973) conducted shear box tests on a number of materials with maximum particle size of 40 mm and found that shear stress at failure increases with normal stress (Figure 2.11). It has also been found that the principal effective stress ratio at failure was much greater for tests with low confining pressure than the tests carried out with higher values of confining pressure (Marsal, 1973). Others (Bishop, 1966, Marsal, 1967, Vesic and Clough, 1968, Charles and Watts, 1980 and Indraratna *et al*, 1993), have shown that the shear strength values increase with confining pressures but the friction angles reduce.

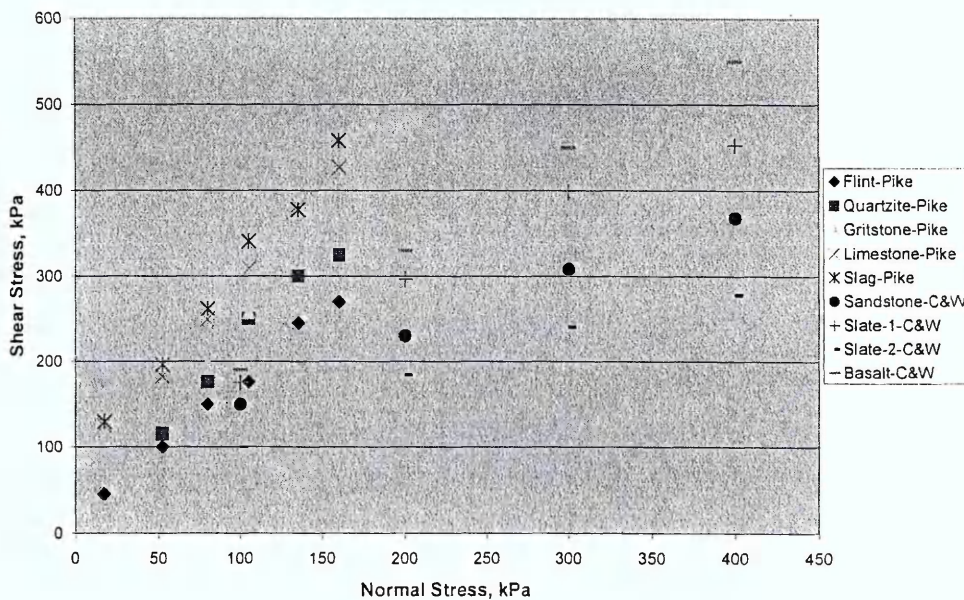


Figure 2.11: Effect of normal stress on shear stress of granular material

2.4.4 Density

Zeller and Wulliman (1957) observed that the friction angles increase with relative density for granular materials of D_{max} of 10, 30 and 100 mm (Figure 2.12).

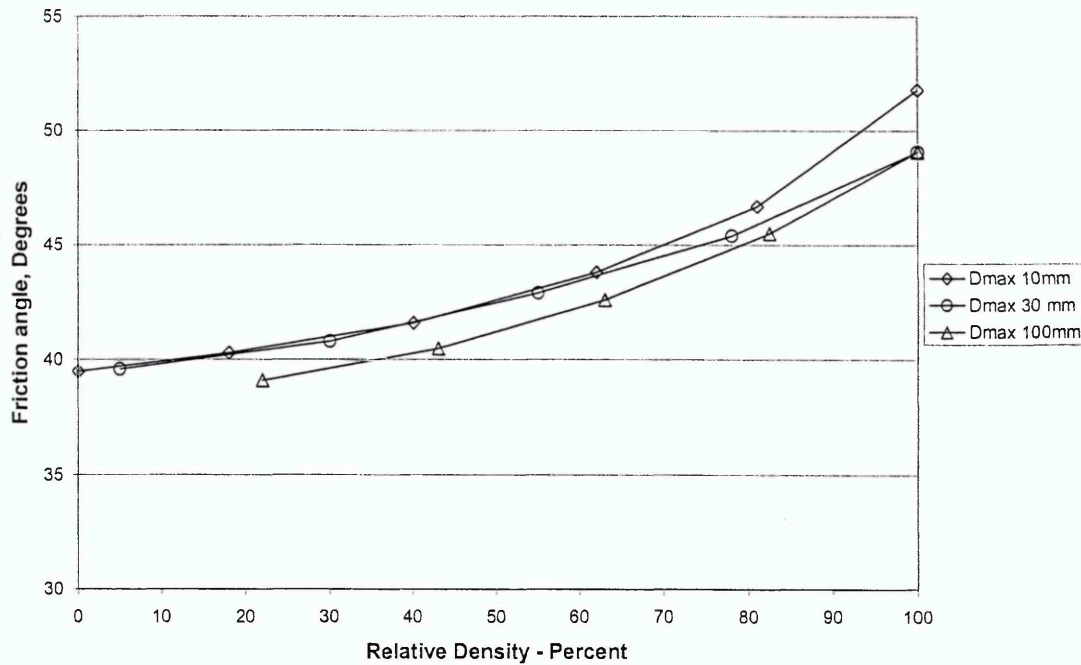


Figure 2.12: The effect of relative density on friction angles (after Zeller and Wulliman, 1957)

Marsal (1973) reported that the variations in friction angles between different densities was in the range of 3° to 4° for material tested at normal stress of 65 kPa. In their paper, Indraratna *et al* (1993) note that the degree of compaction and hence the initial porosity of rockfill has a major effect on shear strength.

2.4.5 Particle Crushing

The crushing of particles can influence the behaviour of granular materials in terms of strength, volume change characteristics, permeability, stress-strain behaviour and pore-pressure distributions (Lee and Farhoomand, 1967 and Lade *et al*, 1996). Permeability is of particular importance if the material is going to be used as engineering fill where it can affect the pore-pressure distributions and seepage quantities (Lade *et al*, 1996).

Marachi *et al* (1969) conducted tests on three different granular materials and found that there is a relationship between the breakage of the particles and the specimens' friction

angles (Figure 2.13) for materials with three different maximum particle sizes (2.8, 12 and 36 inches).

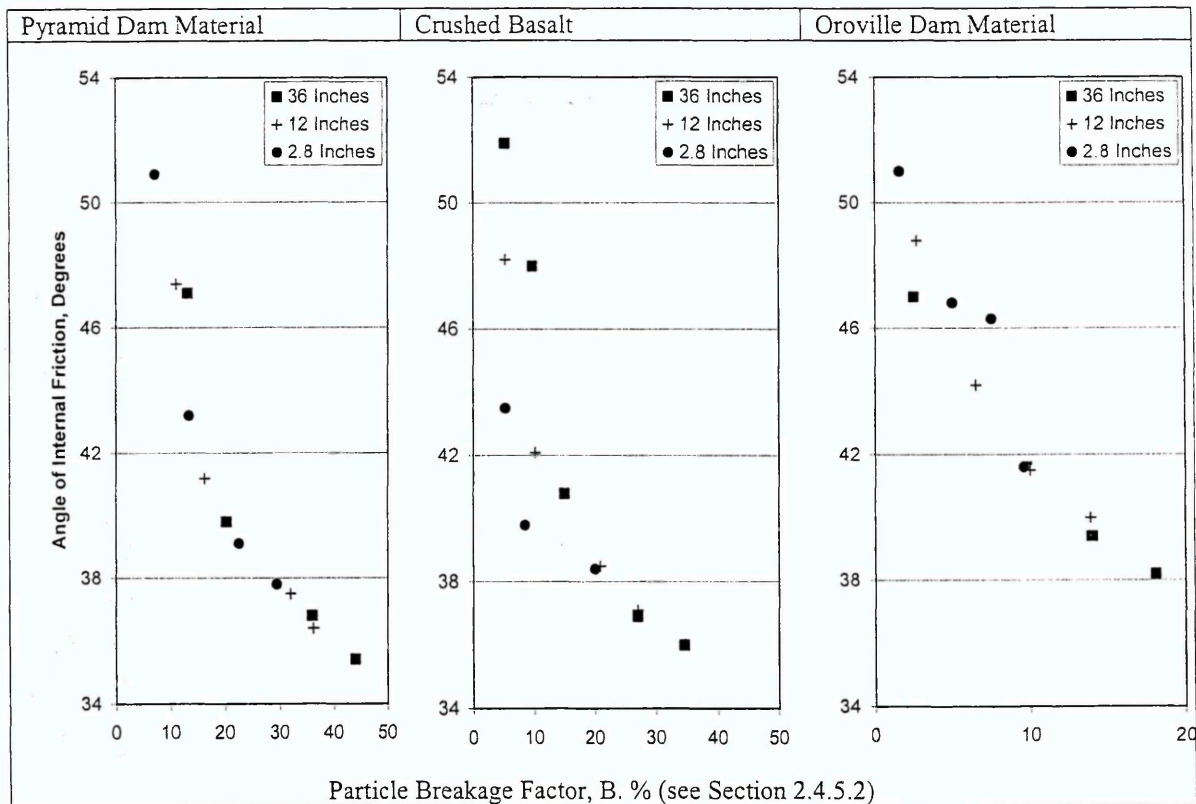


Figure 2.13: Angle of internal friction against breakage factor (after Marachi *et al*, 1969)

2.4.5.1 Factors affecting Particle Crushing

The factors affecting particle breakage have been investigated extensively and the findings may be summarised as follows:

1. The amount of breakage is affected by many factors, such as the stress level and the stress path applied to them (Lee and Farhoomand, 1967, Lade *et al*, 1996).
2. Yamamuro and Lade (1993) established that the crushing of particles depends on the types of materials tested and continues with time, even when the material is under constant stress.
3. Particle size is also a factor that affects the degree of breakage of a material. Larger particles are thought to be more prone to breakage than the smaller ones due to the fact that they contain more defects and/or micro-cracking (Hardin, 1985). This is probably a result of the smaller particles being created from the larger ones fracturing along these defects, and therefore as the process continues fewer and fewer defects exist within the smaller particles (Hardin, 1985).

4. Increased angularity increases particle breakage, as the stresses can concentrate along their smaller dimension and fracture it more easily (Lade *et al*, 1996). The concentration of stresses at angular points of contact causes fractures at those points (Yamamuro and Lade, 1993). The same researchers also found that well-graded soils do not break as easily as uniform soils, probably because when more particles surround each particle, the average contact stress tends to decrease.
5. It has been noticed that the addition of water in materials increases the particle breakage (Hardin, 1985; Lade *et al*, 1996), probably due to the softening of particles
6. Extensive coverage of particle crushing has been conducted by Nakata *et al* (1999). They performed individual particle strength testing, and triaxial tests in which marked (painted) particles of the same composition, size and shape as the individual tests were placed within the triaxial test sample. This was done to identify the behaviour of the particles individually and as part of granular specimens. The results were inconclusive as to if the crushing behaviour of the particles changed when they were part of a triaxial specimen.

2.4.5.2 Particle crushing quantification

Almost all the investigations concerning testing of granular materials have noted particle breakage (e.g. Barden *et al*, 1969; Murphy, 1971; Hagerty, 1993), even at relatively low pressures. Many attempts have been made to quantify and measure this problem with the use of breakage factors, most of them based on the changes of grain size distribution of the materials before and after testing.

The most widely used breakage factors are the ones developed by Marsal (1967) and Lee and Farhoomand (1967):

- Marsal noticed significant amounts of breakage of particles while performing large-scale triaxial tests on rockfill materials. His breakage factor, B_f , uses the sum of the percentage differences, for each sieve, between the initial and final gradation curves.
- The breakage factor of Lee and Farhoomand (1967) is based on the change before and after testing, of a single particle diameter namely the 15% finer on the grain distribution curve. Their factor ($D_{15(\text{Initial})} / D_{15(\text{Final})}$) was the ratio between the initial and final grain size corresponding to 15% fines line. The

relations of this breakage factors to the grading curves of the materials are given in Figure 2.14.

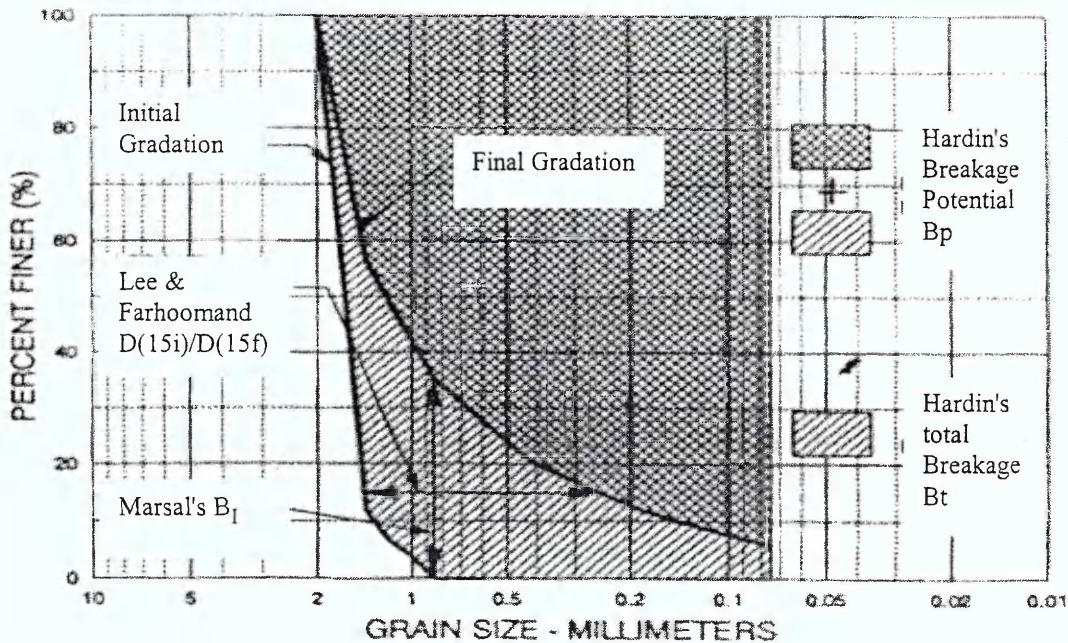


Figure 2.14: Breakage Factors (Lade, Yamamuro & Bopp, 1996)

Particle breakage quantification is based on the grading curves before and after shearing. Despite this though, it is almost impossible to obtain a direct relationship between particle breakage (and the properties affecting it), and shear strength since the amount of breakage depends on other factors. For example different materials with identical gradations, undergoing the same shear testing, will exhibit different amounts of crushing if other properties like particle shape and individual particle strength are different.

2.4.6 Relation between permeability and particle crushing

Duncan *et al* (1972) and Lade *et al* (1996) have also investigated the relationships between particle gradation and size with permeability. Hazen (1911) developed a formula relating the grain size with permeability:

$$k = 100 \times (D_{10})^2$$

where k is the permeability coefficient (cm/s)

D_{10} is the effective grain size.

Taking this formula into consideration, Lade *et al* (1996), developed an alternative breakage factor B_{10} based on D_{10} particle size and on the effective grain size before the test (D_{10i}) and after the test (D_{10f}):

$$B_{10} = 1 - (D_{10f} / D_{10i})$$

The minimum value of the factor is zero, where no breakage occurs and the upper value is one, where infinite breakage occurs.

2.4.7 Summary

Table 2.2 presents a summary of the parameters and their possible effect on shear strength/friction angle according to literature.

Table 2.2: Summary of parameters affecting shear strength

Parameter	Comment
Particle Shape	Shear strength increases with particle angularity
Sample Gradation and Maximum Particle Size	Broader gradation increases strength but parameters and their effect too interlinked to be able to safely conclude which has the biggest effect
Confining Pressure	Shear strength increases with confining pressure but the friction angle appears to reduce
Density	Shear strength and friction angle increase with density.
Particle Crushing	Friction angle tends to reduce with increasing particle crushing

2.5 Compaction

For natural coarse granular materials, the density is generally understood to be related to the moisture content and the compactive effort. At low moisture contents the soil has low workability and is therefore difficult to compress. By adding water the material is provided with the lubricant that it needs to move more freely (Watson, 1989). The introduction of excessive water leads to higher saturation levels which keep the particles apart during compaction, which reduces the density of the material. The control of moisture during compaction therefore becomes one of the most important factors to consider in earthworks control (Wignall *et al*, 1999). Optimum moisture content is defined as the moisture level at which maximum dry density of the material is achieved.

The value of optimum moisture content is different for different types of granular material. For sands and gravel mixtures it is typically 5-7% and for sands 8-10% (Watson, 1989).

Testing of granular materials in the laboratory can not exactly mirror field conditions and it is very difficult to test undisturbed samples of granular materials obtained from sites. Therefore, for laboratory studies, materials need to be compacted at densities representative of the field (Hoff *et al*, 2004). Many studies (e.g. Nowak *et al*, 1998, Knight *et al*, 1995, Richard, 2005 and Lumay and Vandewalle, 2005) have stated the fact that the dynamics of granular material compaction is a complex process and there have been many theoretical models for estimating/predicting their compaction behaviour (Boutreux and de Gennes, 1997, Levin *et al*, 2001 and Arenzon *et al*, 2003). Analysis of these methods though is outside the scope of this project.

Many methods for laboratory compaction exist, such as Proctor impact hammer, modified proctor hammer, vibratory table and vibratory hammer. There are differences in the behaviour of the materials compacted with these methods, even when the same dry density is achieved. Hoff (1998) found that samples of the same materials compacted with gyratory compactor exhibited higher CBR values than when compacted by modified proctor hammer. Hoff *et al* (2004) also showed that Gneiss from Askøy, Norway, when compacted to the same density by the vibratory table, produced higher failure angles than the same material compacted by impact methods (hammer).

Carga and Madureira (1985) found that the difference between the maximum dry densities for standard and intermediate energies is independent of the percentage of gravel fraction, and that the compacted density was essentially independent of the gradation of the gravel fraction. They also found for a number of samples tested that the particle size does not dramatically affect the maximum dry density, for 40-60% gravel content and for the equipment used in the research. No information was given about materials with gravel content outside the range of 40-60%.

2.6 Compressibility

2.6.1 Introduction

Granular materials suffer changes in volume and void ratio when subjected to a load due to the rearrangement, distortion and crushing of the particles. Roberts and De Souza (1958) showed that the volume changes of sands at low stresses is a result of the

compression of the soil skeleton and particle rearrangement. Even though at low stresses there is some crushing on sands, it becomes the dominating factor of the compressibility of sands at higher stresses (Lee and Farhoomand, 1967, Hardin, 1985 and Hagerty *et al*, 1993). Similar behaviour has been observed for larger granular materials, and their compressibility has been attributed to the rearrangement of particles during loading and the breakage of highly stressed points (Marsal, 1967, Lade *et al*, 1996, Yamamuro and Lade 1993). The compressibility of granular materials, as a whole and not on the individual particle level, depends on many factors such as gradation, particle size and shape (Rowe, 1955, Roberts and De Souza, 1958, Schultze and Moussa, 1961), and the literature on the influence of each factor is reviewed separately below.

2.6.2 Effect of Particle Shape

Hagerty *et al* (1993) found that material that contained angular particles showed a greater degree of compressibility than material with the same median grain size and composition that contained spherical particles. These results are in agreement with the findings of Pestana and Whittle (1995) and Pigeon (1996). They attributed the behaviour to the fact that angular particles crush more easily than rounded, and therefore it is easier to fill the air voids with crushed material and to have rearrangement of the particles within the material. Cho *et al*, (2006) also found that the compression and decompression indices reduce with increased regularity calculated as $(\text{Sphericity} + \text{Roundness})/2$, and it is shown in Figure 2.15.

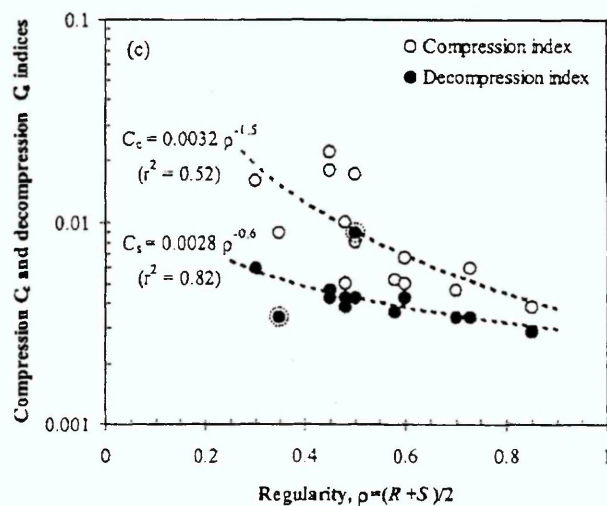


Figure 2.15: Compression and decompression indices against particle shape (after Cho *et al*, 2006)

Note: The compression index is calculated by drawing a curve along the compression line against different loading (1 kPa and 10 kPa or 2 kPa and 20 kPa) and at different void ratios. The index is calculated by subtracting the two void ratios. The opposite gives the decompression index.

2.6.3 Effect of Individual Particle Strength

Tests performed by Pestana and Whittle (1995) on two types of sands found that Ottawa sand was more difficult to compress than Quiou sand. This was a result of the fact that the main constituent of Ottawa sand is quartz and the main constituent of Quiou sand is calcitic shell fragments. Quartz is stronger and therefore more difficult to crush than calcitic shell fragments. Similarly Yamamuro *et al* (1996) found that that material with relatively weaker, in terms of strength, particles showed a “faster” compression response to stresses, which was attributed by the researchers to the fact that soft grains allowed the material to flow plastically and fill the voids easier and faster.

2.6.4 Effect of Material Void Ratio (dry density)

Roberts and de Souza (1958) observed that void ratio is one of the main factors that affects the compressibility of sand and ground quartz. Tests performed by Hite (1989) on loose and dense samples of sand showed that the compressibility of the materials decreased with increased density. However when the stresses reach a level when particle breakage occurs, then the degree of influence of the initial void ratio decreases and becomes minimal (Hendron, 1963, Vesic and Clough, 1968 and Hagerty *et al*, 1993). This was also noticed by Yamamuro *et al* (1996), who observed that the effect of the initial void ratio was eliminated at high pressures. Pestana and Whittle (1995) also reached the same conclusion, but noted that cementation might play a role in the behaviour but did not proceed to a more detailed investigation of the subject.

2.6.5 Effect of Material Grading

In tests triaxial tests by El-Sohby (1964) and Pigeon (1969) it was found that the material compressibility decreases as their grading broadens. The same behaviour was observed during an investigation of the effects of the grading and density on the mechanical properties of crushed dolomite by Thom and Brown (1988). On the other hand Marsal (1966) performed drained triaxial tests on coarse gravel and broken rock and observed that the coarser materials compressed more as grading broadens. The

apparent contradiction of the effect of grading on the compressibility of the materials possibly indicates that other factors, especially listed in this paragraph, play a more important part than grading in the behaviour of the materials.

2.6.6 Effect of time

Special attention has also been given to the compression with time relation. De Souza (1958), Roberts and De Souza (1958) and Pestana and Whittle (1995), all found in their research, that included triaxial and one dimensional compression testing, that the compression of granular materials starts almost from the time, the load is applied to them and continues with time but at a decreasing rate, as long as the load is applied continuously. This is similar to the phenomenon of secondary compression or creep effects, observed with clay soils (Lee and Farhoomand, 1967). This continuous compression is attributed to the continuous deformation, re-arrangement and breakage of the particles under load (Roberts and De Souza, 1958 and Pestana and Whittle, 1995). The exact response of the materials depends on their particles' properties, the magnitude of the load and the stress path(s). This was observed by Houlsby and Psomas (2001) when they tested sand in a one dimensional compression tests at load increments of 28.3 kPa (Figure 2.16)

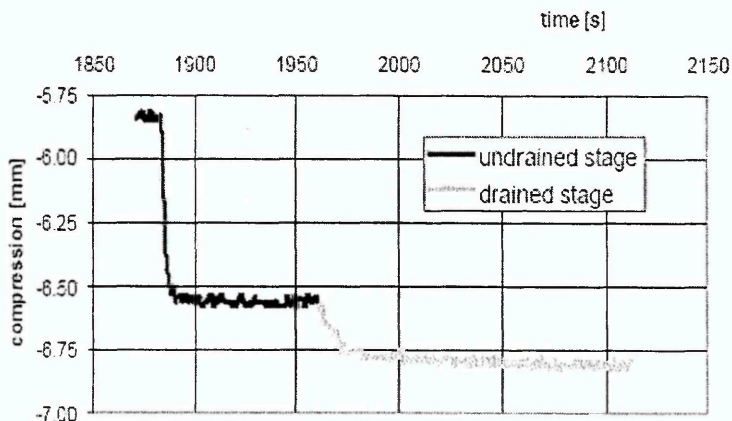


Figure 2.16: Displacement against time for sand (After Houlsby and Psomas, 2001)

2.6.7 Effect of Water

Holestol *et al* (1965) determined by field and laboratory tests that the compressibility of mixes of unweathered granitic gneiss and amphibolite increase with the addition of

water. The same phenomenon was observed by Sowers *et al* (1965) on their tests on broken rock. Miura and Yamanouchi (1975) showed that the introduction of water can affect the compressibility of cohesionless soils by increasing particle breakage (through weakening the individual particles), a phenomenon that is more intense in materials with larger particles (Leslie, 1975). Clements (1981) observed that flooding particle contacts caused additional displacements to the materials tested. Sun *et al* (2004) also found that for identical materials, the saturated specimens exhibit more volumetric strain(dilation) in comparison to the unsaturated specimens for three different normal stresses (Figure 2.17).

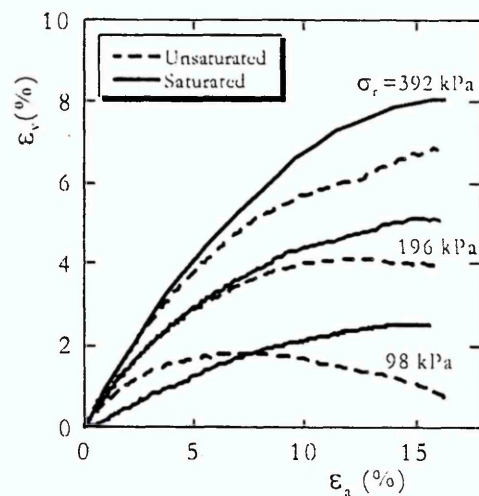


Figure 2.17: Volume change behaviour of saturated and unsaturated materials (after Sun *et al*, 2004)

2.7 Leachate

Leachate is the liquid that drains or 'leaches' from a landfill site or in this project's case from the materials when they are compacted and left to be permeated by precipitation that can groundwater, rain, frost and/or melted snow. It varies widely in composition regarding the type of the landfill or in this case the type of the materials. The production of leachate has the potential to interfere with the mechanical properties of the material. Further more there is a possibility that contamination of the land, and the underground and the surface water systems could result. Little research into the leachate generation characteristics of recycled concrete and bricks has been undertaken. Due to the granular nature of the materials, conceptually it may be assumed that particle size may have an

effect on the amount of produced leachate. Hill (2001) did indeed find that the larger the particles the less likely they are to leach.

Dawson (2001) found that the existence of Ca^{2+} (Calcium ions) in concrete is the most likely chemical to produce leachate, and found also that a high pH reduces the production of leachate. The same research also indicates that of the chemically untreated recycled materials used in road construction, concrete is one of the most unlikely to produce leachate. Dawson showed, using in-situ tests, that the use of recycled materials including crushed concrete does produce a small amount of leachate but its chemical components not only do not exceed the pollution limits but they exist in very small concentrations.

2.8 Recycled aggregates research

This section of the thesis presents some recent research on the use of recycled materials as aggregates and provides information of the types of tests conducted and the results obtained.

McKelvey *et al* (2002) investigated the behaviour of two types of recycled aggregates under repeated load on a series of shear box tests and vertical stresses varying from 60 kPa to 300 kPa. The first type of material (named S1 for this discussion) was crushed concrete obtained from crushing concrete tubes. The second type of materials (named S2) was crushed brickwork containing bricks (of at least 95%) and mortar.

Sivakumar *et al* (2004), also investigated the behaviour of two recycled materials, similar to S1 and S2, during large shear box tests named S3 and S4 for the purpose of this discussion. S3 was crushed concrete obtained from crushing concrete tubes and S4 was crushed brickwork containing bricks (of at least 95%) and mortar. All materials were sieved and had particles between 20 and 40 mm.

The friction angles, determined from a straight line from the origins to the value of shear stress for 300 kPa, were and 39° for S1 and 37° for S2 and 43° for both S3 and S4. McKelvey *et al* (2002) and Sivakumar, *et al* (2004) state that the particle crushing of the materials was high but do not give specific values.

Aurstad *et al* (2005) have tested crushed concrete with particles ranging from 0-63 mm (DG2) and from 20-63 mm (OG2) in a large triaxial apparatus (diameter 300 mm and

height 600 mm). They found that the friction angle of DG2 was always higher than 48° and for material OG2 higher than 60°.

Aurstad *et al* (2005) have also observed that the crushing of particles is low for the grading of the materials from 0-63, but quite significant for the materials when they contain particles from 20-63 mm. Taking into consideration the results of this investigation together with the results presented by Aurstad *et al* (2005), McKelvey *et al* (2002) and Sivakumar *et al* (2004), it appears that recycled materials with minimum particle sizes of 20 mm crush more than the same type of materials containing finer particles. This may be a result of the “ability” of broader gradation to fill more voids and restrict the movement of larger particles. Further testing will be needed though to verify this.

Rathje *et al* (2006) conducted comparative tests on crushed concrete and limestone in respect to utilising them as backfill for mechanically stabilized earth walls. They determined the permeability and friction angle of the materials. The friction angle of both materials was 46° and the coefficient of permeability of the crushed concrete varied from 1×10^{-3} m/s to 8.5×10^{-5} m/s. The crushed limestone exhibited a coefficient of permeability of 1×10^{-2} m/s. They concluded that the friction angle of the crushed concrete is acceptable for the specific backfill engineering applications but the permeability is a concern.

Huurman and Molenaar (2006) have conducted a series of large scale triaxial tests on materials containing 65% of crushed concrete and 35% of crushed masonry with maximum particle size of 40 mm. They used six different gradations but kept the maximum particle size the same. They found that the friction angles of the materials varied from 42° to 46°.

2.9 Concluding Remarks

The literature review on recycled materials has shown that they exhibit significant friction angle values and can be utilised by the industry for field applications. Their behaviour is also similar to natural aggregates and tests used for them can be applied in testing recycled aggregates. It is clear though that there are many types of recycled aggregates in existence and their properties depend on factors such as the type and age of buildings demolished, the amount of processing they have undergone, if more than

one types of materials is used to provide the testing samples and their grading curves. The literature review has also shown that the investigation of the shear strength of the materials should include testing the materials under different "conditions" and "parameters" such as sample density, maximum particle size, particle shape, moisture content.

All these different "conditions" and "parameters" and their effect on the shear strength is have been analysed in this chapter and are summarised below:

- The shear strength, compressibility and crushing of granular materials increases with angularity. In addition to determining the shape of particles with the use of British Standards (BS 812-105), a more complete description can be given by the methods described and used by Rösslein (1941) and Lees (1964).
- The reviewed research has proven inconclusive on the exact effect of the grading on the shear strength and compressibility of granular materials.
- The reviewed research has proven inconclusive on the exact effect of the maximum particle size on shear strength. It has shown though that particle crushing tends to reduce with maximum particle size due to less defects existing in smaller particles.
- The shear strength of granular materials increases with confining pressure but the opposite occurs in their friction angles.
- The increase in the specimens' density results in the increase of shear strength but in the decrease of the compressibility. The effect on the compressibility appear to reduce though when high confining pressures are reached.
- The addition of water appears to increase the compressibility and the crushing properties of the materials.
- When sustained long term stress is applied to granular materials, then particle crushing and compression continues to occur.
- Almost all research on granular materials has shown particle crushing due to loading and the most widely used methods for quantification are the breakage factors after Marsal (1967) and Lee and Farhoomand (1967).
- It is very difficult to produce laboratory specimens representative of site conditions, and therefore great attention should be given to specimen compaction and preparation.

- Crushed concrete creates small amounts of leachate, but the chemical components leached are significantly lower than the permitted limits.

It can be seen therefore that the behaviour of engineering fill is a complicated subject affected by many variables.

Therefore a comprehensive large scale testing schedule that includes the investigation of these different "conditions" and "parameters" together with the shear strength of the materials is needed which will also include the development of large scale testing equipment.

CHAPTER 3

RATIONALE FOR EXPERIMENTAL PROGRAMME

3.1 Fundamental Aspects of Experimental Programme

The objectives of the project were defined in Chapter 1 to be:

1. To provide a base for future research by investigating the physical and mechanical characteristics of crushed recycled aggregates
2. Provide data on the strength of recycled aggregates so they can be utilised by the industry.
3. Compare the properties of recycled materials with other research on recycled and primary aggregates.
4. Compare the characteristics and performance of different types of recycled materials.

The testing programme for this investigation has been derived according to these objectives and the information collected from the literature review. At the outset, it was apparent that fundamental choices had to be made with regard to the maximum particle size to be tested, the focus of the testing work and the number of tests. Each aspect is discussed below in turn. The equipment and procedures used for determining the Physical Properties and the Main Series testing procedures are presented in detail in Chapters 4 and 5 respectively. Chapter 6 presents the three types of materials chosen as representative of crushed concrete and bricks utilised by the industry.

Three types of materials were going to be tested in this investigation. Two types of crushed concrete, one (Material A) removed from a demolition site with no further processing and one (Material B) was furthered processed at a crushing site. The brickwork rubble (Material C) has also been processed in the same crushing site as Material B. A complete description of the materials used and the processes involved in the acquisition of the materials is given in Chapter 6.

3.1.1 Selection of Maximum Particle Size

A significant problem resulting from the large size of the materials is the inability to perform all the necessary tests with existing standardised equipment. Two possible solutions to this obstacle were identified early in the research project:

1. Scale down the materials maximum particle size, or
2. Develop new large scale equipment that can accommodate particle sizes up to 50 mm.

The latter of these was chosen in order to test representative materials of in situ fills, and due to the fact that similarly large particle sizes were used by many researchers (Charles and Watts, 1980, Indraratna *et al*, 1993 and Indraratna *et al*, 1998) for the investigation of the properties of engineered fills. By testing similar maximum particle size materials, the effect of the particle size variable is removed from any comparisons, making them more relevant.

A further consideration in defining the test programme and the maximum particle size of the specimens is the non-uniformity of the materials proposed to be investigated in this project. Observations of crushed concrete indicate that particles larger than about 20mm were made up mainly of concrete whilst the smaller particles were a mixture of:

- The gravel used for the manufacturing of the original concrete
- Composite concrete particles (containing cement and gravel particles)
- Fragments of cement

This non-uniformity would make the scaling down of the materials for testing a procedure that would probably lead to inaccurate results, as it would significantly alter the samples' properties due to, for example, alterations in particle shape and particle strength. It was therefore considered necessary to develop equipment that can accommodate materials with particle sizes up to 50 mm, despite the difficulties that this would present

3.1.2. Testing Programme

Having determined the maximum particle size, it was necessary to define the testing programme. It was necessary to develop a testing programme that would:

1. Be able to describe and classify the materials, and
2. Establish their suitability for their use as engineering fill

In order to achieve these, a testing programme was devised that included two main series. The first, Physical Properties Series (PPS) included tests to determine the physical properties of the materials (see Section 3.2). The second, Main Series Testing (MST), included large scale testing for the determination of the shear strength, particle crushing and permeability (see Section 3.3). It was decided not to investigate the compressibility of the materials due to time and material restrictions.

3.1.3 Number of Tests

Due to the challenges of testing these types of materials, specifically the potential variability of the samples obtained and the reliability of the results from newly established equipment and testing procedures, it was decided to undertake a significantly large number of tests in order to identify any possible effects of sample variability on the results and more fully understand the repeatability of the test data.

3.2 Physical Properties Testing Series

The Physical Properties Series (PPS) was undertaken to identify fundamental material characteristics, using standard methodologies where possible. Table 3.1 summarises the tests included in the PPS programme, together with the aim of each test and the standard used for performing it. The tests were targeted to identify the main characteristics of the materials that may possibly affect properties such as the shear strength and permeability, as has been discussed in the literature review.

Table 3.1: Tests included in the Physical Properties Series

Test	Method Used	Aim of Test
Grading	Mechanical Sieving	Determine the Grading Properties
Particle Shape	BS 812-105.1, 1989	Determine the Flakiness Index
Particle Shape	BS 812-105.2, 1990	Determine the Elongation Index
Particle Shape	Rösslein (1941) and Lees (1964)	Determine three dimensional shape of the particles
Water Absorption	BS 812-2, 1995	Determine the water absorption
Particle Density	BS 812-2, 1995	Determine the particle density
AIV	BS 812-112, 1990	Determine Aggregate Impact Value
ACV	BS 812-110, 1990	Determine Aggregate Crushing Value
Freezing-Thawing	BS EN 1367-1, 1999	Resistance to freeze-thaw cycles and affect on materials' strength
Compaction	BS 1377-4, 1990	Determine compaction characteristics according to BS
Compaction	Large scale dynamic compaction	Determine compaction characteristics for maximum particle size of 50 mm

3.2.1 Shape

The literature available on the effect of particle shape on shear strength of granular materials is somewhat confusing. Even though some researchers (Marsal, 1967; Kirkpatrick, 1965; Leslie, 1963) indicate that the particle shape affects the strength (see Chapter 2), others (Holtz & Gibbs, 1956; Vallerga *et al*, 1957) have shown that there is a negligible effect of particle shape on the behaviour of granular material. As the effect is uncertain, it was decided to determine particle shape as analytically as possible, within the context of this project, using the following methods:

- Flakiness and Elongation Index.
- Description of three dimensional shape according to Rösslein (1941), Zingg (1935) and Lees (1964).

As the materials tested are not homogeneous it was considered necessary to produce results not only for the whole of the materials but also for each of the individual particle sizes fractions in order to establish the effect the size has on the shape of the materials.

3.2.2 Grading

The grading curves of the materials were determined by using the dry sieving method according to BS 812-103, instead of the wet sieving methods. The reasons for this decision were:

- The need to perform sieving tests with large quantities of materials to achieve repeatability given the variability of recycled materials. It was considered impractical due to time and quantity of materials restrictions to proceed with wet sieving for the whole programme. However, a small quantity of each of the three types of the materials was wet sieved at the same stages of the project in order to verify the results of the dry sieving process.
- BS 812-103.1:1985 states that if the materials that are going to be tested do not contain any significant amount of clay materials then the dry sieving method can be applied. This is the case for all three types of materials tested in this project.

It was decided to perform sieving tests on a large quantity of the original materials at different stages of the testing programme in order to verify the effectiveness of the preparation procedure. These tests were carried out at five different points during this project: Before the compaction tests, before the permeability test and before, after half the shear box tests have been completed, and at the end of the shear box testing series.

3.2.3 Compaction

The British Standard 1377-4 test method may only be applied to the crushed concrete materials that have not been furthered processed (Material A, see Chapter 5) according to paragraph 3, note 2. As a result, a non British Standard test method was adopted using a 300 mm diameter mould with the materials compacted using a Kango K900 vibrating hammer. Material A was also tested according to BS 1377-4, 1990 in order to provide data for comparing the two methods.

3.2.4 Aggregate Impact Value (AIV) and Aggregate Crushing Value (ACV)

The AIV and ACV tests give the relative strength of aggregates against impact and crushing loading by determining the ability of an aggregate to resist crushing. The lower the figure the stronger the aggregate, i.e. the greater its ability to resist crushing. The AIV and ACV tests were performed in this investigation for two main reasons:

1. Initial indication of material strength
2. Initial comparison between the recycled materials and industry products

The materials tested according to these standards (BS 812-112:1990 and BS 812-110:1990) should pass through the 14 mm sieve and be retained on the 10 mm sieve. It was appreciated that due to the non-uniform nature of the materials (see paragraph 3.1) it is quite possible, within this particle fraction requirement (14 to 10 mm), to test samples that are not representative of the materials as a whole. Despite the risk of not obtaining results representative of the materials as a whole, it was decided to proceed with the tests according to the standards so the values could be compared with natural materials.

3.2.5 Freezing and Thawing

The materials were tested for their resistance to freezing and thawing by:

1. Conducting freezing and thawing cycles according to BS EN 1367-1
2. Determining the effect it has on their strength by conducting AIV and ACV tests after the freezing and thawing process.

3.3 Main Series Testing (MST)

This paragraph describes the rationale behind the Main Series Testing (MST) programme. This series included large-scale, non-British standard tests in respect of:

- Permeability

- Particle Crushing
- Shear Strength Testing, in a Large Shear Box

This section does not include the description of the equipment and the exact procedures followed in these tests, as these will be given in Chapters 4 and 5 respectively. A summary of the tests performed is given in Table 3.2.

It was intended originally to test the materials for their compressibility and leachate properties. Due to a combination of budget, time and material restrictions this proved to be impossible.

Table 3.2: Tests included in the Main Series

Test	Description of Test	Variables Investigated
Permeability	Constant Head Method on a Large scale permeability cell	N/A
Particle Crushing	Determine the particle crushing of the materials due to shear box testing	Dry density and maximum particle size
Shear Box	Determine the shear strength of the materials using a large scale shear box	Dry density and maximum particle size

3.3.1 Specimen Moisture Content and Dry Density

All three types of materials were to be removed from the storage bays, transported to the laboratory, compacted and tested immediately at their natural moisture content. The moisture content of all the materials was in the range of 2.0 +/- 0.2 % (see Chapter 6).

By testing the materials at the same moisture content the intention was to:

- Eliminate the influence of moisture on the results of the different tests and materials and therefore establish more clearly the effects of other parameters such as maximum particle size and dry density.
- Minimise the extra cost, time and work required to make changes to the moisture content which would not be undertaken in industry due to the significant negative impact on cost of such processing.

Before proceeding with the MST it was necessary to undertake initial compaction trials in order to establish a suitable dry density for testing because of the variability and the

limited information existing on the testing of these types of materials. The trials took place in the shear box (316 mm square by 160 mm deep) and a 300 mm diameter circular mould that was used for the compaction tests (See Chapter 4 for details of the equipment).

The compaction trials procedure was different from the compaction test procedure that was used in this project. The trials were carried out on the materials with moisture content of 2 % (standard deviation of 0.24) and with layer depths of 50 mm. The samples were continuously compacted for a period of 3 minutes, with the use of a Kango K900 vibrating hammer, and it was determined that the dry density achieved under these conditions was 1.83 (+/- 0.13) and 1.84 (+/- 0.19) Mg/m³ (average of 3 trials) for the crushed concrete materials for the circular and shear box moulds respectively. For the crushed brick materials the dry density values were 1.81 (+/- 0.06) and 1.79 (+/- 0.11) Mg/m³. It was therefore decided to proceed with testing of the samples with a dry density of 1.8 Mg/m³, as this value can be achieved with the specific compaction process and compares well with published data from other research (e.g. Indraratna *et al*, 1993 and Varadarajan *et al*, 2003)

3.3.2 Permeability

For the determination of the permeability parameters, the constant head method described in BS 1377-5:1990 was used, but with the cell replaced with one of 300 mm diameter and 600 mm height. The complete specifications and the design of the large permeability cell are given in Section 4.4. Its design and development was based on two requirements:

- BS 1377-5:1990 states that the minimum ratio of height to diameter of the cell should be two.
- Marachi *et al* (1972) and Indraratna *et al* (1993) have suggested that the ratio of the diameter to the maximum particle size be at least 6 to render particle size effects negligible. For the proposed maximum particle size of 50 mm this gives a minimum diameter of 300 mm.

The effect of variation in dry density and maximum particle size were not investigated in the permeability tests due to:

- Time required to design and manufacture the equipment.
- Lengthy sample preparation procedures required and extended duration of work.

3.3.3 Shear Strength Testing

The principal methods of testing granular materials for their shear strength are the shear box and the triaxial test. Originally it was intended to conduct both types of testing by utilising a large shear box apparatus already available and developing a large triaxial cell able to accommodate particles up to 50 mm. This would have provided:

1. A large amount of data from the shear box tests that would have helped in eliminating any possible effects of the variability of the materials on the results
2. A mechanism for checking the accuracy of the newly developed triaxial cell
3. Means for comparing the two methods.

Due to factors outside the control of this research though the development of the triaxial test equipment proved to be impractical. Therefore the investigation of the shear strength of the materials occurred with the use of shear box testing alone.

The shear box already available for this investigation could only accommodate samples with maximum particle size up to 37.5 mm (Bishop and Henkel, 1962). The development of a larger shear box was considered but was impracticable due to the time available for this research. Therefore the maximum particle size of the specimens in the shear strength and particle crushing investigations is restricted to 37.5 mm. The majority of the other tests in this investigation were performed on materials with 50 mm maximum particle size (due to the fact that they had already been performed before the inability to perform large scale triaxial tests became evident).

The different types of shear box tests performed are summarised in Table 3.3. By conducting these tests it was intended to determine any possible effects the dry density and maximum particle size might have on shear strength. The use of the second testing dry density of 1.6 Mg/m^3 was selected because:

- It was not practical to achieve any higher specimen density than 1.8 Mg/m^3 (see Section 3.3.1)
- It was considered that reducing the density to values higher than 1.6 Mg/m^3 would not have been enough to produce clear results on its effect on shear strength
- There has been published data on the properties of granular materials where similar density values have been used (Indraratna *et al*, 1998), and therefore comparisons will be possible.

Table 3.3: Types of shear box tests and variables investigated

Test Type	Dry Density (Mg/m ³)	Maximum Particle Size (mm)
SBT1	1.8	37.5
SBT2	1.6	37.5
SBT3	1.8	28

The materials were tested at five different normal stresses (95, 143, 190, 238 and 317 kPa), the first four chosen to simulate the self load of the materials at depths of 5, 7.5, 10 and 12.5 meters and the fifth being the largest that can be obtained from the equipment used without causing any damage to it (value simulating approximately the self load at 16 meters). This represents typical industry practices where it is unusual to meet fills with depths larger than 15 meters (Goodwin, personal communication).

Table 3.4: Number of tests for each of the materials for all different types of tests for all five different normal stresses

Material	Type and Number of tests		
	Density of 1.8 Mg/m ³ , Max Particle Size of 37.5 mm (SBT1)	Density of 1.6 Mg/m ³ , Max Particle Size of 37.5 mm (SBT2)	Density of 1.8 Mg/m ³ , Max Particle Size of 28 mm (SBT3)
A	50	25	15
B	25	25	15
C	25	25	15

The number of tests performed for each of the materials and for each of the different types of tests is given in Table 3.4. There was a minimum number of three tests performed for each normal stress for all the materials for each of the individual tests. This amount (three) of tests was chosen because is the minimum number of tests the majority of the British Standards suggest in order to obtain representative results for the tests they describe.

The repeatability and accuracy of the test preparation and execution was verified by initially performing a large number of tests for material A and for SBT1, for which there were ten tests performed for each normal load. When good repeatability was achieved the number of repetitions for each of the remaining type of test was reduced.

3.3.4 Particle Crushing

Particle crushing is known to occur under stress (Lee & Farhoomand, 1967, Marsal, 1967, Lade *et al*, 1996) and due to the nature of the materials being tested it was decided that the breakage was needed to be quantified as part of this research.

Based on the literature review and its general acceptance it was decided to use the breakage index (B_I) by Marsal (1967) to quantify crushing.

Particle crushing was measured as part of the shear box work in order to compare the crushability of the materials at different density and maximum particle size values.

The total mass of the all the shear box tests performed for each type of material was sieved at the end to obtain their crushing values. It was considered to sieve the materials tested for each individual normal stress but it was decided that this would not produce robust and representative results due to the relative small mass used for each test. This provided crushing values for Materials A, B and C for two different dry densities and two different maximum particle sizes.

CHAPTER 4

DESCRIPTION OF THE TEST EQUIPMENT

4.1 British Standard Tests

The equipment used in this project for performing the BS tests fell within the specifications stated within the corresponding standard. All the dimensions were measured with a vernier caliper, which in turn was calibrated with the use of a calibration rig with a micrometer head readable to 0.01 mm (+/- 0.01 mm). The basic types of equipment used for sample preparation were all within their required calibration period. A list of the basic equipment used in this investigation is presented in Appendix A.

4.2 Compaction Tests

The compaction mould used for the large scale compaction trials was manufactured from mild steel (Figure 4.1) with stiffening flanges at 1/3 and 2/3 of its height.

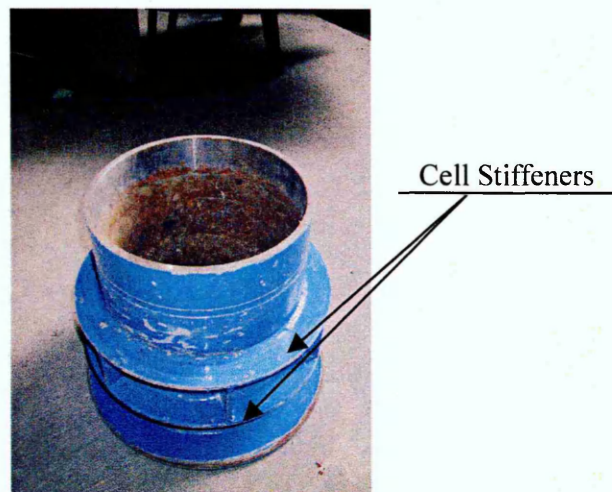


Figure 4.1: The large scale compaction mould

The dimensions of the compaction mould (300 +/- 1 mm diameter and 400 +/- 2 mm depth) was measured before and after each set of tests for the individual moisture contents and it was found that they were not affected by the compaction force applied. From the literature review, it has been established that the best methods for compacting granular materials are the vibratory table or the vibratory hammer (Section 2.6). The

large scale of the equipment used for the shear and permeability tests though makes the use of the vibratory table impractical and therefore the vibratory hammer method was used.

The vibrating hammer used for the mould compaction was a Kango 900K with an output of 1050 W. The force applied to the vibrating hammer (with the tamper attached to it) was in the magnitude of 350 ± 10 N and was calibrated against an Avery Birmingham, type 3205 CLE scale by determining the pressure required to be applied by the user to achieve the necessary compaction force.

4.3 Climatic Chamber

Figure 4.2 shows the chamber system used for the freezing-thawing process of this test.

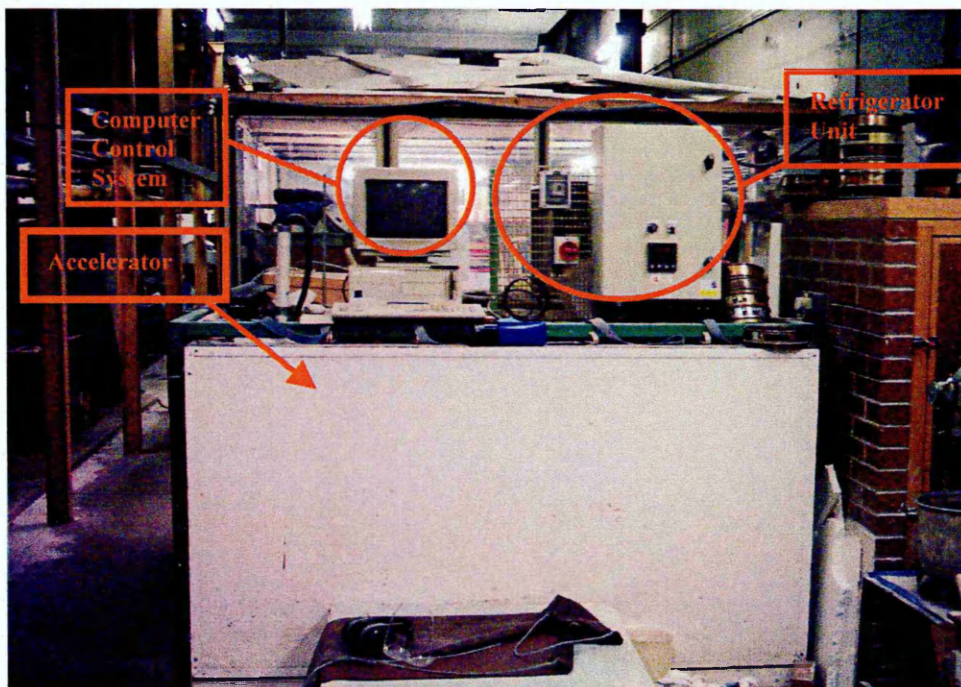


Figure 4.2: The climatic chamber and computer control system

Testing for the resistance of the materials to freezing and thawing took place in accordance with the European Standard EN 1367-1:1999. The climatic chamber used for this test was designed and constructed according to the Ceram research (formerly known as BCRA or the British Ceramics Research Association Ltd) chamber specifications and it is described in more detail in Peake and Ford (1984). In brief, the

accelerator has dimensions of 1.9 m by 2.0 m in the base and it is 1.2m high (external dimensions) with the outer skin having 80mm of insulation between external (ambient) and internal conditions. The specific chamber used in this test was modified by Sheffield Hallam University to facilitate computer control of the cycle such that any period of freezing or thawing could easily be run, with finer control over the number of cycles per day and the maximum and minimum temperatures.

The chamber is mounted in a steel frame which also provides the platform for the refrigeration and the computer control system. The computer display duplicates the display of time and temperature within the chamber, with the use of thermocouple sensors, and is capable of varying the inside temperature profile against time in order to be able to comply with the standards used. Figure 4.3 shows the recorded temperature against time profile for each of the freezing cycles used for the test, which complies with the specifications of EN 1367-1:1999. The temperature profile produced by the logging system was checked by the use of calibrated thermocouples and data loggers with the use of PicoLog software.

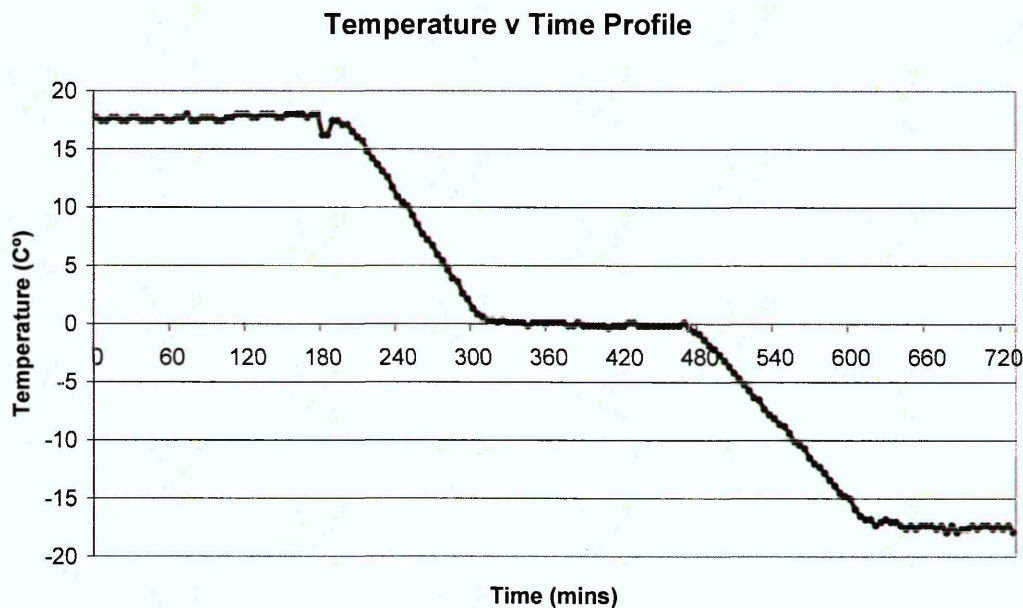


Figure 4.3: Recorded profile of Temperature against Time for the Freezing cycle

4.4 Permeability

The procedure and the equipment incorporate many characteristics of the permeability testing procedure that is described in BS 1377-5:1990 (calculations, constant head

method, dimension specifications), which was modified mainly only in size to accommodate materials with maximum particle size of 50 mm.

The large scale permeability cell used (Figures 4.4, 4.5 and 4.6) was a cylinder of 300 +/- 2 mm drain section pipe made of hardened plastic of a height of 615 mm to accommodate the sealing groove, the permeable mat and the steel mesh and still allow for a specimen of 600 mm height. The wall thickness was 10 mm.

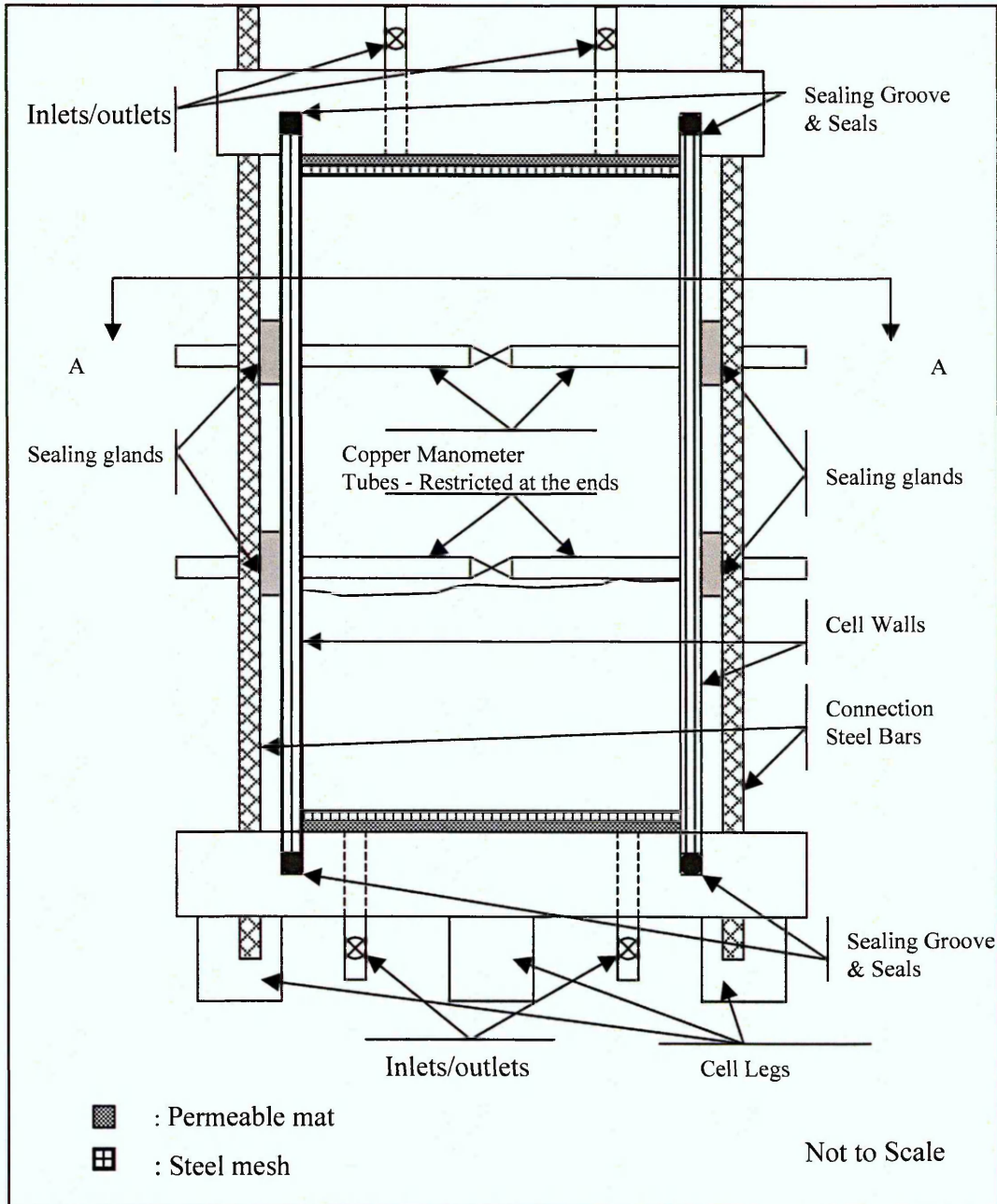


Figure 4.4: Schematic of the large scale permeability cell

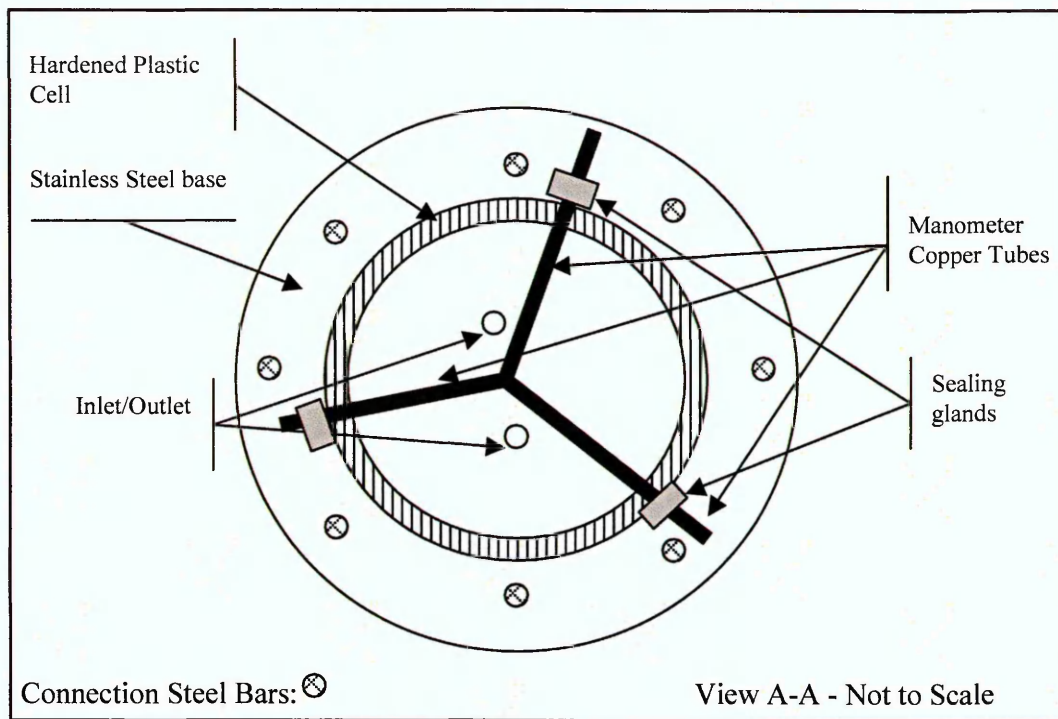


Figure 4.5: Schematic of the Permeability Cell (Plan View)

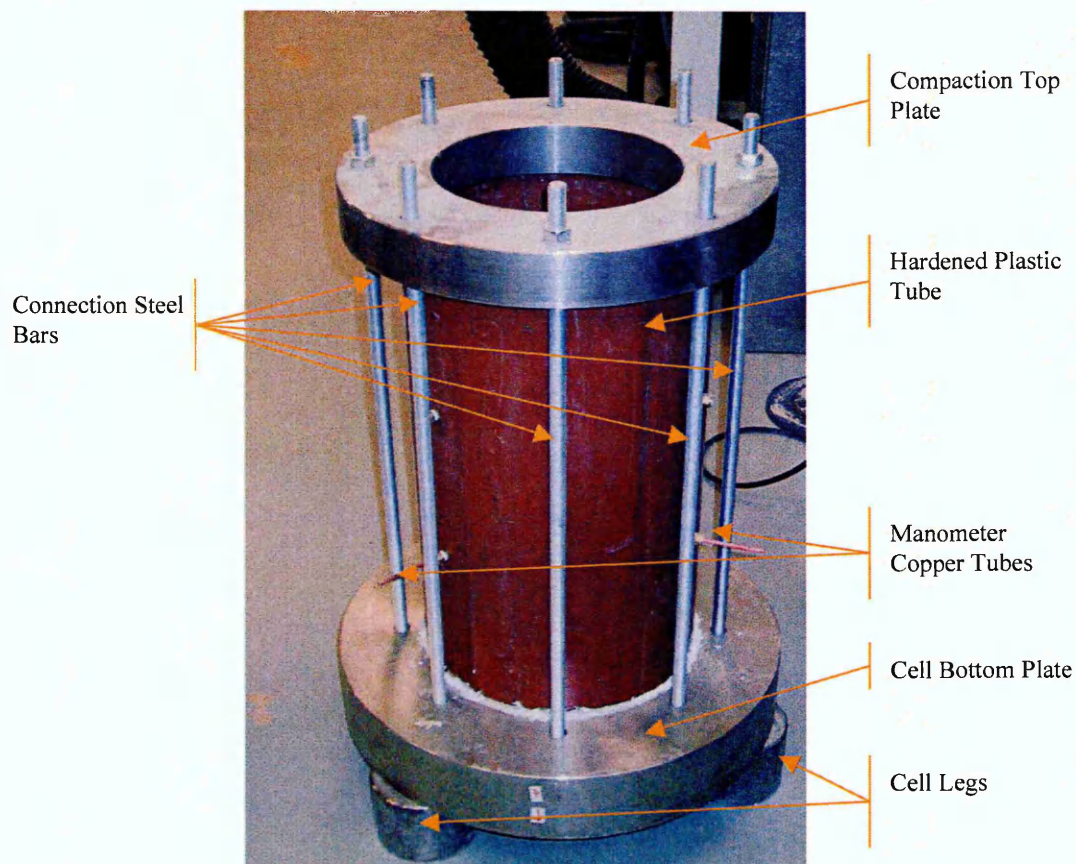


Figure 4.6: Permeability Cell

The key features of the equipment, as shown in the schematic of Figures 4.4 and 4.5 (View A-A) and photo of Figure 4.6, are as follows:

- Stainless steel base plate of 600 mm diameter and 200 mm thickness
- Two top plates: one with a 275 mm hole to allow for compaction and one for performing the actual permeability test.
- Top and bottom plates have a groove of 4 mm width in which a seal is placed
- Both plates also have two valves, as water inlets/outlets
- The bottom and top plates were connected with 8 steel bars
- Copper tubes and cell connections were sealed with modified sealing glands

The large size of the bottom plate was designed to withstand the dynamic compaction force. The base plate was placed on three steel legs to allow space for two bottom valves.

The load applied by the pipe's weight and the force of fixing the connection steel bars restrains the elastic seals and helps to form an airtight seal between the plastic pipe and the end plates. This was checked by filling the empty cell with water and observing that there were no leaks and verified during the testing where no leaks were observed too.

The constant head tank was placed at a height of 2 meters above the cell's point of water insertion. The manometer tubes were connected with copper tubes, which were restricted at the ends by compressing the ends and leaving only a small gap that allowed the flow of water but retained fine particles, in order to minimise migration of fines through them and their effect on the accurate representation of the head. Six tubes were used, at each of two levels, 200 mm apart, three tubes were inserted through the outer wall. The connections of the tubes with the plastic wall were sealed by the use of modified compression glands.

Appendix B presents more details of the equipment used for the large scale permeability tests.

Due to the lack of previous usage of these equipment parts for this type of testing it was necessary to measure and check their dimensions and usage regularly. The checks showed that they did not exhibit any signs of deformation (plastic pipe, sealing grooves and bottom and top plates) or blockage (inlets, outlets, copper and plastic tubes and pump used). The equipment parts therefore did not have to be replaced during the four

tests performed, with the exception of the replacement of the permeable mats and the copper tubes that were damaged by the removal of the materials at the end of each test.

4.5 Shear Box

The shear box equipment used in the test programme is shown in Figure 4.7. The apparatus is free-standing, and consists of a rigid base frame supporting a central horizontal loading jack. The thrust from the jack is applied to the lower half of the ball track mounted 316 ± 2 mm square by 160 ± 3 mm high shear box. The upper half of the shear box is attached to a yoke, which is connected in turn to a 50 kN capacity load cell. The horizontal loading jack is driven via a multi-speed gear box mounted within the base of the machine. Vertical load is applied to each specimen through a rigid loading plate and a vertical loading frame. The lower crosshead of the loading frame passes beneath a horizontal loading beam, which transfers dead load from the end of the beam at a ratio of 20:1. The rate was calibrated by applying dead load (10, 20, 30, 40 and 50 kg) to the loading plate and measuring the force at the other end with the use of the calibrated 50 kN load cell. It was found to be 20.3 (± 0.1):1.

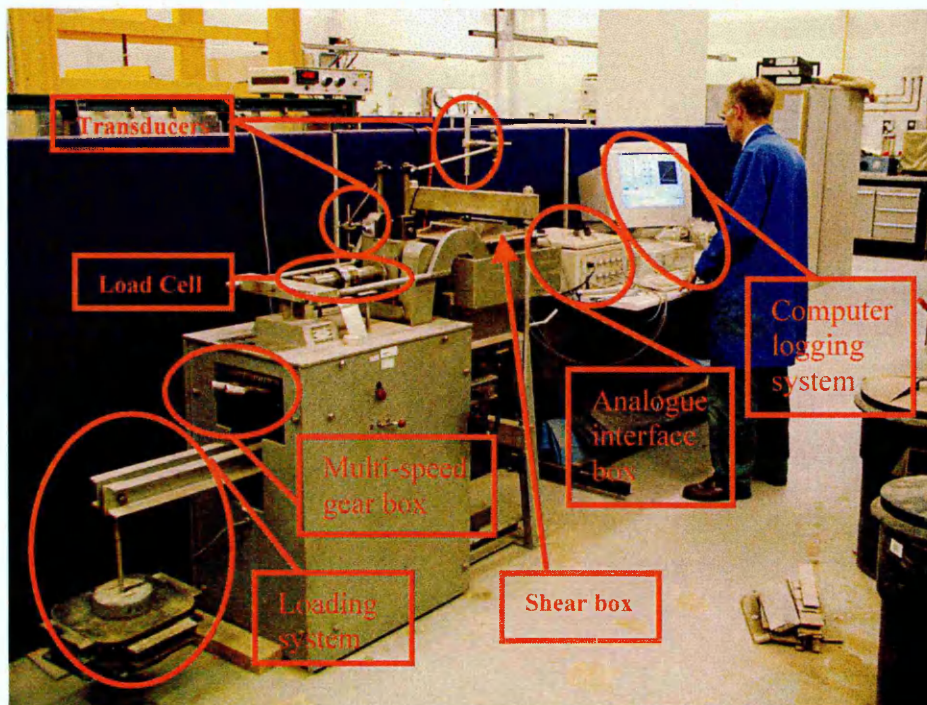


Figure 4.7: The shear box, displacement transducers and computer logging system.

Measurements of the load applied (measured through the load cell) and the vertical and horizontal displacements (measured through transducers) were logged by the computer every minute (Figure 4.7) with the help of a custom made analogue interface box (supply of 250 V). It provides the power needed for the transducers to operate and provides the software with the readings of the voltage changes that are then converted to engineering units. The vertical and horizontal displacements were logged using calibrated transducers. The detailed logging procedure is presented in Appendix C.

The transducers were manufactured by RDP Electronics (type D2/1000A) with a capacity of measuring ± 25 mm when zeroed at the middle (capability of recording to 0.01 mm) and it was calibrated with the use of a calibration rig that was fitted with a micrometer manufactured by Moore & Wright with a capacity of measurements up to 25 mm (readable to 0.01 ± 0.01 mm).

The load cell was a N.C.B./M.R.E. load cell of a capacity of 50 kN manufactured by W.H. Mayes & Son (Windsor) Ltd. It was calibrated in the structures laboratory of Sheffield Hallam University with the use of the concrete tube crushing machine by Avery-Denison Limited to one hundredth of a kN .

Table 4.1: Calibration factors and 95% confidence limits

Equipment Calibrated	Calibration Factor	95 % Confidence Limits	
		Upper	Lower
Load Cell	0.9799	0.9833	0.9751
Vertical Displacement Transducer	0.9841	0.9897	0.9794
Horizontal Displacement Transducer	0.9896	0.9926	0.9842

The calibration procedures took place at three different points of the test series. Before the shear box tests started, at the mid point, and at the end of the shear testing programme. In each of the calibration procedures there were three runs of displacement and load applied. In the load cell calibration the load applied was up to 50 kN and back to zero again, and for the transducers the run went up to 25 mm and back to zero again. Table 4.1 shows the calibration factors and 95% confidence limits for the two transducers and load cell used in the shear box testing.

CHAPTER 5

TEST PROCEDURES

5.1 Introduction

This chapter presents the procedures followed in the individual tests performed in this investigation. For each test, with the exception of the investigation for particle crushing after the shear box tests, fresh materials were used.

Standard tests were undertaken in accordance with the relevant British Standard as follows:

- Water Absorption and Particle Density (BS 812-2:1995)
- Flakiness and Elongation Index (BS 812-105.1:1989 and 812-105:2 1990 respectively)
- Aggregate Impact and Crushing Value (BS 812-112:1990 and BS 812-110:1990 respectively)

Only non-standard, research specific large scale tests are concisely described in this chapter. The results of the physical characteristic tests are presented in Chapter 6 and the results for the main series testing in Chapter 7.

5.2 Physical Properties Testing Series

5.2.1 Material Grading

In each of the grading tests a mass of not less of 500 kg was sieved by the use of a mechanical shaker. To establish the exact sieving procedure, it was necessary to perform some initial trials to check the time required for the materials to pass the apertures and to be retained by the right sieve. Different sieving duration sessions were performed with test times varying from 2.5 minutes to 17.5 minutes in increments of 2.5 minutes. From this, it was determined that a 15 minute duration was satisfactory. Sieving for 17.5 minutes showed that the results were the same as with 15 minutes sieving.

The procedure was further verified by sieving the individual fractions (from the mechanical sieving and for a single test from all three materials) by hand and establishing that no more particles passed through the apertures. Dry sieving was used

to sieve the large quantities of the materials and determine their grading. Smaller quantities of the materials (50 kg) were wet sieved to verify the accuracy of the dry sieving results, as discussed in Chapter 3 above.

5.2.2 Particle Shape

The materials were sieved with the use of a mechanical shaker, following the same process established for the grading tests, and the individual size portions were stored in plastic bags. The Flakiness Index (F_I) and Elongation Index (E_I) were determined according to BS 812-105.1 (BSI, 1989) and BS 812-105:2 (BSI, 1990) respectively. A vernier caliper was used for measuring the dimensions of the particles for the determination of their elongation (q) and flatness (p) ratios. Angularity measurements were undertaken using the chart after Lees, 1964, (Figure 2.4).

Table 5.1: Mass and particle numbers tested for each of the size fractions for Material A, B and C

Sieve Size, mm	Material A		Material B		Material C	
	% Retained	Mass Tested(kg) and No of Particles Measured	% Retained	Mass Tested(kg) and No of Particles Measured	% Retained	Mass Tested(kg) and No of Particles Measured
37.5	7.3	21	14.4	42	14.4	43
28	8.5	25	17	50	16.9	50
20	10.2	30	15.1	44	15.1	45
14	12.4	36	11.2	33	11.2	33
10	11	32	9	27	8.9	26
6.3	17.1	50	12	35	12	36

Due to the difficulty of measuring the dimensions of small particles (with the use of the vernier caliper), the fractions were tested down to materials retained on the 6.3 mm sieve. It was decided to produce the specimens for each size fraction to be tested according to their percentage of mass of the original sample. This way the particle shape of the materials as a whole will be more representative of the type and percentage of the particles existing in each size fraction of the materials. The size fraction with the largest mass percentage retained in the grading tests had a mass of 50 kg tested for the F_I and E_I values, and 50 particles for the measurement of their dimensions for the determination of the three dimensional shape. The mass and number of particles was then reduced depending on the percentage of materials retained on the other size fractions. For

example for Material A, 50 kg and 50 particles were tested for the size fraction of 6.3 mm. For the size fraction of 10 mm, the mass and number of particles was calculated as $(11\% / 17.1\%) \times 50$. Table 5.1 summarises the mass and particle number tested for each of the size fractions. Both of the Indices were determined by testing the same mass of materials, so that the results of both tests will relate to the same particles.

For the visual determination of the degree of angularity, for all size fractions, 10 particles were placed on a clear surface in an arrangement similar to the ones shown in Figure 2.1 were tested. All the particles selected for testing were washed to remove any fines and left to dry naturally in trays in the laboratory for a period of one week, and then stored in clearly labelled plastic bags until testing. The average moisture content of the materials (established immediately after the actual testing) was found to be 2.1 % (standard deviation of 0.2). Each group of 10 particles were placed on a white clear surface, arranged according to Figure 2.1, and photographed from 2 different angles for better accuracy.

The F_1 and E_1 were investigated three times for each of the materials during the duration of this project, at the beginning, after half the shear box tests have been completed and at the end of the investigation, in order to minimise any possible negative effects of the sampling process on the accuracy of the results.

In summary, the procedures established and followed in this project tried to minimise any influence different properties may have on the particle shape results. By using a large number of particles, and utilising the same particles for the F_1 and E_1 tests, the influence of sampling and material variability was minimised. Repeating the tests three times at different points of this research also minimized any possible errors due to sampling procedures and the results show that a great degree of consistency has been achieved (see Chapter 6).

5.2.3 Compaction

As described in Chapter Four, the compaction cell had dimensions of 300 mm diameter and 400 mm depth. This was to accommodate the materials with maximum particle size of 50 mm, for the reasons explained in Section 3.3.1.

For the compaction tests the specimen was formed in the cell in two layers each about 200 mm thick. The second layer was compacted after the maximum (possible) dry

density was achieved for the first layer. Then both layers were compacted until the total mass of the two layers reached the maximum possible dry density. Water was measured and added to dry fresh material to achieve the required moisture contents (eight different moisture contents varying from 0 to 11%). After both layers had been compacted, the specimen occupied about three-quarters of the cell depth of about 300 mm. Every single specimen was sampled after compaction and tested for its moisture content.

The vibrating hammer was equipped with a tamper of a diameter of 290 ± 2 mm and the force applied to each layer during compaction was 350 ± 10 N. Each layer was compacted for a number of periods of 30 (± 1) seconds. Between each time period of compaction the depth of the sample from the top of the compaction cell was measured at five different points (centre and four points on the sample's edges, forming a cross) so that its volume and therefore its dry density could be determined. The compaction testing procedure was designed in this way that there would be an opportunity to determine:

- The effect of moisture content on compaction behaviour.
- The dry density behaviour of the materials against time of compacting effort.
- Any possible differences between the two layers of compaction.

Figure 5.1 shows a typical result. The dry density against time graph for all material types and moisture content are similar with the dry density increasing steadily with time for about the first three minutes of the procedure (Figure 5.1). Thereafter any additional compactive effort had little or no effect on the dry density achieved. The values used in the moisture content against dry density graphs (Section 6.6, Chapter 6) are those achieved for the individual moisture contents after compacting the specimens for 8 periods of 30 seconds each, since compacting the materials for more than a total time of 4 minutes did not increase their dry density to a higher value than the one achieved for compaction time of 4 minutes.

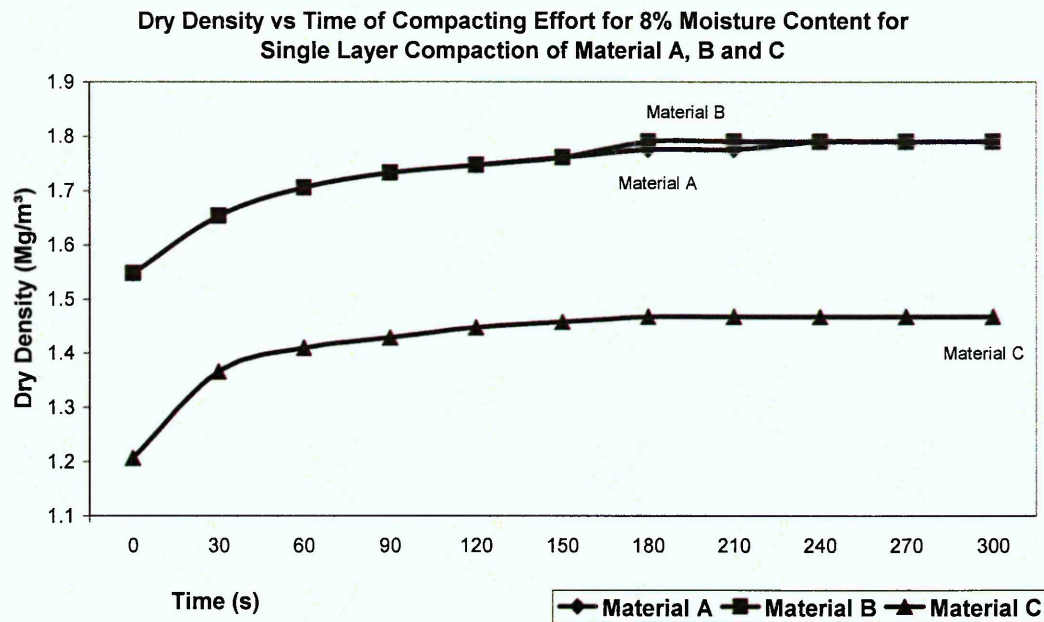


Figure 5.1: Behaviour of Materials A, B and C when compacted with 8 % moisture content

5.2.4 Resistance to Freezing and Thawing

Particles passing the 50 mm sieve and retained on the 10 mm sieve were used for the test, which was undertaken in accordance with EN 1367-1, 2000. After ten cycles of the freezing - thawing process the materials were passed through the 5 mm sieve. The resistance of materials to freezing and thawing is calculated as a percentage of materials passing a sieve size half the size of the minimum particle size tested. In this project the resistance of the three materials to freezing and thawing was established as a percentage of materials passing the 5 mm sieve.

Following the freezing process in the climatic chamber the containers with the frozen materials (Figure 5.2) were transferred to a tank containing water at a temperature of 20 °C. The containers were placed at distances of at least 50 mm from each other and the walls of the tank and the water temperature was tested every 15 minutes at six points in the tank. Water temperature was adjusted to maintain the precise levels (20 °C) throughout the specified thawing time.

The AIV and ACV of the materials after freezing and thawing were also determined by testing them after they have undergone the freezing and thawing process. After the

materials went through the freezing-thawing process, they were dried and the AIV and ACV were performed.



Figure 5.2: The containers (with material A) in the thawing tank after the freezing cycle

5.3 Main Series testing

5.3.1 Permeability

This section summarises the permeability test procedure. A detailed description of the equipment was presented in Chapter 4. The detailed testing procedure accompanied by photos and schematics is presented in Appendix B.

The permeability of the test materials, as discussed in the literature review, depends on their compaction level. The compaction level of all the three types of materials used for the purposes of this specific test was the same as that used in the majority of the other tests of the research programme (1.8 Mg/m^3). The materials were compacted to the required density dynamically in the cell with the use of the vibrating hammer. For the compaction purposes the cell was fitted with the compaction top plate (Figure 5.3). This way access to the Kango Hammer for sample compaction purposes was allowed

Before compaction began, a high flow permeable mat (>10 l/hr) was placed on the bottom of the cell to restrict the migration of fines and was protected by the use of a 3 mm thick steel mesh. Both the permeable mat and steel mesh had a diameter of 300 mm.

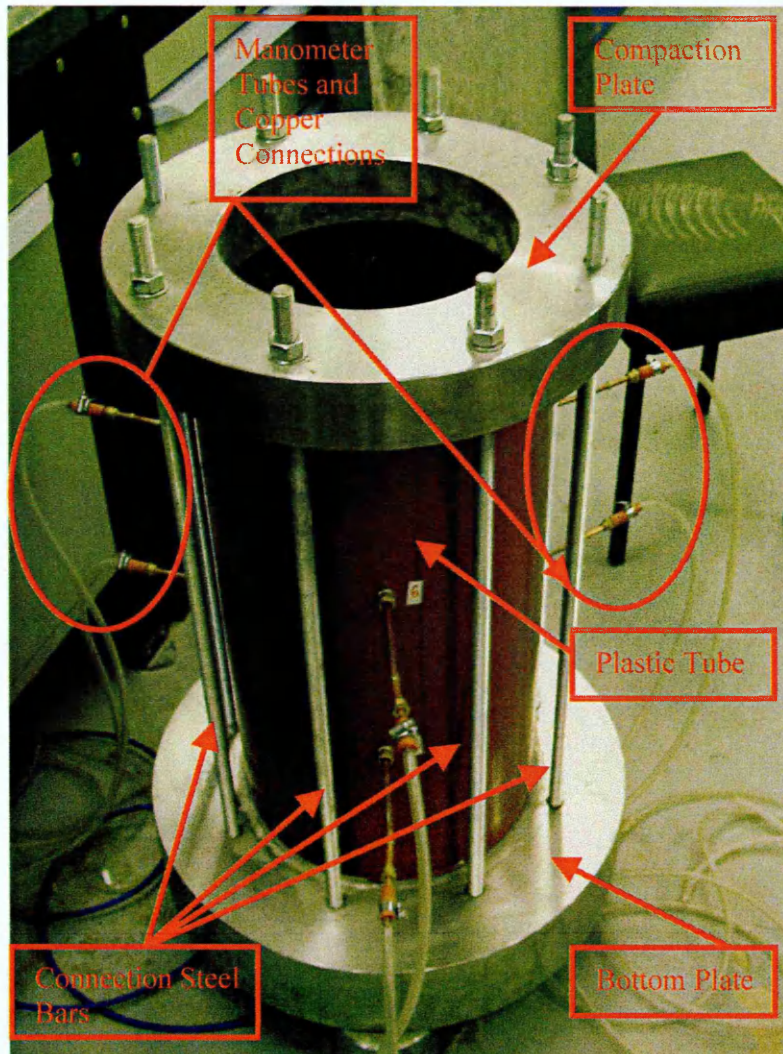


Figure 5.3: The permeability cell with the compaction plate

The materials were compacted in 6 layers, each up to a specific depth to achieve a uniform density of 1.8 Mg/m^3 throughout the specimen. The copper tubes were inserted into the cell when the materials reached the tube placement level on the cell, in order to avoid any possible damage to them, and the compaction continued to the next layer. At the end of the compaction process the compaction plate was removed carefully in order to avoid any disturbance to the sample and replaced by the top plate. A permeable mat and a steel mesh, both of the same specification as the ones used at the bottom, were

also used between the materials and the top plate. The copper tubes were then connected with the manometer pipes that lead to a bank of manometers, which had been numbered according to their position in the cell. The permeability testing arrangement also included a constant head and a supply tank.

The saturation process of the materials was undertaken using clean tap-water in accordance with BS 1377-5:1990, paragraph 5.2.4. Water was inserted to the cell from the bottom valve and once water started coming out from the top valve suction with the use of a suction pump was applied to the sample to speed up the process. The saturation procedure lasted for four weeks for all three material types tested, after which period there were no signs of air trapped in the sample. This was verified by the fact that during the last week of saturation the application of continuous suction did not yield any trapped air from the outlet pipes.

After the flow and the manometer readings were stable for a period of one week 10 measurements were obtained for all the materials. Five were taken by measuring the volume of water passing through in a period of ten minutes and five by measuring the time it takes to obtain 500 (± 5) ml of water.

The coefficient of permeability (k) is calculated by equation 5.1 (after BS 1377-5:1990, Section 5.6.2)

$$k = \left(\frac{q}{i} \right) \left(\frac{R_t}{A} \right) \quad \text{eq 5.1}$$

where

k is the coefficient of permeability in m/s

q is the flow of water through the specimen in l/s

i is the hydraulic gradient

R_t is the temperature correction factor for the viscosity of water and can be derived from BS 1377-5: 1990, Figure 4.

A is the cross sectional area of the specimen in m^2

The hydraulic gradient is calculated from equation 5.2

$$i = \frac{h}{y}$$

eq 5.2

where

h is the difference between the two manometer levels in m

y is the difference between the height of the corresponding monitoring points in m

5.3.2 Particle Crushing

The procedure followed for the determination of the crushability of the materials was essentially the same as the one followed during the grading tests. After each shear box test, the materials were removed from the box and placed in labelled plastic bags. After the individual shear box series (SBT1, SBT2 and SBT3) was completed for each of the materials, they were sieved following the process established for the grading tests. The individual sieve fractions were then weighed and the after-shear grading curves were established.

5.3.3 Shear Box Testing

A detailed description of the shear box equipment (Figure 5.4) is presented in Chapter 4, and the exact testing procedure accompanied by photos and schematics in Appendix C. This section presents a summary of the shear box testing undertaken in this project in order to provide an initial picture to the reader of the processes followed.

The complete testing programme required a very large quantity (about 2500 kg) of each material to be prepared, but due to storage limitations it was not feasible to obtain sufficient amount of the material from the suppliers to allow quartering of the samples strictly in accordance with British Standards requirements. Rather, the entire mass of each material required for the shear box tests was placed on a clean concrete floor. The materials were passed through a 37.5 mm sieve and the fraction coarser than 37.5mm was then removed to reduce the ratio between the minimum dimension of the test specimen and the maximum particle size to within acceptable limits. The remainder was then mixed thoroughly on a clean concrete floor. The mixed material was sub-divided to prepare each sub-sample in turn via a process of quartering, with the remaining sample being retained each time for further re-mixing and quartering for the preparation of the next samples. The same process was followed for all the different types of shear box

tests, with materials larger than 28 mm removed for the investigation of the effect of maximum particle size on shear strength (SBT3).

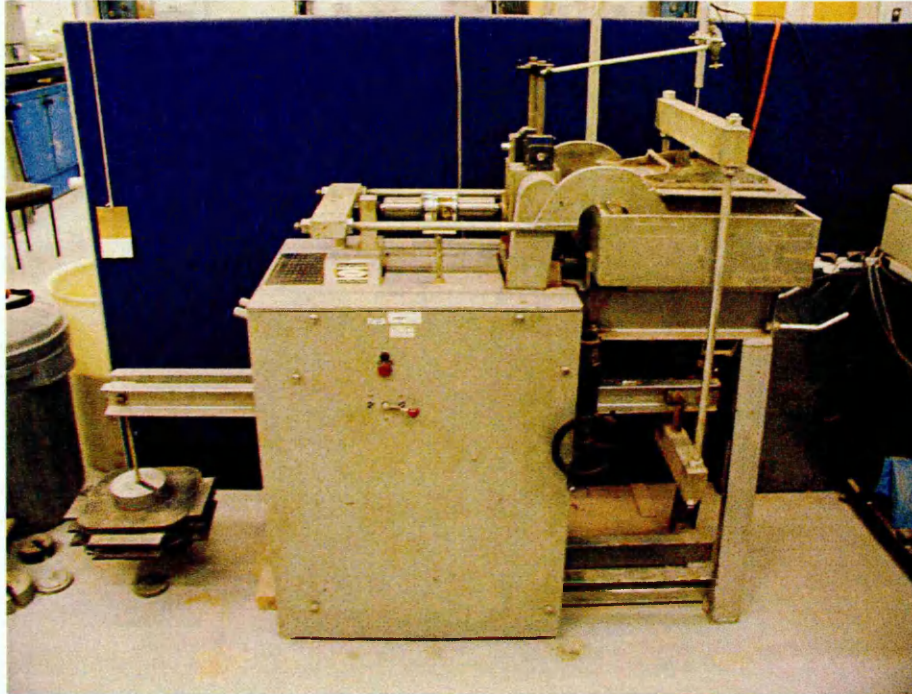


Figure 5.4: The shear box apparatus

To ease specimen preparation and avoid damage to the shear box frame, compaction of the materials in the shear box was undertaken with the shear box removed from its frame and placed on the concrete floor. Figure 5.5 shows the shear box on the floor after Material C had been compacted to specimen specifications for SBT1.

Both halves of the shear box were secured together with the locating screws, and a vibrating hammer used to compact a mass of 8.6 kg of the material at their natural moisture content into the box for each of the three layers to achieve the target dry density for each test specimen of 1.8 Mg/m^3 . A mass of 7.6 kg was used for each layer to achieve the target dry density of 1.6 Mg/m^3 . A rubber pad of 5 mm thickness was placed between the compaction plate and the materials to minimise the risk of breakage of the materials' sharp edges. Three layers were adopted to avoid coexistence of the shear plane with layer interfaces, and to promote a uniform density throughout the specimens. After the required density was achieved the top plate was placed in position and the whole box placed within the test frame. The locating screws and four clamps

placed on each size of the shear box ensured that the disturbance of the sample during its placement in the test frame was kept to as minimum levels as possible.

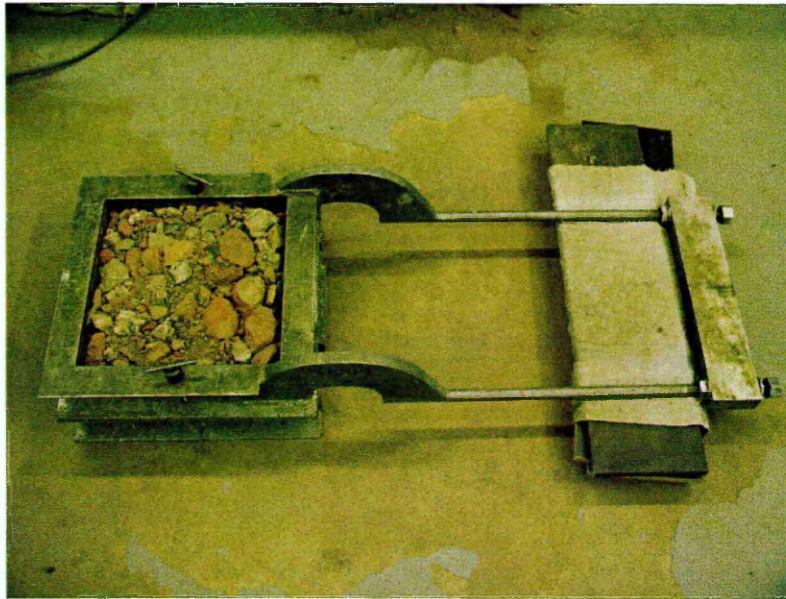


Figure 5.5: The shear box on the floor with Material C compacted in it

The displacement rate used for the shear box tests was determined based on two parameters:

1. Time restrictions
2. The necessity to perform a large number of shear box tests

It was estimated that it would be necessary to perform three tests per day to complete the testing schedule and a rate of displacement of 0.125 mm/minute made this possible. It was important to conform with BS1377-7:1990, and for this reason a total of five trials (two for Material A and C and one for Material B) were performed. It was established that this displacement rate falls within the specifications of the displacement rate according to BS1377-7:1990. The displacement rate specifications were also verified from the displacement rates that were measured during the shear box tests and their results.

The tests were carried out until the real time graph showed that the ratio of shear strength to horizontal displacement was reducing (BS 1377-7: 1990, Paragraph 7.2.4.9).

This did not allow for analytical observations of the post peak behaviour of the materials but did allow for the large number of tests necessary to minimise the effects of the materials' variability.

Chapter 6 Test Materials

CHAPTER 6
TEST MATERIALS

6.1 Introduction

This chapter describes the types of materials tested in this project and their physical characteristics. The three material types (Table 6.1) tested in this investigation were purposefully selected as being representative of commercial operational and crushing processes, in preference to the crushing of the materials in the laboratory using artificial procedures. The first type of crushed concrete (Material A) was removed from a demolition site with no further processing and the second (Material B) was obtained from a crushing site. The brickwork rubble (Material C) has also been processed in the same crushing site as Material B. A description of the materials used and the processes involved in the acquisition of the materials is given in this chapter.

Table 6.1: Initial similarities and relations between the three types of materials

Material	Concrete Based	Brick Based	Furthered Processed
A	✓	X	X
B	✓	X	✓
C	X	✓	✓

6.2 Principles of Acquisition, Transportation, Handling and Storage

The handling of the materials on site made the acquisition of samples according to all the British Standards (BS 812-101:1984, BS 812-102:1984 and BS 5930:1999) controls impracticable. This was due to the constant movement of the materials within the site, and the fact that large quantities of materials were required for testing.

Nevertheless every effort was made to obtain as representative a sample as possible by:

1. Mixing the stockpiled materials on site several times with the use of heavy site plant available at the processing site, before any sampling from stockpiles was undertaken
2. Obtaining approximately equal proportions of each sample from the top, middle and bottom of the mixed stockpiles.

The ideal situation, from a repeatability perspective, may have been to obtain materials that did not contain any other materials rather than the desired crushed concrete and

bricks. However such materials would not be typical of the industrial wastes produced by demolition and crushing of concrete and brick structures. The removal of all the impurities (sizes from 40 mm to fine particles) would be a lengthy and costly procedure for industry. Typically only large particles such as timber and metals are removed in practice, the latter via the use of magnets. It was therefore decided to similarly test the materials without removing any impurities other than metal components and large pieces of timber. The quantity of the impurities after the sieving tests (100 kg of each material were sampled) was found to be less than 1 % (range 0.2 - 0.8 %).

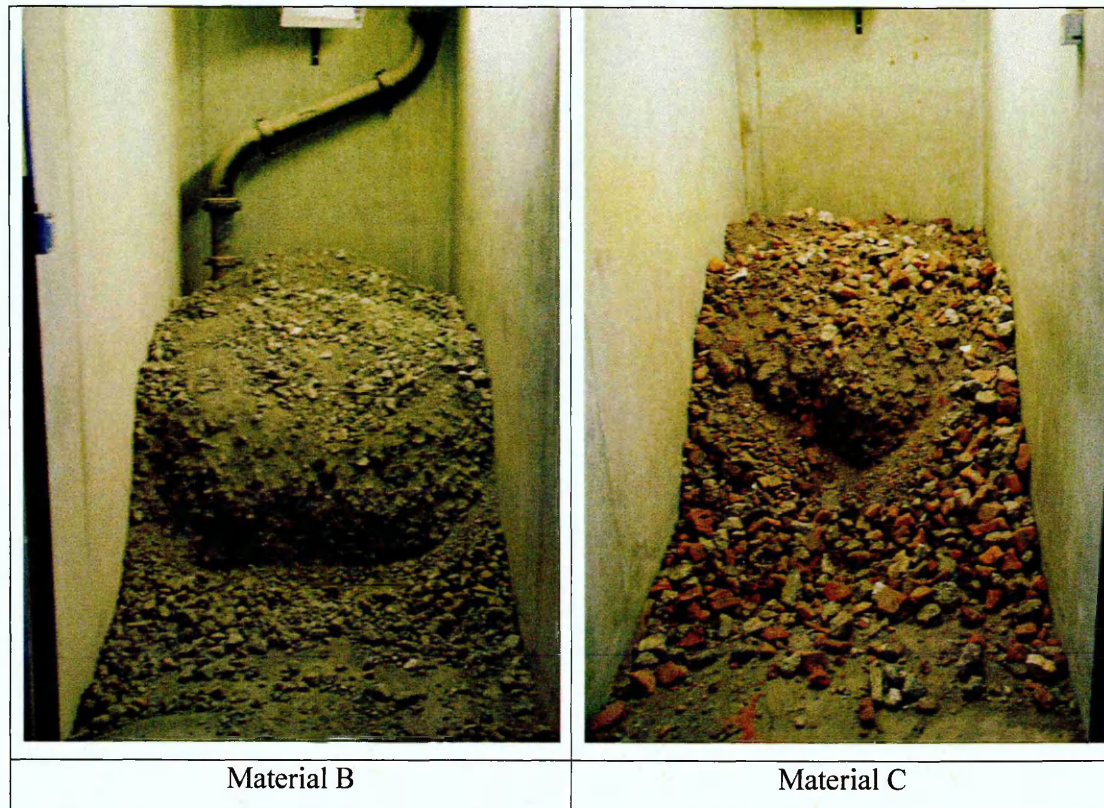


Figure 6.1: Material B and C in the laboratory storage bays

After the materials were transported to the laboratory they were placed in storage bays (indoor storage, Figure 6.1) that kept them protected from adverse weather conditions such as extreme temperatures, rain, snow and wind.

6.3 Source and Description of Materials

The materials produced by the demolition of concrete and brick structures can be used and processed in various ways, on or off site. The industrial processes employed are generally similar to the ones used in quarries for the extraction of primary aggregates. A more detailed description of the procedures commonly used is presented in Section 2.2. Examination of these procedures had led this investigation into choosing the following three types of materials, to represent in part the range of processing methods:

Material A: Produced at a Sheffield city centre location from the demolition of a late 20th century concrete building in 2001. The grading curve (format based on BS EN 933-1:1997 and determined by mechanical sieving) of Material A is presented in Figure 6.2. The demolition waste was crushed on site using heavy demolition plant, and in excess of four tonnes of the material were transported directly to the university laboratories. The material mainly comprised crushed concrete, as the demolition and processing method adopted on site had led to the removal of the vast majority of other structural components. Laboratory inspection procedures revealed that impurities such as steel reinforcement accounted for less than 1% by mass of the sample delivered. All remaining metallic materials, such as electricity cables, were manually removed in the laboratory prior to testing.

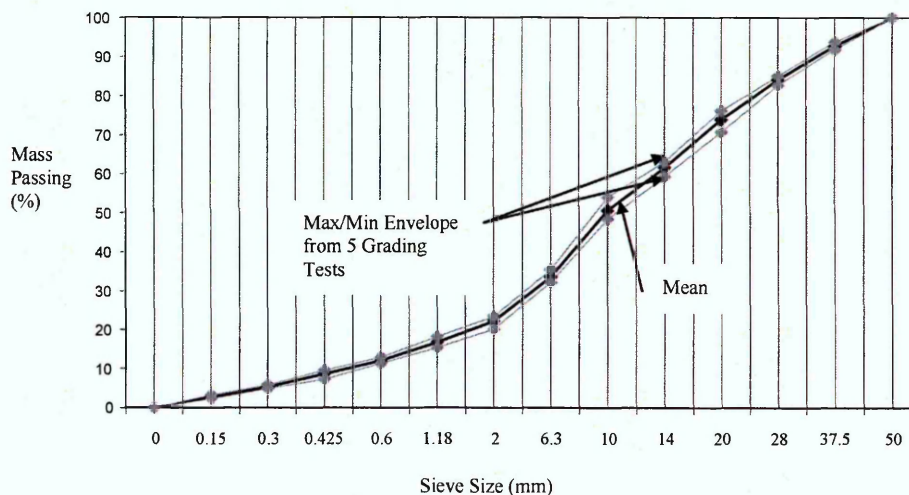


Figure 6.2: Grading curve for Material A

Materials B and C: These materials were of crushed concrete and crushed brick respectively, and were both obtained from a demolition waste processing site in Hull operated by Sam Allon (Contracts) Ltd. Both the concrete and brick had been sourced originally from unknown developments, and subsequently transported to and processed at the crushing site. Their grading curves are presented in Figure 6.3 (format based on BS EN 933-1:199). A range of commercial products are prepared at the site, and the products used in this research project were selected as being compliant with industry standard specifications. Material B was selected as meeting the grading requirements of RCA (Recycled Aggregates) (ii) of Table 1 of Digest 433 B.R.E (Building Research Establishment, 1998), whilst Material C was chosen to meet the grading requirements of RCA (i) of Digest 433 B.R.E. (Building Research Establishment, 1998).

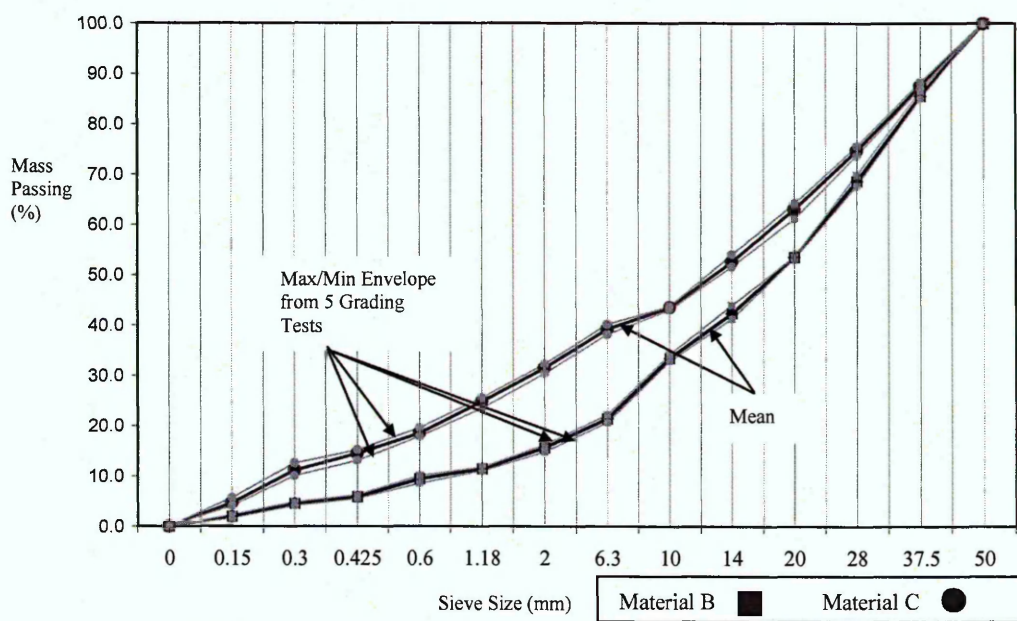


Figure 6.3: Grading curves for Material B and C

The minimum and maximum envelopes of the grading curves, of all the sampled materials, indicate that the materials collected were consistent.

The average grading curves of all the materials are shown in Figure 6.4 and their grain size characteristics are summarised in Table 6.2.

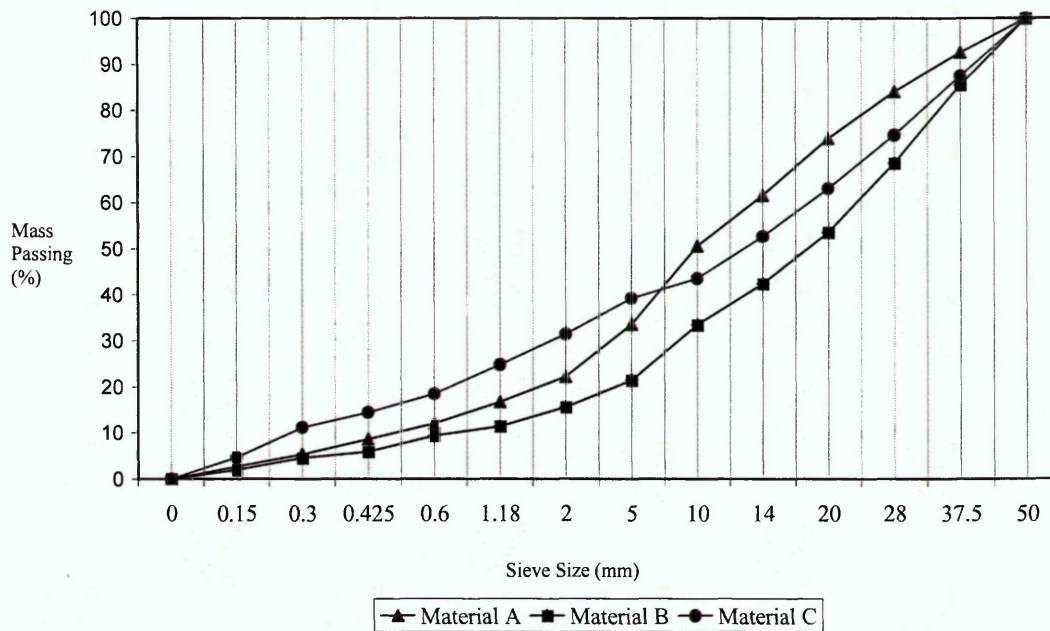


Figure 6.4: Average grading curves for Material A, B and C

Table 6.2: Summary of Grain Size characteristics of test materials.

Characteristics (Mean values)							
Material	d_{\max}	d_{10}	d_{30}	d_{50}	d_{60}	C_u	C_z
A	50 mm	0.47 mm	4.6 mm	10.1 mm	13.5 mm	32.9	0.7
B	50 mm	0.62 mm	8.5 mm	17.9 mm	23.6 mm	33.3	2.1
C	50 mm	0.29 mm	1.8 mm	12.9 mm	18.3 mm	46.6	1.0

The results show that even though there is a difference in the effective sizes of the particles in Materials A and B, their Uniformity Coefficient (C_u) values are almost identical. There is a larger range of particle sizes in Material C, and a larger C_u .

Materials B and C, that had been crushed further to the specifications of Digest 433 B.R.E. (1998), are well graded according to their C_z value. This is also verified by their Coefficient of Curvature (C_z), as they both are within the limits of 1 – 3 for well-graded soils. Material A has a value of C_z of 0.7, and may be described as poorly to well graded. The difference in Materials A and B may be explained by the further crushing Material B would have undergone during processing, or through artificial selection at the site.

As stated in section 5.2.1, it was necessary to perform wet sieving in a smaller quantity of all the materials in order to verify the validity of the dry sieving results. A mass of 100 kg of each of the materials was wet sieved according to BS 1377-2:1990 and the results are presented in Table 6.3. From this data it can be seen that the differences between the percentages passing between the wet and dry sieving tests are small. Therefore the grading curves of Figure 6.4 can be considered accurate representation of the materials' particle distribution.

Table 6.3: Comparison between wet and dry sieving results

Sieve Size (mm)	Percentage of Mass passing for Dry and Wet Sieving Tests					
	Material A		Material B		Material C	
	Dry	Wet	Dry	Wet	Dry	Wet
0	0	0	0.0	0	0.0	0
0.15	2.8	2.2	2.0	2.7	4.7	4.3
0.3	5.4	4.2	4.6	3.7	11.2	11.2
0.425	8.7	6.9	5.9	5.1	14.5	13.6
0.6	12.1	11.5	9.5	8.9	18.5	18.2
1.18	16.8	16.5	11.5	11.4	24.8	24.6
2	22.2	22.7	15.7	15.5	31.5	32.0
5	33.5	33.4	21.5	21.9	39.2	38.9
10	50.6	51.6	33.5	34.1	43.5	43.8
14	61.6	63.2	42.4	43.6	52.7	52.6
20	74.0	75.2	53.6	54.2	63.1	62.7
28	84.2	85.1	68.7	70.1	74.7	73.5
37.5	92.7	93.6	85.6	87.7	87.5	87.3
50	100	100	100	100	100	100

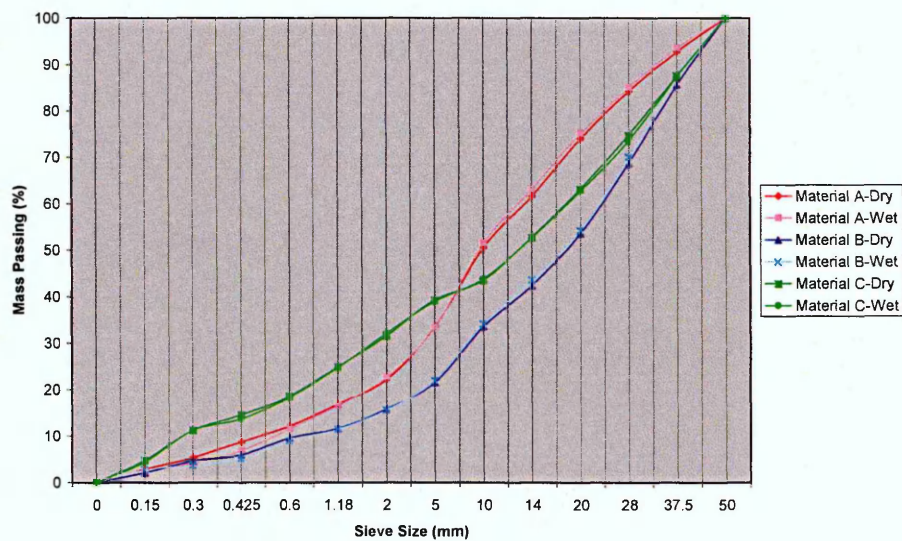


Figure 6.5: Wet and dry grading curves

Table 6.4 shows that there is a degree of variability in the grading curves of the materials, especially for Material A. The variability, as expressed with values of maximum differences (i.e. range of results for each fraction), shows that the Material B and C are more consistent materials, with maximum differences reaching 2.7 %. This is probably a result of them have been processed further and crushed to precise specifications. On the other hand Material A, that was obtained straight from a demolition site, exhibits a greater variability and the maximum differences reach a value of 5.6 % (for sieve size of 10 mm). This is a variation of ± 2.8 %, which as a percentage of the total percentage passing ($2.8 / 50.6$) is 5.5 % variation. This is double the maximum difference presented for Materials B and C.

Table 6.4: Variability of grading results for all materials

Average Percentage (of 5 tests) Passing and Maximum Difference between the Minimum and Maximum Values of all Grading Tests for each Individual Sieve Size						
	Material A		Material B		Material C	
Sieve Size (mm)	Mean (%)	Max Difference	Average (%)	Max Difference	Average (%)	Max Difference
0.15	2.8	0.9	2.0	0.6	4.7	1.6
0.3	5.4	0.9	4.6	0.7	11.2	2.5
0.425	8.7	2.3	5.9	0.7	14.5	2.1
0.6	12.1	1.6	9.5	1.5	18.5	1.7
1.18	16.8	2.9	11.5	0.7	24.8	2.1
2	22.2	3.3	15.7	1.4	31.5	1.8
5	33.5	3.3	21.5	1.5	39.2	2.0
10	50.6	5.6	33.5	1.3	43.5	0.7
14	61.6	3.7	42.4	2.7	52.7	2.4
20	74.0	5.5	53.6	0.3	63.1	3.0
28	84.2	2.3	68.7	2.1	74.7	1.8
37.5	92.7	1.9	85.6	1.5	87.5	1.2
50	100	0.0	100	0.0	100	0.0

Max Difference means the difference between the maximum and minimum value of the materials passing the specific sieve

6.4 Water absorption and particle density

The water absorption and particle density results (established according to BS 812-2:1995) for each material are summarised in Table 6.5. The results for the concrete based materials, A and B, are identical, except for their degree of variation, which is very low and can be considered negligible. The value of water absorption is higher and particle density is lower for the brick based material (Material C). The differences in consistency may be attributed to the nature of the materials since the procedures established in this project should minimise the effects of differences in sample preparation and variability.

Table 6.5: Particle density and water absorption values

Material	Water Absorption (%)		Particle Density (Mg/m ³)	
	Value	SD	Value	SD
A	5.5	0.068	2.2	0.04
B	5.5	0.091	2.2	0.03
C	13.2	0.212	1.9	0.06

Note: SD means Standard Deviation

6.5 Particle Shape

6.5.1 Flatness and Elongation Ratios

The results from the calculations of the particles' flatness and elongation ratios are presented in graphical form in Figures 6.6, 6.7 and 6.8 for Material A, B and C respectively (graphs with their averages are presented in Appendix D). The elongation q and flatness p ratios are given by:

$$q = b/a$$

$$p = c/b$$

where a , b and c are the longest, intermediate and shortest lengths of a particle, respectively.

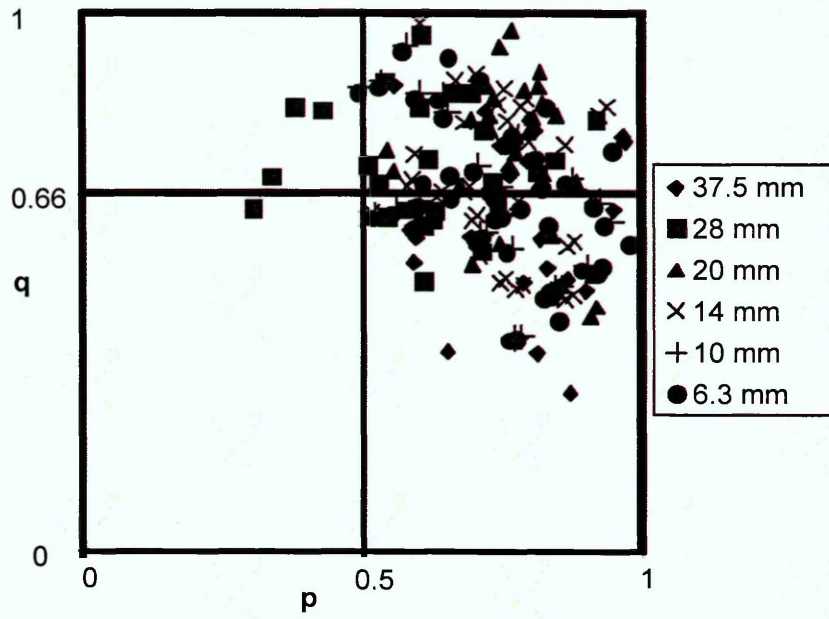


Figure 6.6: Shape categories for all the size fractions for Materials A(after Rösslein, 1941)

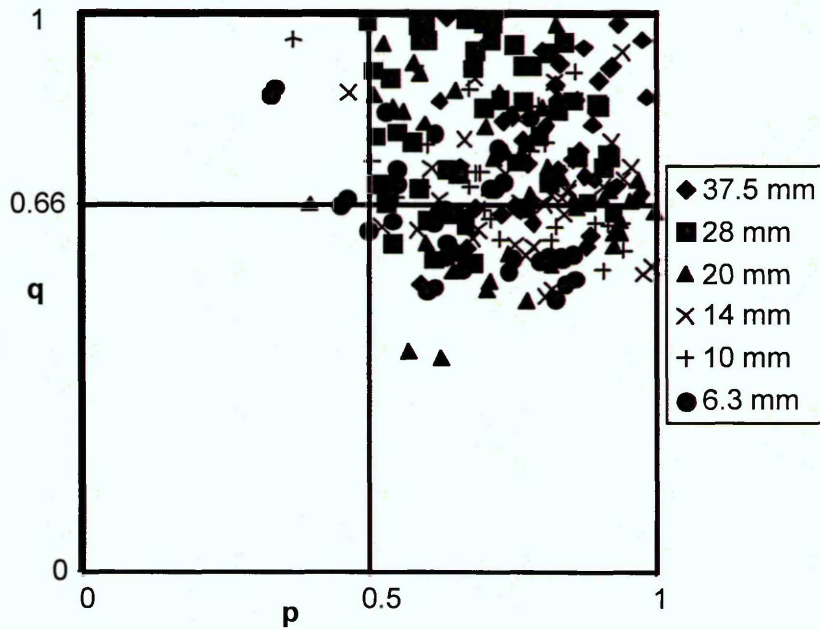


Figure 6.7: Shape categories for all the size fractions for Materials B(after Rösslein, 1941)

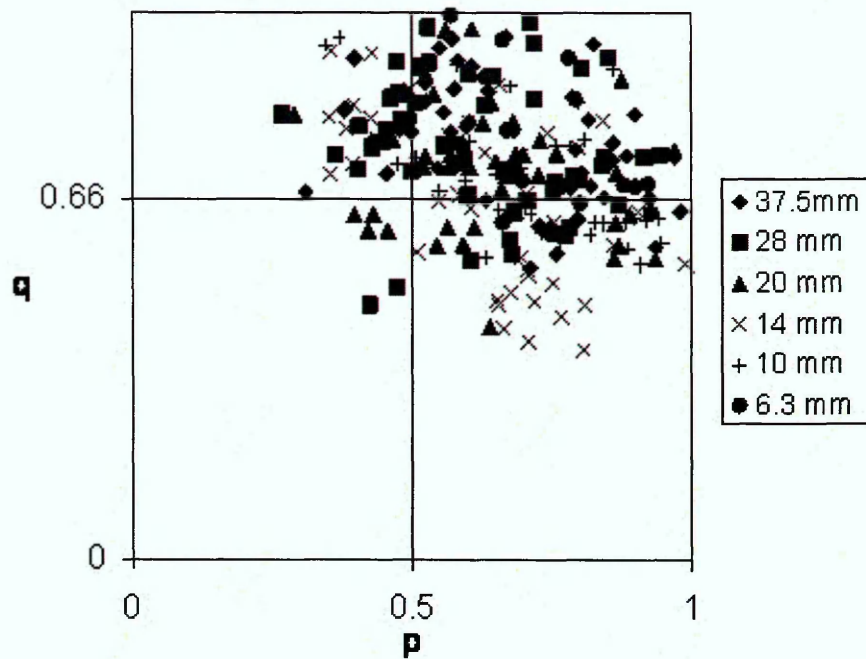


Figure 6.8: Shape categories for all the size fractions for Materials C (after Rösslein, 1941)

6.5.2 Flakiness and Elongation Index

Table 6.6 presents the values of all the types of F_I and E_I for materials A, B and C. The number of particles measured for each of the individual sieve size fractions were given in table 5.1.

Table 6.6: Values of all the Flakiness and Elongation Indices for all the Materials

Sieve Size, mm	Material A		Material B		Material C	
	$F_{I,1}$	$E_{I,1}$	$F_{I,1}$	$E_{I,1}$	$F_{I,1}$	$E_{I,1}$
37.5	20.2	20.9	11.1	6.3	17.2	15.5
28	11.3	26.9	6.3 (50)	16.4	11.1	28.3
20	8.9	23.4	5.1 (44)	16.2	13.5	27
14	12.6	24.2	7.7 (33)	13.7	10.3	27
10	13.1	24.2	8.6 (27)	16.3	7.3	17.5
6.3	11.6	23.4	4.9 (35)	9.9	6.2	9.7
Total	$F_I=12.9$	$E_I=23.9$	$F_I=7.3$	$E_I=13.1$	$F_I=10.9$	$E_I=20.8$

To allow for different intended uses of the data, the results are presented in two ways:

- The total Elongation (E_D) and Flakiness (F_D) index of the materials, and
- The values of each individual size fraction ($F_{L, 1}$ and $E_{L, 1}$).

Table 6.7 presents the average values and the difference between the maximum and minimum values of the F_I and E_I for all the materials.

Table 6.7: Summary of F_I and E_I values for all the materials

Material	Flakiness Index (F_I)		Elongation Index (E_I)	
	Mean	Range	Mean	Range
A	12.9	1.7	23.9	0.8
B	7.3	1.8	13.1	2.6
C	10.9	2.5	20.8	1.3

6.5.3 Angularity Values

Table 6.8 summarises the angularity values for Material A, B and C for all the sieve fractions that were investigated.

Table 6.8: Angularity values for all materials (after Lees, 1964)

Angularity Values, after Lees (1964)			
Sieve Size, mm	Material A	Material B	Material C
37.5	500-599	600-699	600-699
28	600-699	500-599	700-799
20	600-699	500-599	700-799
14	600-699	500-599	700-799
10	600-699	400-499	600-699
6.3	500-599	400-499	500-599
Average	600-699	500-599	700-799

6.5.4 Complete Shape Description

Taking all the information and results of the particle shape tests under consideration, the complete descriptions of the particle shape for Materials A, B and C are:

1. Materials A: Equi-dimensional with low angularity (600-699) according to Rösslein (1941), and equi-dimensional to discs with low angularity (600-699) according to Zingg (1935), with F_I 12.9 and E_I 23.9.
2. Materials B: Equi-dimensional with low angularity (500-599) according to Rösslein (1941) and Zingg (1935), with F_I 7.3 and E_I 13.1.
3. Materials C: Equi-dimensional with low angularity (700-799) according to Rösslein (1941), and discs to equi-dimensional with low angularity (700-799) according to Zingg (1935), with F_I 10.9 and E_I 20.8.

In some of the particle shape descriptions two categories are named. That means that the largest percentage of particles fall within the first-mentioned category but it is not the overall majority (> 50 %). In this case the second most populated category is included in the description (e.g. for Material C, description according to Zingg, 1935, discs account for 43 % of the particles and equi-dimensional particles for 39 %).

6.6 Compaction

For the test methods described in Section 5.2.3 the measured values of the maximum dry density (average of five tests) and the moisture content are summarised in Table 6.9. Material A was also tested in a California Bearing Ratio mould, which complies with the specifications of Figures 12 and 13 of BS 1377-4:1990. All three tests, using a 2.5, 4.5 kg and a vibrating hammer, were performed in order to allow for comparison with the results from the large scale mould testing and establish any differences in the materials' behaviour. Five of each of the BS tests were performed in order to obtain more representative results.

Table 6.9: Maximum dry density and corresponding moisture content values

Type of Test	Material Type					
	A		B		C	
	m/c	ρ_d	m/c	ρ_d	m/c	ρ_d
Mould Compaction	5	1.84	5	1.84	7.5	1.79
2.5 kg Hammer	6	1.77	N/A	N/A	N/A	N/A
4.5 Kg Hammer	6	1.80	N/A	N/A	N/A	N/A
Vibration Compaction	6	1.83	N/A	N/A	N/A	N/A

Dry Density Values (ρ_d) in (Mg/m^3), and Moisture Content (m/c) in %

The dry density (ρ_d) values of the different air and moisture contents are calculated by:

$$\rho_d = \frac{G_s \times (1-A) \times \rho_w}{(1+w \times G_s)} \quad \text{eq. 6.1}$$

where:

G_s is the Specific Gravity of the soil particles

A is the air content (%)

ρ_w is the density of water (Mg/m^3)

w is the water content (%)

The Specific Gravity (G_s) is given by:

$$G_s = \rho_s / \rho_w \quad \text{eq. 6.2}$$

Where ρ_s is the particle density (Mg/m^3)

For the particle densities the calculated values of Section 6.4 were used.

The results are presented graphically in Figure 6.9.

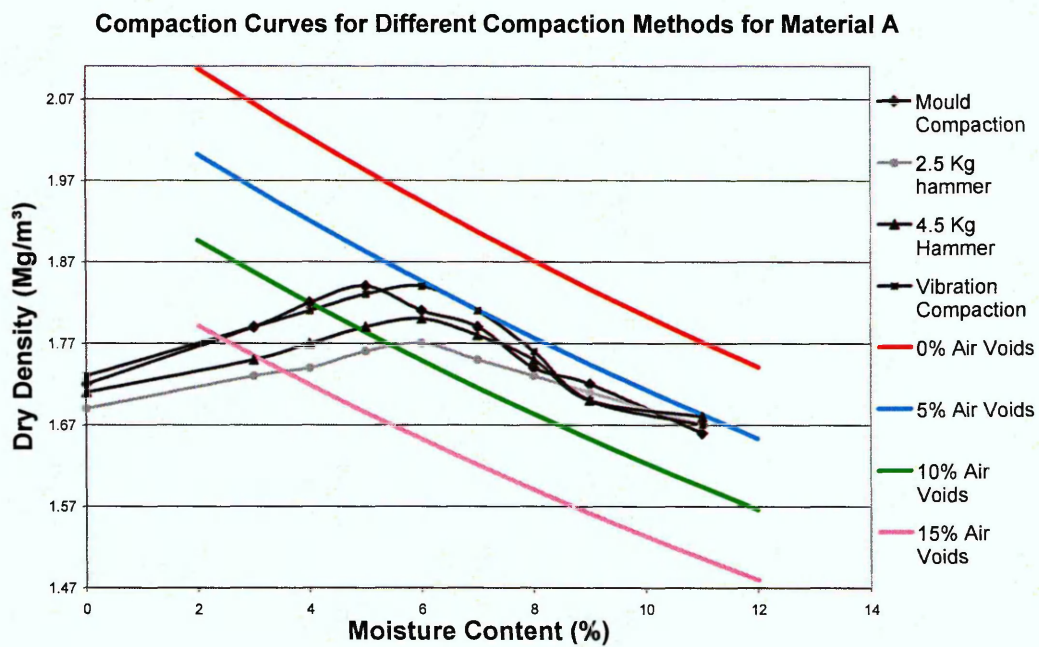


Figure 6.9: Compaction Curves for all the types of compaction for Material A

Figure 6.10 presents the range of results for each of the moisture content for all points for all the tests. The variation of any of the values was not larger than 0.11 Mg/m^3 indicating good consistency.

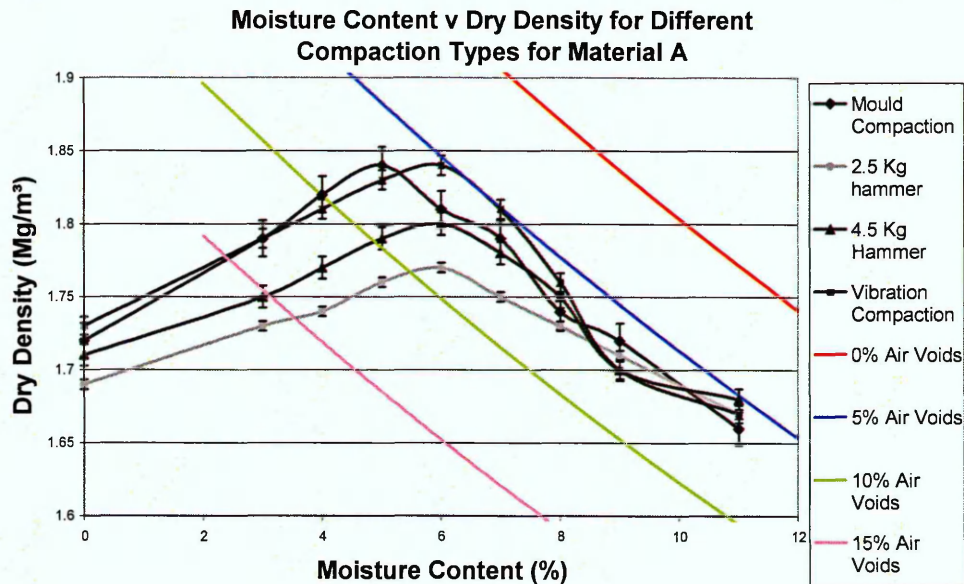


Figure 6.10: Variability of compaction results for Material A

The results of the BS compaction tests performed for Material A show reasonable consistency (Figure 6.10), with the mould compaction tests of Material A indicating a larger variability from the BS compaction tests, with the larger variation reaching 0.11 Mg/m^3 for 4 % moisture content, which is a very low value (of about 6 %) variation that can be considered negligible.

Figures 6.11 and 6.12 show the compaction results for Material A for one and two layer compaction respectively. As explained before the compacting took place in two stages. One layer of the material was compacted to the maximum possible density and then a second identical layer was used, on top of the first one and also compacted to the maximum possible density. this was done in order to check if the compaction of the second layer on top of the first layer affected the total dry density achieved. The corresponding results for Material B are given in Figures 6.13 and 6.14.

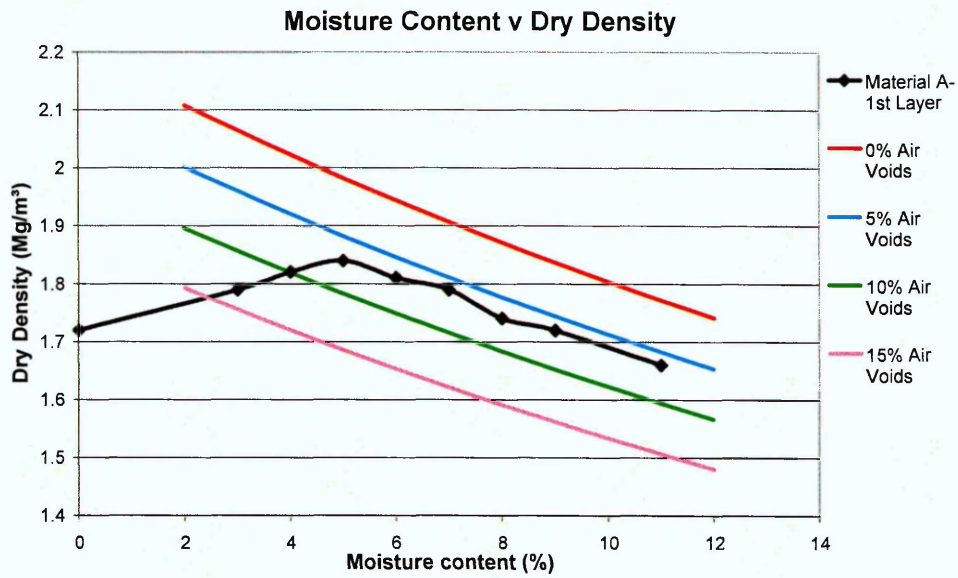


Figure 6.11: Large scale compaction curves for Material A (1st layer)

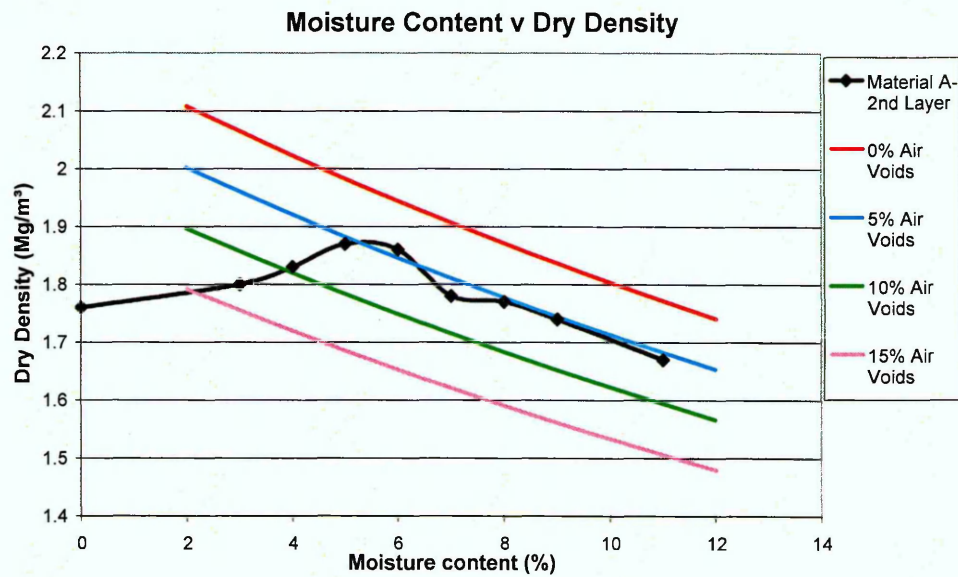


Figure 6.12: Large scale compaction curves for Material A (2nd layer)

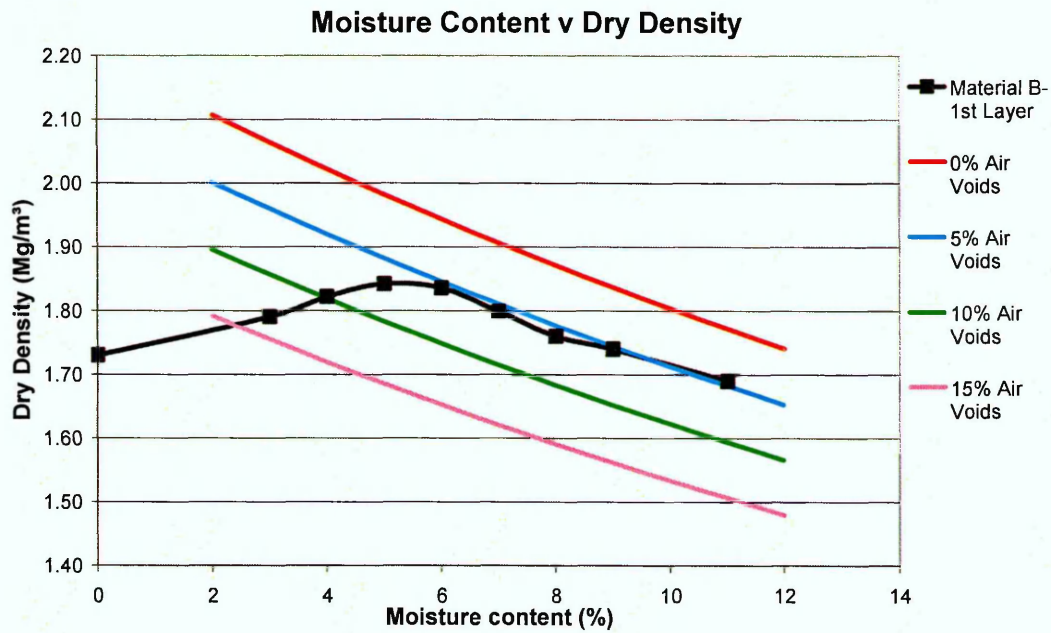


Figure 6.13: Large scale compaction curves for Material B (1st layer)

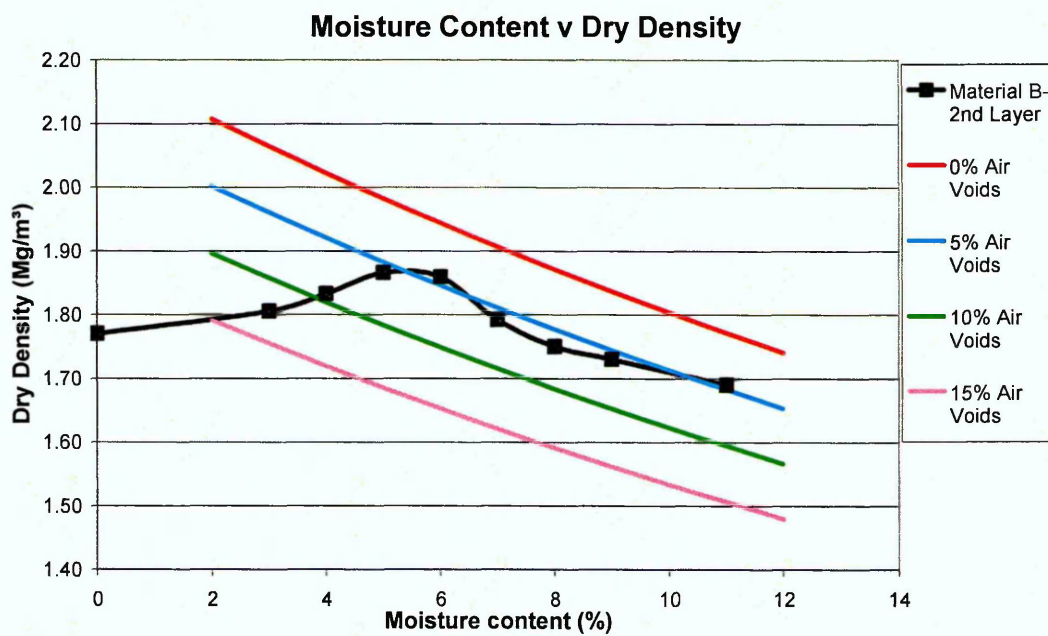


Figure 6.14: Large scale compaction curves for Material B (2nd layer)

The compaction graphs show that the behaviour of Material A and B appear to be similar, and that the brick based materials achieve a lower maximum dry density.

Figure 6.15 shows the compaction curves for Material C for both layers of compaction.

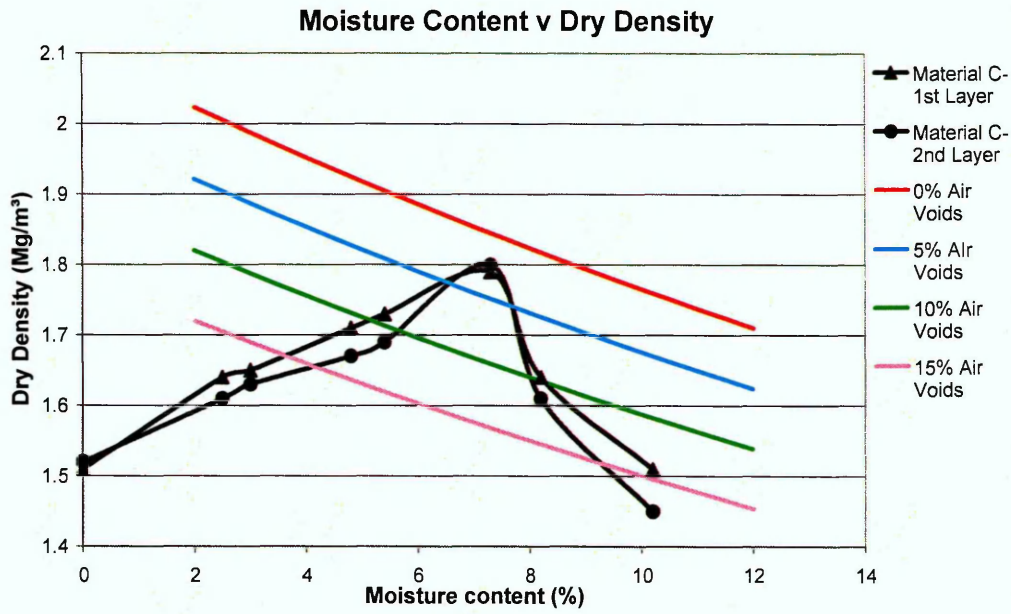


Figure 6.15: Large scale compaction curves for Material C

Figures 6.16 and 6.17 show the average compaction curves for all the materials for one layer and two layer compaction respectively.

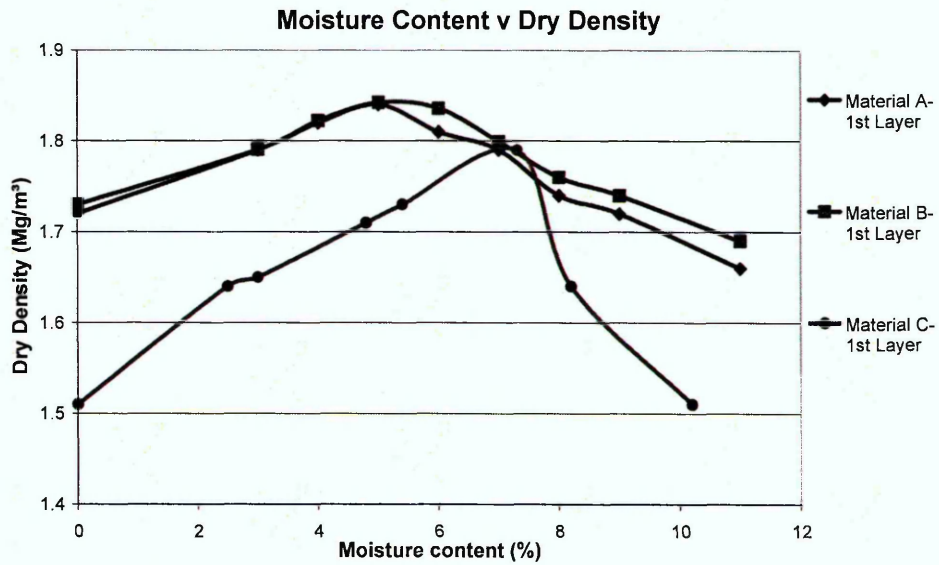


Figure 6.16: Compaction curves for all Materials – 1st Layer

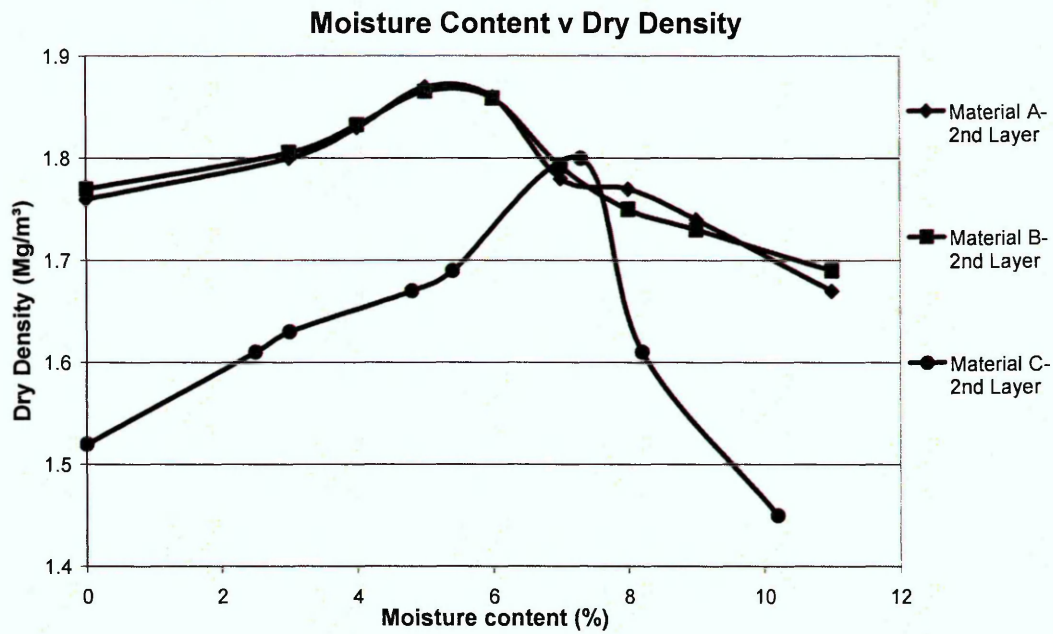


Figure 6.17: Compaction curves for all Materials – 2nd Layer

Table 6.10 presents the variability of the mould compaction results for Material A and B. The results for Material C are given in Table 6.11.

Table 6.10: Variability of dry density results for Material A and B

Dry Density Values and their variations for Materials A and B (in Mg/m³)				
Moisture Content (%)	Material A		Material B	
	Dry Density	Differences	Dry Density	Differences
0	1.72	-0.05/+0.04	1.73	-0.06/+0.07
3	1.79	-0.03/+0.10	1.79	-0.05/+0.05
4	1.82	-0.08/+0.11	1.82	-0.06/+0.02
5	1.84	-0.08/+0.08	1.84	-0.03/+0.01
6	1.81	-0.05/+0.06	1.84	-0.06/+0.03
7	1.79	-0.09/+0.08	1.80	-0.04/+0.12
8	1.74	-0.08/+0.07	1.76	-0.02/+0.06
9	1.72	-0.08/+0.10	1.74	-0.07/+0.05
11	1.66	-0.09/+0.06	1.69	-0.08/+0.04

Table 6.11: Variability of dry density results for Material C

Dry Density Values and their variations for Material C (in Mg/m ³)		
Moisture Content (%)	Dry Density	Differences
0	1.51	-0.02/+0.03
2.5	1.64	-0.01/+0.03
3	1.65	-0.06/+0.09
4.8	1.71	-0.11/+0.08
5.4	1.73	-0.3/+0.04
7.3	1.79	-0.05/+0.05
8.2	1.64	-0.02/+0.04
10.2	1.51	-0.06/+0.02

Summarising it can be said:

- The variability of the results (Tables 6.10 and 6.11) for the mould compaction of all the materials shows that there is a good degree of repeatability
- The BS compaction tests appear to be slightly more consistent than the mould compaction tests for Material A.
- Material C had a smaller degree of variability than the concrete based materials, probably due to their more homogeneous nature.

6.7 Aggregate Impact and Aggregate Crushing Values

The average values for the AIV and ACV tests, together with the standard deviation values (SD), for the three types of materials are presented in Tables 6.12 and 6.13 respectively. They include the values of the dry (D) and soaked (S) tests and the reductions of the AIV and ACV values of the materials when they are soaked compared to being dry.

The percentage reductions are calculated by the following formula:

$$\frac{\text{AIV or ACV under soaked conditions} - \text{AIV or ACV under dry conditions}}{\text{AIV or ACV under dry conditions}}$$

Table 6.12: Dry and soaked AIV and their Standard Deviation (SD) values for all the materials

Material	AIV _D (%)		AIV _S (%)		Reduction in Strength between Dry and Soaked Testing Values (%)
	Results	SD	Results	SD	
A	17.7	0.8	18.9	0.7	6.2
B	29.5	0.6	31.1	0.7	5.4
C	27.8	0.5	29.2	0.5	5.0

Table 6.13: Dry and soaked ACV and their Standard Deviation (SD) values for all the materials

Material	ACV _D (%)		ACV _S (%)		Reduction in Strength between Dry and Soaked Testing Values (%)
	Results	SD	Results	SD	
A	25	0.8	26.8	0.7	7.3
B	28.6	0.7	30.3	0.8	0.9
C	33.3	0.5	35.3	0.5	5.5

6.8 Resistance to Freezing and Thawing

Table 6.14 shows the percentage of the materials tested that passed the 5 mm sieve after ten freezing/thawing cycles. It includes the results for:

- The actual freezing/thawing tests, with particle size ranging from 50 to 10 mm and
- the results for the materials, with particle size of 14 to 10 mm, that were used for determining the affect of the freezing/thawing process in their strength (through AIV and ACV tests).

Table 6.14: Results of the particle percentage passing the 5 mm sieve after the weathering process

Materials	BS EN 1367-1,2000 test (Particle size 50 - 10 mm)		Preparation for AIV and ACV tests (Particle size 14 - 10 mm)	
	Results	SD	Results	SD
Material A	2 %	0.2	1.2 %	0.2
Material B	2.4 %	0.3	1.6 %	0.2
Material C	2.1 %	0.2	1.1 %	0.1

Table 6.15 shows the values of the ACV_w and AIV_w (w indicates AIV and ACV tests after freezing-thawing and both tests conducted on dry materials) together with their standard deviation after the freezing – thawing process of all the materials.

Table 6.15: ACV and AIV for all the materials after the freezing – thawing process

Materials	AIV_w (%)		ACV_w (%)	
	Results	SD	Results	SD
Material A	19.5	0.698	27.6	0.786
Material B	33.9	0.598	32	0.657
Material C	30.9	0.532	35.9	0.476

CHAPTER 7

MAIN SERIES TEST RESULTS

7.1 Introduction

This chapter presents the factual results of the Main Series Testing. These are presented in the following order:

1. Section 7.2 - Large scale permeability testing
2. Section 7.3 - Shear box testing to investigate the effects of maximum particle size and specimen dry density in a 305 mm square shear box
3. Section 7.4 - Particle crushing during shear

7.2 Permeability

The large scale permeability tests, under steady state conditions, were performed in specimens of 1.8 Mg/m^3 dry density and dimensions of 600 mm height and 300 mm diameter. This gave a cross sectional area of 70685.8 mm^2 . As discussed previously (Section 5.3.1) the readings of the manometer tube differences (between points 200 mm apart) and flow through the samples were taken after they have been stabilised for a period of about a week. The values of flow and manometer differences are presented in Figures 7.1 and 7.2 respectively.

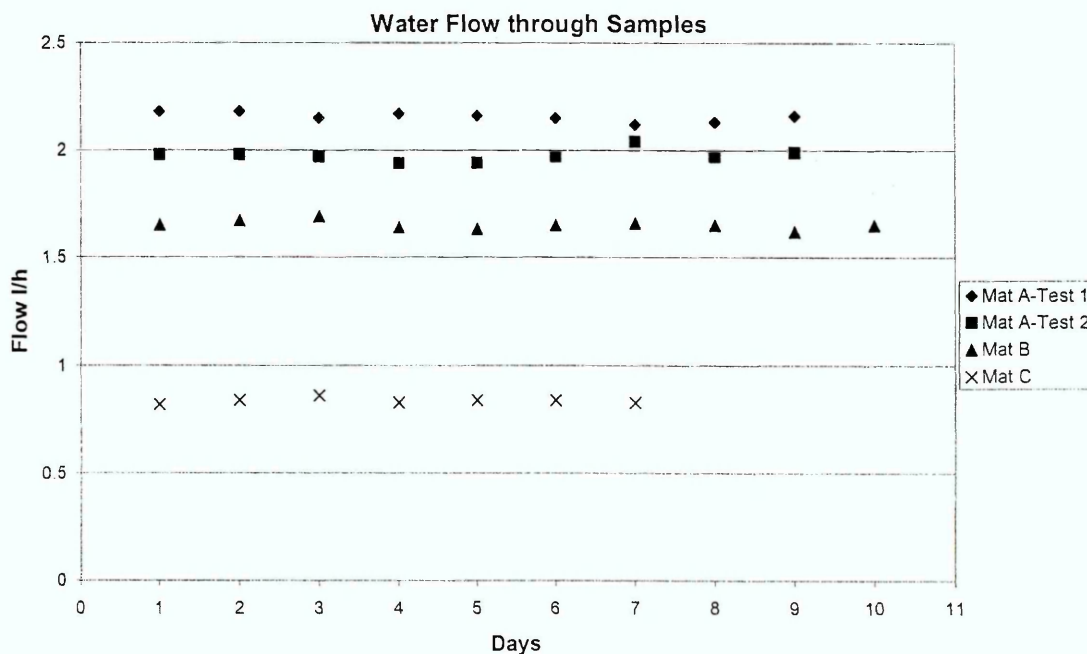


Figure 7.1: Water flow through permeability specimens

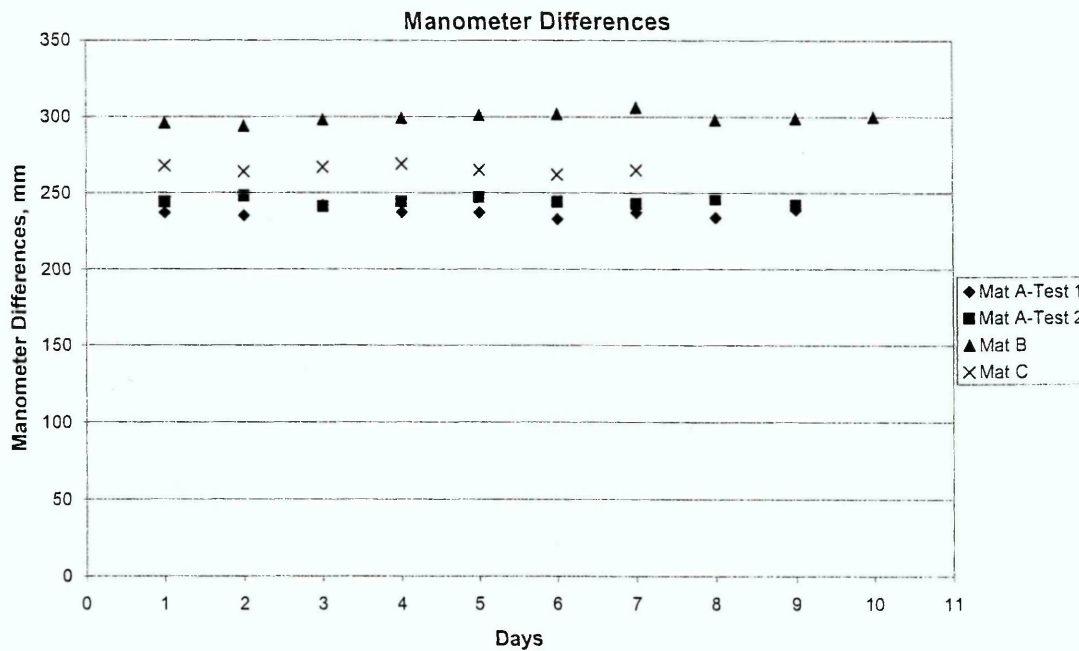


Figure 7.2: Manometer differences for permeability tests

The results of the water flow through the samples, together with the calculated Coefficient of Permeability (k) values and their standard deviation (SD) are presented in Table 7.1 for all four tests. The temperature of the laboratory, measured twice daily, throughout the four permeability tests performed was 20-22 °C degrees. The mean temperature was 21 °C, with a standard deviation of 0.8. This gave a temperature correction factor (R_t) for the viscosity of water (derived from BS 1377-5: 1990, Figure 4) of 0.96 for all tests (The value of 21 °C was used for calculating the R_t).

Table 7.1: Values of the Coefficient of Permeability (k) for all the Materials

Material	Flow	Coefficient of Permeability and SD	
	Values (l/h)	k (m/s)	SD
Material A (Test 1)	2.16	2.5×10^{-5}	5.4×10^{-6}
Material A (Test 2)	1.98	2.2×10^{-5}	8.2×10^{-6}
Material B	1.65	1.5×10^{-5}	1.1×10^{-6}
Material C	0.84	8.5×10^{-6}	1.9×10^{-6}

The restricted number of tests performed for the determination of the permeability of the materials does not allow for safe observations, but the values of flow, manometer

differences, coefficient of permeability and standard deviation show the good repeatability of the procedures used.

7.3 Shear Box Testing

This paragraph presents the results from the shear box tests. Table 7.2 summarises the parameters of the specimens tested, which were applied for all three materials. Table 7.3 presents the particle shape characteristics for SBT1 and SBT3. SBT1 and SBT2 have identical particle shape parameters.

Table 7.2: Specimen parameters for shear box tests, for all Materials

Test Type	Max Particle Size, mm	Density, Mg/m ³	Moisture Content, %	Square Sample Dimensions
SBT1	37.5	1.8	2 ±0.2	305×305
SBT2	37.5	1.6	2 ±0.2	305×305
SBT3	28	1.8	2 ±0.2	305×305

Table 7.3: Particle shape for maximum particle size of 37.5 and 28 mm

Maximum Particle Size	Material A		Material B		Material C	
	F _I	E _I	F _I	E _I	E _I	F _I
37.5 mm (SBT1, SBT2)	11.5	23.8	6.5	14	20.3	9.7
28 mm (SBT3)	11.6	24.4	6.6	14.5	21.9	9.3

The results are presented in terms of:

1. Shear Stress against longitudinal displacement and axial strain (Section 7.3.1)
2. Shear Stress - Normal Stress Values (Section 7.3.2)
3. Volume Change Behaviour - volumetric (ϵ_v) against average axial (ϵ_a) strain (Section 7.3.2)

The three different materials, the large number of tests and the two different parameters (density and maximum particle size) investigated in these tests have resulted in huge amounts of data. There were two choices of presenting this data. Place indicative graphs in this paragraph and the rest in Appendices or present all the graphs for all three materials for SBT1, SBT2 and SBT3. The second was chosen because it was felt that

this will give the reader a complete initial idea of the behaviour of the materials under different conditions of testing. These results show the average values of the tests. All the graphs for every single test performed in this project are presented in Appendices E and F.

7.3.1 Stress-Strain Behaviour

The shear stress values are calculated for each measurement point by constantly compensating for the reduction in cross sectional area of the specimens due to the horizontal displacements. For example, the shear stress of Material B, for 95 kPa normal stress after 30 minutes (30 reading) after the beginning of the test is calculated:

$$\text{Shear stress } (\sigma) = \text{load (kN)} / \text{cross sectional area (m}^2\text{)}$$

Load at 30 minutes is 11.26 kN

Horizontal Displacement at 30 minutes is 3.04 mm

Cross sectional area at 30 minutes is $0.305 \times (0.305 - 0.00304)$

The shear stress at 30 minutes is 122.26 kN/m² (kPa)

Figures 7.3 and 7.4 present the shear stress against horizontal displacement for Material B and C respectively, for SBT1, at 143 kPa normal stress. The graphs for all the shear box tests performed in this project are presented in Appendix E

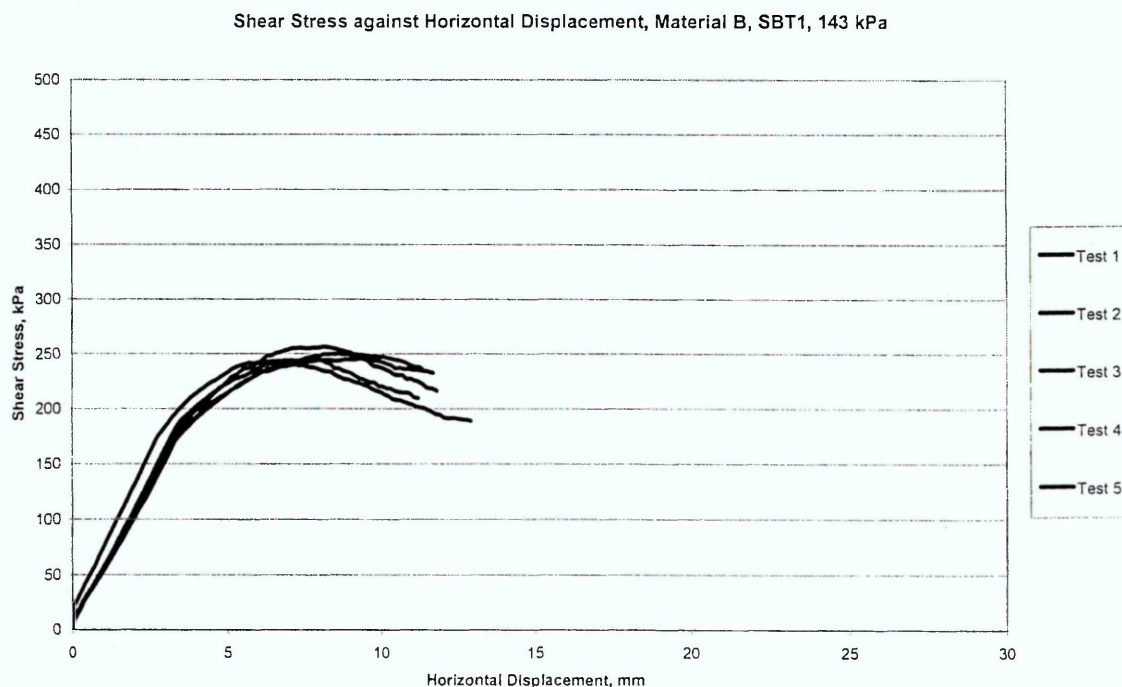


Figure 7.3: Shear Stress against Horizontal Displacement for Material B

Shear Stress against Horizontal Displacement, Material C, SBT1, 143 kPa



Figure 7.4: Shear Stress against Horizontal Displacement for Material C

The axial strain value at each recording time point is calculated as the percentage of the horizontal displacement at that point over the whole length of the specimen.

The average shear stress values at specific axial strains are obtained by identifying the shear stress values at similar axial strains and then obtaining the average shear stress values. For example, for Material B and normal stress 143 kPa. For axial strain of 2% the shear stress values are 249, 238, 245, 247 and 243 kPa. This gives an average of shear stress of 244.4 kPa.

The results in the form of graphs of shear stress against axial strain for each of the materials tested, for SBT1, SBT2 and SBT3 and for all the normal stresses (95, 143, 190, 238, and 317 kPa) are presented in the following Figures:

- Figures 7.5, 7.6 and 7.7 present the graphs for Materials A for SBT1, SBT2 and SBT3 respectively
- Figures 7.8, 7.9 and 7.10 present the graphs for Materials B for SBT1, SBT2 and SBT3 respectively
- Figures 7.11, 7.12 and 7.13 present the graphs for Materials C for SBT1, SBT2 and SBT3 respectively

Stress-Strain Behaviour for Material A, SBT1

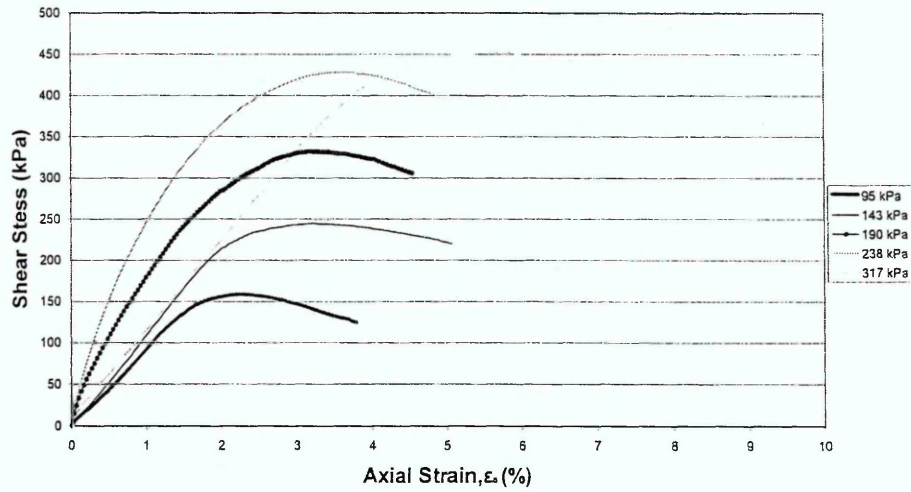


Figure 7.5: Stress-Strain behaviour of Material A for SBT1

Stress-Strain Behaviour for Material A, SBT2

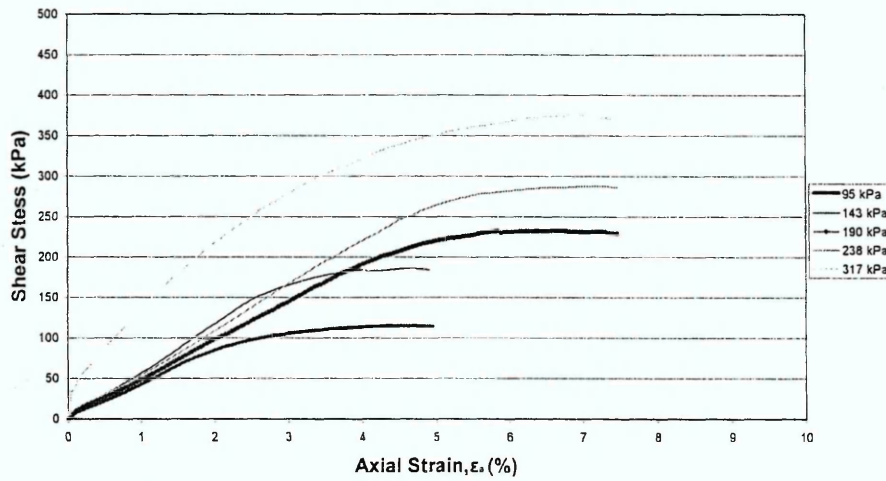


Figure 7.6: Stress-Strain behaviour of Material A for SBT2

Stress-Strain Behaviour for Material A, SBT3

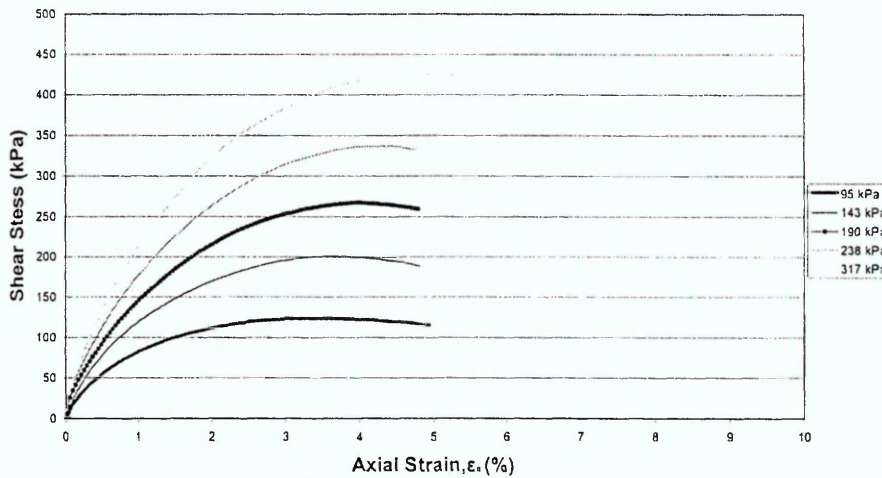


Figure 7.7: Stress-Strain behaviour of Material A for SBT3

Stress-Strain Behaviour for Material B, SBT1

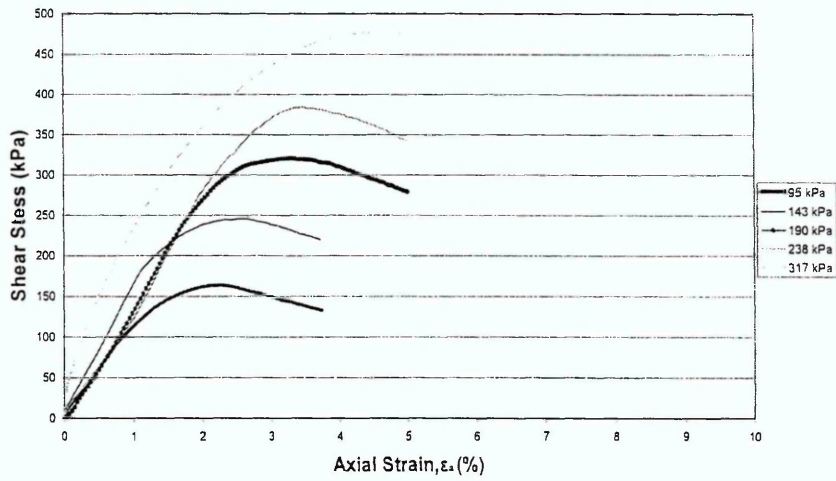


Figure 7.8: Stress-Strain behaviour of Material B for SBT1

Stress-Strain Behaviour for Material B, SBT2

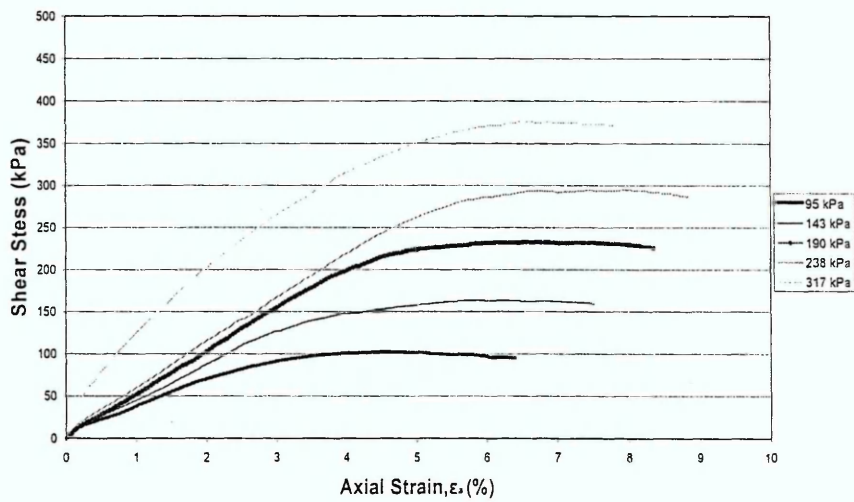


Figure 7.9: Stress-Strain behaviour of Material B for SBT2

Stress-Strain Behaviour for Material B, SBT3

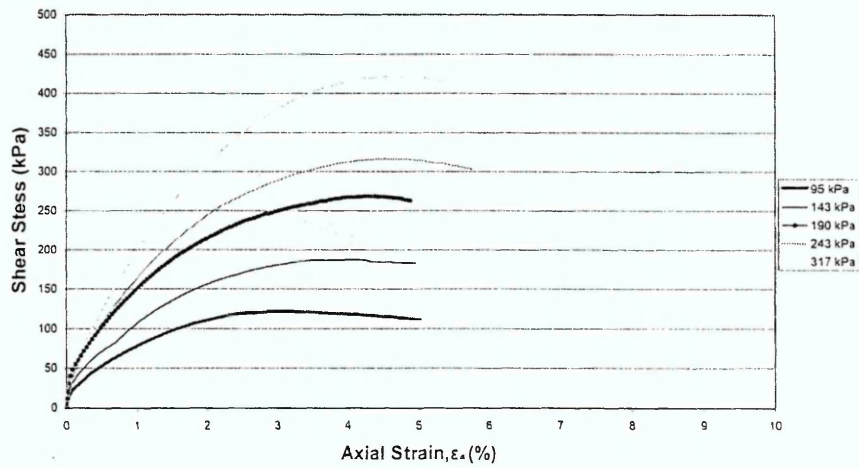


Figure 7.10: Stress-Strain behaviour of Material B for SBT3

Stress-Strain Behaviour for Material C, SBT1

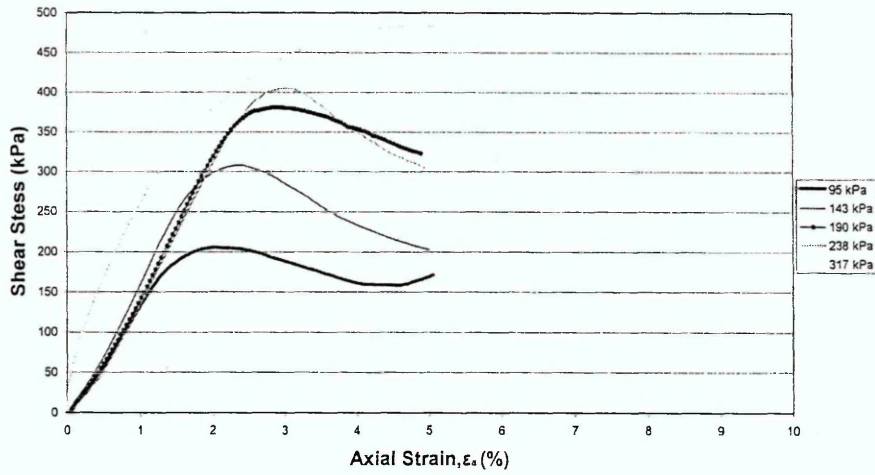


Figure 7.11: Stress-Strain behaviour of Material C for SBT1

Stress-Strain Behaviour for Material C, SBT2

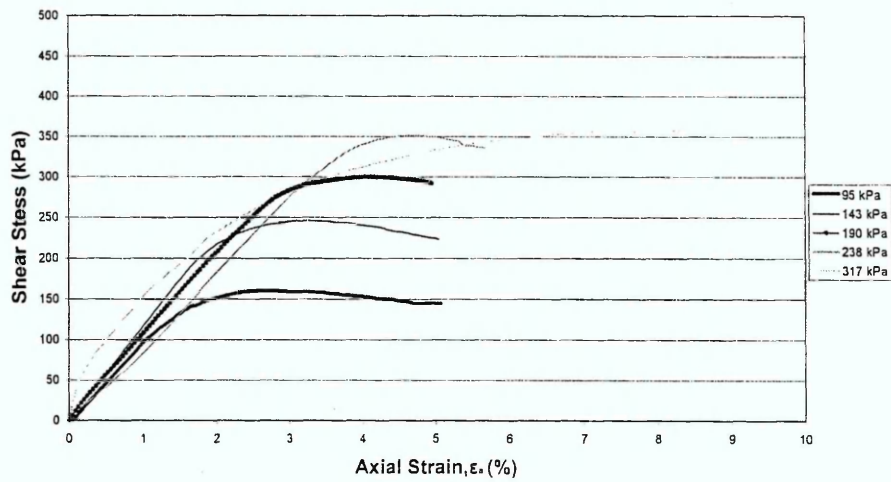


Figure 7.12: Stress-Strain behaviour of Material C for SBT2

Stress-Strain Behaviour for Material C, SBT3

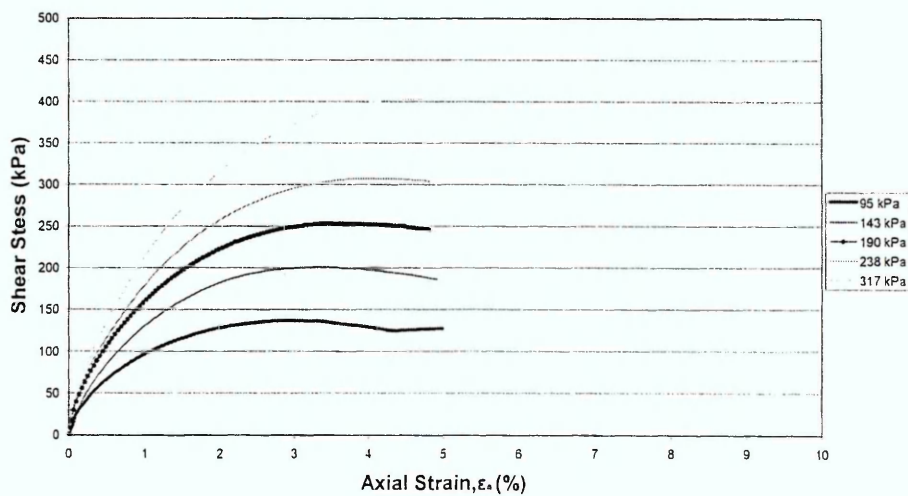


Figure 7.13: Stress-Strain behaviour of Material C for SBT3

7.3.2 Shear Stress Values

Table 7.4 summarises the mean peak values of the calculated shear stress at failure, σ_f , (kPa) for all of the materials for tests SBT1, SBT2 and SBT3 for all the normal stresses investigated. Their Standard Deviation values are shown in Table 7.5.

Table 7.4: Mean peak Shear Stress values (in kPa) for all the materials

Materials	Type of Test	Normal Stresses (σ_n), kPa				
		95.0	143.0	190.0	238.0	317.0
A	SBT1	176.1	246.7	343.2	441.8	454.7
A	SBT2	116.7	187.6	236.4	289.6	388.2
A	SBT3	123.9	202.1	268.9	338.1	434.3
B	SBT1	164.9	248.1	324.9	394.1	481.9
B	SBT2	103.1	165.1	231.1	298.5	378.4
B	SBT3	122.8	187.9	269.3	317.2	422.1
C	SBT1	209.9	309.1	384.8	409.9	486.0
C	SBT2	167.0	249.6	301.6	352.9	363.5
C	SBT3	137.8	203.6	254.1	308.2	404.1

Table 7.5: Mean peak shear stress Standard Deviation values (kPa) for all the types of shear box tests for all the materials

σ_n (kPa)	Material A			Material B			Material C		
	Standard Deviation			Standard Deviation			Standard Deviation		
	SBT1	SBT2	SBT3	SBT1	SBT2	SBT3	SBT1	SBT2	SBT3
95	8.1	4.4	6	4.6	2.7	9.3	11.6	10.3	7
143	15.3	5.6	5.5	5.3	12.3	10.5	8.3	18.8	11.2
190	19.5	11.7	10.1	4.7	16.8	5.5	33.5	10.4	8.5
238	23.6	15.9	7	5.4	16.8	4.9	27.9	13.7	8
317	26.1	25.4	12.9	33.9	12.2	30.6	29.8	33.5	21.1

The shear box results indicate that the variations in the results of the mean peak shear stress are not of significantly high level and taking into account the difficulties involved initially in obtaining the materials from site, in taking representative samples and in the large scale of the tests, the results can be characterised as being representative.

7.3.3 Volume Change Behaviour

Figure 7.14 presents the volumetric against axial strain for Material A, SBT1 and 95 kPa normal stress. Appendix F, presents the volumetric (ϵ_v) against axial (ϵ_a) strain for every single test performed in this investigation.

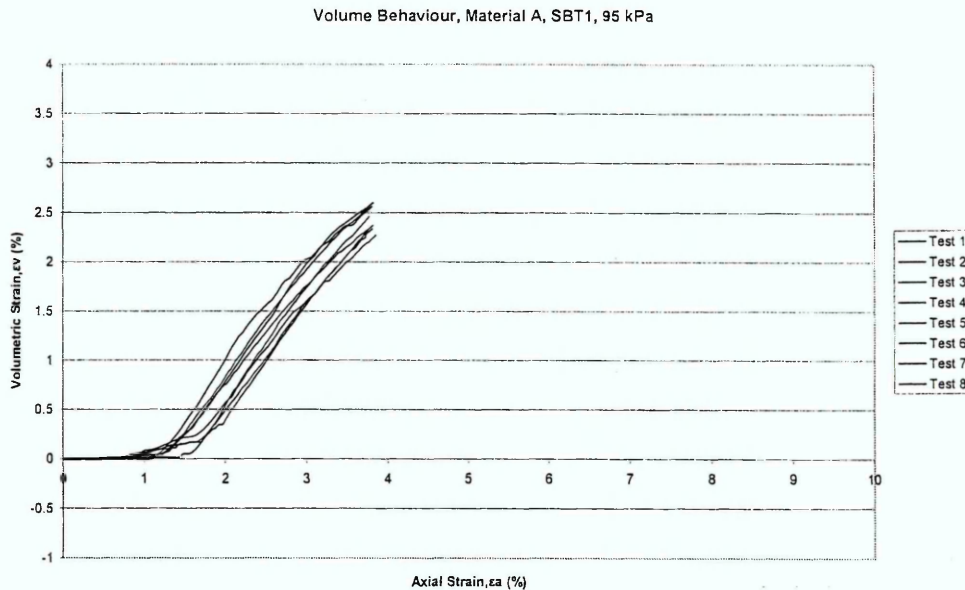


Figure 7.14: Volume Behaviour for Material A, SBT1 at 95 kPa

The average volumetric strain values at specific axial strains are obtained by identifying the volumetric strain values at similar axial strains and then obtaining the average volumetric strain. For example Material A and normal stress 95 kPa. For axial strain of 3% the volumetric strain values are 2.05, 1.74, 1.76, 1.62, 1.97, 1.64, 1.63 and 2%. This gives an average shear stress of 1.81 %.

The results are presented as follows:

- Figures 7.15, 7.16 and 7.17 present the graphs for Materials A for SBT1, SBT2 and SBT3 respectively
- Figures 7.18, 7.19 and 7.20 present the graphs for Materials B for SBT1, SBT2 and SBT3 respectively
- Figures 7.21, 7.22 and 7.23 present the graphs for Materials C for SBT1, SBT2 and SBT3 respectively

In the figures of this paragraph the positive values of volumetric strain indicate sample expansion and the negative ones compression.

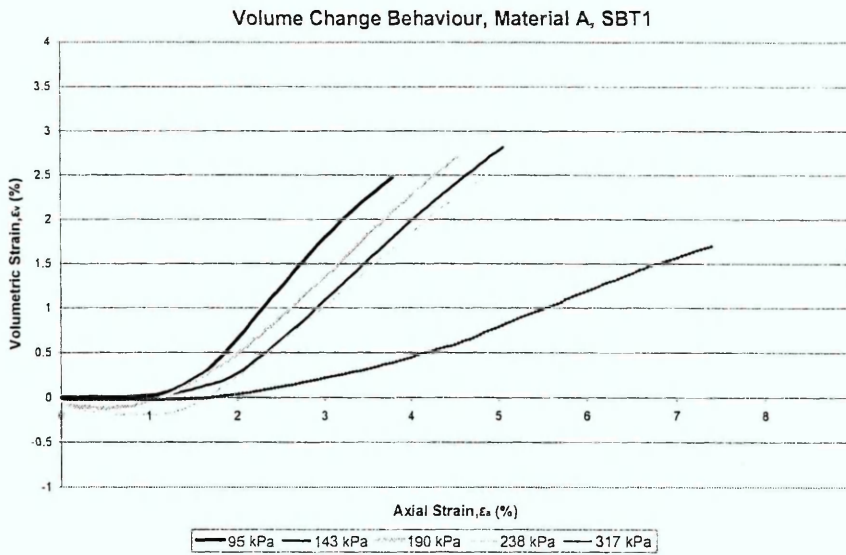


Figure 7.15: Volume Change behaviour for Material A, SBT1

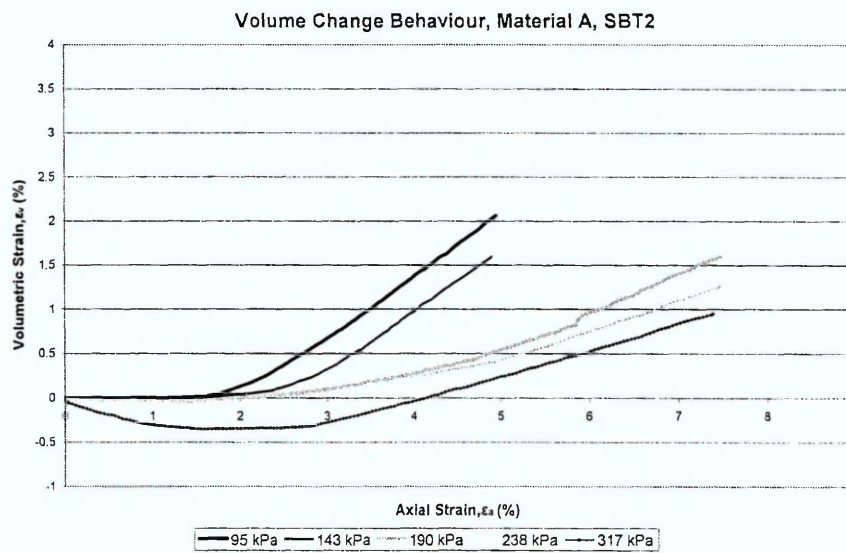


Figure 7.16: Volume Change behaviour for Material A, SBT2

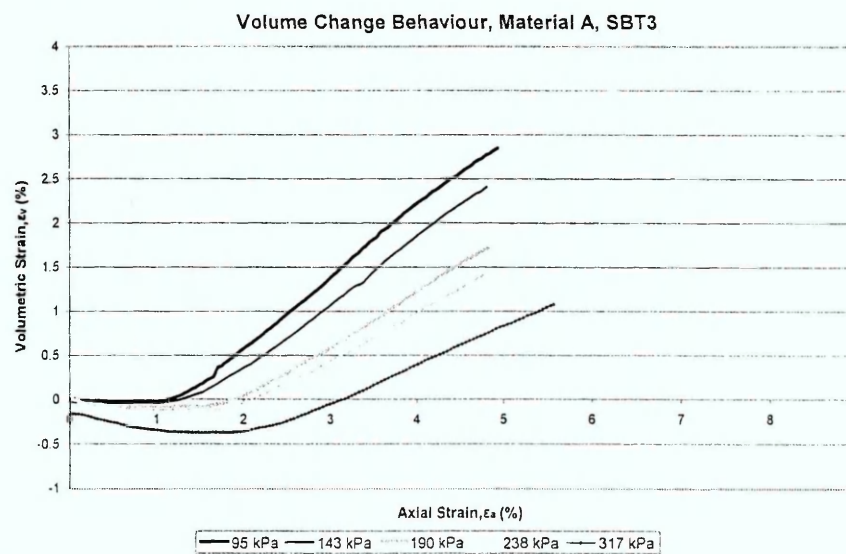


Figure 7.17: Volume Change behaviour for Material A, SBT3

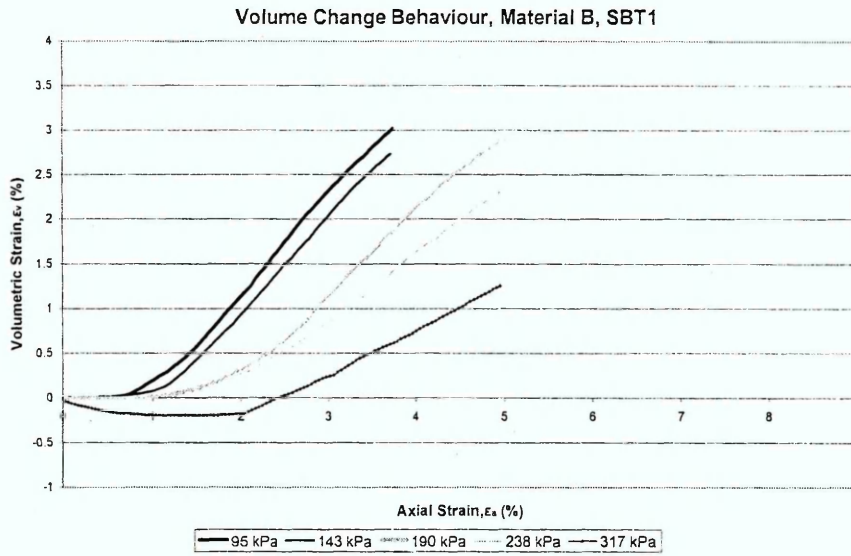


Figure 7.18: Volume Change behaviour for Material B, SBT1

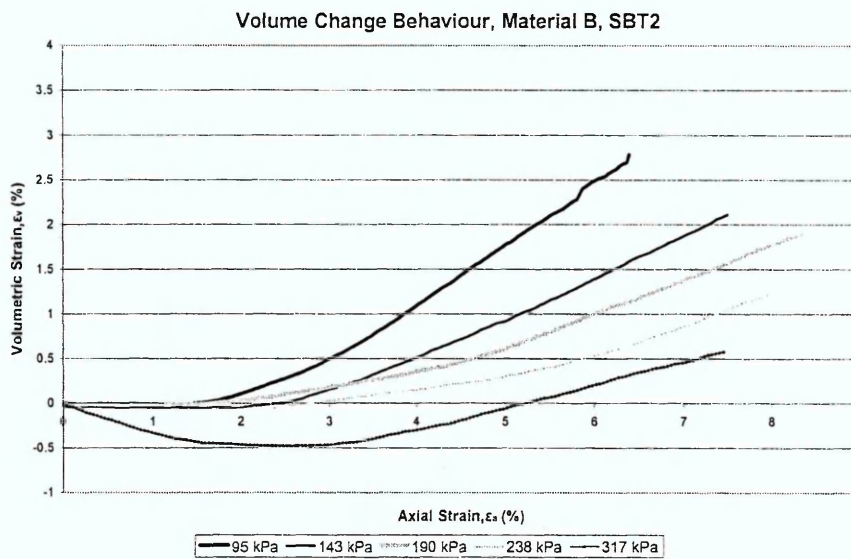


Figure 7.19: Volume Change behaviour for Material B, SBT2

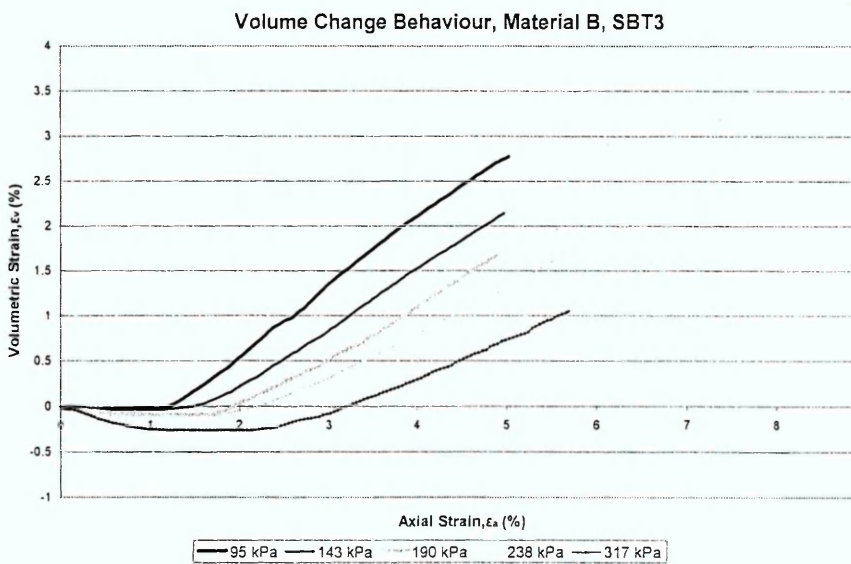


Figure 7.20: Volume Change behaviour for Material B, SBT3

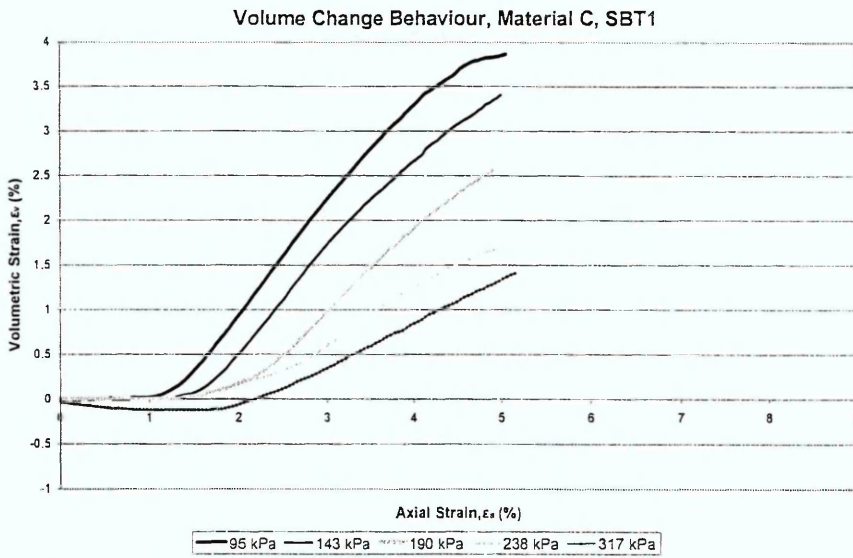


Figure 7.21: Volume Change behaviour for Material C, SBT1

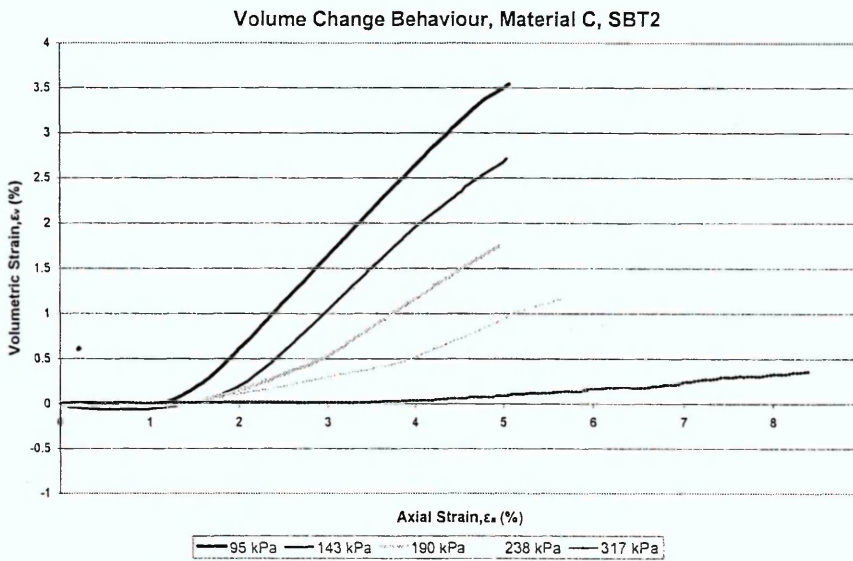


Figure 7.22: Volume Change behaviour for Material C, SBT2

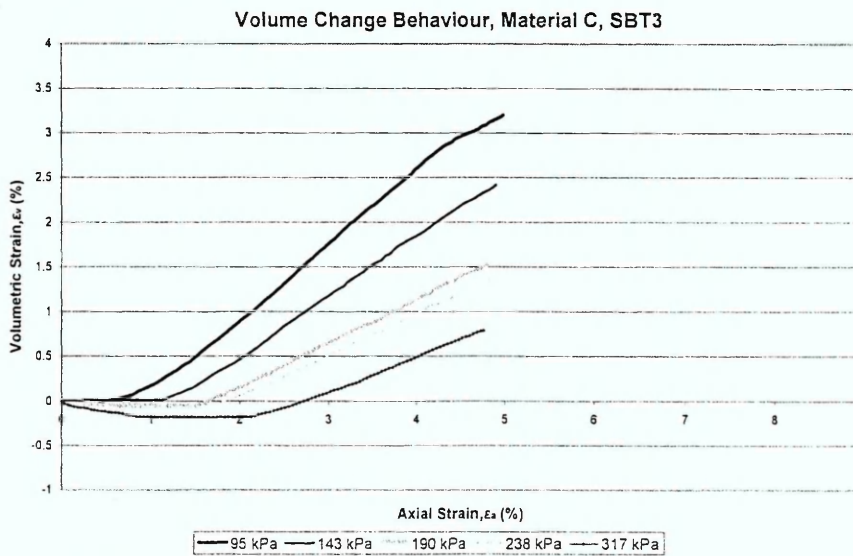


Figure 7.23: Volume Change behaviour for Material C, SBT3

7.3.4 Repeatability of Results

The results of the shear box tests, as presented with the values of shear stress, volumetric against axial strain and shear stress against axial strain show great repeatability. Table 7.6 presents the standard deviation values as a percentage of the shear stress values for every normal stress investigated.

Table 7.6: Standard deviation as a percentage of mean peak shear stress values

Standard Deviation as a percentage of the Mean Peak Shear Stress Value for each Test						
Materials	Test Type	Normal Stress, kPa				
		95	143	190	238	317
A	SBT1	5	6	6	5	6
A	SBT2	4	3	5	5	7
A	SBT3	5	3	4	2	3
B	SBT1	3	2	1	1	7
B	SBT2	3	7	7	6	3
B	SBT3	8	6	2	2	7
C	SBT1	6	3	9	7	6
C	SBT2	6	8	3	4	9
C	SBT3	5	6	3	3	5

From the Table 7.6 it can be seen that the repeatability of the results is good. All the values fall below 10 %, which proves that the specimen preparation procedure used managed to minimise any possible effect of the variability of materials. The largest values of standard deviation (in percentage terms) are met by Material C and reach 9%. It can be observed that:

- There is different behaviour between differently based crushed materials (concrete and bricks)
- The different degree of processing between Material A and B has not altered their behaviour to a significant degree.

Further analysis is needed, though, in order to verify these statements. It would be very useful to test more than one crushed brick based material and more types of processed and unprocessed crushed concrete based materials, in order to identify any possible behavioural trends.

Observing Figures 7.10, 7.11, 7.12, 7.22 and 7.23 and the graphs of Appendices E and F it is clearly seen that the repeatability of the test is very satisfactory. The mean values used for the presentation and discussion of results therefore can be considered representative of the actual properties of the materials, and also verifies the high level of consistency in the specimen preparation procedures.

Table 7.7 presents the upper and lower limits of the envelopes of the mean volumetric-axial strain curves for all materials, shear box test types and normal stresses. The values used show the maximum difference of volumetric strain encountered throughout the graph and applied throughout the curve showing the volumetric-axial strain relations. For example for Material A, SBT1 and 95 kPa the upper and lower limit curves will show the "worst case scenario" of the variability of the materials. This difference is highest (0.36% of volumetric strain) and it is met at an axial strain of 2.164 %. This value is applied throughout the curve and creates the upper and lower envelopes, both being parallel to the average curve at "distances" of 0.36%.

Table 7.7: Upper and lower limits of the envelopes of the volumetric-axial strain curves

Limits of Upper and Lower Envelopes for Mean Volumetric-Axial Strain Curves, %						
Material Type	Test Type	Normal Stress, kPa				
		95	143	190	238	317
A	SBT1	± 0.36	± 0.45	± 0.21	± 0.43	± 0.36
A	SBT2	± 0.34	± 0.10	± 0.28	± 0.29	± 0.11
A	SBT3	± 0.27	± 1.28	± 0.52	± 0.21	± 0.34
B	SBT1	± 0.51	± 0.24	± 0.76	± 0.74	± 0.35
B	SBT2	± 0.67	± 0.29	± 0.63	± 0.48	± 0.31
B	SBT3	± 0.19	± 0.38	± 0.22	± 0.18	± 0.34
C	SBT1	± 0.39	± 0.52	± 1.23	± 0.36	± 0.41
C	SBT2	± 0.66	± 0.62	± 0.51	± 0.26	± 0.48
C	SBT3	± 0.40	± 0.37	± 0.32	± 0.15	± 0.22

7.4 Particle Crushing

This section of the Thesis presents the results of particle crushing of the materials after the shear box tests. As discussed previously, the results for each type of shear box

(SBT1, SBT2 and SBT3) are plotted and calculated by sieving the whole quantity of the materials tested for the five normal stresses and do not include any tests on individual normal stresses. Figures 7.24, 7.25, and 7.26 present the grading curves of all the materials before and after the shear box tests.

From these three Figures and the differences in percentages passing, between before and after shear box testing, the B_I value according to Marsal (1967) can be calculated by adding the differences of these percentages from the individual sieves. The values are presented in Table 7.8.

The values of B_I for SBT1, SBT2 and SBT3 for all the materials are shown in Table 7.8.

Table 7.8: Breakage Index, B_I , for SBT1, SBT2 and SBT3

Material	Breakage Index, B_I (%)		
	SBT1	SBT2	SBT3
A	8.8	4	4.4
B	12.1	7.1	5.5
C	4.3	2.5	2.1

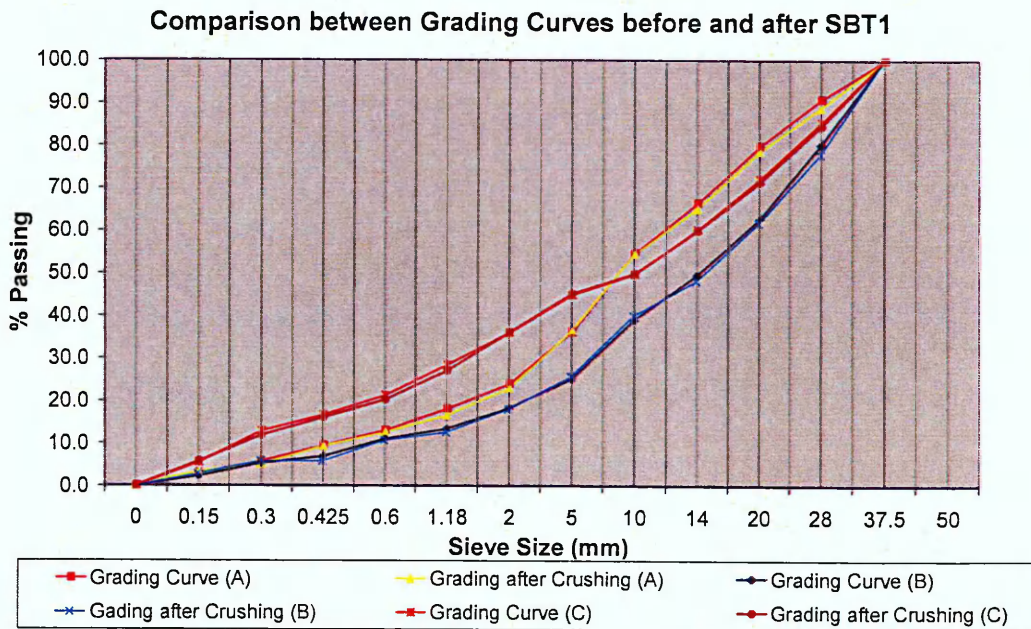


Figure 7.24: Grading curves for all the Materials after SBT1

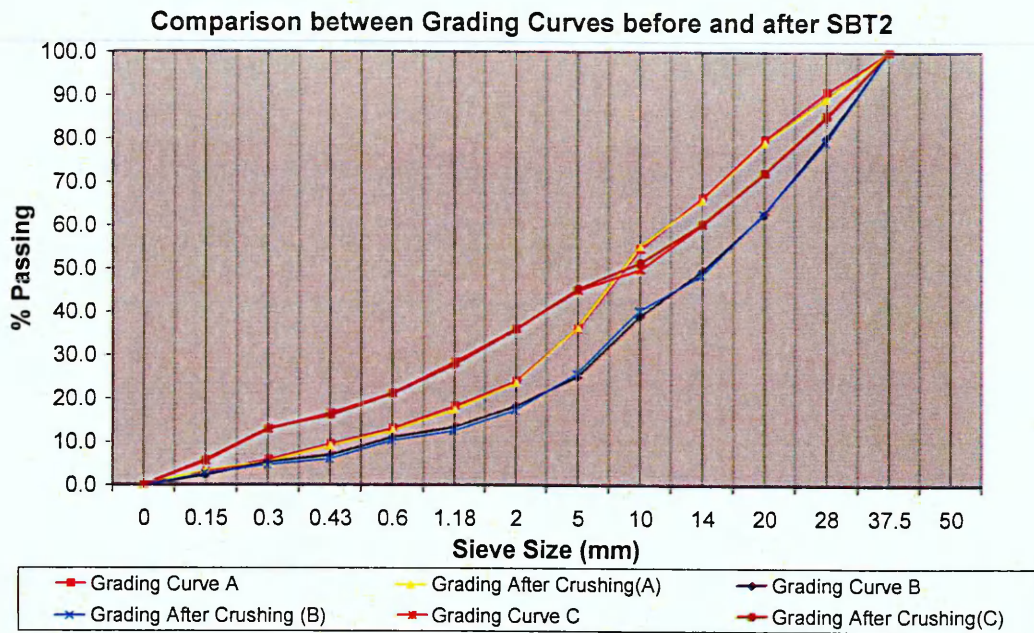


Figure 7.25: Grading curves for all the Materials after SBT2

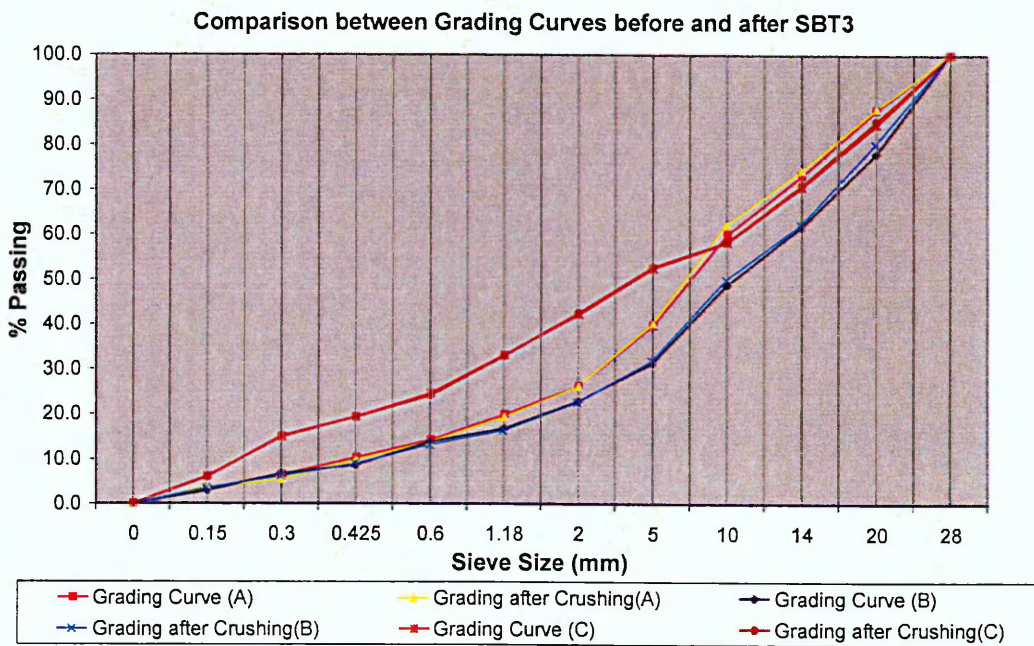


Figure 7.26: Grading curves for all the Materials after SBT3

CHAPTER 8

DISCUSSION OF RESULTS

8.1 Introduction

The test programme discussed in Chapter 5 was designed to investigate the physical and mechanical characteristics of the demolition waste materials. Chapter 6 and 7 in turn have presented the physical and mechanical properties of the materials as they were determined by the test programme. This Chapter analyses and discusses the results of the test programme in the following order:

- Particle shape
- Aggregate Impact and Aggregate Crushing Value Tests
- Freezing and thawing tests
- Permeability
- Particle crushing
- Shear strength

8.2 Particle Shape

Table 8.1 summarises the F_I and E_I values for Materials A, B and C.

Table 8.1: Flakiness and Elongation Indexes

Material A		Material B		Material C	
F_I	E_I	F_I	E_I	F_I	E_I
12.9	23.9	7.3	13.1	10.9	20.8

The flatness and elongation ratios plotted in Figures 6.6, 6.7 and 6.8 show that a large population of particles, 64% of Material A, 74% of Material B and 55% for Material C, fall within the equidimensional category.

From the results it can be observed:

1. Between Materials A and B, F_I decreased by 5.6 percentage points and E_I decreased by 10.8 percentage points.
2. There is a 10 percentage point increase in equidimensional particles in Material B compared to Material A is probably caused by the additional processing and therefore crushing of the materials into more rounded particles.

3. There are almost no blades (particles described as being elongated and flaky) in Material A, B or C.

The most likely explanation for these observations is the manner in which the materials fracture when subjected to mechanical crushing. Lade *et al* (1996) found that particles fracture easier along their smaller dimensions, and Yamamuro and Lade (1993) observed that the concentration of stresses at the angular points of particles causes fracture more easily than at non-angular points. It is therefore possible to infer although further testing is required, that angular and flaky particles will tend to break into particles with more equidimensional shapes during crushing.

The F_I and E_I values for Material C fall between those for Material A and B. The most possible explanations for this are the way the materials crush and the degree of processing.

- The particles are less flaky and elongated compared with Material A due to greater processing and therefore crushing of the particles into more rounded ones
- The particles are more flaky and elongated than Material B. Though both materials have undergone similar processing, Material B probably crushes more easily and therefore produces "more rounded" and/or "more cubic" particles.

8.3 Aggregate Impact and Aggregate Crushing Value Tests

8.3.1 Comparison between Material A, B and C

Table 8.2 presents the results for the AIV and ACV tests for both dry and soaked state and Table 8.3 the ratios of AIV to ACV tests.

Table 8.2: AIV and ACV results

	AIV _D (%)	ACV _D (%)	AIV _S (%)	ACV _S (%)
Material	Results	Results	Results	Results
A	17.7	25.0	18.9	26.8
B	29.5	28.6	31.1	30.3
C	27.8	33.3	29.2	35.3

Table 8.3: AIV over ACV ratios

Material	AIV _D /ACV _D (%)	AIV _s /ACV _s (%)
A	70.8	70.5
B	103.1	102.6
C	83.5	82.7

The results show:

- Material A appears to be the strongest with Material B the weakest for the AIV test. For the ACV tests though, Material A are still the strongest with Material C the weakest. The age of the original structures that were demolished to produce Material A and B is unknown and therefore this factor can not be taken into consideration.
- Material A and C behave similarly as their AIV is higher than the ACV and their AIV/ACV is similar, but Material B exhibit a slightly higher ACV than AIV. These two findings might be a result of the particle properties of the materials that either break easily under crushing or impacting load.
- The strength of all three materials decreases when they are soaked.

The AIV and ACV tests have been widely used as characterising the strength of natural homogeneous materials. Schouenborg, *et al.*, (2007) have found that the abrasion of alternative (recycled) aggregates is best described when the material is tested as a unit (the entire grading) and that tests such as LA-Test, AIV and ACV tests are less relevant for heterogeneous materials. Since the three types of materials investigated in this project are not homogeneous it is possible that the AIV and ACV results presented are not representative of the materials as a whole. Tests that can provide information about the strength of the materials as a unit are the shear box tests and the Breakage Index. As the results of these two tests are analysed there would be a comparison with the AIV and ACV results in an effort to verify or refute the applicability of the AIV and ACV tests for recycled materials testing.

8.3.2 Comparison with Industry Products

It would be impossible to investigate all the properties of all the industry materials available, so the values of Table 8.4 are just a representative of some of the main granular materials used in construction.

Table 8.4: Values for ACV, AIV, F_1 and water absorption for Material A, B and C and industry products

Materials	Properties		
	ACV (%)	AIV (%)	Water Absorption (%)
A	25	17.7	5.5
B	28.6	29.5	5.5
C	33.3	27.8	13.2
Limestone ¹	25	20	0.3
Granite ¹	27	N/A	0.33
Microtonalite ¹	13	15	2.1
Limestone ²	N/A	<30	<2
Gabbro ²	N/A	8-10	0.2-0.7
Limestone ³	23	N/A	0.18

¹ values obtained from CMS Quarries Sdn Bhd website from 3 different quarries in Malaysia

² values obtained from Stevin Rock website from 2 different quarries in United Arab Emirates

³ values obtained from S. Morris Ltd website from their quarry at

Comparing the ACV and AIV values of all the materials it can be seen that Material B and C appear to be weaker. On the other hand Material A seem to be of the same strength as far as their behaviour under the specific tests is concerned. This is probably a result of the crushing process the materials undergo. As it has been explained in previous sections, Material B and C have been further processed, comparing to A, and therefore is possible that they have micro-cracking on their particles which might cause the extra crushing under the ACV and AIV tests.

From the three types of materials investigated in this project, these specific tests are more applicable to Material C, which have a more homogeneous composition (Material A and B are composed by concrete particles, cement particles and virgin aggregates particles, while C from crushed brick particles). Therefore, taking into consideration the values of Limestone¹, for which both values of ACV and AIV are available and

comparing them with Material C it is noticeable that both materials behave similarly, crushing less under the AIV tests (impacting load in comparison with crushing load). The difference between the two tests for both materials is also similar (5.5 % for Material C and 5 % for Limestone¹). Obviously, the values of a single industry product is not enough to form a complete behavioural picture of material C but it appears that they behave similarly to natural aggregates (as far as the differences of their ACV and AIV values are concerned).

8.4 Freezing and Thawing Tests

Table 8.5 summarises the results of the freeze-thaw tests for all materials and Table 8.6 shows the values of the ACV_w and AIV_w before and after the freeze-thaw process of all the Materials, together with their percentage reductions.

Table 8.5: Freezing thawing results

Materials	Freezing Thawing values (% passing)	
	Results	SD
Material A	2 %	0.2
Material B	2.4 %	0.3
Material C	2.1 %	0.2

Table 8.6: ACV and AIV for all the materials before and after the freeze-thaw

Material Type	Before Freeze-Thaw		After Freeze-Thaw		Reduction (%)	
	AIV (%)	ACV (%)	AIV_w (%)	ACV_w (%)	AIV	ACV
Material A	17.7	25.0	19.5	27.6	10.2	10.4
Material B	29.5	28.6	33.9	32	14.9	11.9
Material C	27.8	33.3	30.9	35.9	11.2	7.8

The values indicate that the materials are marginally affected by the freezing and thawing process but the alterations in their particle size distribution is not significant. For example, for Material A, the difference caused by freezing and thawing will be that the percentage of material passing through the 5 mm sieve would be 35.6 instead of 33.6 (average values from 5 tests).

The main conclusions of these tests are:

- All three types of Materials change their grading, but not considerably, when subjected to freezing and thawing process.
- All materials show a reduction in the strength of their particles based on AIV and ACV tests.
- Materials B are affected more than Material A. This might be a result of the extra process they underwent that might have caused micro-cracks in their particles which when filled with water and frozen and thawed can crack further. Microscopic analysis of the materials in order to investigate this suggestion was not feasible due to the time frame of this investigation
- Material C which have also been further processed do not present such a large reduction in particle strength compared to Materials A and B and for the ACV results. When the AIV results are compared then Material C are affected more than Material A but less than Material B. These results might be due to their individual properties. There can not be a direct comparison though since Material C are brick based and the original sources of all the materials are unknown.

It is important to note though that the age of the structures that were demolished for the production of the three types of Materials is unknown, and therefore this factor can not be taken into consideration when comparing the materials. The type of cement and aggregates used in the manufacturing of the original concrete (that was crushed to produce materials A and B) is also unknown and therefore this factor can not also be taken into consideration.

8.5 Permeability

The measured permeability of the materials is 2.4×10^{-5} (average of two tests), 1.5×10^{-5} and 8.5×10^{-6} m/s for Material A, B and C respectively.

Due to the limited number of tests (only two tests for Material A and one for Material B and C were performed) the results may not be regarded to be representative of recycled materials generally. However the two tests performed for Material A show that the procedure for the preparation, saturation and testing of the sample are reproducible. The small difference in the k values (0.3×10^{-5} m/s, which is 13% of the mean k value

measured) may be a result of the variability of the materials and therefore can not be confidently attributed to shortfalls in the sample preparation process.

The permeability of the Materials is considered to be quite small. Values of 1×10^{-5} m/s have been observed though by other researchers for limestone (Brown, 1988; Mackenzie and McDonald, 1985), but for coarser materials of particles sizes 100 mm.

In conclusion it can be said that:

- The equipment and the procedure followed for the compaction, saturation and flow stabilisation for the permeability can be easily reproduced
- The permeability of all the Materials is quite low
- There is a difference of about 60% between the permeability of Material A and B, that can be result of the differences in gradings.
- More tests are required to determining the range of permeability values for the materials, including varying parameters such as density of specimens

8.6 Test Parameters Investigated in the Shear Box and Particle Crushing Tests

The literature review has identified that the following factors may affect the shear strength and particle breakage behaviour of granular materials:

- Moisture content
- Freeze Thaw
- Maximum particle size
- Particle shape
- Specimen density

It would have been impossible to investigate the effect of every parameter. The parameters varied and kept stable are as follows:

1. Moisture content - As all the materials in this investigation were tested with the same moisture content for the reasons mentioned previously (Section 3.4.1), it is not possible to comment on the influence of moisture content.
2. Weathering - Weathering is thought to induce greater particle breakage (and lower strength) due to weakening of individual particles (Chrismer, 1985). The results from the freeze-thaw tests (2, 2.4 and 2.1 % for Material A, B and C respectively) have shown that the materials exhibit very similar degradation under freeze-thaw conditions and no samples were tested in the shear box after

being subjected to any weathering effects. Therefore it is not possible to comment on the effect of weathering on particle crushing and material strength in this investigation. Also the degree of weathering of the materials' source(s) is unknown and therefore is impossible to comment on that effect on the strength of the crushed materials.

3. Maximum particle size - The materials were tested for two maximum particle sizes, 37.5 mm (SBT1) and 28 mm (SBT3), both with the same specimen density of 1.8 Mg/m³.
4. Particle shape - As the reduction of the maximum particle size caused minimal change to the flakiness and elongation Indices of the materials (Table 8.7) it is not possible to comment on the effect of this parameter.

Table 8.7: Flakiness and Elongation Indexes values for SBT1 and SBT3

Maximum Particle Size	Material A		Material B		Material C	
	F _I	E _I	F _I	E _I	E _I	F _I
37.5 mm (SBT1)	11.5	23.8	6.5	14	20.3	9.7
28 mm (SBT3)	11.6	24.4	6.6	14.5	21.9	9.3

5. Specimen density - The effect of dry density on shear strength and particle crushing was investigated by testing at densities of 1.8 Mg/m³ (SBT1) and 1.6 Mg/m³ (SBT2), but keeping the maximum particle size at 37.5 mm. On these tests the specimens' moisture content, maximum particle size, particle shape and grading were kept identical for both SBT1 and SBT2.

8.7 Particle Crushing

Table 8.8 summarises the breakage index values for all Materials for SBT1, SBT2 and SBT3.

Table 8.8: Breakage Indices

Material	Breakage Index, B _I (%)		
	SBT1	SBT2	SBT3
A	8.8	4.0	4.4
B	12.1	7.1	5.5
C	4.3	2.5	2.1

Comparing the values from Table 8.8 it is evident that Material B crushes the most and Material C the least, for all types of shear box testing. This is thought to be a result of:

- Concrete based particles (Material A and B) crushing more than brick based particles (Material C) due to the weaker nature of their cement to cement and / or cement to aggregate bonds.
- The further processed concrete based material (B) having more micro-cracking on their particles, which may lead to greater crushing in Material B during shear.

Angular particles crush more during shear tests, but there is no obvious correlation between the results of the Flakiness and Elongation ratios with the amount of particle breakage of the materials. Therefore the differences in ease of breakage do not appear to be an effect of particle shape.

As discussed in Section 8.6, the two parameters varied during the shear box tests were the maximum particle size and specimen density. Their effect on particle crushing is discussed below:

1. Maximum particle size - From Table 8.7 it can be seen that there is approximately 50% less crushing occurring in SBT3 compared to SBT1, for all three materials. This increase in the degree of crushing with increasing particle size has been previously reported for natural aggregates (Hardin, 1985, MacDowell and Bolton, 1998 and Indraratna *et al* 1998).
2. Specimen density - The decreases in Breakage Index between SBT1 and SBT2 are given in Table 8.9.

Table 8.9: Reduction in values of B_I between SBT1 and SBT2

Material Type	SBT1	SBT2	Reduction of B_I
Material A	8.8	4.0	4.8 (54%)
Material B	12.1	7.1	5.0 (41%)
Material C	4.3	2.5	1.8 (41%)

Particle crushing reduces with reducing density. This has been observed by others (De Souza, 1958, Hendron 1963 and Hagerty *et al*, 1993) and is mainly attributed to the fact, that since the materials are not compacted so densely then they have the ability to rearrange during shear rather than to crush.

Table 8.10 compares the AIV and ACV tests and breakage factors. The numbers 1, 2 and 3 rank the amount of particle crushing with 1 showing the materials that crush the least and 3 the most.

Table 8.10: Comparison of AIV and ACV tests with particle crushing results

Mat	AIV	ACV	Particle Crushing		
			SBT1	SBT2	SBT3
A	1	1	2	2	2
B	3	2	3	3	3
C	2	3	1	1	1

The comparison shows that there is no direct connection between the amount the materials crush as a whole and on the AIV and ACD tests. It is believed that for the specific three types of materials investigated the AIV and ACV tests do not provide reliable information on the strength of the particles.

Demolition waste materials crush under stress application, with the amount of crushing reducing with maximum particle size and specimen density. This behaviour has also been observed for natural granular materials. Material C crushed less than Material A and B and this was attributed to individual particle strength due to the existence of the weaker cement to cement and cement to aggregate bond in the crushed concrete particles. This might cause the composite particles (crushed concrete particles) to break more than the homogeneous ones (crushed brick particles). Further testing, of the strength of individual particles' strength, is needed though to verify this.

8.8 Introduction to Shear Box Testing

As discussed in Section 8.6 the parameters investigated in this project as for their effect on shear behaviour are specimen density (SBT2), maximum particle size (SBT3) and normal stress (SBT1, SBT2 and SBT3). The moisture content of the samples was kept the same throughout the shear box test programme and the change in maximum particle size was not associated with any changes in the particle shape of the materials.

The discussion of the behaviour of the materials under shear are presented as follows:

1. Initial Observations on Behaviour under Shearing - Section 8.9
2. Influence of Specimen Density - Section 8.10
3. Influence of Maximum Particle Size - Section 8.11

4. Influence of Normal Stress - Section 8.12
5. Comparison with Natural Granular Materials - Section 8.13
6. Engineering Fill Applications - Section 8.14
7. Comparison with other Recycled Aggregates – Section 8.15

8.9 Initial Observations on Behaviour during Shearing

Figure 8.1 shows the mean stress-strain behaviour curves (τ - ϵ_a curve) of all the materials for SBT1, SBT2 and SBT3, at 95 kPa normal stress. A similar graph form was observed for all normal stresses for the different shear box tests.

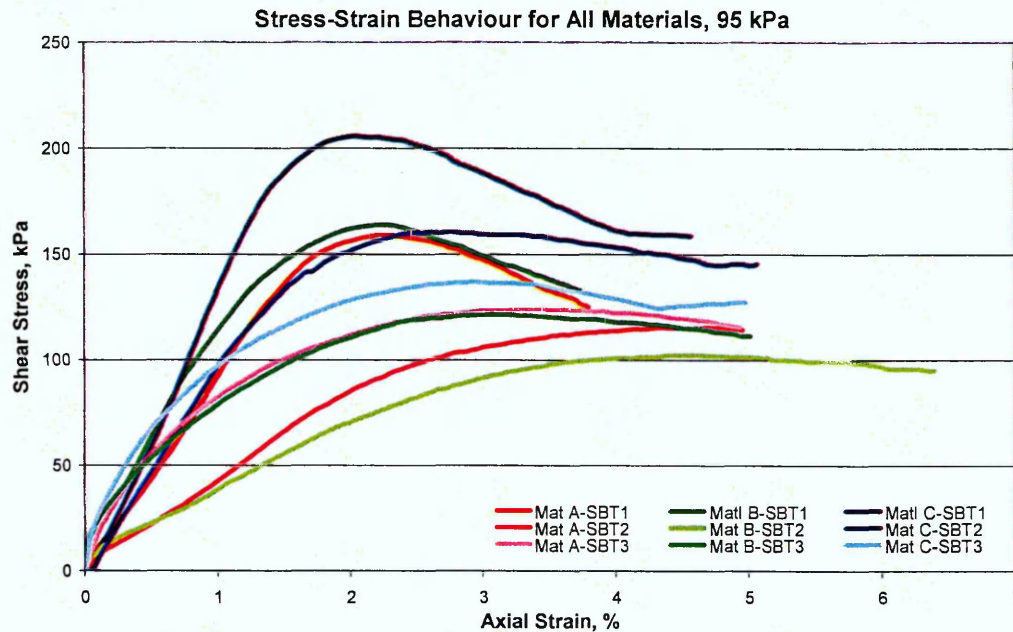


Figure 8.1: Mean stress-strain behaviour curves at 95 kPa normal stress

All the materials exhibit a strain-softening behaviour observed in well-compacted soils for SBT1. The behaviour of the Materials for SBT2 tends towards a less well-compacted soil and for SBT3 this less well-compacted soil behaviour is more evident. This behaviour is believed to be related to the particle crushing of the materials which is the highest in SBT1 and lowest in SBT3. It can also be a result of the density and degree of packing of the materials. Comparing SBT1 and SBT2 it can be said that the higher degree of compaction, in SBT1 compared to SBT2 and SBT3, causes a more sharp rise in the shear stress with axial strain. This is due to the denser packing of the particles and therefore there is less re-arrangement of the particles compared to SBT2 and SBT3.

In the majority of the results (apart from SBT1, 143 and 238 kPa and from SBT2, 143 kPa) the stress strain curves of Material A and B appear to be closely spaced despite the differences in their properties (gradation, particle shape, crushing and AIV and ACV). This demonstrates a similarity in the behaviour of the concrete based materials, as far as their stress strain behaviour is concerned. This can be a result of:

1. The differences in parameters of these two specific materials may have minor effect and other parameters such as normal stress may be the dominating factor on their shear-strain behaviour
2. These parameters may be "cancelling out" the effect of each other. For example, Material A crushes less and is more angular than Material B which, according to Literature Review, would mean that Material A should have higher values of shear strength. Material B though is more broadly graded and this would mean that they have higher shear strength. The accumulative effect of these three parameters, though, may cause Material A and B to exhibit similar stress-strain behaviour.

The behaviour of Material C differs from Materials A and B something that was expected since it has a different composition (brick based). It exhibits higher values of shear stress and this is believed to be a result of its lower particle breakage and higher Cu value (Indraratna *et al*, 1998). It is thought that the differences existing between the Flakiness Indices of Material A and B and Material C (12.9, 7.3 and 10.1 for A, B and C respectively) are quite low and they do not affect their differences in the shear strength levels.

Figure 8.2 shows this trend for all three materials, SBT1 and two different normal stresses.

In all the types of tests, for all the materials, the volumetric behaviour in the later stages of the tests where failure (peak of τ - ϵ_v graph) occurs is of volumetric expansion as has been illustrated in Section 7.3.3. All graphs are not repeated in this section of the thesis for ease of reading.

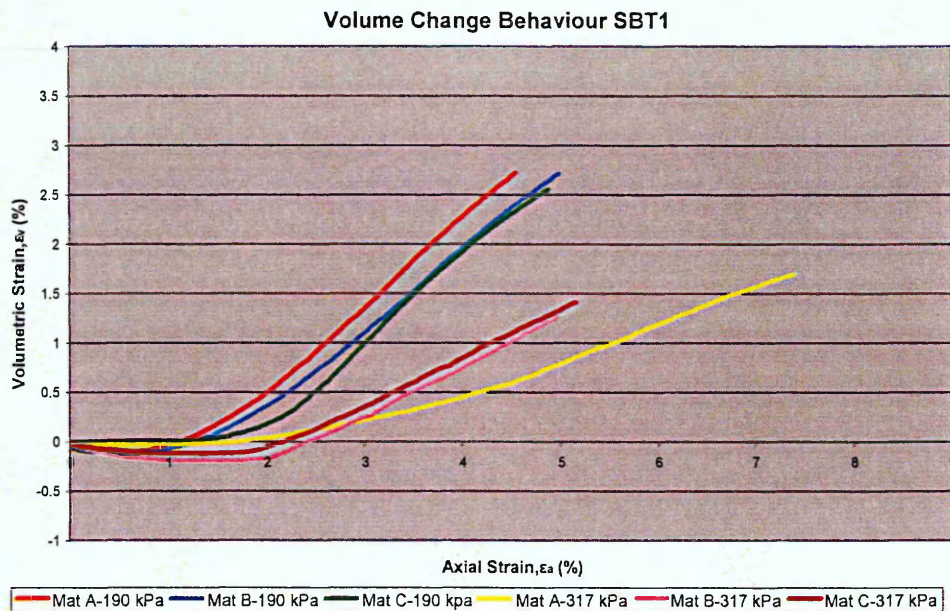


Figure 8.2: Volumetric behaviour for SBT1, 190 and 317 kPa normal stress levels

Figure 8.3 presents the average peak shear to normal stress behaviour of the three materials for SBT1.

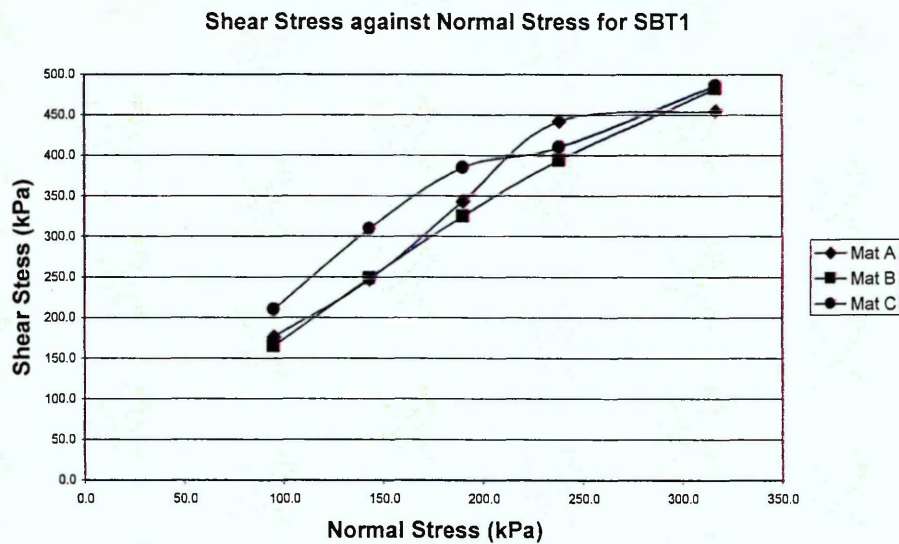


Figure 8.3: Normal against shear strength for SBT1

Figure 8.3 shows that the shear-normal stress graphs display curvature and probably pass through the origin of the axes (zero cohesion). The curvature phenomenon has been observed in shear strength investigations for natural granular materials by others

(Marachi *et al*, 1972, Charles and Watts, 1980, Indraratna *et al*, 1993, Indraratna *et al*, 1998). The curvature is more evident for Material C and less for Material B.

The friction angles (based on a straight line from the origin to the measured shear at 317 kPa) were calculated to be 55°, 57° and 57° for Material A, B and C respectively. The values for Material A and C appear to be quite high compared to natural aggregates, but values of about 60° have been observed by Charles and Watts (1980) for sandstone and basalt of maximum particle size of 38 mm. Indraratna *et al* (1998) have found friction angles of 66 and 67° for basalt at low normal stresses and attributed them to the interparticle stresses being less than the crushing strength of the materials and the ability of particles to dilate more. Further, Fannin *et al* (2005) have calculated friction angles up to 71° for in situ tests in mountain soils at British Columbia. Concluding:

1. The materials behaviour is of well compacted materials for SBT1 and well to poorly compacted materials for SBT2 and SBT3. This has been attributed to particle crushing
2. All materials exhibit volumetric expansion at failure, typical of densely packed materials.
3. The shear-normal stress relation exhibits curvature and the values of friction angles appear to be quite high when compared to natural aggregates.

8.10 Influence of Specimen Density on Behaviour during Shearing

8.10.1 Influence on stress-strain behaviour

Figure 8.4 shows the axial strain values at failure (peak of $\tau - \varepsilon_a$ graph) for Material A, B and C for SBT1 and SBT2.

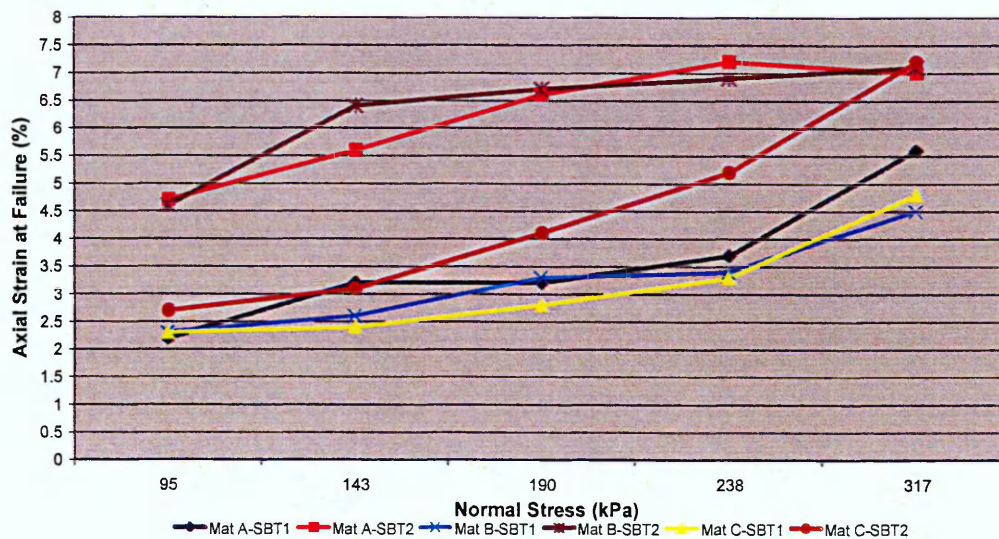


Figure 8.4: Axial strain values at failure for SBT1 and SBT2

From the results, it can be concluded that the axial strain at failure (peak of τ - ϵ_a graph) increases, quite significantly when the dry density reduces. This behaviour has been observed by others for natural aggregates (Pike, 1973, Charles and Watts, 1980) and it has been attributed to the more loose packing of the particles (Charles and Watts, 1980). Particles undergo compression, rearrangement, compression and breakage stages under shearing forces (Varadarajan *et al*, 2003). Looser packing allows for more rearrangement of particles and therefore larger axial strain is required for failure.

8.10.2 Influence on volume change behaviour

Figure 8.5 presents the volumetric strain values at failure for SBT1 and SBT2 for all three materials.

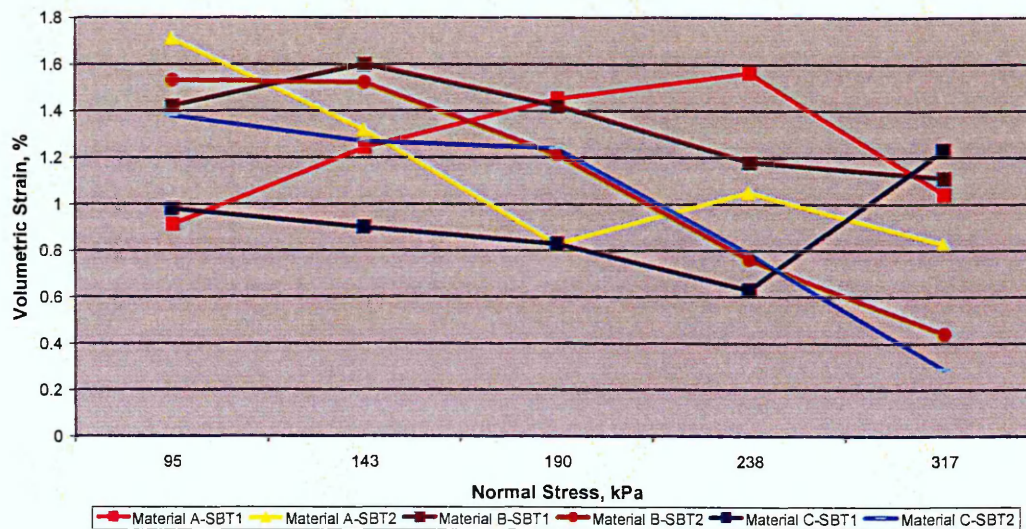


Figure 8.5: Volumetric strain values at failure for SBT1 and SBT2

The results present a mixed picture of the volumetric behaviour of the materials when the specimen density changes. Particle breakage decreases with the reduction in dry density and it was expected that, if that was the dominant factor, the volumetric dilatancy would increase. This does not occur though and the volumetric dilatancy at failure (between SBT1 and SBT2) increases at lower normal stresses but appears to decrease as the normal stress increases. There is not therefore a specific pattern of influence on the volumetric strain from the change in the specimen density. This may be due to the fact that the change in dry density was not large enough to produce any specific pattern on its influence on volumetric behaviour and at this level of change

normal stress is the dominant factor on the volumetric behaviour of the materials. Further testing with higher range of densities is required to verify or refute this conclusion.

8.10.3 Influence on shear strength

Figure 8.6 presents the shear-normal stress curves for SBT1 and SBT2 in the form of best fit trendlines.

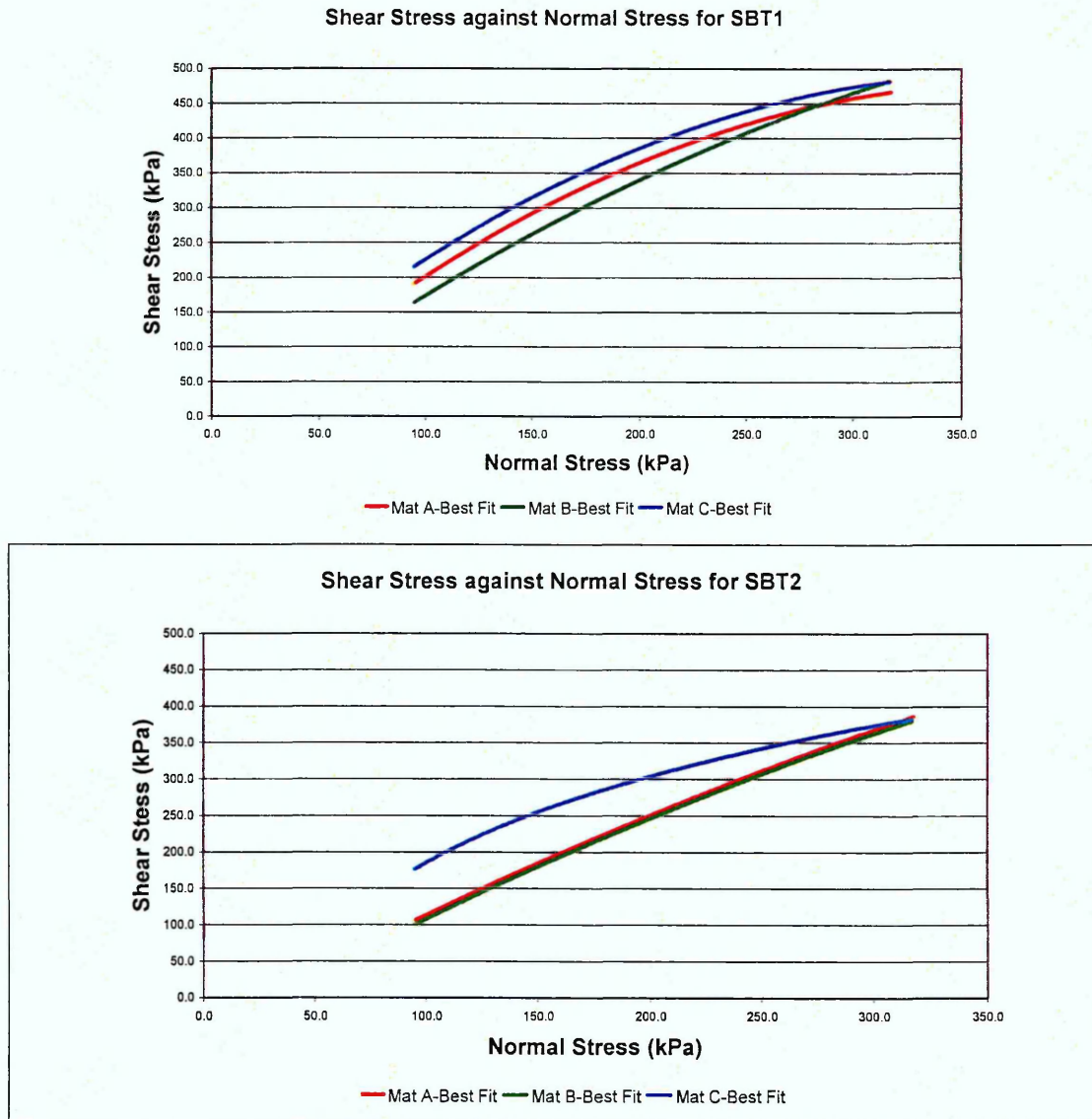


Figure 8.6: Shear-normal stress curves for SBT1 and SBT2

Six different trendline types were applied in the graphs. All the best fit trendlines pass through the axes origin point (0, 0). The best fit graphs presented in this discussion are

produced by the type of trendline that has a coefficient of determination (R^2) closest to one. The coefficient of determination indicates how closely the estimated values for the trendline correspond to the data. A trendline is most reliable when its coefficient of determination value is at or near 1.

The best fit graphs for SBT1 and for Material A, B and C had a coefficient of determination of 0.98, 0.99 and 0.99 respectively. For SBT2 the coefficients of determination were 0.99 for all three materials.

As discussed previously the shear to normal stress graphs display curvature and pass through the origin of the axes for SBT1. For SBT2 though this behaviour is only observed for Material C. There is no obvious reason for this and further testing with more types of brick based materials is required to determine if this is a trend generally met for brick-based materials or specifically for Material C. The further processed concrete based material (B) and the concrete based material obtained straight from the demolition site (A) exhibit an almost linear and identical relation in the SBT2 tests. The possible reasons for this similarity have been discussed in Section 8.9.

Table 8.11 tabulates the values of friction angles, for all normal stresses for all three materials together with their percentage reductions from SBT1 to SBT2. The friction angles have been calculated as secant values from the origin to the normal stress level indicated.

Table 8.11: Friction angle values for SBT1 and SBT2

Percentage reduction, % given by: (friction angle for SBT1-friction angle for SBT2)/friction angle of SBT1									
Normal Stress, kPa	Material A			Material B			Material C		
	SBT1	SBT2	%	SBT1	SBT2	%	SBT1	SBT2	%
95.0	62	51	17	60	53	13	66	60	8
143.0	60	53	12	60	55	9	65	60	8
190.0	61	51	16	60	55	8	64	58	9
238.0	62	51	17	59	55	7	60	56	7
317.0	55	51	8	57	54	5	57	54	5

The results show that the friction angles decrease when the specimen density reduces as expected due to the reduced packing of particles at lower densities. Particle breakage

also decreases with reduced density and this could cause an increase in the strength of the materials (Varadarajan, *et al*, 2003). In this discussion, though, friction angles increase with density and despite the reduced particle crushing. Particle breakage appears therefore to:

1. Not affect the behaviour of the materials, or
2. is a secondary factor to specimen density and its effect may not be visible.

The largest reductions of friction angles are met for Material A. Material A, which is the less processed from all three materials, has the least broad gradation. This results in reduced capacity of filling the voids in the specimen during rearrangement of particles under shearing. For the same materials, when the density reduces the amount of voids increases. Material B and C with more broad gradation may be able to fill this increased amount of voids faster and therefore exhibit smaller percentages of friction angle reduction. This is a possible explanation and more testing with manufactured gradings of the same type of materials is needed to verify it.

The reductions are more significant for lower normal stresses. At higher values of normal stress the reduction percentages are smaller (5-8%), which may also be an indication that the effects of dry density is minimised as the normal stress increases. A more comprehensive discussion on the influence of normal stress on the behaviour of the materials under shear is given in Section 8.12.

8.10.4 Summary of conclusions

The discussion on the influence of specimen density has shown:

- The axial strain at failure (peak of τ - ϵ_a graph) increases with reduced specimen density
- The volumetric strain decreases or increases with reduced density and the changes appear to be influenced by the levels of normal stress
- The friction angles reduce with reduced density

8.11 Influence of Maximum Particle Size on Behaviour under Shearing

8.11.1 Influence on stress-strain behaviour

Figure 8.7 shows the axial strain values at failure (peak of τ - ϵ_a graph) for Material A, B and C for SBT1 and SBT3.

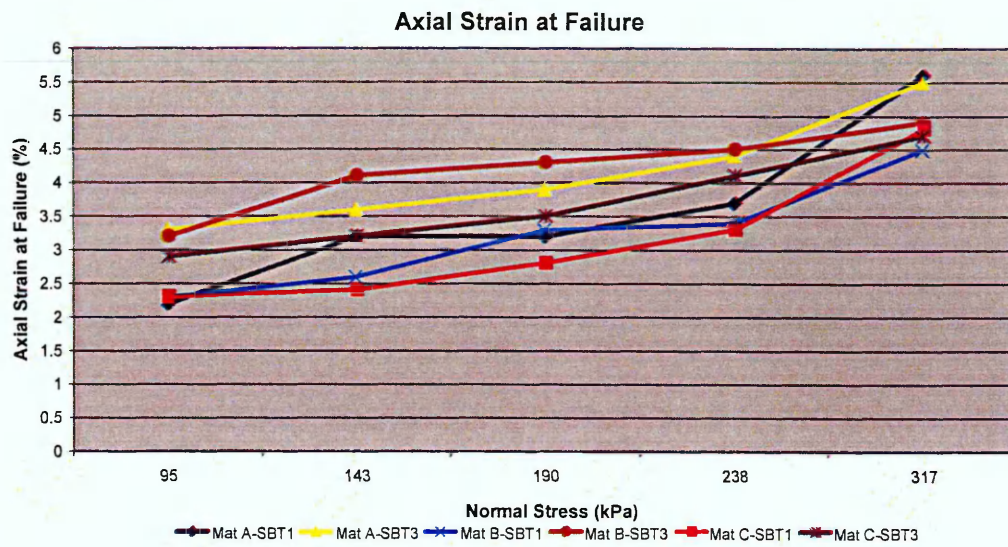


Figure 8.7: Axial strain values at failure for SBT1 and SBT3

The results show that the reduction of maximum particle size used in this experimental programme increases the axial strain at failure.

Particle crushing reduces with reduced maximum particle size, as also shown by McDowell and Bolton (1998) and this could be a reason for the increased axial strain values. On the other hand though, Varadarajan *et al* (2003) have shown that the axial strain at failure increases with maximum particle size when they tested two materials (of alluvial and metamorphic rock origin) with maximum particle sizes of 25, 50 and 80 mm. The difference in the behaviour between these natural and recycled materials can be due to:

- Particle crushing being the dominant factor in the stress-strain behaviour of the materials when maximum particle size reduces or
- The difference in maximum particle sizes is not large enough to show any clear, similar to natural aggregates, trends.

Testing the materials with larger maximum particle size differences would be able to determine which of the above explanations are true.

Another interesting observation is that the effect of maximum particle size become small at higher normal stresses where differences of -0.1, 0.4 and 0.1% are met for material A, B and C respectively at 317 kPa normal stress. This has also been encountered by Indraratna *et al* (1993) for material with maximum particle sizes of 38.1

and 25.4 mm for normal stresses above 300 kPa. A more comprehensive discussion on the influence of normal stress on the behaviour of the materials under shear is given in Section 8.12.

8.11.2 Influence on volume change behaviour

Figure 8.8 presents the volumetric strain values at failure for SBT1 and SBT3 for Material A (concrete based and obtained straight for a demolition site), B (concrete based but furthered processed) and C (brick based and furthered processed) and for all normal stresses investigated in this project.

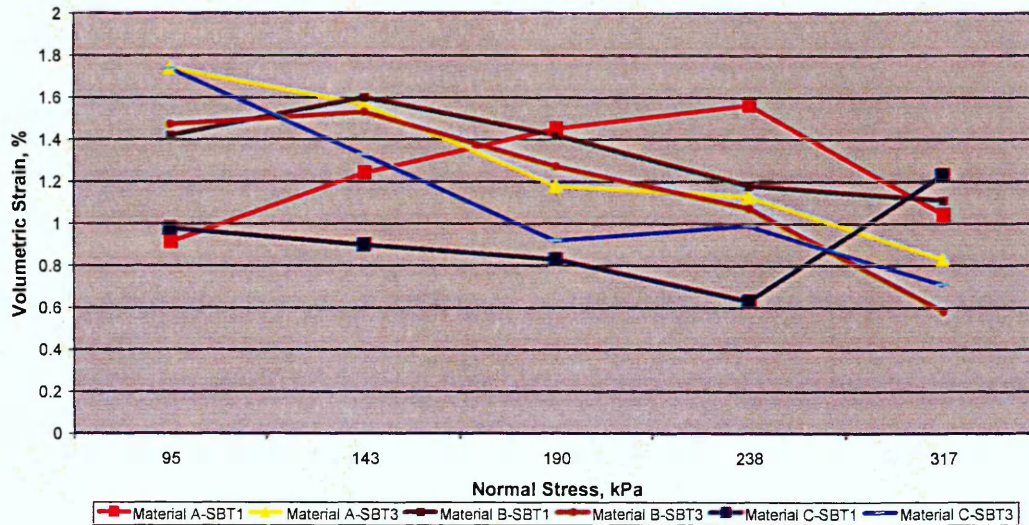


Figure 8.8: Volumetric strain values at failure for SBT1 and SBT3

The results on the effect of maximum particle size on volumetric behaviour present a mixed picture, as in the discussion on the influence of specimen density on volumetric behaviour of the materials (Section 8.10.2). The volumetric dilation at failure (between SBT1 and SBT3) increases at lower normal stresses but appears to decrease as the normal stress increases. This may be a result of the fact that the change in maximum particle size was not large enough to produce any specific pattern on its influence on volumetric behaviour as discussed for the stress-strain curves in Section 8.11.1. Further testing with higher range of maximum particle sizes is required though to verify or refute this conclusion.

The changes in volumetric strains at failure appear to depend on the normal stress levels and that is discussed in Section 8.12.

8.11.3 Influence on shear strength

Figure 8.9 presents the shear-normal stress curves for SBT1 and SBT3 in the form of best fit trendlines. The coefficients of determination were 0.99 for all three materials.

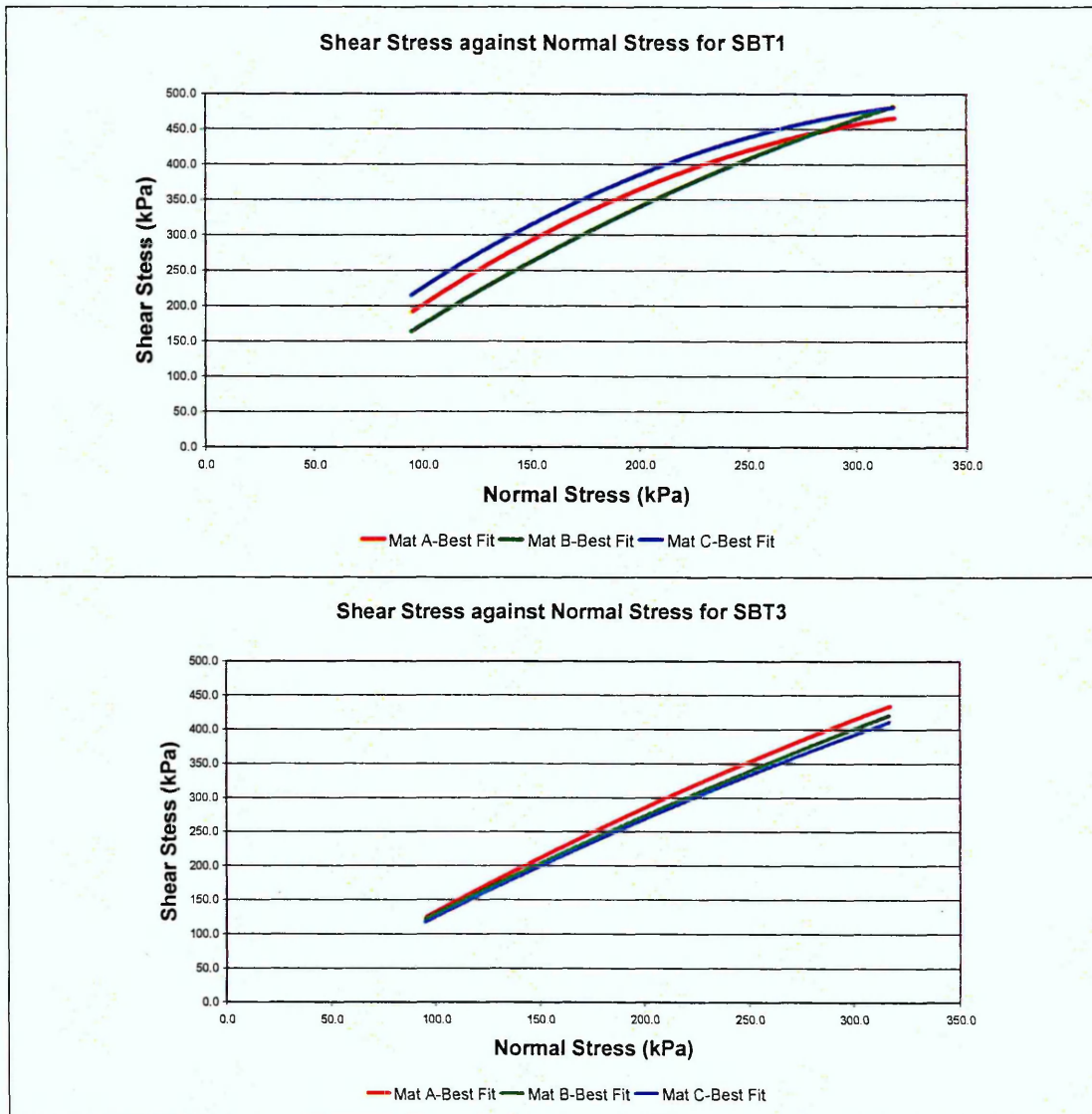


Figure 8.9: Shear-normal stress curves for SBT1 and SBT3

As discussed previously the shear to normal stress graphs display curvature and pass through the origin of the axes for SBT1. For SBT3 though behaviour of all the materials appear to be linear. This is believed to be a result of the significantly reduced particle breakage of particles (by 50%, 55% and 51% for Material A, B and C respectively).

As established in the Literature Review, the effect of maximum particle size on the friction angles of materials can not be generalised for all materials. Table 8.12 presents

the values of friction angles, all three materials together with their percentage reductions from SBT1 to SBT3. The friction angles have been calculated by as secant values from the origin to the normal stress level indicated, because the graphs curve and pass through the origin of the axes, exhibit zero cohesion.

Table 8.12: Friction angle values for SBT1 and SBT3

Percentage reduction, % given by: (friction angle for SBT1-friction angle for SBT2)/friction angle of SBT1									
Normal Stress, kPa	Material A			Material B			Material C		
	SBT1	SBT3	%	SBT1	SBT3	%	SBT1	SBT3	%
95.0	62	47	23	60	52	13	66	55	16
143.0	60	49	18	60	53	12	65	55	16
190.0	61	51	17	60	55	8	64	53	16
238.0	62	51	16	59	53	10	60	52	13
317.0	55	50	9	57	53	6	57	52	9

The values of Table 8.12 show that the friction angles of all the materials reduce when the maximum particle size decreases from 37.5 mm to 28 mm. Particle breakage also decreases with the reduced maximum particle size. As discussed in Section 8.10.3 this could cause an increase in the strength of the materials (Varadarajan, *et al*, 2003). In this discussion, though, friction angles increase with maximum particle size despite the reduced particle crushing. Particle breakage appears therefore to:

1. Not affect the behaviour of the materials, or
2. is a secondary factor to maximum particle size and its effect may not be visible.

8.11.4 Summary of conclusions

The discussion on the influence of maximum particle has shown:

- The axial strain at failure increases with reduced maximum particle size
- The volumetric strain vary with reduced maximum particle size, with no clear correlations, and the changes appear to be affected by the normal stress levels
- The friction angles reduce when maximum particle size is reduced

Comparing the discussions on both Sections 8.10 and 8.11 it is evident for the three materials and two different maximum particle sizes (37.5 and 28 mm) and specimen densities (1.8 and 1.6 Mg/m³) that:

- The stress-strain relations are affected more from the reduction in density than in maximum particle size
- The influence on the volumetric behaviour of the materials is inconclusive for both maximum particle sizes and densities
- The friction angles are affected more by the reduction in maximum particle size than the reduction in specimen density

It has to be noted though that these observations are true for the specific materials and values of maximum particle size and specimen density parameters. Larger changes in these parameters may show different trends and this needs further investigation.

8.12 Influence of Normal Stress on Behaviour under Shearing

8.12.1 Influence on stress-strain behaviour

The graphs of Section 7.3.1 on the stress-strain relations of all the materials show that the axial strain at failure (peak of τ - ϵ_a graph) increases with normal stress (graphs are not repeated for ease of reading). The values of axial strain at failure are plotted against normal stresses (as best fit trendlines) for Material A, B and C in Figure 8.10.

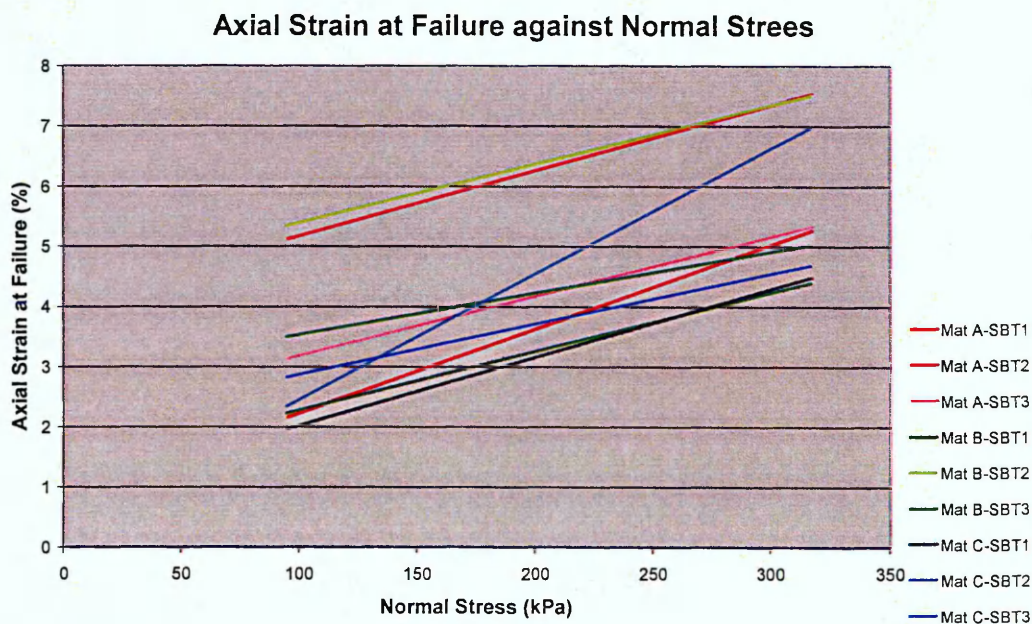


Figure 8.10: Influence of normal stress on axial strain at failure

The results indicate that the amount of axial strain at failure (peak of τ - ϵ_a graph) increases with normal stress, something that has been observed by others (Marsal, 1967, Charles and Watts, 1980, Indraratna et al, 1993, Indraratna et al 1998 and Varadarajan, *et al*, 2003) when testing granular materials.

The best fit graphs appear to be of similar gradients for SBT1 and SBT3, but exhibit completely different trends between SBT1 and SBT2. As discussed in Section 8.11.4 the changes in specimen density affect the stress-strain relations of the materials more than the reductions in maximum particle size. The best fit trendlines of Figure 8.10 appear to verify these observations.

8.12.2 Influence on volume change behaviour

Figure 8.11 presents the influence of normal stress on mean volumetric strain at failure (peak of τ - ϵ_a graphs). It shows the actual value points for each material and test and the linear best fit trendlines.

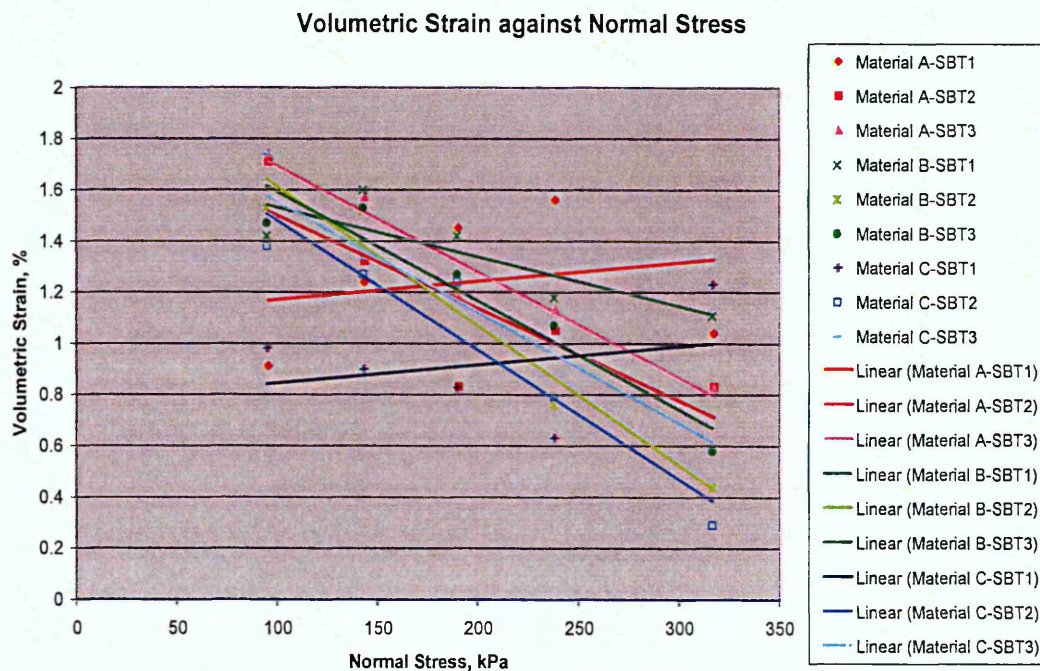


Figure 8.11: Influence of normal stress on volumetric strain at failure

The level of volumetric strain (dilatancy for all the tests performed in this investigation) reduces with normal stress apart from SBT1 for Material A and C. Others (e.g. Marsal, 1967, Charles and Watts, 1980, Brown, 1988, Indraratna *et al*, 1993, Indraratna *et al*,

1998 and Varadarajan *et al*, 2003) have observed this for natural aggregates and shown that at high normal stresses materials exhibit compression.

Varadarajan *et al* (2003) attributed the reduction of volumetric dilatancy to the increased particle breakage and therefore increased compression behaviour at higher normal stresses. Similar results were observed by Lade *et al* (1996). This can not be verified for these results though because no particle crushing tests were performed for individual normal stresses.

The materials exhibit the largest particle crushing when sheared with the largest density (1.8 Mg/m^3) and maximum particle size (37.5 mm) for SBT1. There is a possibility therefore that their behaviour is heavily related to the crushing of particles for them to exhibit any specific trend of volumetric dilatancy reduction with increasing normal stress.

Figure 8.12 presents the best fit trendlines for all the materials for SBT2 and SBT3 and their possible continuations after the normal stress of 317 kPa. These have been based on their graphical form and assume that the rates will not change dramatically at higher normal stresses. They show the level of normal stress at which it is estimated the volumetric behaviour of the materials at failure (peak of τ - ϵ_a graphs) will change from dilatancy to compression.

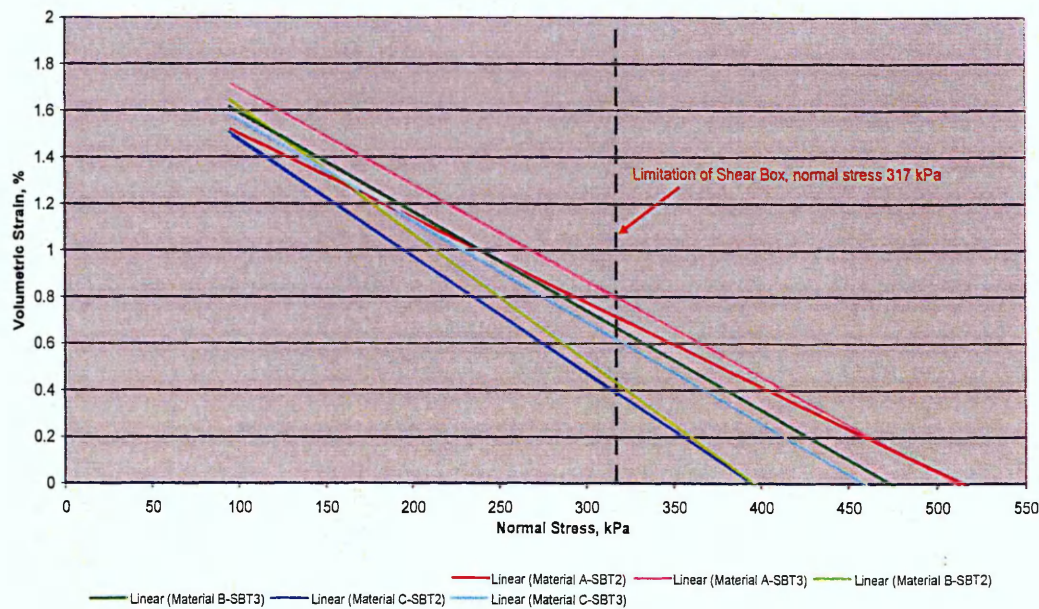


Figure 8.12: Possible continuations of the best fit graphs for Materials A, B and C

Figure 8.12 shows that at high normal stress levels the volumetric behaviour of the three materials is possibly of compression. This is another indication that the recycled materials behave similarly to natural aggregates. The estimations of this section are based on the materials and the range of normal stresses investigated in this project. Further testing with values outside the range of 95 to 317 kPa is required though to confirm or refute this.

Figure 8.13 shows the percentage changes in volumetric strain (ϵ_v) at failure (peak of $\tau - \epsilon_a$ graphs) for the different normal stresses investigated in this project.

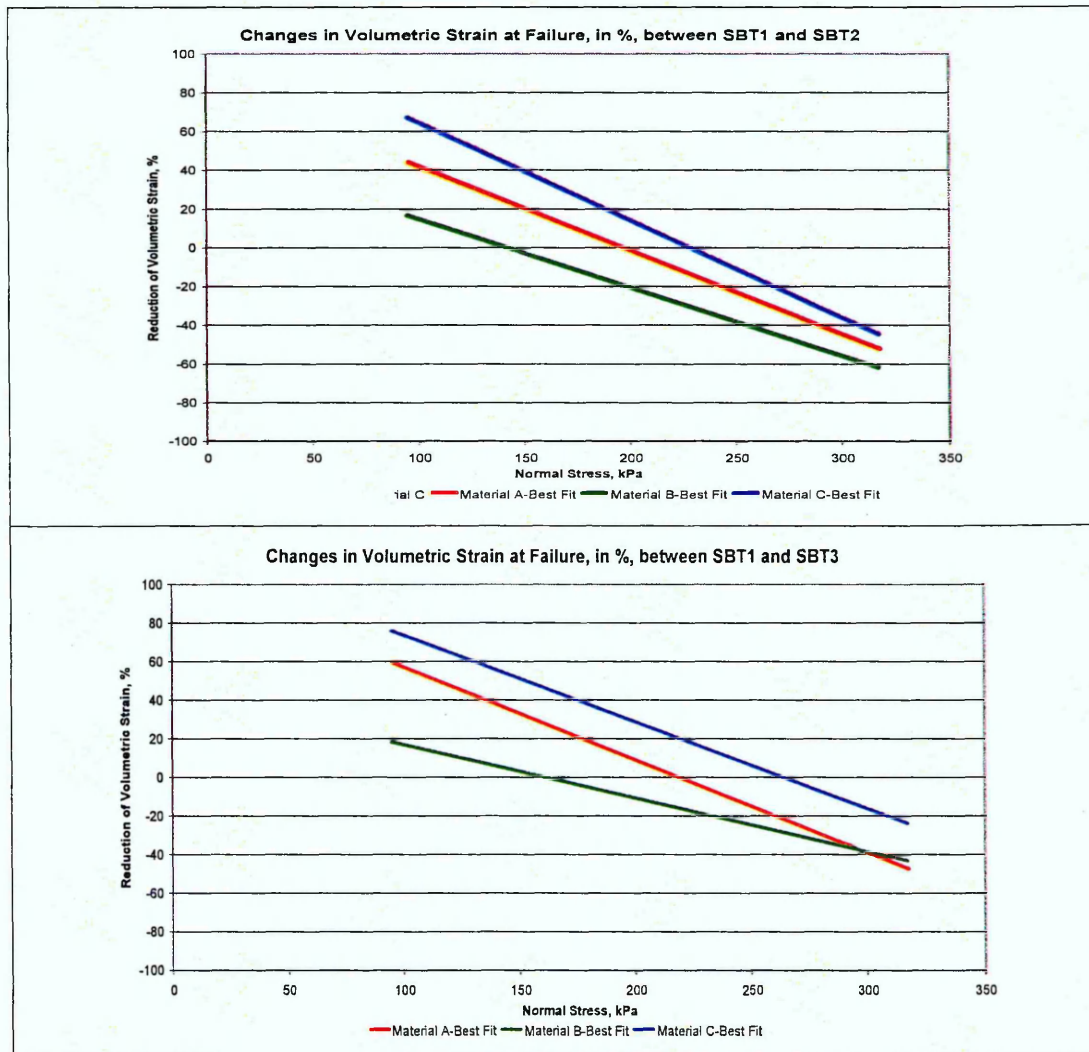


Figure 8.13: Changes in ϵ_v between SBT1 and SBT2 and SBT1 and SBT3

It has been discussed in Sections 8.10.2 and 8.11.2 that the volumetric strains at failure for all three materials reduce or increase when the specimen density or maximum

particle size decreases, i.e. there is no specific correlation on the effect of maximum particle size. The lack of specific trends was attributed to the normal stress being the dominant factor. The percentages are calculated by:

$$\frac{\epsilon_v \text{ at SBT1} - \epsilon_v \text{ at SBT2 or SBT3}}{\epsilon_v \text{ at SBT1}}$$

Positive values indicate increase in ϵ_v and negative decrease.

At low normal stresses there is an increase in the ϵ_v , when the values of SBT2 and SBT3 are compared with the values of SBT1. As the normal stress increases though, this increase in ϵ_v reduces and at specific normal stresses for each of the Materials becomes a volumetric strain decrease.

This level of normal stress where the difference of volumetric dilatancy becomes zero would be called "point of zero ϵ_v change" for the purposes of this discussion. Table 8.13 summarises the calculated normal stresses at the ϵ_v change inversion points.

Table 8.13: Point of zero ϵ_v change between SBT1 and SBT2 and SBT1 and SBT3

Normal stress, kPa		
Materials	SBT1 to SBT2	SBT1 to SBT3
A	195	220
B	145	165
C	230	270

The results of Table 8.13 show that Material B reaches the point of zero ϵ_v change at the lowest normal stress and Material C at the highest. The particle crushing results show that Material B crush the most and Material C the least. Varadarajan *et al* (2003) and Lade *et al* (1996) have found that at higher normal stresses increased particle breakage and therefore increased compression occurs. It is possible therefore that the materials that crush the easiest reach the point at which dilatancy decreases at lower normal stresses than stronger material.

As far as the volumetric behaviour of the materials is concerned it has been shown that:

1. The level of normal stress appear to be the dominant factor
2. There is a level of normal stress at which the effect on the volumetric strain of the specific changes of maximum particle size and specimen density, of this investigation,

becomes zero. These points have been estimated graphically and testing at these specific normal stresses is needed to establish these levels more accurately.

8.12.3 Influence on shear strength

Apart from affecting the shear stress, it has been well documented (Marsal, 1967, Leps, 1970, Marachi *et al*, 1972, Indraratna *et al* 1993 and Fannin, 2005) that an increase in normal stress reduces the friction angle of the materials. Figures 8.14 shows the values of friction angle in relation to normal stress in the form of polynomial best fit trendlines. The friction angles are based on a straight line from the axes origin to the measured shear stress at the investigated normal loads and are presented in the form of comparison between SBT1 and SBT2 and SBT1 and SBT3.

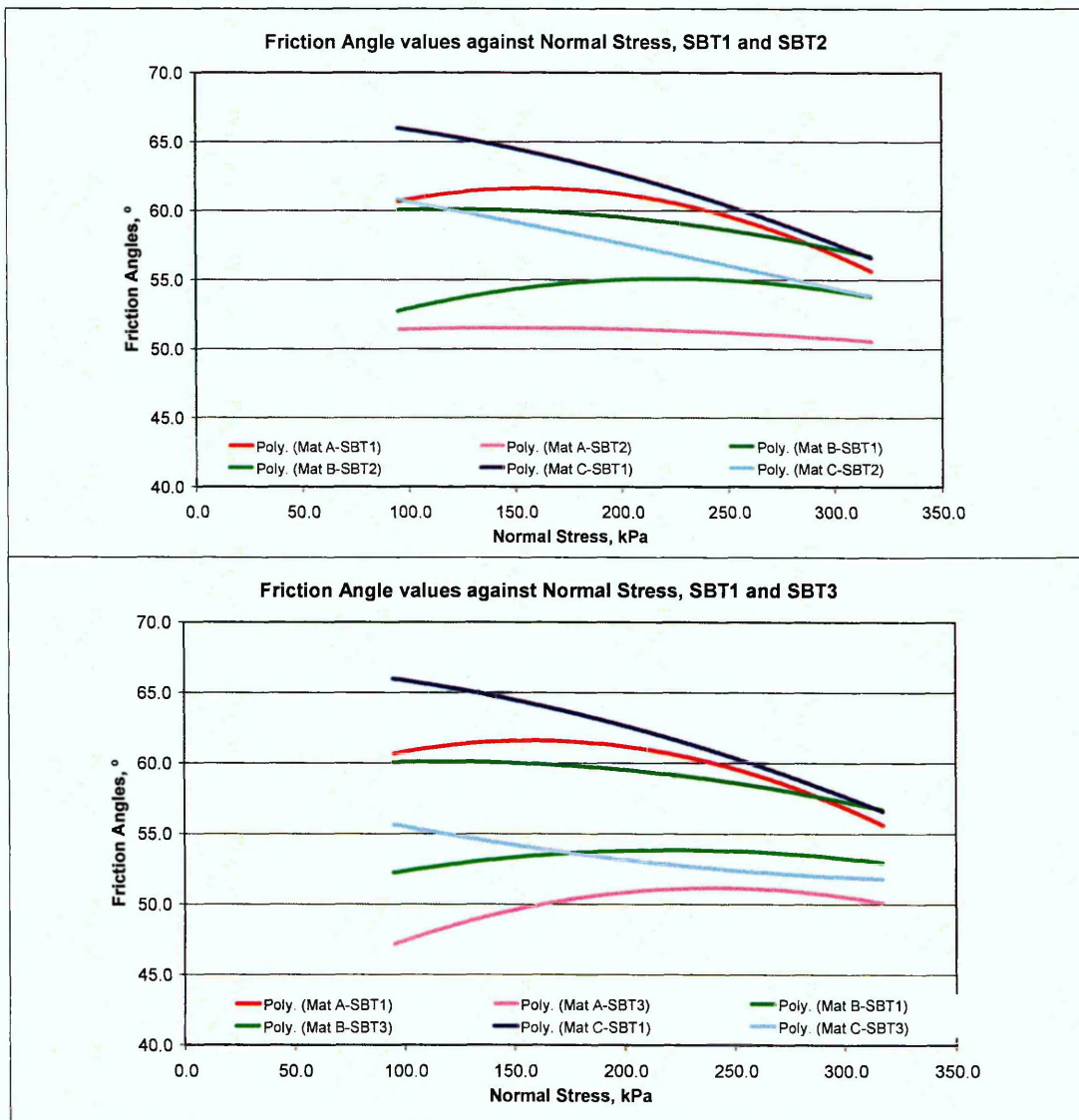


Figure 8.14: Friction angle values in relation to normal stress levels

From figure 8.14 it is observed that:

- For SBT1: The friction angles of Material A and B remain almost stable at 50° from 95 to 238 kPa and then drop by 7° and 3° respectively. The friction angles of Material C reduce continuously and from 66° at 95 kPa reach 57° at 317 kPa. This is close to reductions observed by Charles and Watts, 1980 (friction angle of basalt from about 60° to 50° from 100 to 300 kPa). On the other hand though, the reductions, though significant, appear to be less striking than the ones observed by Indraratna *et al* (1998) who noticed drops of friction angles from 67° to 46.8° from 20 kPa to 250 kPa.
- For SBT2: There is almost no effect on the friction angles for Material A and B from the values of 95 kPa to the values of 317 kPa. This indicates that under the test conditions of SBT2, and for the range of normal stresses investigated their friction angle is not affected. Material C exhibits a reduction on the friction angles of about 6.5°.
- For SBT3: The friction angles of the crushed concrete based materials do not appear to be affected by the increase in normal stresses. The friction angles of Material C reduce by approximately 3.5°. This reduction is significantly lower than the one observed for SBT2

Materials C appear to have the higher friction angles at low normal stresses. There is no clear correlation of this with particle shape since Materials C are not the most angular and therefore stronger materials. It is though possible that Material C exhibits the higher friction angles due to:

1. Higher Cu value that provides better packing of particles (Indraratna *et al*, 1998)
2. Having the least particle crushing, and therefore higher stiffness.

The differences in the values of friction angle, between SBT1 and SBT2 and SBT1 and SBT3, appear to reduce with increasing normal stress. Indraratna *et al* (1998) found that at higher normal stresses (< 400 kPa) the effects of particle size on the friction angles of the materials reduces. The same trend appears for the reduction in specimen density. Further testing at higher normal stresses is desirable, though, to be able to verify this conclusion.

The differences of the friction angles of Material C with those of the concrete based materials reduce as the level of normal stress increases. It is believed, though further

testing is needed, that there may be a specific level of normal stress at which the friction angles of the materials are similar despite their differences in individual properties. This indicates that at high normal stresses the differences in the properties of the three types of recycled materials (such as particle shape, grading and particle crushing) may not play a significant role and the normal stress dominates their behaviour under shear.

8.12.4 Summary of conclusions

The analysis of the results for the effect of normal stress on the behaviour of the materials under shear has shown:

- The axial strain at failure (peak of τ - ϵ_a graph) increases with normal stress
- The level of volumetric strain (dilatancy) reduces with normal stress
- The friction angles of the materials appear to reduce with normal stress levels

8.13 Comparison of Friction Angles with AIV and ACV Tests

The validity of the AIV and ACV tests in showing the strength of materials as a unit has been questioned for heterogeneous materials. This section compares these two tests with the friction angles of the materials in order to verify or refute this for the specific recycled aggregates investigated.

Table 8.14 and 8.15 present the values of AIV, ACV and friction angles for Materials A, B and C for SBT1 and SBT2, and SBT3 respectively. The numbers 1, 2 and 3 indicate the strength of the materials with 1 being the stronger, according to their friction angle and shear strength values, in that specific test. Where there are two matching numbers in a column, the results of those materials are too close and therefore considered identical.

Table 8.14: Comparison of ACV and AIV tests with SBT1 and SBT2

Mat	AIV	ACV	SBT1					SBT2				
			95	143	190	238	317	95	143	190	238	317
A	1	1	2	2	2	1	2	3	3	3	3	2
B	3	2	3	2	3	3	1	2	2	2	2	1
C	2	3	1	1	1	2	1	1	1	1	1	1

Table 8.15: Comparison of ACV and AIV tests with SBT3

Mat	AIV	ACV	SBT3				
			95	143	190	238	317
A	1	1	3	3	3	3	3
B	3	2	2	2	1	1	1
C	2	3	1	1	2	2	2

From the results it can be seen that there is no clear correlation between the values of the friction angles and the AIV and ACV tests. There is only one result that correlates between the different tests (For SBT1 at 238 kPa with the AIV). For the specific three types of the materials investigated in this project, the AIV and ACV tests can not be used to characterise their strength as a unit (i.e. their complete grading), and this is due to the heterogeneous nature of the materials.

8.14 Comparison with Natural Granular Materials

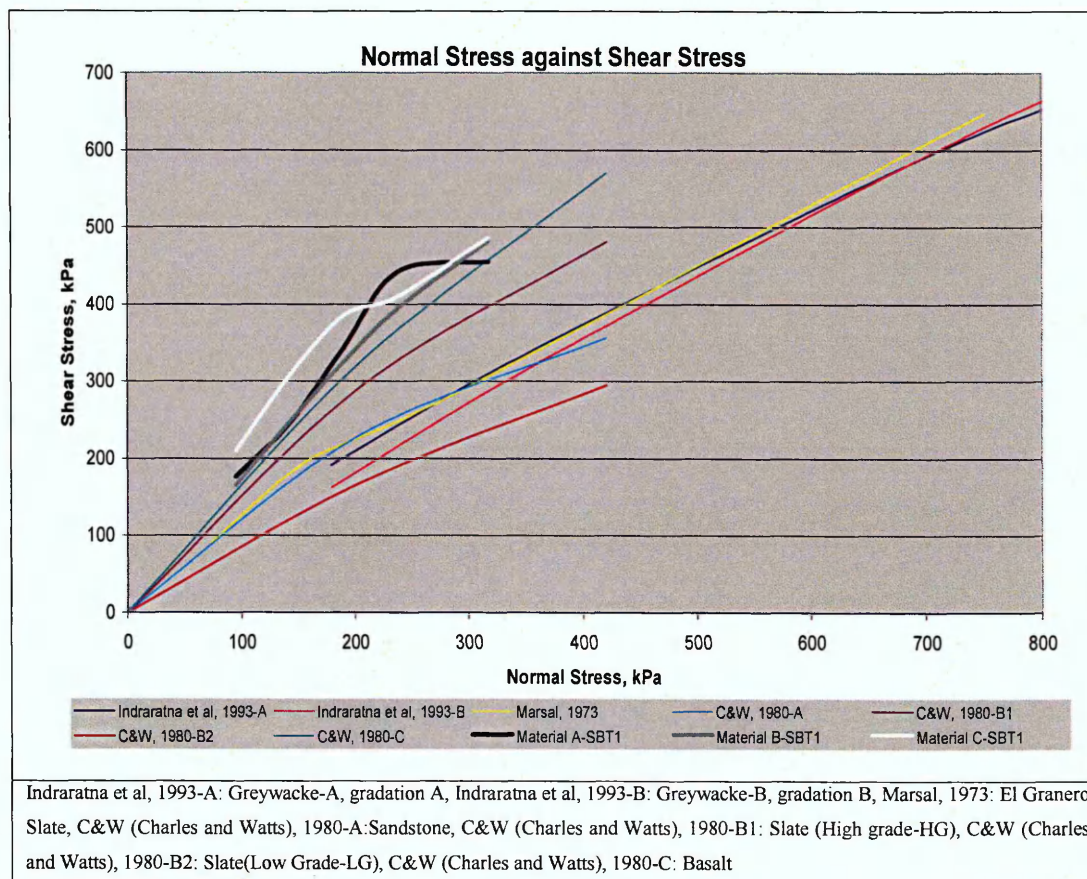


Figure 8.15: Shear-normal stress envelopes

Figure 8.15 presents the shear-normal stress envelopes for Materials A, B and C for SBT1 together with the envelopes of other investigations. Table 8.16 summarises the characteristics of all these Materials.

Table 8.16: Characteristics of the tests compared in Figure 8.15

Type of Material	d_{\max} (mm)	Specimen Size Ratio	Density
Greywacke-A	38	8	1.85 Mg/m ³
Greywacke-B	25	12	1.85 Mg/m ³
El Granero Slate	200	5.7	1.9 Mg/ m ³
A: Sandstone	38	6	2 Mg/ m ³
B1: Slate (HG)	38	6	2.1 Mg/ m ³
B2: Slate (LG)	38	6	1.8 Mg/ m ³
C: Basalt	38	6	2.1 Mg/ m ³
Material A-SBT1	37.5	8.1	1.8 Mg/ m ³
Material B-SBT1	37.5	8.1	1.8 Mg/ m ³
Material C-SBT1	37.5	8.1	1.8 Mg/ m ³

The specific natural materials were chosen because they have similar maximum particle size and density to the parameters of SBT1. The natural granular materials compared were tested in large triaxial equipment and the specimen size ratio is the ratio of the maximum particle size over the diameter of the specimen. For the crushed demolition waste materials the ratio of the maximum particle size over the size of the shear box side was used.

The envelopes of Figure 8.15 show that the demolition waste materials exhibit the steepest rise in shear stress with normal stress (i.e. greater stiffness). Not all data needed (e.g. particle shape and breakage indices) for a direct comparison is available. The graphs though, provide an indication on the strength and shear-normal stress behaviour of natural and demolition waste material:

1. They show the curvature on the envelopes of natural granular materials, which is another indication of the similarity of behaviour of natural aggregates with Material A, B and C.

2. It is possible that, with the curvature exhibited by Materials A, B and C, at higher normal stresses, the envelopes of demolition waste and natural materials meet - Further investigation is needed thought to substantiate this.
3. The higher values of shear stress at any given strain exhibited by Materials A, B and C might be a result of higher individual particle strength. Unfortunately no such data is available for the materials compared and the results of the AIV and ACV tests can not be used reliably as an indication of particle strength for Material A, B and C.

Pike (1973) conducted shear box tests on 300 mm square specimens for number of materials. Figure 8.16 presents the shear-normal stress envelopes for Materials A, B and C for SBT1 together with the envelopes of five granular materials tested by Pike (1973).

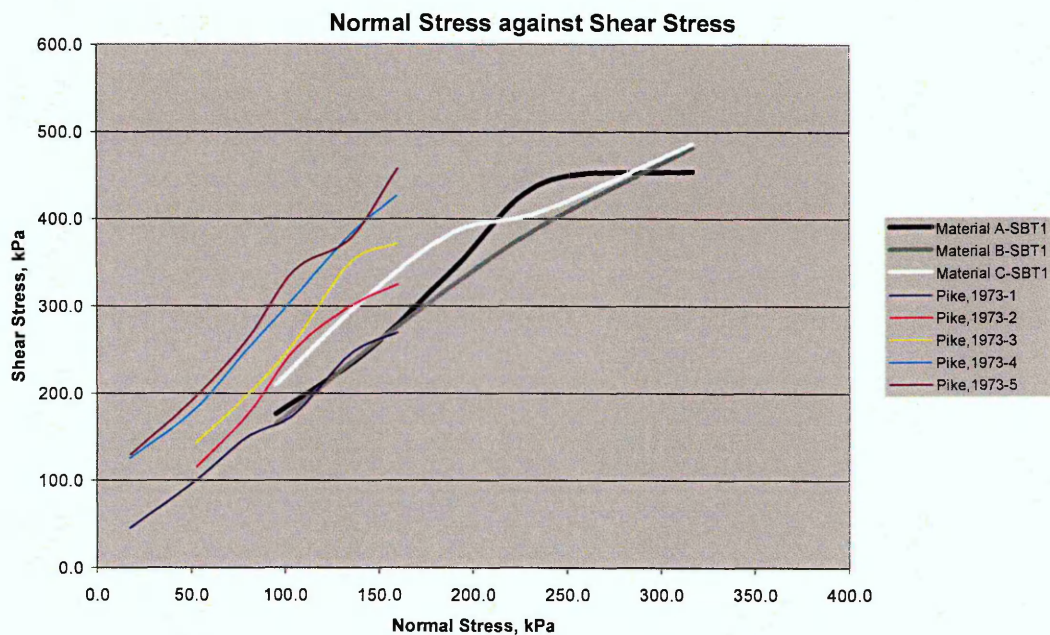


Figure 8.16: Shear-normal stress envelopes comparison

The envelopes of Figure 8.16 show that the demolition waste materials exhibit the similar rise in shear stress with normal stress compared to materials 1, 2 and 3. Materials 4 and 5 appear to have greater stiffness than Material A, B and C.

Table 8.17 shows the types of materials presented in figure 8.16 and their testing parameters.

Table 8.17: Characteristics of the Materials compared in Figure 8.16

Materials	$d_{max}(mm)$	Specimen Size Ratio	Density
A	37.5	8.1	1.80 Mg/m ³
B	37.5	8.1	1.80 Mg/m ³
C	37.5	8.1	1.80 Mg/m ³
Pike, 1973-1, Bridport, Flint	40	7.5	1.83 Mg/m ³
Pike, 1973-2, Rugeley, Quartzite	40	7.5	1.82 Mg/m ³
Pike, 1973-3, Stanley Ferry, Gritstone	40	7.5	1.76 Mg/m ³
Pike, 1973-4, Holcombe, Limestone	40	7.5	1.82 Mg/m ³
Pike, 1973-5, Corby, Slag	40	7.5	1.75 Mg/m ³

Since the densities investigated are similar between the five materials and Materials A, B and C this can not be the reason for these differences. Also material 4 are characterised as rounded and material 2 as mixed so there is no direct correlation between size and strength. Pike (1973) tested the materials dry and Materials A, B and C were tested with a moisture content of 2%. Due to this the moisture content could not have had a significant effect on the strength properties of the materials in this comparison. Adding to this the maximum particle size differences are very small to have contributed significant to the differences in values exhibited. The most probable reason for the differences between the five materials and Materials A, B and C is their particle strength, but due to the lack of data for the five materials tested by Pike (1973) and the unreliability of the AIV and ACV tests this can not be verified.

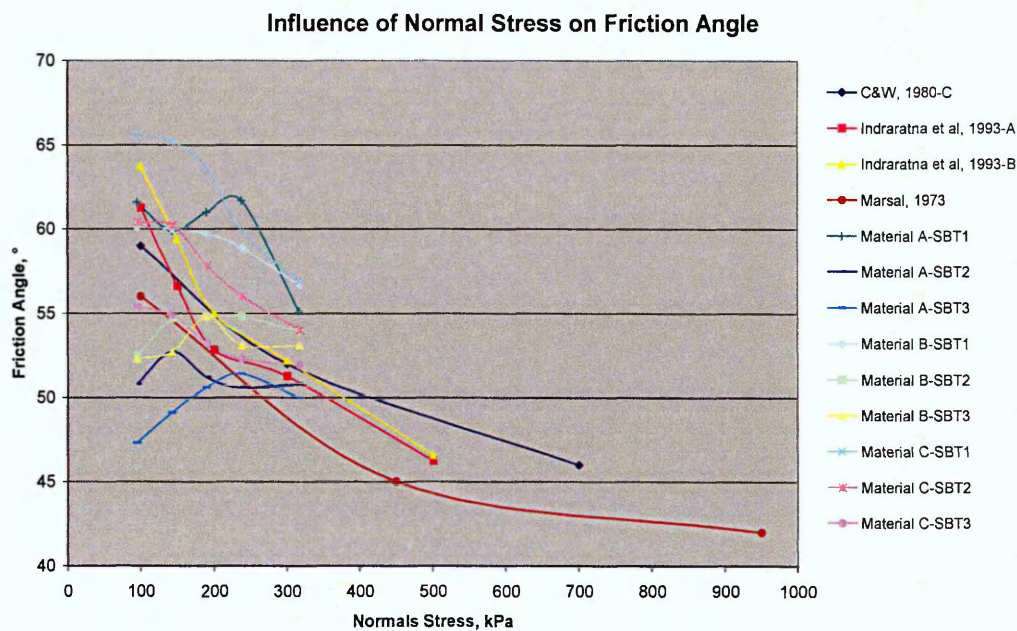


Figure 8.17: Influence of normal stress on friction angles

Figure 8.17 presents the influence of normal stress on the friction angle (average value) for Material A, B and C, for all the types of shear box together with the data from three natural aggregates obtained from the figures presented in the individual papers.

The more striking observations from Figure 8.17 are:

- The friction angles of Material A, B and C for SBT1 are higher than any of the natural materials presented in the graph. Again this can be a result of the individual particle strength and needs to be further investigated. After 238 kPa they appear to follow the reduction patterns set by the natural aggregates.
- For the materials A and B the friction angles for SBT2 and SBT3 are below the values for the natural aggregates for the lower normal stresses but after 238 kPa they appear to follow the reduction patterns set by the natural aggregates
- Material C show the greatest consistency, since for all types of shear box they follow similar reduction patterns as the natural granular materials

These observations of convergence are possibly a result of the minimisation of the effects of particle properties (such as particle shape and maximum particle size) at higher normal stresses (Indraratna *et al*, 1993).

8.15 Engineering Fill Applications

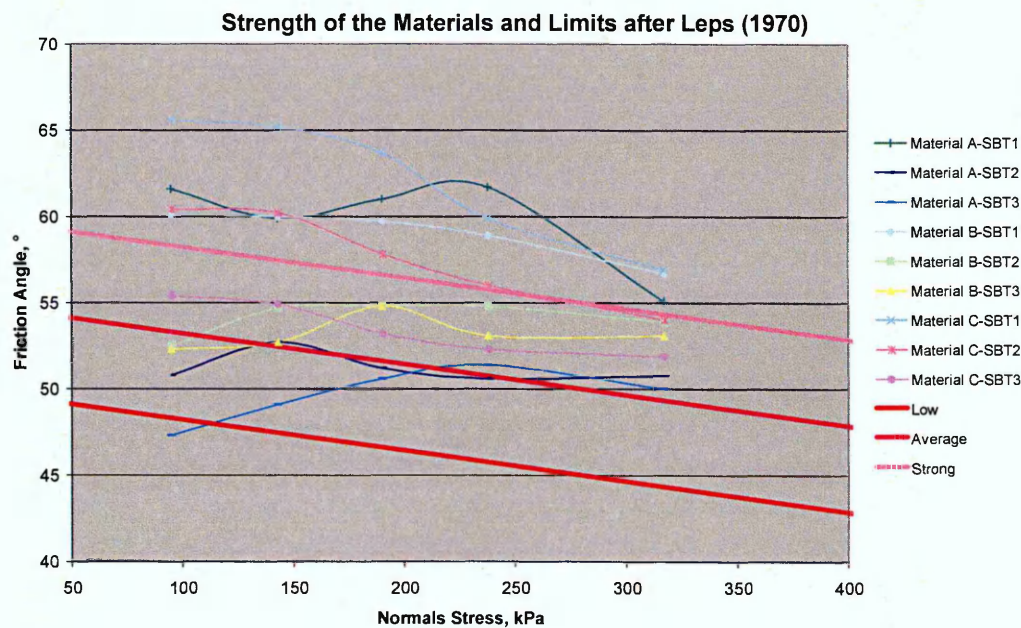


Figure 8.18: Friction angles of Materials and rockfill strength limits (after Leps, 1970)

As far as the industrial application of granular materials for fill engineering is concerned, Leps (1970) proposed limits of friction angles for low and high strength rockfill materials. Figure 8.18 presents all the data from this investigation together with the limits recommended by Leps.

Figure 8.18 shows that almost all the values (apart from Material A, SBT3, 95 kPa) fall above the lower strength limit set by Leps (1970). It is noticeable that all the results for SBT1 and the result for Material C SBT2 are above the higher strength limit which again shows the high values of friction angle exhibited by the materials. This most probably shows the high strength of the materials' particles and/or the high degree of friction existing between them, but since there is no available data, this can not be verified. In general though, it appears that the materials belong in the category of average to high strength rockfill.

8.16 Comparison with other Recycled Aggregates

This paragraph presents a comparison of the results for Material A, B and C with the results of the recycled materials research that has been mentioned in Section 2.8. Some wording and analysis is repeated and this is done for ease of reading.

McKelvey *et al* (2002) investigated the behaviour of two types of recycled aggregates under repeated load on a series of shear box tests and vertical stresses varying from 60 kPa to 300 kPa. The first type of material (named S1 for this discussion) was crushed concrete obtained from crushing concrete cubes. The second type of materials (named S2) was crushed brickwork containing bricks (of at least 95%) and mortar.

Sivakumar *et al* (2004), also investigated the behaviour of two recycled materials, similar to S1 and S2, during large shear box tests named S3 and S4 for the purpose of this discussion. S3 was crushed concrete obtained from crushing concrete cubes and S4 was crushed brickwork containing bricks (of at least 95%) and mortar. All materials were sieved and had particles between 20 and 40 mm. The specific volumes of the materials were 1.97 for S1 and 2.04 for S2. The materials were sheared at a rate of 1.5 mm/min. All four materials were sieved and had particles between 20 and 40 mm. The specific volumes of the materials were 1.97 for S1 and 2.04 for S2, 2.08 for S3, 1.90 for S4. The materials were sheared at a rate of 1.5 mm/min.

The shear rate used was about 10 times higher than the one utilised in this project, which shows that the rate used in this investigation was quite low. This allowed this

research to determine more accurately the behaviour of the materials, since the failure point was not missed and the rise in shear with axial strain was recorded in regular points.

The friction angles, determined from a straight line from the origins to the value of shear stress for 300 kPa, were and 39° for S1 and 37° for S2 and 43° for both S3 and S4. These values are significantly lower than the ones obtained for Material A, B and C at 317 kPa for all types of shear box. McKelvey *et al* (2002) and Sivakumar, *et al* (2004) state that the particle crushing of the materials was high but do not give specific values. The lower values of friction angles of S1, S2, S3 and S4 are most probably due to:

1. Their higher level of particle crushing and/or
2. The fact that Materials A, B and C have broader grading curves

Material S1 and S2 (no data is presented for material S3 and S4) behave similarly volumetrically with Material A, B and C since they exhibit dilatancy at low normal stresses that reduces with increasing normal stress levels.

Aurstad *et al* (2005) have tested crushed concrete with particles ranging from 0-63 mm (DG2) and from 20-63 mm (OG2) in a large triaxial apparatus (diameter 300 mm and height 600 mm). Table 8.18 summarises the friction angle of Material A, B, C, DG2 and OG2 together with the test characteristics.

Table 8.18: Comparison of Material A, B, C, DG2 and OG2

Material Type	Particle size (mm)		Density (Mg/m ³)	Friction Angle, °
	Max	Min		
A	37.5	0	1.80	55
A	37.5	0	1.60	51
A	28	0	1.80	50
B	37.5	0	1.80	57
B	37.5	0	1.60	54
B	28	0	1.80	53
C	37.5	0	1.80	57
C	37.5	0	1.60	54
C	28	0	1.80	52
DG2	63	0	2.16	>48
OG2	63	20	1.82	>60

Table 8.18 shows that the values observed between DG2 and OG and the three materials tested in this investigation are similar (the friction angles for OG2 are higher for all the tests but lower for DG2). They conclude that materials with strength properties like the ones exhibited by OG2 and DG2 “should perform excellently as unbound sub-base layer in roads”. Even though larger in-situ testing is required, it appears that Material A, B and C could be utilised in the construction of sub-base layers.

Aurstad *et al* (2005) have also observed that the crushing of particles is low for the grading of the materials from 0-63mm, but quite significant for the materials when they contain particles from 20-63 mm. Grading curves, for the materials with 0-63 mm particle size range, of before and after shearing are presented in their paper and show that they are almost similar, which shows that there is almost no particle crushing. Taking into consideration the results of this investigation together with the results presented by Aurstad *et al* (2005), McKelvey *et al* (2002) and Sivakumar *et al* (2004), it appears that recycled materials with minimum particle sizes of 20 mm crush more than the same type of materials containing finer particles. This may be a result of the “ability” of broader gradation to fill more voids and restrict the movement of larger particles and to provide better support. Further testing will be needed though to verify this.

Rathje *at al* (2006) conducted comparative tests on crushed concrete and limestone in respect to utilising them as backfill for mechanically stabilized earth walls. They determined the permeability and friction angle of the materials. The friction angle of both materials was 46° and the coefficient of permeability of the crushed concrete varied from 1×10^{-3} m/s to 8.5×10^{-5} m/s. The crushed limestone exhibited a coefficient of permeability of 1×10^{-2} m/s. They concluded that the friction angle of the crushed concrete is acceptable for the specific backfill engineering applications but the permeability is a concern. If the same specifications are applied to Material A, B and C it is obvious that in regard to strength they are acceptable for backfill engineering. The permeability of the materials needs further investigation though, since there was a limited amount of tests performed.

Huurman and Molenaar (2006) have conducted a series of large scale triaxial tests on materials containing 65% of crushed concrete and 35% of crushed masonry with maximum particle size of 40 mm. They used six different gradations but kept the

maximum particle size the same. They found that the friction angles of the materials varied from 42° to 46°. The friction angles of Material A, B and C are higher than the ones obtained by Hurman and Molenaar (2006). A complete comparison though can not be done since information as the specimen density is not given.

The comparison of Material A, B and C with other investigations has shown that the friction angles of all three materials appear to be higher apart from material OG2 tested by Aurstad *et al* (2005). It is important to note though that in all the investigations there are different parameters (such as the mixing of concrete and bricks and the crushing of concrete in the laboratory) that affect the relevance of the comparison. It is very difficult though to find two investigations that test the same type of recycled aggregates since they are too variable and almost certainly are obtained from different sources. It is the opinion of the authors that this remains the biggest problem into characterising the properties and behaviour of demolition waste as a whole.

CHAPTER 9

CONCLUSIONS AND RECOMMENTATIONS

9.1 Introduction

In Section 1.2, the technical issues in need of investigation were stated, along with the objectives of the project:

1. To provide a base for future research by investigating the physical and mechanical characteristics of crushed recycled aggregates
2. Provide data on the strength of recycled aggregates so they can be utilised by the industry.
3. Compare the properties of recycled materials with other research on recycled and primary aggregates.
4. Compare the characteristics and performance of different types of recycled materials.

Extended experimental work was carried out to determine the physical and mechanical characteristics of crushed demolition waste. It was necessary to test a large number of samples to try and minimise the effects of material variability and large particle size.

This Chapter presents the main and secondary conclusions of this research.

9.2 Main Conclusions

Suitability for industrial applications: The shear strength of the recycled aggregates has been compared with natural and other recycled aggregates and it has been shown that they can be utilised by the industry for construction purposes since they are of considerable strength. Adding to that, when the friction angles of materials A, B and C and all shear box tests are plotted together with the limits of rockfill strength (after Leps, 1970), they are above the lower strength limits.

Similarity with natural aggregates: The behaviour of Material A, B and C exhibited a number of similarities with natural aggregates:

1. The shear strength reduces with reducing specimen dry density.
2. The friction angle reduces with increasing normal stress.
3. The shear strength increases with axial strain and normal stress.
4. The shear-normal stress envelopes exhibit curvature at low normal stresses.
5. The materials exhibit dilatancy at low normal stresses that decreases with increasing normal stress.

6. The friction angles and shear stress although a bit higher is of similar values when compared with the specific natural aggregates given in Section 8.14.

Comparison between different types of recycled aggregates: This investigation tested three different types of recycled aggregates to determine the differences between concrete based, further processed (Material B) and not (Material A), and brick based (Material C) materials. The main conclusion of this comparison are:

Physical Characteristics: Material A and B exhibit almost identical coefficients of uniformity, water absorption and particle density values and dry density during the compaction tests that is met at the same optimum moisture content. The only main differences are their Flakiness and Elongation Indices, which as has been explained is probably a result of the further processing. Material C on the other hand does not exhibit any similar properties with the concrete based materials (with the exception of the freezing thawing results).

Shear Behaviour: Material A and B exhibit numerous similarities as far as their behaviour during shear box testing is concerned. The shear stress values at failure have some small differences but taking into account their standard deviation and the almost identical values of friction angles, then it can be concluded that their shear strength is similar. The shear stress decreases more with dry density than with maximum particle for both materials. The stress-strain and axial-volumetric strain relations also appear to be similar enhancing the argument that the effect of further processing of crushed concrete is minimal. Material C exhibit different results and behaviour to the concrete based materials, something that was expected due to the difference in the nature of the materials.

Concluding, it is apparent that the behaviour of similarly based recycled materials is similar, despite the different degrees of processing, but this applies to the specific materials tested in this investigation and generalising this for all demolition waste aggregates would be unsafe before further research is undertaken.

9.3 Secondary Conclusions

Large Scale Testing Equipment: The large scale compaction mould and permeability cell were designed to accommodate materials with particle sizes up to 50 mm. The durability of the materials used and the design of both pieces of equipment have allowed for performing numerous tests without the need of complicated procedures

and/or replacing of the large majority of parts used. It can be stated with confidence therefore that the design of the equipment and the materials used for it, with maybe the exception of replacing the mild with stainless steel for the compaction mould, are acceptable for these types of large scale testing.

Result variability: The main conclusion drawn from all the tests is that despite the possible effects of variability, non-homogeneous nature and large particle size the results show great consistency and repeatability. The consistency of the results has also been proved by the standard deviation values and graphs of Appendices E, F and G. This shows that the methods employed have minimised these effects.

Conclusions: This section presents the conclusions that do not fall in any of the other categories of this chapter.

- Dry sieving is an acceptable method for determining the grading curves of the materials.
- All materials' particle shape is classified as equi-dimensional with low angularity but Material A are more flaky than B and C.
- All materials exhibit very good resistance to freezing and thawing
- The compaction tests have indicated that both concrete based materials behave almost identically.
- The aggregate impact and crushing values tests are not considered by the authors as a valid method for determining the strength of crushed concrete materials and/or their particles because of the non-homogeneous nature of the materials.
- All materials exhibit crushing after shear box testing that reduces with maximum particle size and dry density.
- The shear strength of the Materials A and B reduces more with reduced dry density than maximum particle size, but the opposite occurs for Material C.
- The rate of reduction on shear stress with maximum particle size and dry density depends and reduces with normal stress.

It has to be noted that these conclusions apply to the specific types of demolition waste tested in this project and should not be generalised without further testing

9.4 Recommendations

The investigation conducted in this project has produced some interesting results on the behaviour and characteristics of three demolition waste materials and should provide valuable information for future research on the subject. Some of the aspects of the investigation though require further examination:

1. More different types of concrete and brick based materials need to be tested to establish if the results of this investigation can be generalised.
2. It is important to investigate the composition of the materials at different size fractions to determine how that affects properties of the materials such as aggregate impact and value tests and particle shape.
3. Further testing to confirm or refute the conclusions about the validity of the aggregate crushing and impact value tests is recommended, since these tests are used widely by the industry and it is important that valid results are produced.
4. More testing of the large scale permeability of the materials is required since the number of tests performed in this investigation was restricted. Different maximum particle and dry densities should also be investigated to provide information on the effects of materials' properties on their permeability.
5. The shear box tests should be carried out at higher and lower normal stress levels than the ones used in this project to determine the full effect of normal stress on the behaviour of the materials.
6. At least another value of maximum particle size and dry density should be used for testing, to determine if there are any relations between them and shear stress.
7. Investigation of the post peak behaviour of the materials is also suggested since it can provide valuable information about the axial strain-stress and axial-volumetric strain behaviour of the materials.
8. Particle crushing of the materials should be more analytically investigated, by determining its values after compaction of the specimens and at different normal stress levels.
9. It is highly recommended therefore to conduct tests for determining the particle strength since it will enhance the analysis of the materials behaviour.

REFERENCES

Aurstad, J., Aksnes, J., Dahlhaug, J.E., Bernsten, G. and Uthus, N., 2005, "Unbound Crushed Concrete in High Volume Roads - A Field and Laboratory Study", 7th International Conference on the Bearing Capacity of Roads, Railways and Airfields, Trodheim, Norway

Barden, L., Ismail, H., and Tong, P., 1969, "Plain Strain Deformation of Granular Material at Low and High Pressures", *Geotechnique*, 19(4), 441-452

Becker, E., Chan, C.K. and Bolton Seed, H., "Strength and Deformation Characteristics of Rockfill Materials in Plain Strain and Triaxial Compression Tests ", *Geotechnical Engineering TE 72-3*, University of California, Berkeley, U.S.A.

Bishop, A.W., 1966, "The Strength of Soils as Engineering Materials", *Geotechnique*, 16 (2), 91-129

Bishop, A.W., and Henkel, D.J., 1962, "The Measurement of Soil Properties in the Triaxial Test", Edward Arnolds, London

Boutreux, T., Raphael, E. and de Gennes, P.G., 1997, "Propagation of a Pressure Step in a Granular Material: The Role of Wall Friction", *Physical Revision, E 55*, 5759 - 5773 Issue 5

Brampton, A., Wallis, M., and Holliday, E., 2004, "Potential Use of Alternatives to Primary Aggregates in Coastal and River Engineering", CIRIA, C590

British Standards Institution, "Code of practice for site investigations", British Standard 5930, Milton Keynes, United Kingdom, 1999

British Standards Institution, “Methods of test for soils for civil engineering purposes-Part 2: Classification Tests”, British Standard 1377-2, Milton Keynes, United Kingdom, 1990

British Standards Institution, “Methods of test for soils for civil engineering purposes-Part 4: Compaction-Related Tests”, British Standard 1377-4, Milton Keynes, United Kingdom, 1990

British Standards Institution, “Methods of test for soils for civil engineering purposes-Part 5: Compressibility, Permeability and Durability Tests”, British Standard 1377-5, Milton Keynes, United Kingdom, 1990

British Standards Institution, “Methods of test for soils for civil engineering purposes-Part 7: Shear Strength Tests (total stress), British Standard 1377-7, Milton Keynes, United Kingdom, 1990

British Standards Institution, “Road aggregates – Part.1: Specification for single-sized aggregate for general purposes”, British Standard 63-1:1987, Milton Keynes, United Kingdom, 1987

British Standards Institution, “Specification for aggregates from natural sources for concrete”, British Standard 882:1992, Milton Keynes, United Kingdom, 1992

British Standards Institution, “Testing aggregates. Method for determination of particle size distribution. Sieve tests”, British Standard 812-103.1, Milton Keynes, United Kingdom, 1985

British Standards Institution, “Testing aggregates. Methods for determination of density”, British Standard 812-2, Milton Keynes, United Kingdom, 1995

British Standards Institution, "Testing Aggregates: Guide to Sampling and Testing Aggregates - Part 101", British Standard 812-101, Milton Keynes, United Kingdom, 1984

British Standards Institution, "Testing Aggregates: Methods for Determination of Aggregate Crushing Value (ACV) - Part 110", British Standard 812-110, Milton Keynes, United Kingdom, 1990

British Standards Institution, "Testing Aggregates: Methods for Determination of Aggregate Impact Value (AIV) - Part 112", British Standard 812-112, Milton Keynes, United Kingdom, 1990

British Standards Institution, "Testing Aggregates: Methods for Determination of Moisture Content - Part 109", British Standard 812-109, Milton Keynes, United Kingdom, 1990

British Standards Institution, "Testing Aggregates: Methods for Determination of Particle Shape – Section 105.1 Flakiness index", British Standard 812-105.1, Milton Keynes, United Kingdom, 1989

British Standards Institution, "Testing Aggregates: Methods for Determination of Particle Shape – Section 105.2 Elongation index of coarse aggregate", British Standard 812-105.2, Milton Keynes, United Kingdom, 1990

British Standards Institution, "Testing Aggregates: Methods for Sampling - Part 102", British Standard 812-102, Milton Keynes, United Kingdom, 1989

British Standards Institution, "Tests for geometrical properties of aggregates. Determination of particle shape. Flakiness index", British Standard 933-3, Milton Keynes, United Kingdom, 1997

- British Standards Institution, "Tests for geometrical properties of aggregates. Determination of particle size distribution. Sieving method", British Standard 933-1, Milton Keynes, United Kingdom, 1997
- British Standards Institution, "Unbound and hydraulically bound mixtures", British Standard 13286-4, Milton Keynes, United Kingdom, 2003
- Brown, A.J., 1988, "Use of Soft Rockfill at Evretou Dam, Cyprus", *Geotechnique*, 38, 333-354
- Building Research Establishment, 1998, "Digest 433: Specifications for Recycled Aggregates", Watford, United Kingdom
- Carga, V.K, and Madureira, C.J., 1985, "Compaction Characteristics of River Terrace Gravel" *J. Geotech. Eng.*, Vol. 111, 987-1007
- Chang, C.S., Chang, Y., and Kabir, M.G., 1992, "Micromechanics Modeling for Stress Strain Behaviour of Granular Soils. I: Theory", *J. Geotech. Eng.*, Vol. 118, No. 12, 1959-1974
- Charles, J.A., 1973, "Correlation between Laboratory Behaviour of Rockfill and Field Performance with Particular Reference to Scammonden Dam ", Ph.D Thesis, University of London, London, UK
- Charles, J.A., and Watts, K.S., 1980, " The Influence of Confining Pressure on the Shear Strength of Compacted Rockfill", *Geotechnique*, 30(4), 353-367
- Chen, L.S., 1948, "An Investigation of Stress-strain and Strength Characteristics of Cohesionless Soil", *Proceedings of the Second International Conference on Soil Mechanics and Foundation Engineering*, Vol. 5, 35-43

- Cho, G.C, Dodds, J. and Santamarina, J.C., 2006, "Particle Shape Effects on Packing Density, Stiffness and Strength: Natural and Crushed Sands", *Journal of Geotechnical and Geoenvironmental Engineering*, Volume 132, Issue 5, 591-602
- Chrismer, S.M., 1985, "Considerations of Factors Affecting Ballast Performance", *Bulletin 704 AREA - AAR Research and Test Department Report No. WP-110*
- Clemens, R.P., 1891, "The Deformation of Rockfill: Inter-particle Behaviour, Bulk Properties and Behaviour in Dams", PhD Thesis, Faculty of Engineering, King's College, London University, London, UK
- Dawson, A., 2001, Presentation on "The Utilisation of Recycled and Secondary Aggregates in Road Construction: European and UK Developments", Nottingham, United Kingdom
- Department of the Environment, Transport & the Regions, 2000, "Waste Strategy 2000 for England and Wales-Part 1", DETR, London, May 2000
- Department of the Environment, Transport & the Regions, 2000, "Waste Strategy 2000 for England and Wales-Part 2", DETR, London, May 2000
- Department of the Environment, Transport & the Regions, 1994, "Guidelines for aggregates provision in England", DETR, London, , Minerals Planning Guidance MPG06
- De Souza, R.J., 1958, "Compressibility of Quartz Sand at High Pressure", M.Sc. Thesis, Massachusetts Institute of Technology, Cambridge
- Duncan, J.M., Witherspoon, P.A., Mitchell, J.K., Watkins, D.J., Hardcastle, J.H., and Chen, J.C., 1972, "Seepage and Groundwater Effects Associated with Explosive Cratering", Rep. No. TE-72-2, University of California, Berkeley, California

Dunn, S., and Bora, P.K., 1972, "Shear Strength of Untreated Road Base Aggregates Measured by Variable Lateral Pressure Triaxial Cell", *Journal of Mechanics*, Vol. 7, 131-142

Eerola, M., and Ylosjoki, M., 1970, "The Effect of particle Shape on the Friction Angle of Coarse-grained Aggregates", *Proceedings of the 1st International Congress of the International Association of Engineering Geology*, Paris, France, Vol. 1, 445-456

El-Shohby, M., A., 1964, "The Behaviour of Particulate Materials under Stress", PhD Thesis, University of Manchester, Manchester, UK

European Standard, "Tests for Thermal and Weathering Properties of Aggregates - part 1: Determination of Resistance to Freezing and Thawing", *European Standard EN 1367-1*, Brussels, Belgium, 1999

European Standard, "Tests for mechanical and physical properties of aggregates. Methods for the determination of resistance to fragmentation", *European Standard EN 1097-2*, Brussels, Belgium, 1998

European Standard, "Tests for geometrical properties of aggregates. Determination of particle shape. Flakiness index", *European Standard 933-3*, Brussels, Belgium, 1997

Fannin, R.J., Eliadorani, A. and Wilkinson, J.M.T., 2005, "Shear Strength of Cohesionless Soils at Low Stress" *Geotechnique* 55, No.6, 267-478

Forth, J., P., Zoorob, S., E., and Thanaya, I., N., A., "Development of Bitumen-Bound Waste Aggregate Building Blocks", *Construction Materials*, 159, CMI, 23-32

Ghataora, G., S., Alobaidi, I., Faragher, E., Grant, S., 2006 "Use of Recycled Aggregates for Cementitious Backfill", *Waste and Resource Management*, 159, WRI, 23-28

- Gur, Y., Shklarsky, E. and Livnech, M., 1978, "Effect of Coarse-fraction Flakiness on the Strength of Graded Materials " Proceedings of the Third Asian Regional Conference on Soil Mechanics and Foundation Engineering, Haifa, Israel, Vol.1, 276-281
- Hagerty, M.M., Hite, D.R., Ullrich, C.R., and Hagerty, D.J., 1993, "One-Dimensional High-Pressure Compression of Granular Media", J Geotech. Engineering, ASCE, 119(1)
- Hardin, B.O., 1985, "Crushing of Soil Particles", J. Geotech. Engineering, ASCE, 111(10), 1177-1192
- Hazen, A., 1911, "Discussion of 'Dams on Sand Foundations', by A.C. Koenig", Trans., ASCE, New York, N.Y., Volume 73
- Hendron, A.J., 1963, "The Behavior of Sand in One-dimensional Compression, Ph.D Dissertation, University of Illinois, U.S.A
- Hill, A., 2001, "Environmental Assessment of Alternative Materials for Road Construction", Presentation Given on November 2001 at University of Nottingham
- Hite, D.R., 1989, "High Pressure Consolidation Tests on Sand", M.Engng. Thesis, Univ. of Louisville, Louisville, U.S.A., 53-67
- HM Treasury, 2004, "An Assessment of Options for Recycling Landfill Tax Revenue, Final Report", London, UK
- Holestol, K., Kjaernsli, B. and Torblaa, I., 1965, "Compression of Tunnel Spoil at Venemo Dam", Proceedings of 6th International Conference of Soil Mechanics and Foundation Engineering, Montreal, Canada

Holtz, W.G., and Gibbs, H.J., 1956, "Triaxial Shear Tests on Perviously Gravelly Soils", Journal of Soil Mechanics and Foundation Engineering Division, ASCE, Vol. 82, No. SM1, Proceedings Paper 867, January, 1-22

Hoff, I. and Baklokk, L.J., 1998, "Materialegenskaper for Grus-ogpukkmaterialer " SINTEF Report STF22 A98459 (Delprosjektrapport KPG 18)

Hoff, I., Baklokk, L.J. and Aurstad, J., 2004, "Influence of Laboratory Compaction Method on Unbound Granular Materials" Proceedings of 6th International Symposium on Pavements Unbound !, Nottingham, UK

Houlsby, G.T. and Psomas, S., 2001, "Soil Conditioning for Pipejacking and Tunnelling: Properties of Sand/Foam Mixtures", Proc Underground Construction 2001 Int Exhibition and Symp Oxford, UK, 128-138

Hurley, J.W., McGrath, C., Fletcher, .S.L. & Bowes, H.M., "Deconstruction and Reuse of Construction Materials", Building Research Establishment Ltd, 2001

Huurman, R. and Molenaar, A.A.A., 2006, "Permanent Deformation in Flexible Pavements with Unbound Base Courses", Transportation Research Board 2006 Annual Meeting CD-ROM, Washington DC, U.S.A.

Indraratna, B., Wijewardena, L.S.S., and Balasubramaniam, A.S., 1993, "Large-Scale Triaxial Testing of Greywacke Rockfill", Geotechnique, 43, 37-51

Indraratna, B., Ionescu, D., and Christie, H., D., 1998, "Shear Behaviour of Railway Ballast based on Large-Scale triaxial Tests", Journal of Geotech. Eng., Vol. 124, 439-449

- Klugar, K., 1975, "A contribution to Ballast Mechanics ", Proceeding of Symposium of Railroad Track Mechanics and Technology, Princeton University, New Jersey, U.S.A., Pergamon Press
- Kirkpatrick, W.M., 1965, "Effects of Grain Size and Grading on the Shearing Behaviour of Granular Materials", Proceedings of the Sixth International Conference on Soil Mechanics and Foundation Engineering, Montreal, Vol. 1, 273-276
- Knight, J.B., Fandrich, C.G., Lau, C.N., Jaeger, H.M. and Nagel, S.R., 1995, "Density Relaxation in a Vibrated Granular Material ", Physical Review E, Volume 51, No. 5
- Koerner, R.M., 1970, "Effects of Particle Characteristics on Soil Strength", Journal of soil Mechanics and Foundation Engineering Division, Vol. 96, Proceedings Paper 7393, 1221-1234
- Lade, P.V., Yamamuro, J.A., and Bopp, P.B., 1996, "Significance of Particle Crushing in Granular Materials", J. of Geotech. Eng., Vol. 122, 309-316
- Lanaro, F., and Tolppanen, P., "3D Characterization of Coarse Aggregates," *Engineering Geology*, 65, 2002, pp. 17-30
- Lee, K.L., and Farhoomand, I., 1967, "Compressibility and Crushing of Granular Soils in Anisotropic Triaxial Compression", Can. Geotech. J., 4(1), 68-86
- Lee, Y.H., 1986, " Strength and Deformation Characteristics of Rockfill", PhD Thesis, Asian Institute of Technology, Bangkok
- Lees, G., "The measurement of Particle Shape and its Influence in Engineering Materials," *Journal of British Granite and Whinstone Federation*, United Kingdom, 4, No. 2, 1964, pp. 17-38

- Leps, T.M., 1970, "Review of Shearing Strength of Rockfill", Journal of the Soil Mechanics and Foundations Division, Proc. Of the American Society of Civil Engineers, 1159-1171
- Leslie, D.D., 1963, "Large Scale Triaxial Tests on Gravelly Soils", Proceedings of the Second Pan American Conference on Soil Mechanics and Foundation Engineering, 181-202
- Leslie, D.D., 1975, "Shear Strength of Rockfill", Physical Properties Engineering Study No. 526, US Army Corps of Engineers, Sausalito, California, U.S.A
- Levin, Y., Arenzon, J.J., and Sellitto, M., 2001, "Aging Dynamics and Density Relaxation in Kinetic Lattice gases Under Gravity ", Europhysics Letters, Volume 55, No. 6
- Lumay, G., Ludewig, F. and Vendewalle, N., 2006, "Compaction of Granular Materials: Experiments and Contact Dynamics Simulations ", Journal of Physics Conference Series 40, 133-143
- MacKenzie, P.R. and McDonald, L.A., 1985, "Mangrove Creek Dam - Use of Soft Rockfill", Proc. Symp. Concrete Face Rockfill Dams, Detroit, 208-230, New York: ASCE
- Marachi, N.D., Chan, C.K., and Seed, H.B., 1972, "Evaluation of Properties of Rockfill Materials", Journal of Soil Mechanics and Foundation Engineering Division, ASCE, Vol. 98, Proceedings Paper 8672, 95-113
- Marachi, N.D., Chan, C.K., Seed, H.B., and Duncan, J.M., 1969, "Strength and Deformation Characteristics of Rockfill Materials", Report TE-69-5, University of California, Berkeley.
- Marsal, R.J., 1967, "Large Scale Testing of Rockfill Materials", Journal of the Mechanics and Foundation Engineering Division, ASCE, Vol. 93, Paper 5, March, 27-43

- Marsal, R.J., 1973, "Mechanical Properties of Rockfill", Embankment Dam Engineering, Casagrande Vol. Wileys, New York, 109-200
- Marsal, R.J., 1976, "Mechanical Properties of Rockfill Soil Mixtures", Douzieme Congres Des Grands Barages, Mexico, 179-209
- McDowell, G.R. and Bolton, M.D., 1998, "On the Micro Mechanics of Crushable Aggregates", Geotechnique 48, No. 5, 667-679
- McKelvey, D., Sivakumar, V., Bell, A. and McLaverty, G., 2002, "Shear Strength of Recycled Construction Materials Intended for Use in Vibro Ground Improvement", Ground Improvement, Vol. 6, No. 2, 59-68
- Miura, N. and Yamanouchi, T. (1975). "Effect of Water on the Behavior of a Quartz-Rich Sand under High Stressed.", Soils and Foundations, Vol. 15, No. 4, 23-34.
- Murphy, D.J., 1971, "High Pressure Experiments on Soil and Rocks", Proceedings, 13th Symposium of Rock Mechanics, 691-714
- Nakata, Y, Hyde, A.F.L., Hyodo, M., and Murata, H., 1999, "A Probabilistic Approach to Sand Particle Crushing in the Triaxial Test", Geotechnique, 49(5), 567-583
- Naylor, D.J., Maranhã, J.R., Maranhã das Neves, E., and Veiga Pinto, A., 1997, " A Back Analysis of Beliche Dam", Geotechnique, 48(2), 221-233
- Nowak, E.R., Knight, J.B., Ben-Naim, E., Jaeger, H.M., and Nagel, S.R., 1998, "Density Fluctuations in Vibrated Granular Materials" Physical Review, Volume 57, No. 2

Office of the Deputy Prime Minister, 2004, "Survey of Arisings and Use of Construction, Demolition and Excavation Waste as Aggregate in England in 2003", HMSO, London

Office of the Deputy Prime Minister, 2002, "Strategic Planning for Sustainable Waste Management: Guidance on Option Development and Appraisal", HMSO, London

Peak, F. and Ford, R.W., 1984, "A Panel Freezing Test for Brickwork", British Ceramics Research Association, Technical Note 358

Pestana, J.M., and Whittle, A.J., 1995, "Compression Model for Cohesionless Soils", *Geotechnique*, 45(4), 611-631

Pestana, J.M., and Whittle, A.J., 1998, "Time Effects in the Compression of Sands", *Geotechnique*, 48(5), 695-701

Pigeon, Y., 1969, "The Compressibility of Rockfill, PhD Thesis", Imperial College of Science and Technology, London, UK

Pike, D.C., 1973, "Shear-box Tests on Graded Aggregates", Transport and Road Research Laboratory, Department of the Environment, TRRL Report LR 584, Materials Division, Highways Department, Crowthorne, Berkshire, England

Rathje, E., Trejo, D., and Folliard, K., 2006, "Potential Use of Crushed Concrete and Recycled Asphalt Pavement as Backfill for Mechanically Stabilizes Earth Walls", Project Summary Report O-4177-S, Center for Transportation Research, The University of Texas at Austin, U.S.A.

Richard, P., Nicodemi, M., Delannay, R., Ribiere, P. and Bideau, D., 2005, "Slow Relaxation and Compaction of Granular Systems", *Nature Materials*, Volume 4, No.2

- Rico, A., Orozco, J.M., and Atzegui, T.T., 1977, "Crushed Stone Behaviour as Related to Grading", Proceedings of the Ninth International Conference on Soil Mechanics and Foundation Engineering, Vol. 1, 263-265
- Roberts, J.E., and De Souza, J.M., 1958, "The Compressibility of Sands", Proc. Am. Soc. Tes. Mater. 58, 1269-1277
- Roberts, J.E., 1964, "Sand Compression as a Factor in Oil Field Subsidence ", Ph.D Thesis, Massachusetts Institute of Technology, Cambridge, Massachusetts, U.S.A.
- Roner, C.J., 1985, "Some Effects of Shape, Gradation and Size on the Performance of Railroad Ballast", M.S. Degree Project Report, Report No. AAR85-324P, Department of Civil Engineering, University of Massachusetts, Amherst, June
- Roscoe, K.H., Schofield, A.N., and Thurairajah, A., 1963, "An Evaluation of Test Data for Selecting a Yield Criterion for Soils", Laboratory Shear Testing of Soil, ASTM Special Technical Publication 362, American Society for Testing and Materials, 111-128
- Rösslein, D., 1941, "Steinbrecheruntersuchungen unter besonderer Berücksichtigung der Kornform" Forsch. a.d. Strassenwesen Band 32, Berlin, Germany. See also translation by F.A. Shergold, Quarry Managers' Journal 30 (4),
- Rothenburg, L., and Bathurst, R.J., 1989, "Analytical Study of Induced Anisotropy in Idealized Granular Materials", Geotechnique 39, No. 4, 601-614
- Rothenburg, L., and Bathurst, R.J., 1992, "Micromechanical Features of Granular Assemblies with Planar Elliptical Particles", Geotechnique 42, No.1, 79-95
- Rowe, P.W., 1955, "A Stress Strain Theory for Cohesionless Soil with Applications to Earth Pressures at Rest and Moving Walls", Geotechnique, No.4, 70-88

- Shultze, E. and Moussa, 1961, "Factors Affecting the Compressibility of Sand", Proc. of the Fifth International Conference on Soil Mechanics and Foundation Engineering, Paris, France
- Sivakumar, V., McKinley J. D. and Ferguson, D., 2004, "Reuse of construction waste: performance under repeated loading", Journal of Geotechnical Engineering, Proceedings of the Institution of Civil Engineers, Vol 157, Issue GE2, pp91-96
- Sowers, G.F., Williams, R.C., and Wallace, T.S., 1965, "Compressibility of Broken Rock and Settlement of Rockfills", Proc. 6th ICSMFE, Montreal, 2, 561-565
- Sun, D.A, Matsuoaka, H., Muramatsu, D., Hara, T., Kudo, A., Yoshida, Z. and Takezawa, S., 2004, "Deformation and Strength Characteristics of Weathered Soft Rock Using Triaxial Tests" International Journal of Rock Mechanics and Mineral Science, Vol. 41, No.3
- Thom, N.H., and Brown, S.F., 1988, "Effect of Grading and Density on the Mechanical Properties of a Crushed Dolomitic Limestone", 14th ARRB Conference, 7: 94-148
- Thom, N.H., and Brown, S.F., 1989, "The Mechanical Properties of Unbound Aggregates from Various Sources", Unbound Aggregates in Roads, Jones and Dawson Editions, Butterworth, London
- Tombs, J.A., 1969, "Strength and Deformation Characteristics of Rockfil", Ph.D Thesis, University of London, London, UK
- U.S Department of Transportation, 2000, "Recycled Materials in European Highway Environments: Uses, Technologies, and Policies", Research undertaken by Turner-Fairbank Highway Research Center, FHWA Publication Number: FHWA-PL-00-025

Vallerga, B.A., Seed, H.B., Monismith, C.L., and Cooper, R.S., 1957, "Effect of Shape, Size and Surface Roughness of Aggregate Particles on the Strength of Granular Materials", ASTM STP 212, 63-76

Varadarajan, A., Sharma, K.A., Venkatachalam, k., and Gupta, A.K., 2003, "Testing and Modeling two Rockfill Materials", Journal of Geotechnical and Geoenvironmental Engineering, Vol 129, No. 3, 206-218

Vesic, A.S., and Clough, G.W., 1968, "Behavior of Granular Materials under High Stress", J. Soil Mech. and Found. Div., ASCE, 94(3), 661-688

Watson, J.P., 1989, "Highway Construction and Maintenance", Longman Scientific & Technical, John Wiley & Sons, New York

Wignall, A., Kendrick, P.S., Ancill, R., and Copson, M., 1999, " Roadwork Theory & Practice", Butterworth Heinemann, 4th Edition

Waste & Resources Action Programme (WRAP), 2005, "Construction Update: Materials Resource Efficiency in Construction",

Yamamuro, J.A., and Lade, P.V., 1993, "Effects of Strain Rate on Instability of Granular Soils", Geotech. Testing J., 16(3), 304-313

Yamamuro, J.A., Bopp, P.A., and Lade, P.V., 1996, "One-Dimensional Compression of Sands at High Pressures", J. Geotech. Engng Div., ASCE, 122(2), 147-154

Zeller, J. and Wulliman, R., 1957, "The Shear Strength of the Shell Materials for the Goschenalp Dam (Switzerland)", Proc. 4th International Conference on Soil Mechanics and Foundation, Vol. 2,399-404, London, UK

Zingg, T., 1935, Beitrag zur Schotteranalyse", Schweiz. Mineral. Petrog. Mitt., 15: 39-140

www.metsominerals.com

www.sanger.net

List of equipment used in the BS tests of this investigation

1. Laboratory test sieves, Endecotts Ltd
2. Mechanical sieve shaker, Pascall Engineering co Ltd
3. Scales, Precisa 30000D, with capacity of 30 kg and readable to 0.1 g and Precisa 300M, with capacity of 300 g and readable to 1 mg, both calibrated by Barry Platts, precision Balance Engineer
4. Avery Birmingham, type 3205 CLE scale, 250 kg capacity scale, readable to 100 g. Calibrated by Avery Berkel, maintenance and calibration
5. Ovens, by APEX Construction Ltd, type A140E and Gallenkamp, type 7B1810C, both producing temperatures of 0-300 °C
6. For the ACV test the equipment used was a concrete tube crushing machine by Avery-Denison Limited (i.d. 7226/D/T85248) with a capacity of 3000 kN and the capability of following the procedures stated in BS 812-110:1990. It was calibrated by the Denison Mayes Group
7. The equipment used for the BS compaction tests fell within the specifications stated in the corresponding standard (BS 1377-4:1990). For the completion of the BS tests the ELE International compaction equipment (product No. 24-9090/01) was used and fell within the standard specifications.
8. The dimensions of the apertures of the sieves used for the establishment of the flakiness and elongation ratios values were measured by the vernier calibre used for this project and they were found to comply with the values set at BS 812-105.1:1989 and BS 812-105:2 1990 respectively.

Permeability Testing Procedure

1. The elastic seal is placed in the bottom plate groove (figure C.1)

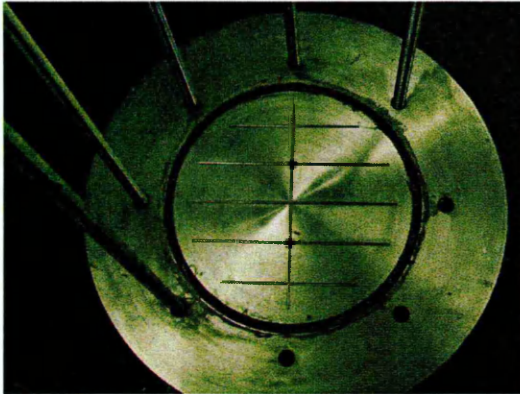


Figure C.1: The seal in the groove of the bottom plate

2. The plastic cell is placed on the bottom cell and after the compaction top plate is in position they are fixed together with the use of 8 steel bars, which seals the bottom plate with the cell (figure C.2)



Figure C.2: The permeability cell with the top compaction plate

3. The permeable mat is placed at the bottom of the cell and on top of that a 3mm thick steel mesh is positioned to protect it from the compaction forces
4. The materials are compacted in the cell in 6 layers
5. The copper tubes were restricted at the end to constrain the migration of fines (figure C.3)



Figure C.3: Restrained Copper pipe

6. After the 2nd layer of materials is compacted the lower level copper pipes were inserted in the tube (figure C.4.a). They were water tightly fixed to the cell with modified glances (figure C.4.b)

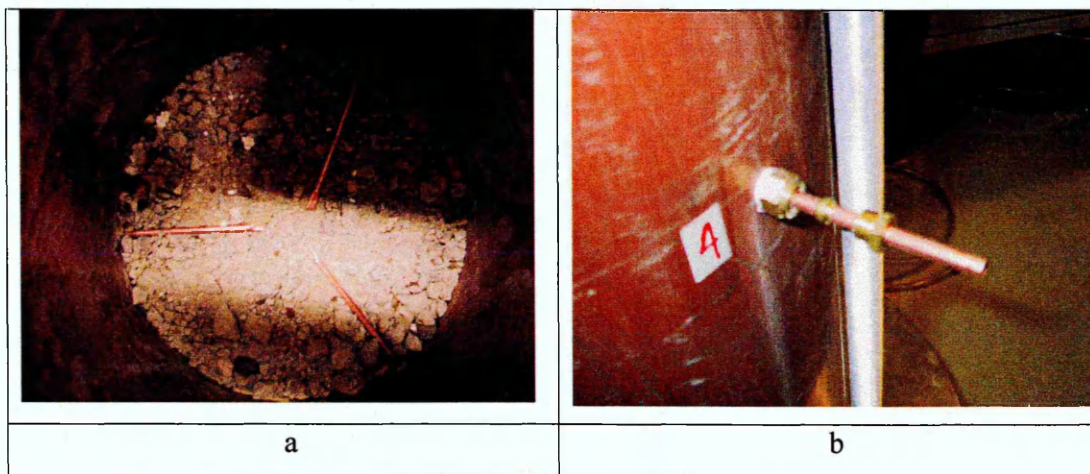


Figure C.4: The copper pipes placed in the cell after the compaction of the first layer (a) and the water tight fixings of the pipes to the cell (b)

7. The compaction of the materials was continued for another two layers and then the copper tube insertion procedure was repeated for the top level copper tubes. All the copper tubes were replaced after every test.

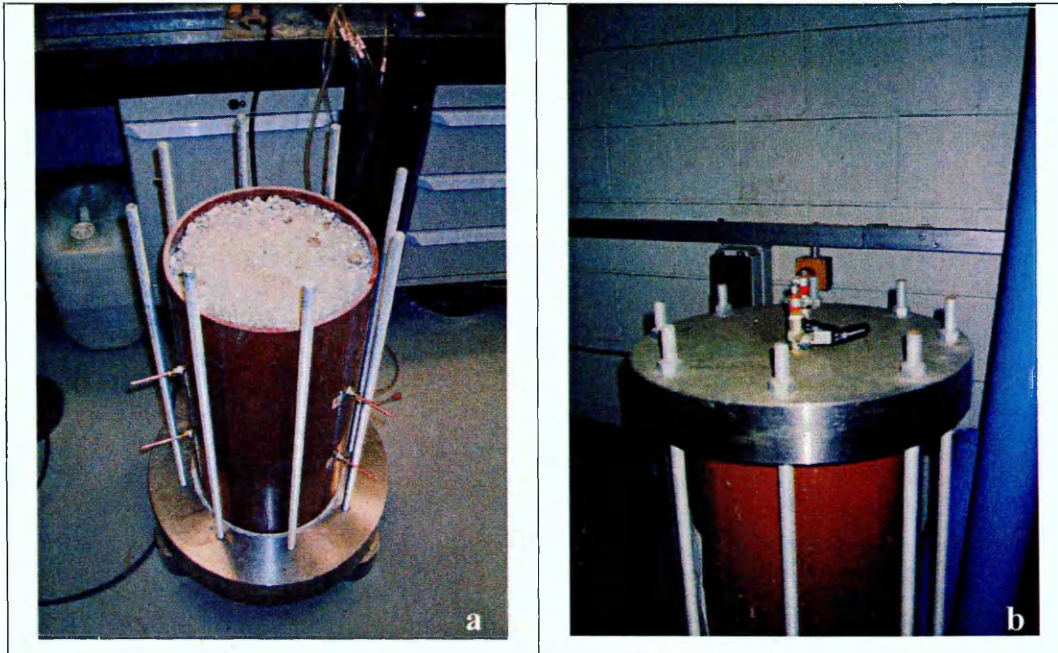


Figure C.5: The compacted sample with the compaction plate removed (a) and the cell with the top plate fixed in place (b)

8. After the compacted materials reached the top level of the tube the compaction plate was carefully removed (C.5.a) and replaced with the top permeability test plate that had a elastic seal in its groove (C.5.b). A permeable mat and a steel mesh, identical with the ones positioned at the bottom of the cell, were placed between the materials and the top plate

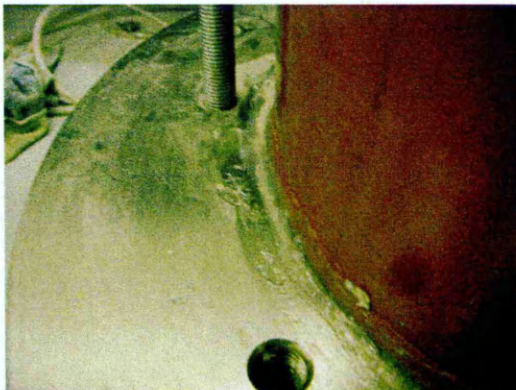


Figure C.6: The extra silicon seal

9. After the copper tubes, cell, top and bottom plates are fixed together, silicon is applied to the contact points for further sealing (figure C.6)

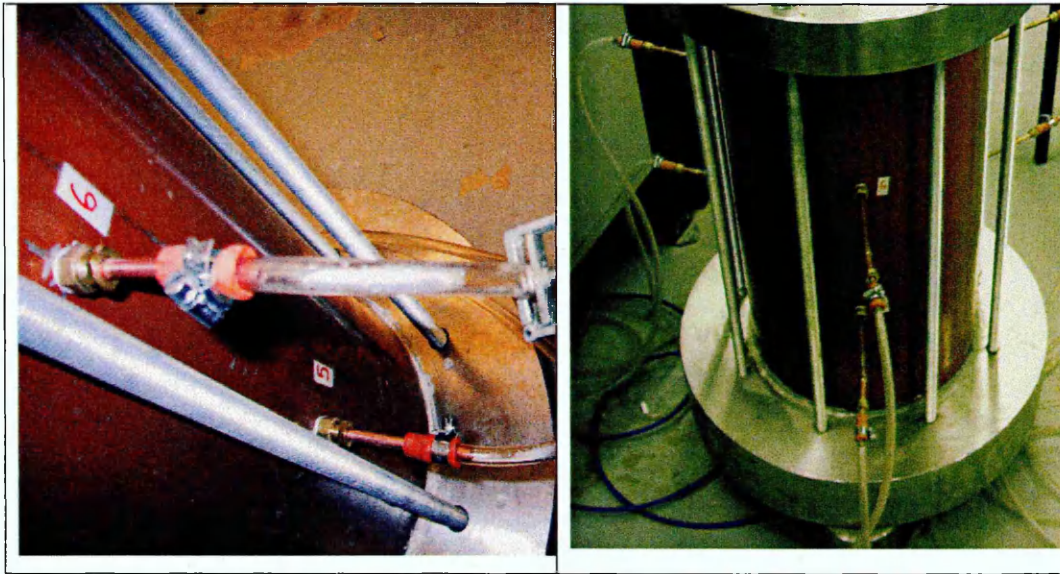


Figure C.7: Connection of the copper pipes with manometer tubes

10. The copper tubes are water tightly connected with the manometer pipes (figure C.7), which lead to a band of manometers (figure C.8), with restricting fixings. All the copper tubes and manometers positions are numbered according to their position in the cell



Figure C.8: Band of Manometer tubes

11. The permeability testing arrangement also included a constant head tank with an overflow and a supply tank fitted with a pump capable to supply the water to the constant head tank and to circulate the water in the supply tank.

12. Once the assembly of the cell apparatus was completed the saturation process of the materials started. Water was inserted to the cell from the bottom plate inlet valve (figure C.9) and once water started coming out from the top valve (figure C.5.b) suction was applied to the sample to speed the process.



Figure C.9: Bottom plate inlet/outlet

13. The saturation procedure lasted for four weeks for all three types of materials and after this period there were no signs of air trapped in the sample. This was verified by the fact that during the last week of saturation the application of continuous suction did not yield any trapped air from the outlet pipes. It was impossible to provide de-aerated water for the whole duration of the test, and therefore the water used was clean tap-water which is acceptable according to the BS 1377-5:1990, paragraph 5.2.4.

14. The permeability cell is then connected to the constant head tank by the top plate water inlet.

15. The flow (Volume/time) was measured from the water coming out from the bottom plate outlet

16. The measurements and calculations of the permeability testing were done in accordance to BS 1377-5:1990.

Shear Box Testing Procedure

This appendix describes the procedure followed in all the shear box tests. It includes numbered references (Ref1,Ref2 etc) to figure D.3. There are also some close up photographs of some of the components of the shear box testing equipment arrangement

1. The shear box was removed from the shear box frame and placed on the floor for compaction (figure D.1). The top and bottom halves were tightly secured together with screws

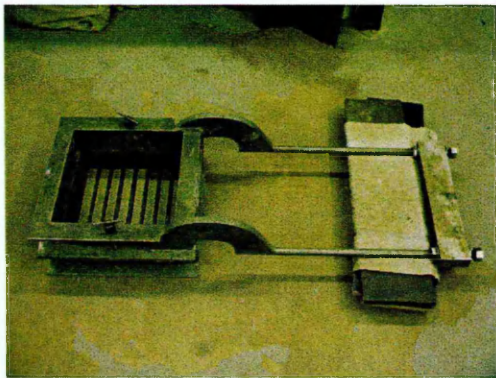


Figure D.1: The shear box ready for compaction

2. The sample was compacted with the use of a Kango 900 K vibrating hammer in three layers in order to avoid the coexistence of the shear plane and the layer interfaces figure (D.2). The Kango hammer was fitted with a compaction plate and a rubber pad of 5 mm thickness was placed between the compaction plate and the materials to minimise the risk of breakage of the materials' sharp edges



Figure D.2: The shear box with the sample (of material C) compacted

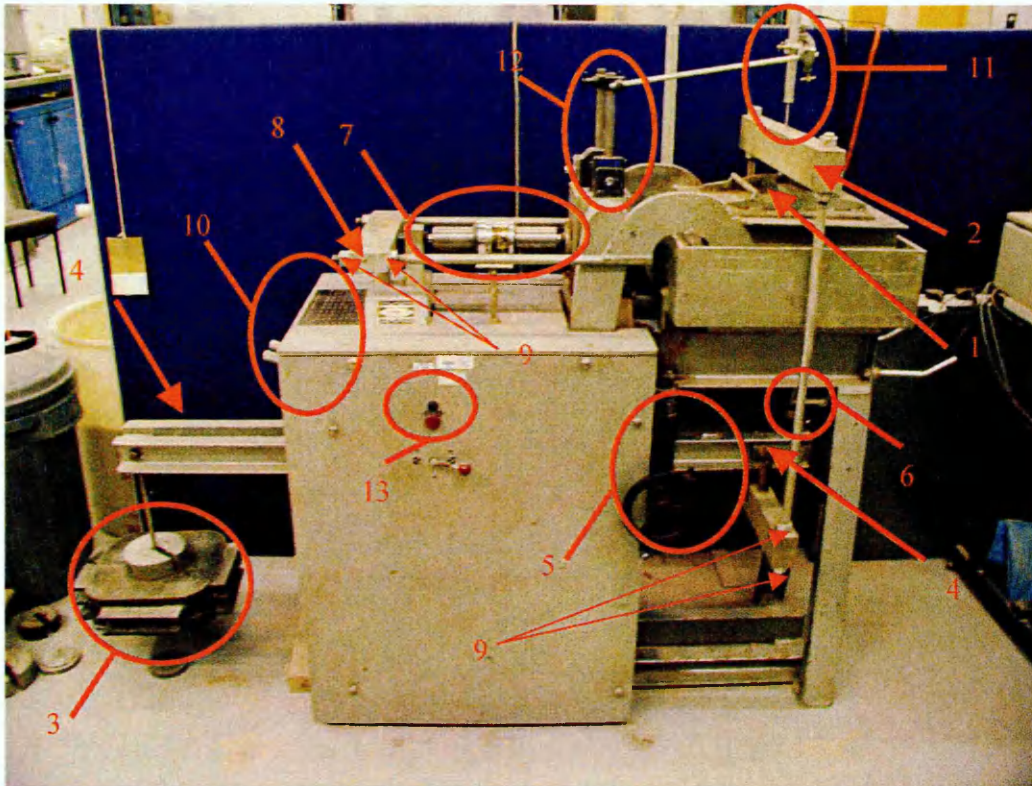


Figure D.3: The shear box frame

3. After the sample was compacted, the box was placed onto the shear box frame (figure D.3).
4. The top plate was then placed onto the shear box (Ref 1), the screws removed and it is connected to the horizontal loading jack by a steel frame (Ref 2)
5. The weights are then placed to the loading platform (Ref3) and the horizontal loading jack (Ref 4) is then levelled by the use of a hydraulic pump system (Ref 5). The normal stress is applied to the shear box via the steel frame (Ref 2) and the vertical loading jack (Ref 6 and figure D.4).



Figure D.4: The vertical loading jack

6. A 50 kN load cell (Ref 7 and figure D.5.a) is connected to the to the horizontal loading yoke (figure D.5.b) that connects to the top half of the shear box with the help of a horizontal loading frame (Ref 8)

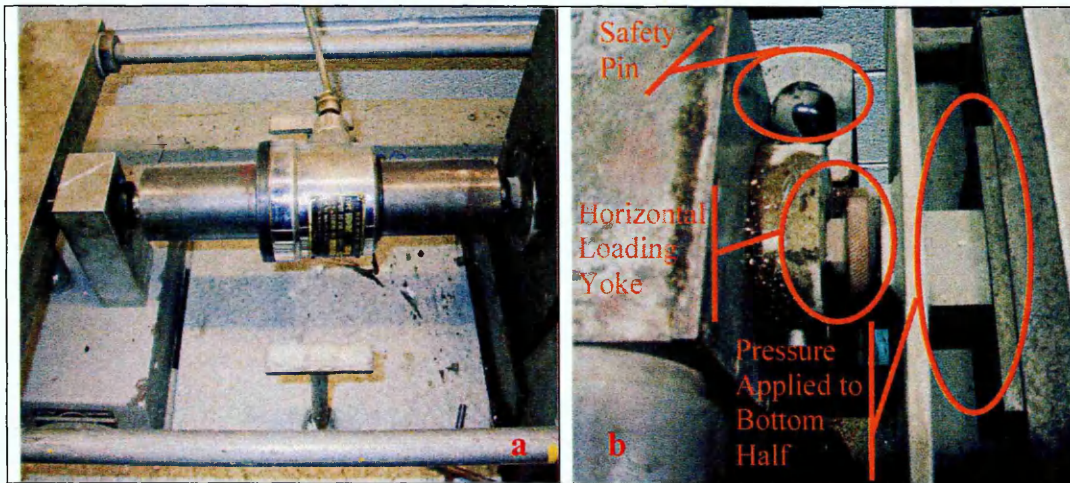


Figure D.5: The load cell (a) and the horizontal loading yoke (b)

7. All the frames and the yokes of the shear box apparatus were tied together with the use of bolts (Ref 9)

8. The speed of movement of the horizontal yoke was then applied via a multi speed gear box (Ref 10 and figure D.6)

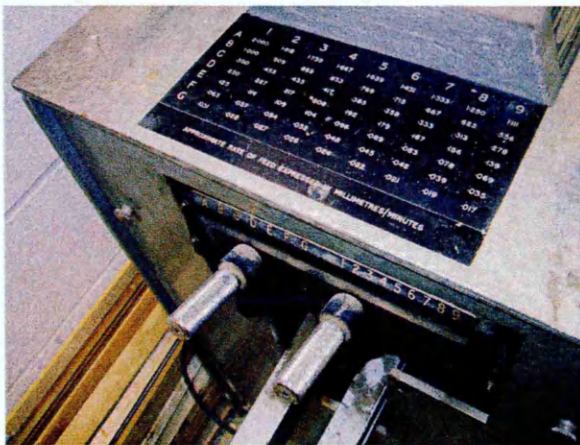


Figure D.6: The control unit of the multi speed gear box

9. The horizontal and vertical transducers (Ref 11) were then fitted to the shear box with the help of magnetic bases (Ref 12)

10. The measurements of the displacements and the load applied were recorded to the computer with the help of those transducers and an analogue interface box (figure D.7)



D.7: The transducers and the interface box used for measuring the displacement and load

11. The values of the horizontal and vertical displacements and the load applied were zeroed in the computer logging system.

12. Finally the tests were initiated by the start/stop button (Ref 13) at the same time as the logging process at the computer. All the measurements were recorded in the computer system, which also produced a real time graph of the readings (figure D.8).

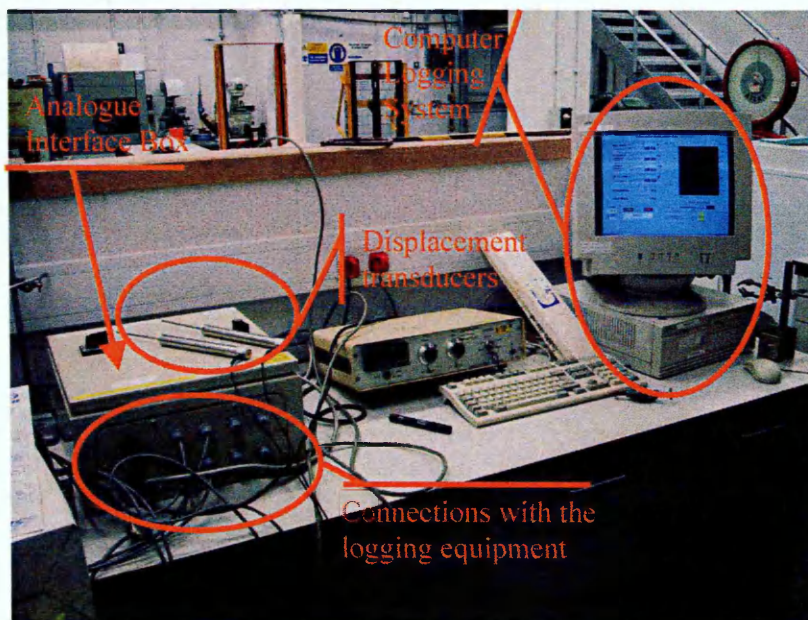
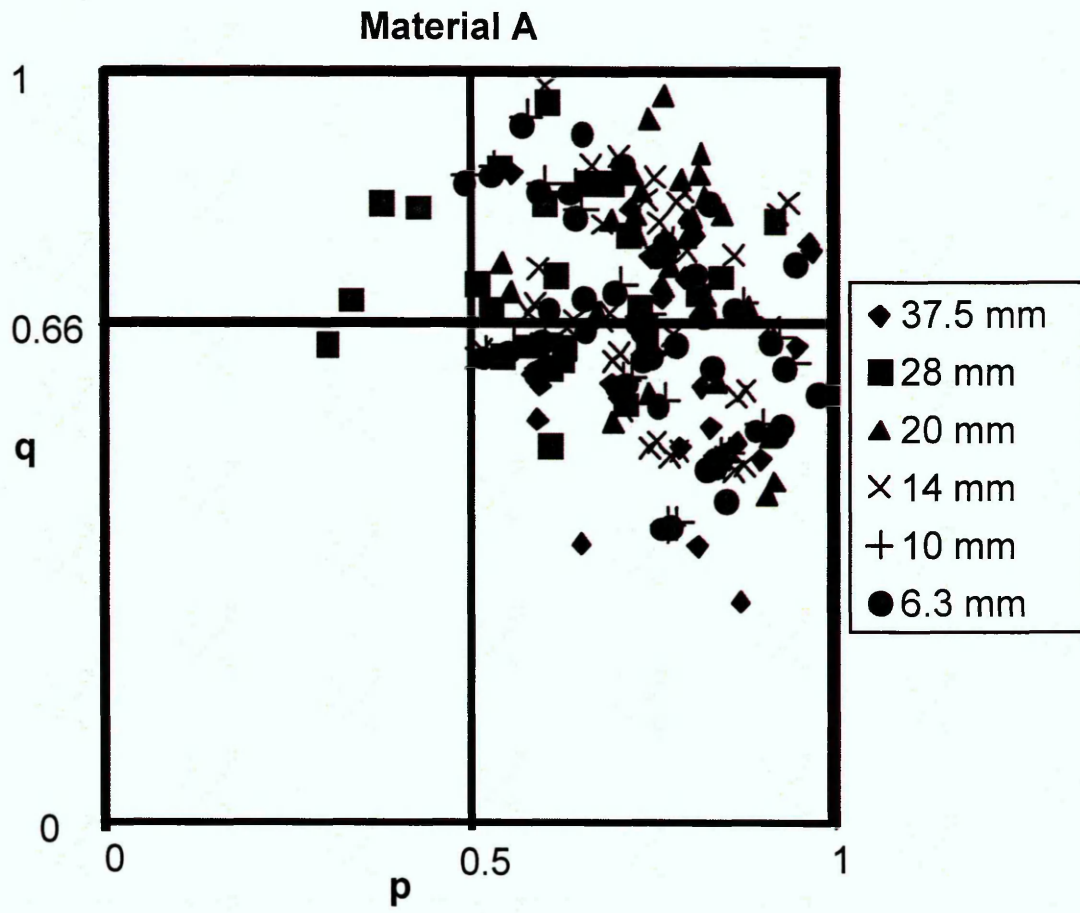
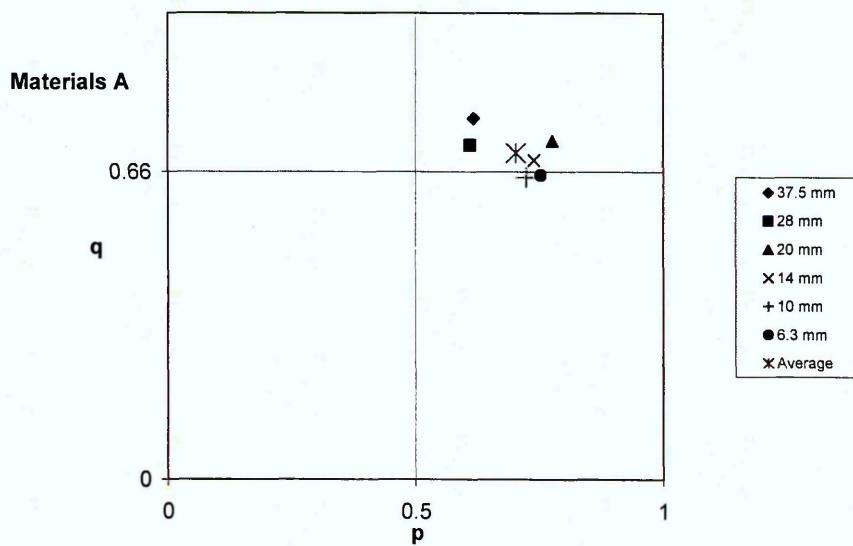


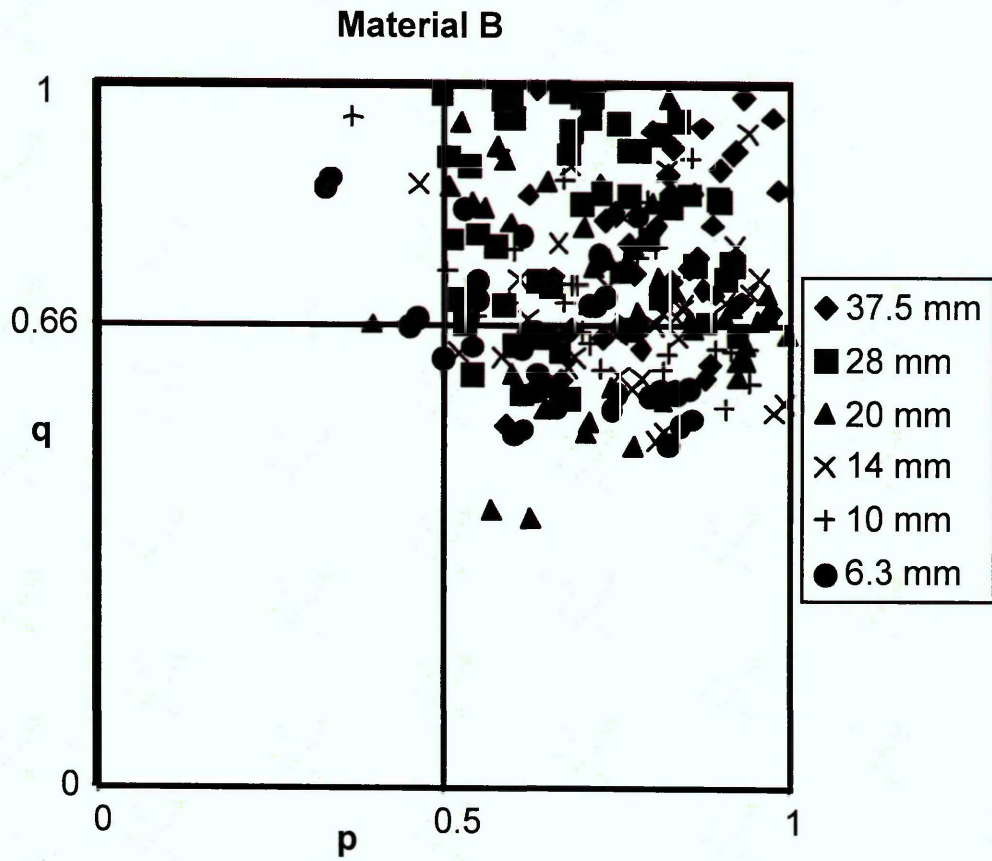
Figure D.8: The computer logging system



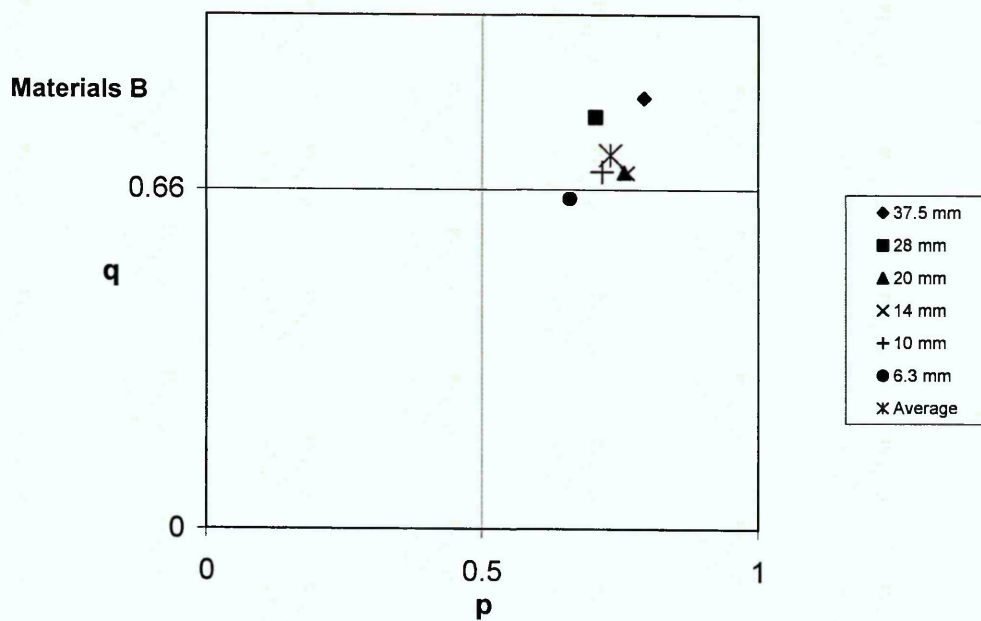
Shape categories for all the size fractions for Materials A (after Rösslein, 1941)



Average values for all the size fractions for Materials A (after Rösslein, 1941)

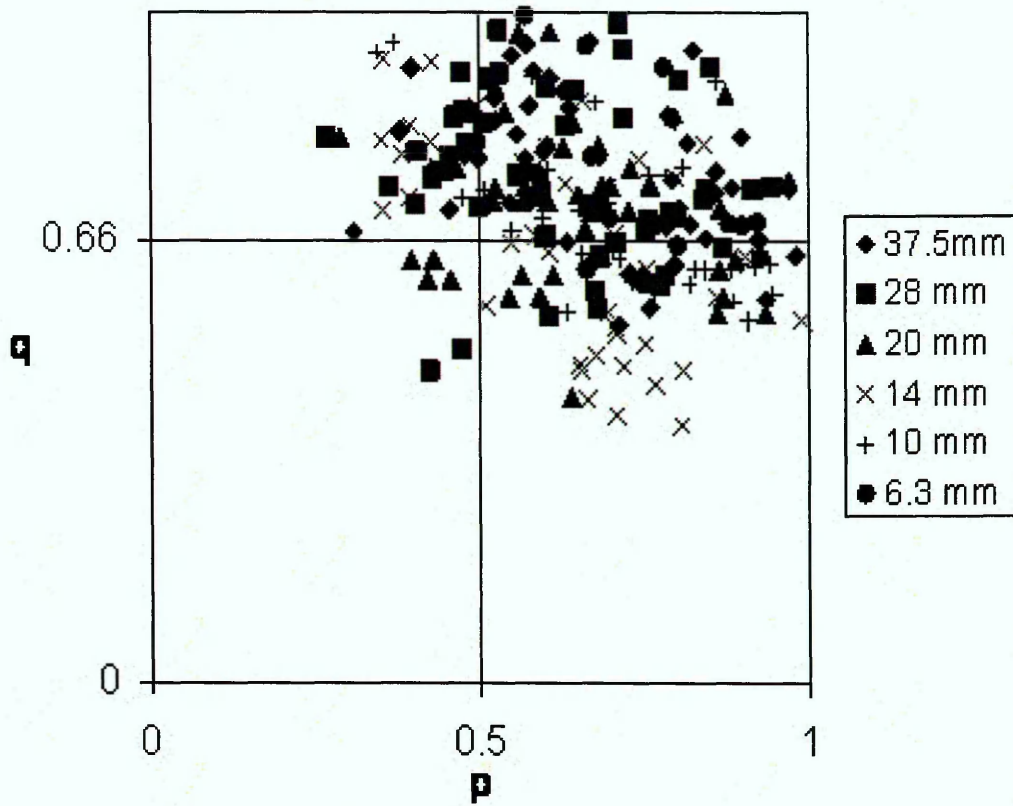


Shape categories for all the size fractions for and B (after Rösslein, 1941)

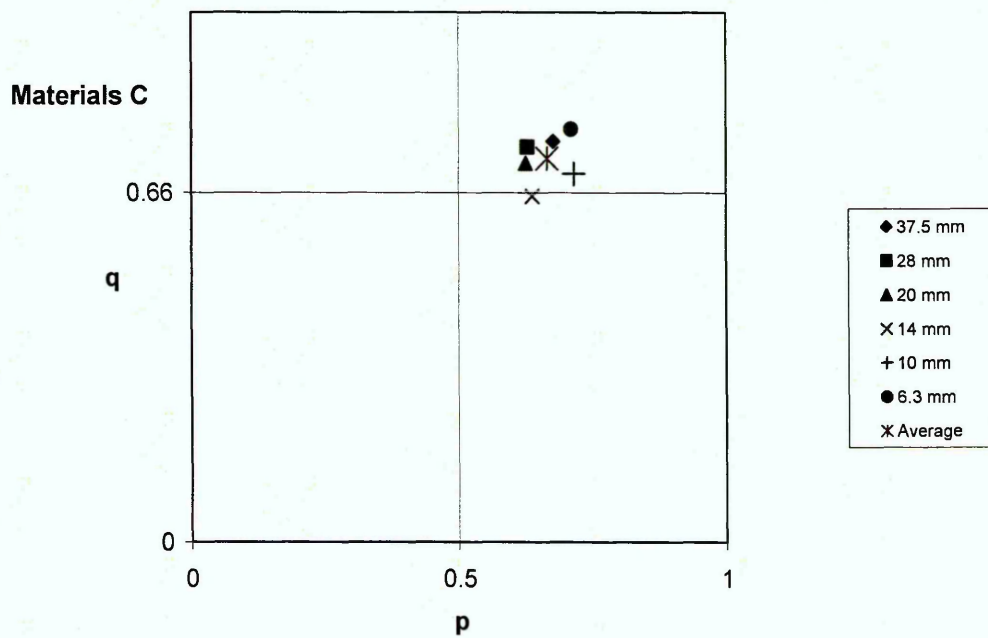


Average values for all the size fractions for Materials B (after Rösslein, 1941)

Materials C



Shape categories for all the size fractions for Materials C (by Rösslein, 1941)

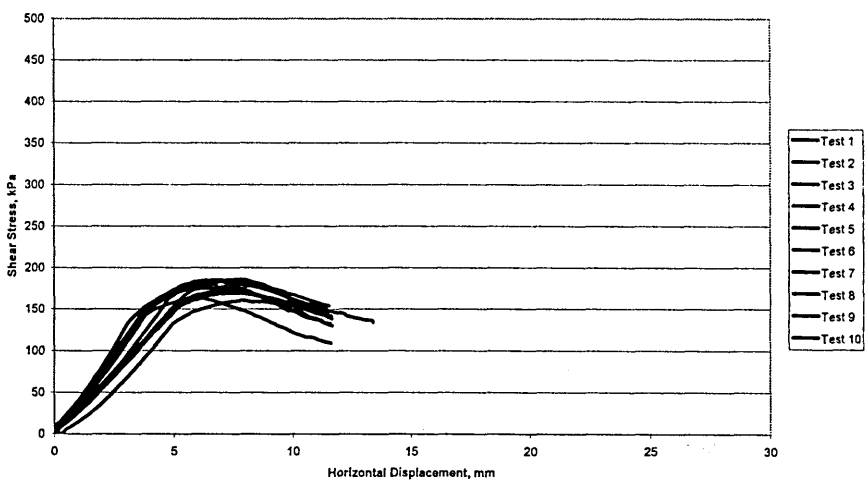


Average values for all the size fractions for Materials B (after Rösslein, 1941)

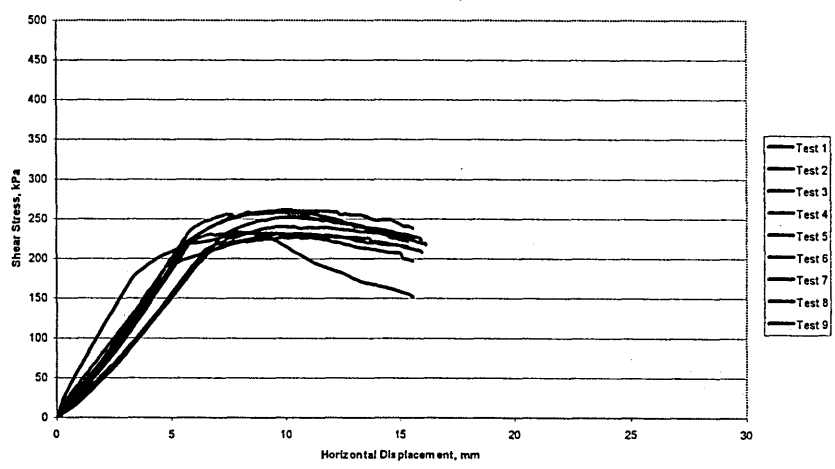
APPENDIX E

MATERIAL A

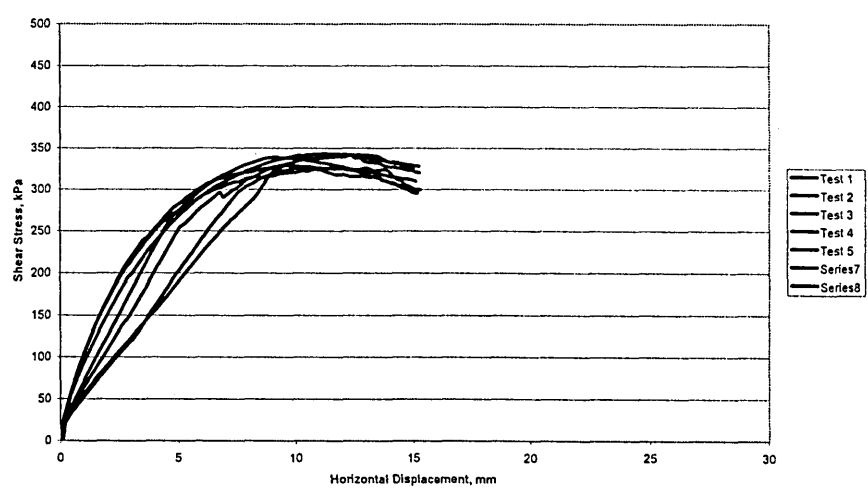
Shear Stress against Horizontal Displacement, Material A, SBT1, 95 kPa



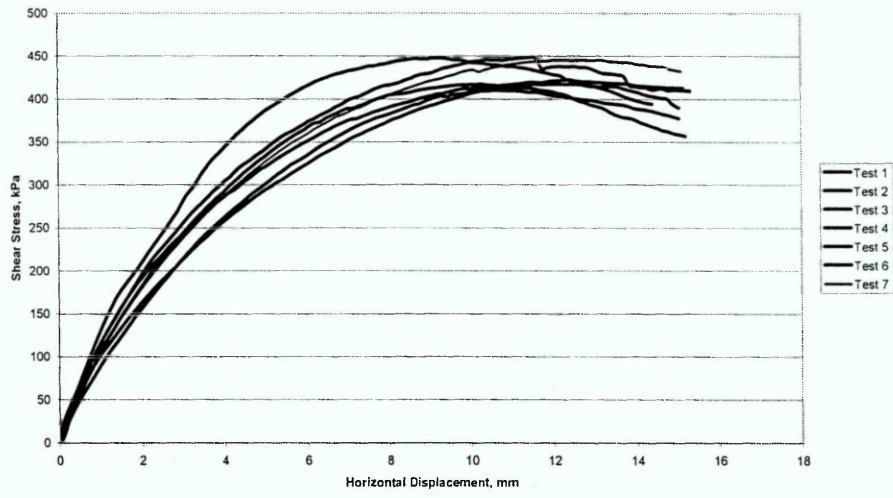
Shear Stress against Horizontal Displacement, Material A, SBT1, 143 kPa



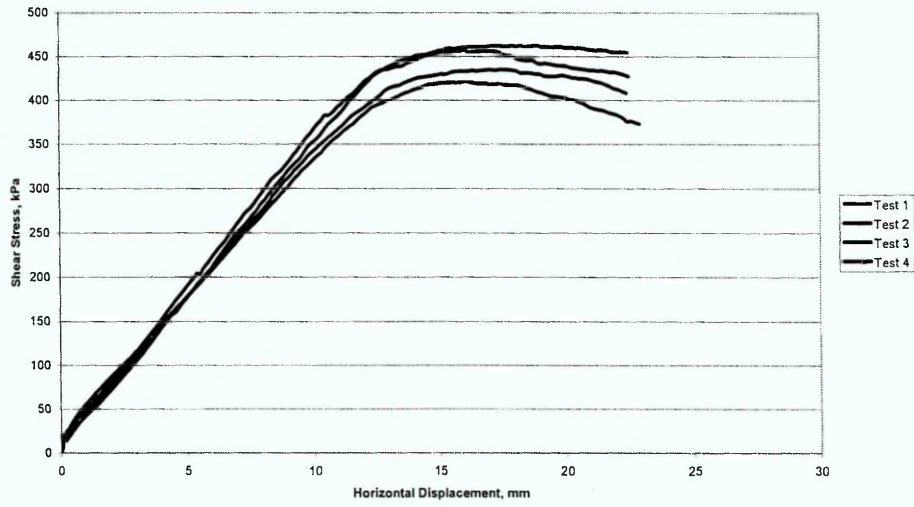
Shear Stress against Horizontal Displacement, Material A, SBT1, 190 kPa



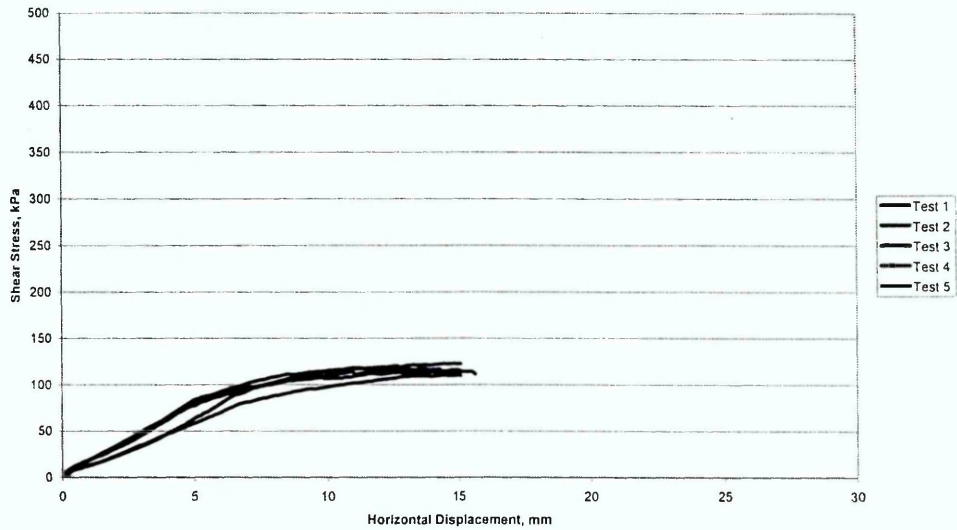
Shear Stress against Horizontal Displacement, Material A, SBT1, 238 kPa



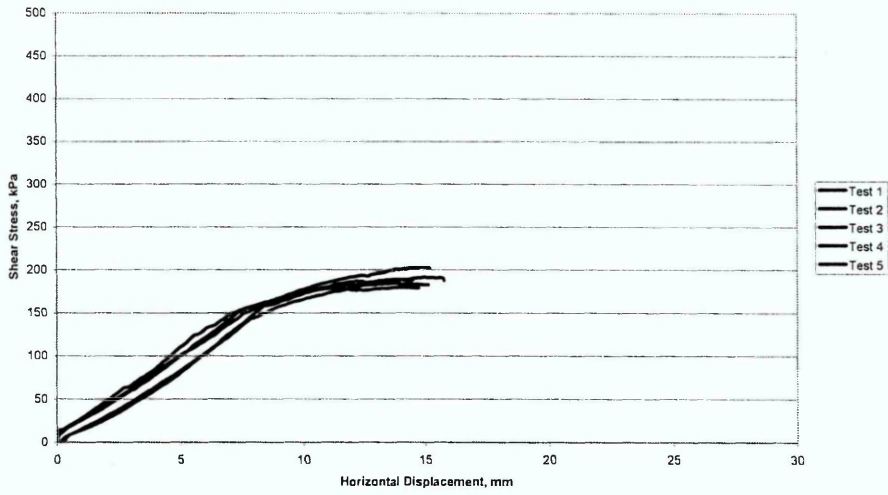
Shear Stress against Horizontal Displacement, Material A, SBT1, 317 kPa



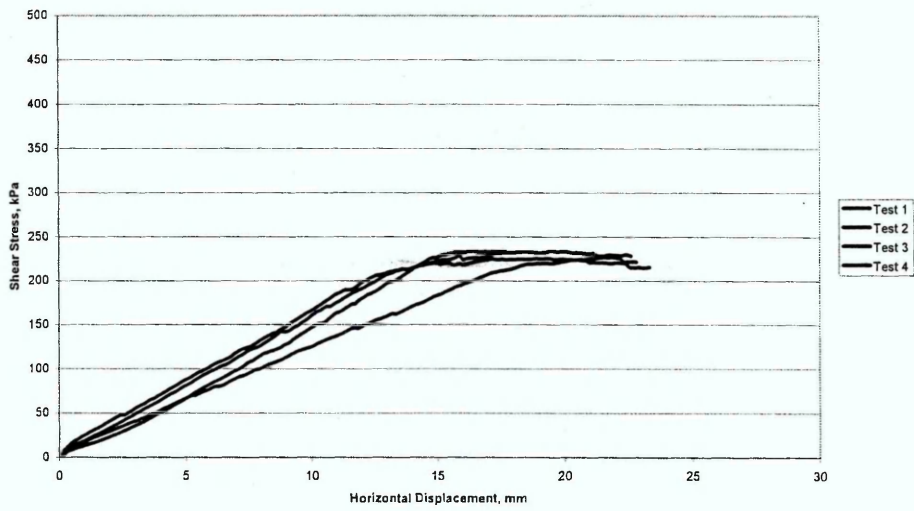
Shear Stress against Horizontal Displacement, Material A, SBT2, 95 kPa



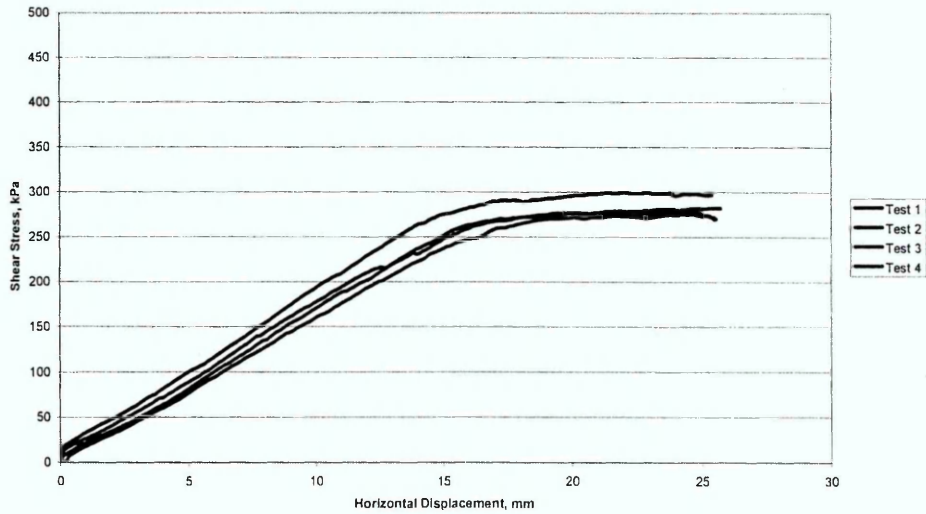
Shear Stress against Horizontal Displacement, Material A, SBT2, 143 kPa



Shear Stress against Horizontal Displacement, Material A, SBT2, 190 kPa



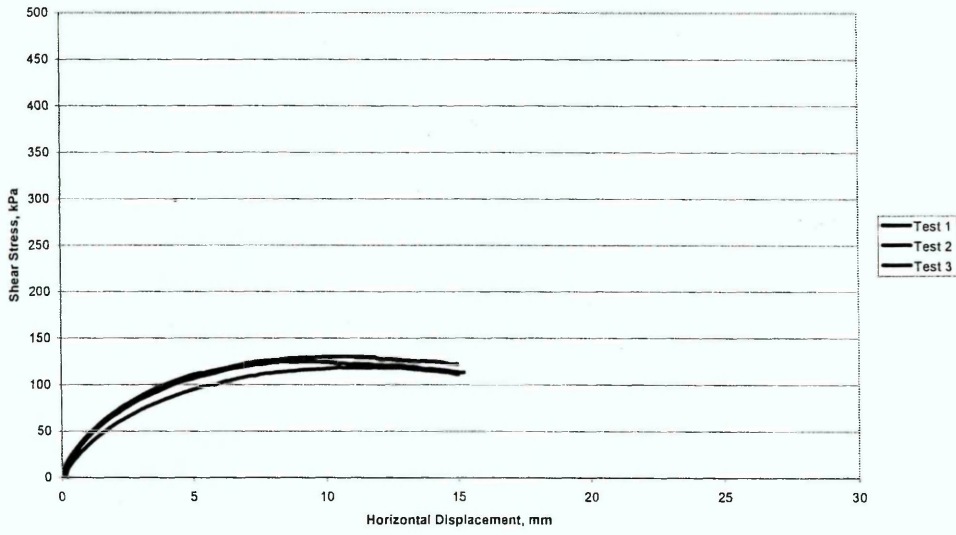
Shear Stress against Horizontal Displacement, Material A, SBT2, 238 kPa



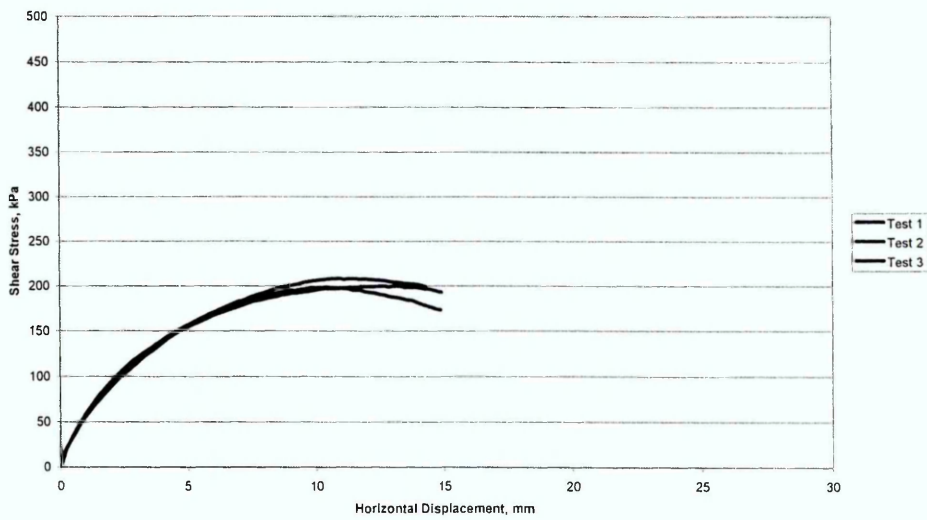
Shear Stress against Horizontal Displacement, Material A, SBT2, 317 kPa



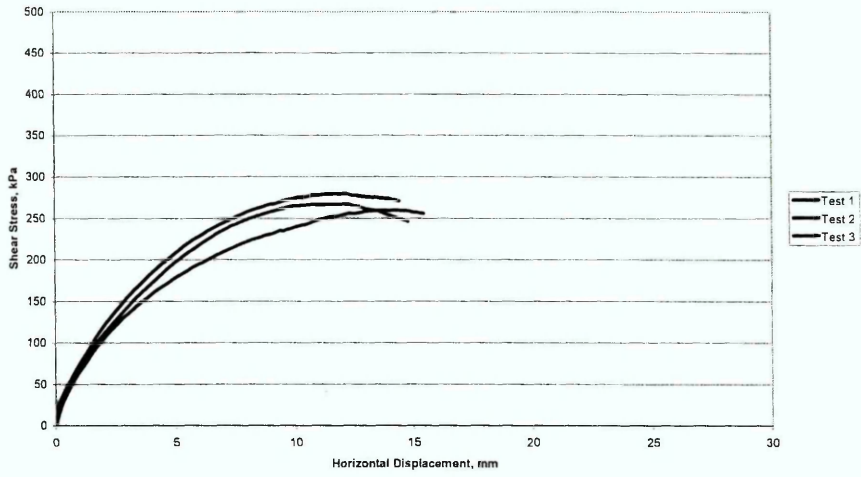
Shear Stress against Horizontal Displacement, Material A, SBT3, 95 kPa



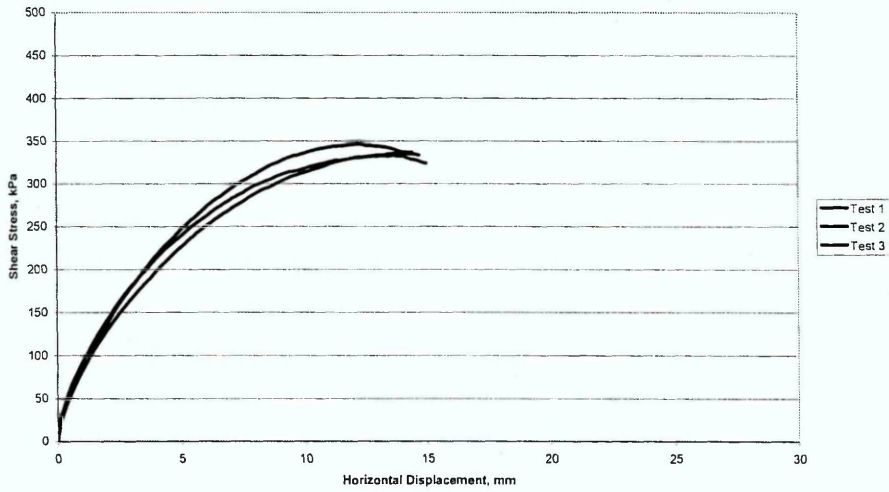
Shear Stress against Horizontal Displacement, Material A, SBT3, 143 kPa



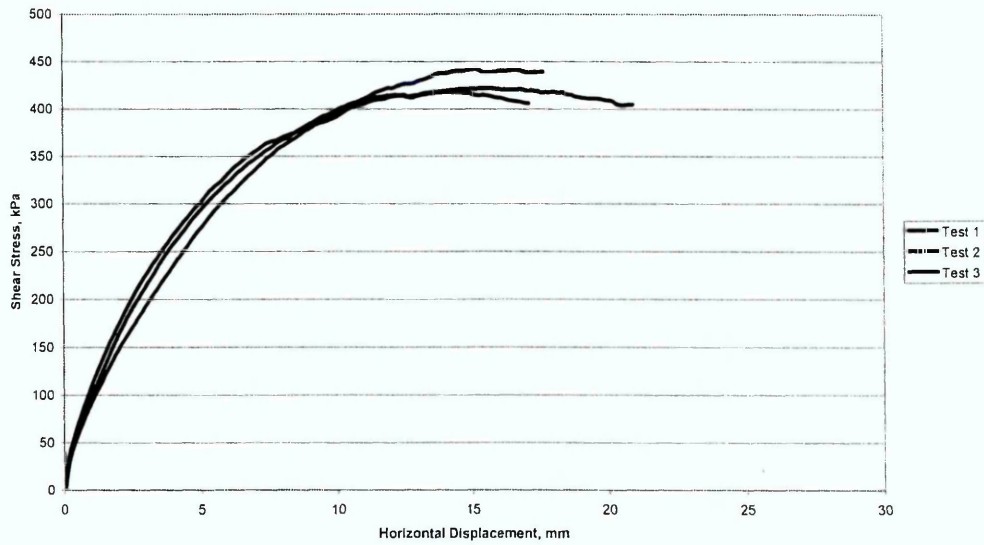
Shear Stress against Horizontal Displacement, Material A, SBT3, 190 kPa



Shear Stress against Horizontal Displacement, Material A, SBT3, 238 kPa

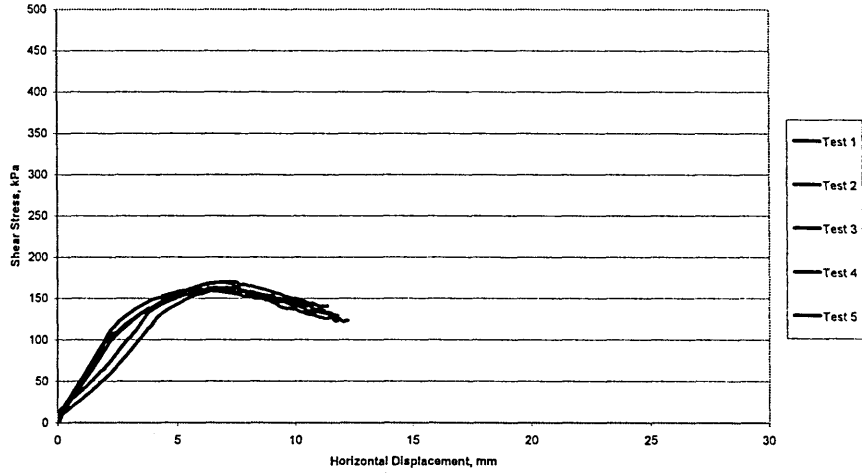


Shear Stress against Horizontal Displacement, Material A, SBT3, 317 kPa

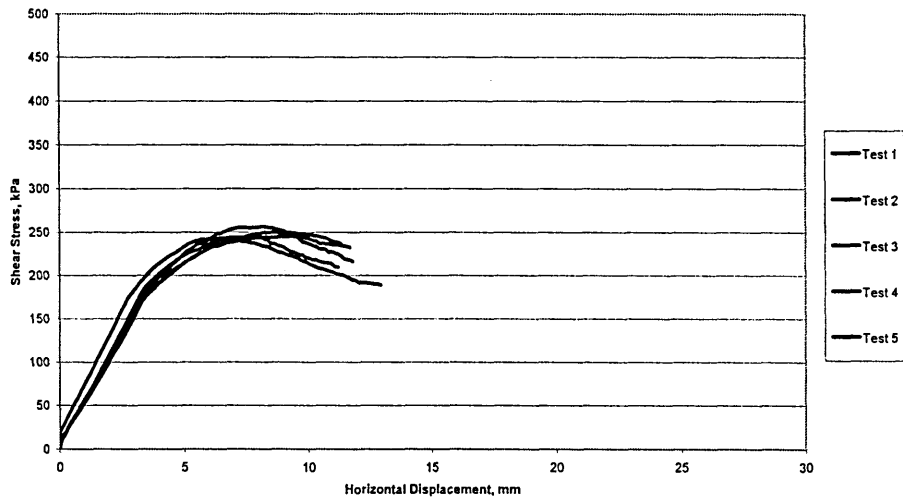


MATERIAL B

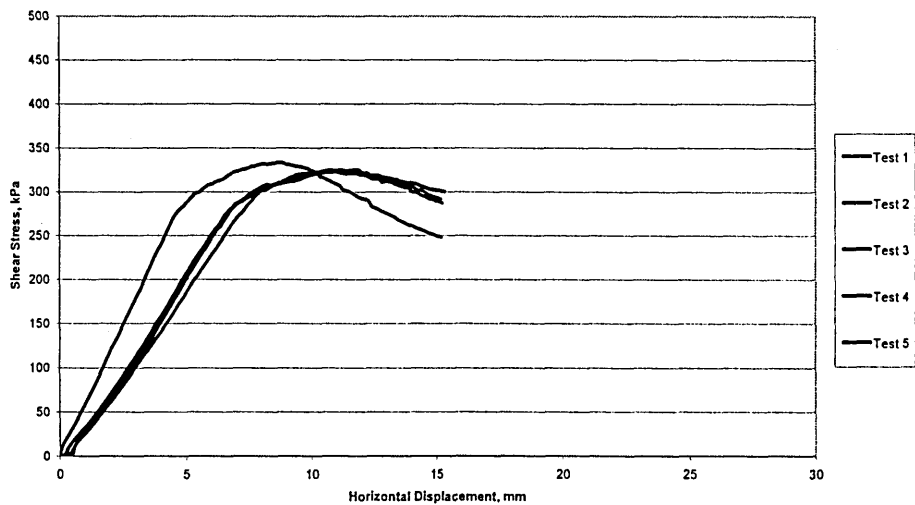
Shear Stress against Horizontal Displacement, Material B, SBT1, 95 kPa



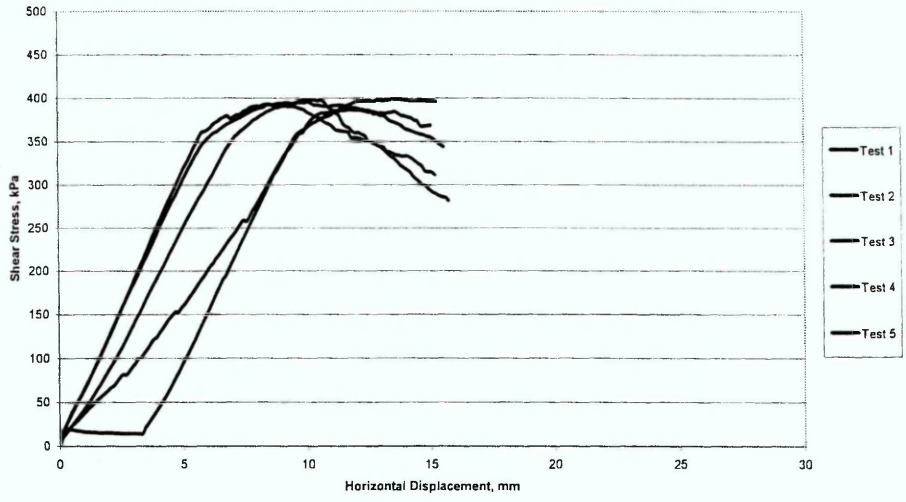
Shear Stress against Horizontal Displacement, Material B, SBT1, 143 kPa



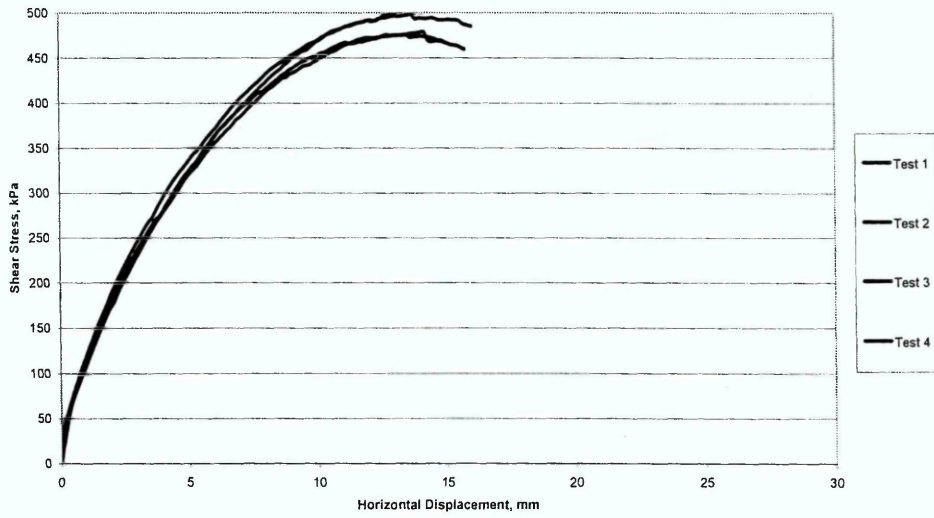
Shear Stress against Horizontal Displacement, Material B, SBT1, 190 kPa



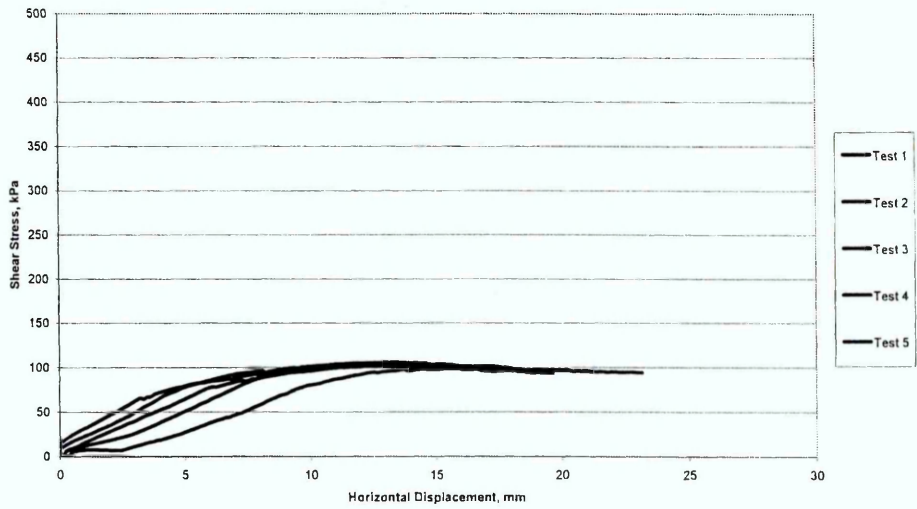
Shear Stress against Horizontal Displacement, Material B, SBT1, 238 kPa



Shear Stress against Horizontal Displacement, Material B, SBT1, 317 kPa



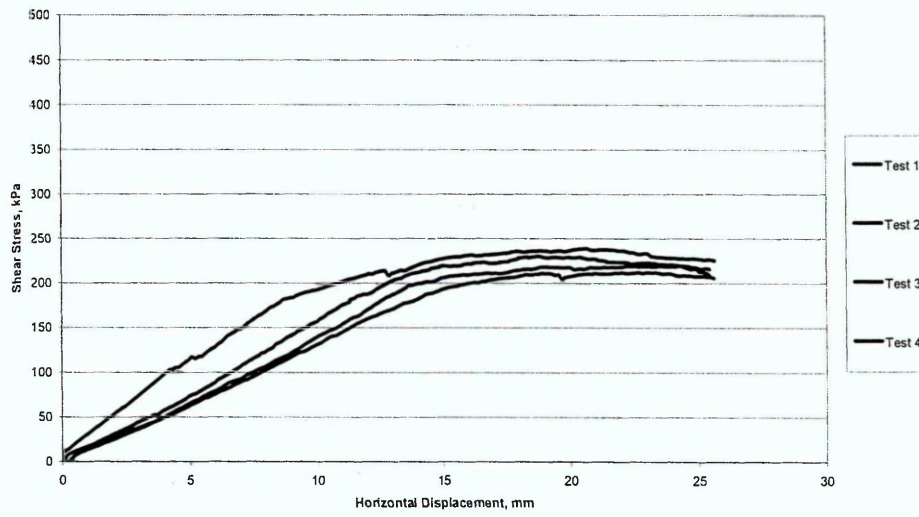
Shear Stress against Horizontal Displacement, Material B, SBT2, 95 kPa



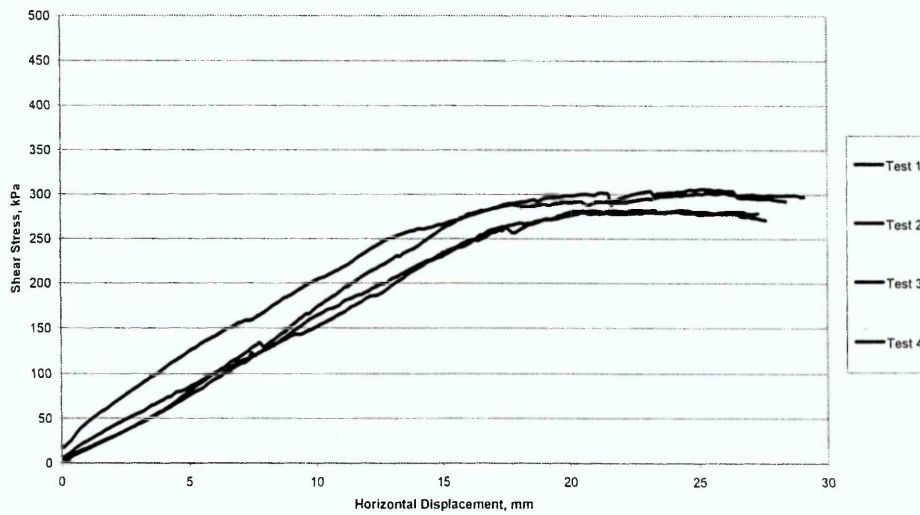
Shear Stress against Horizontal Displacement, Material B, SBT2, 143 kPa



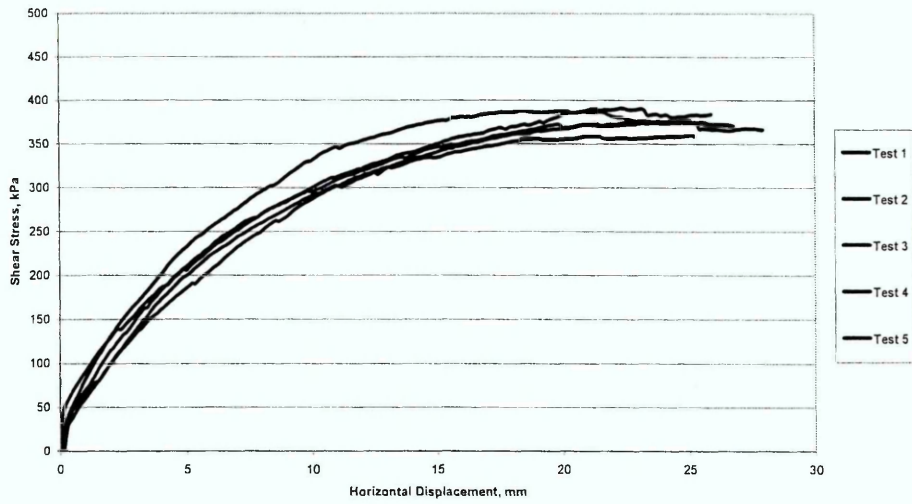
Shear Stress against Horizontal Displacement, Material B, SBT2, 190 kPa



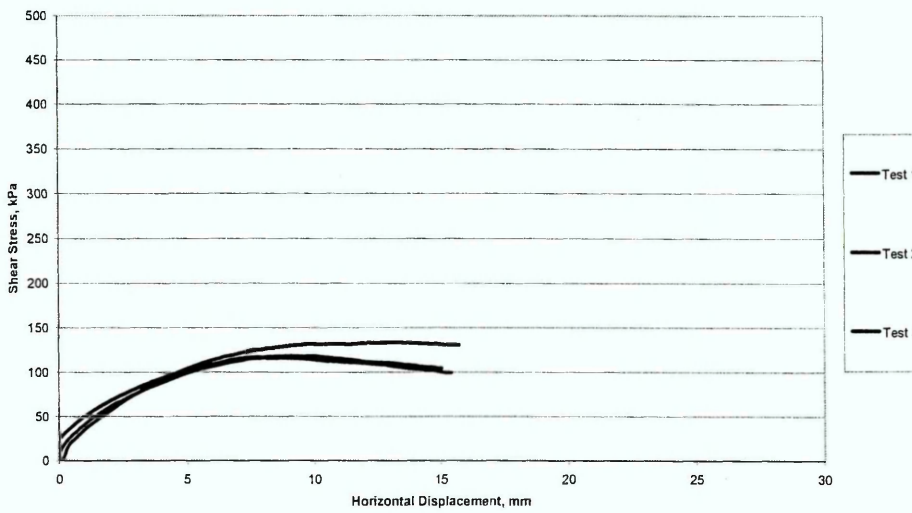
Shear Stress against Horizontal Displacement, Material B, SBT2, 238 kPa



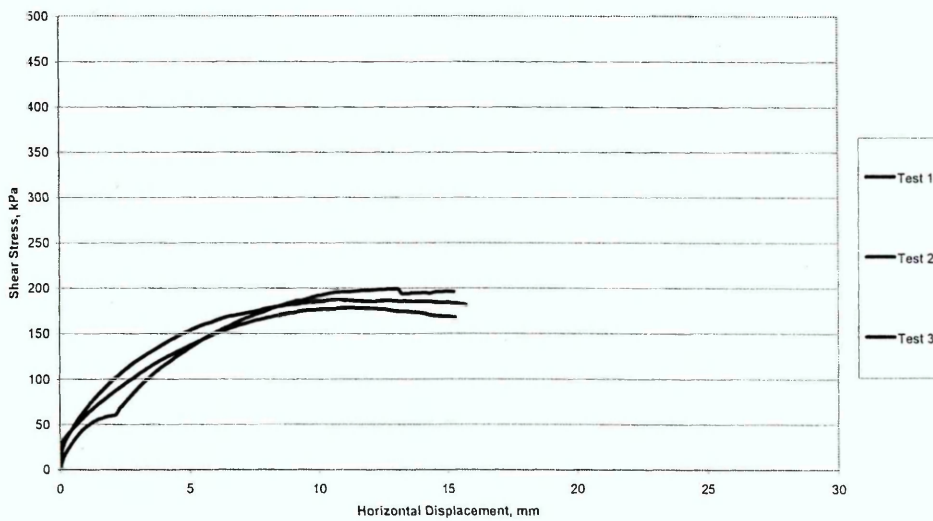
Shear Stress against Horizontal Displacement, Material B, SBT2, 317 kPa



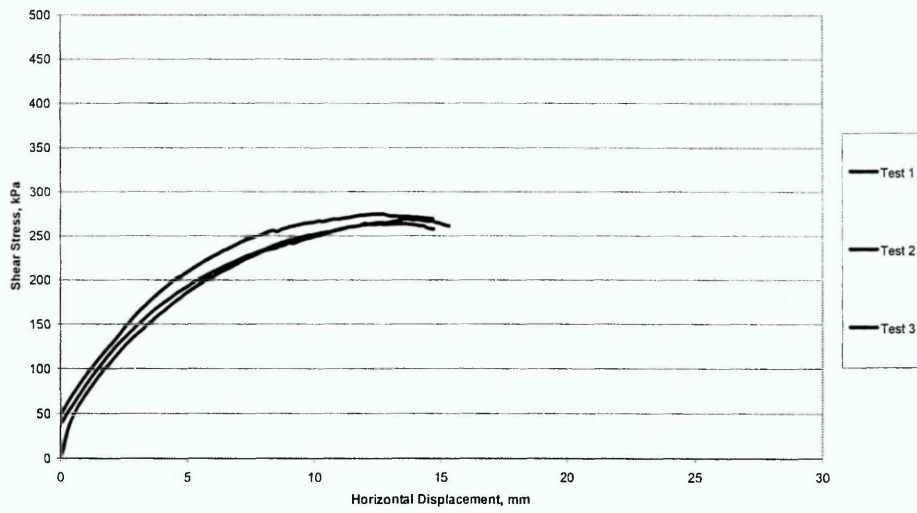
Shear Stress against Horizontal Displacement, Material B, SBT3, 95 kPa



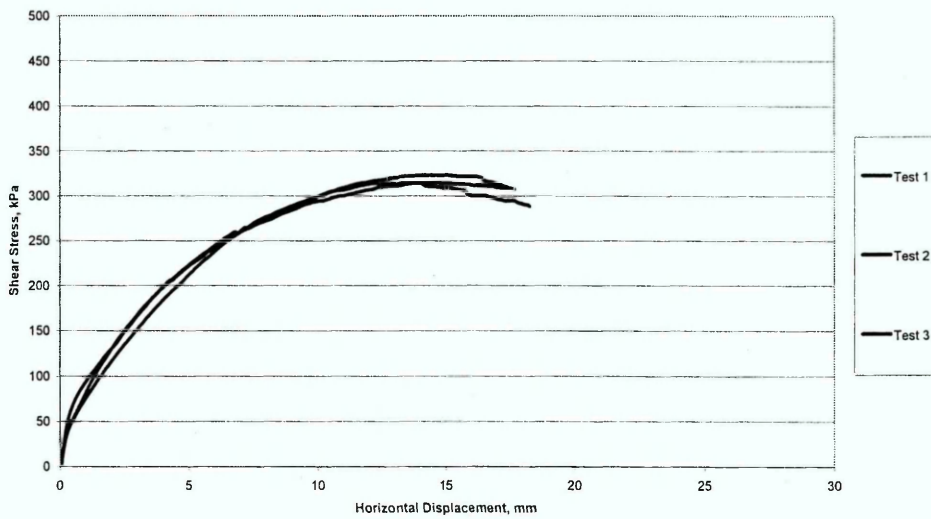
Shear Stress against Horizontal Displacement, Material B, SBT3, 143 kPa



Shear Stress against Horizontal Displacement, Material B, SBT3, 190 kPa



Shear Stress against Horizontal Displacement, Material B, SBT3, 238 kPa

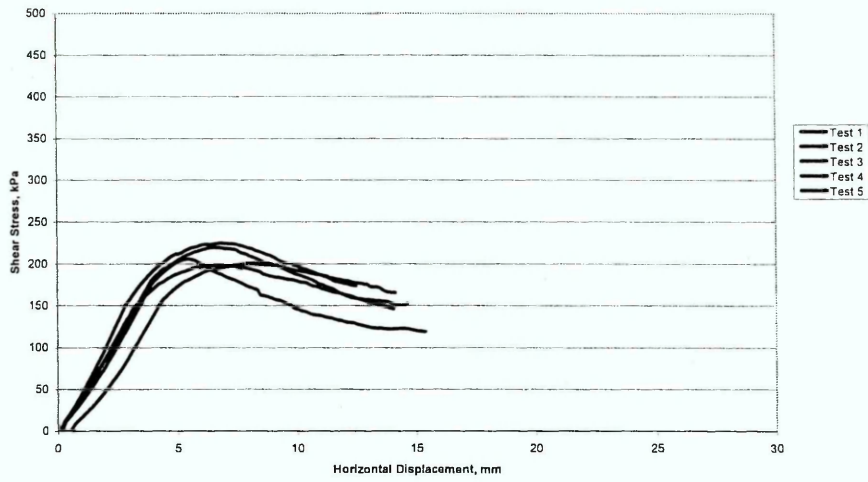


Shear Stress against Horizontal Displacement, Material B, SBT3, 317 kPa

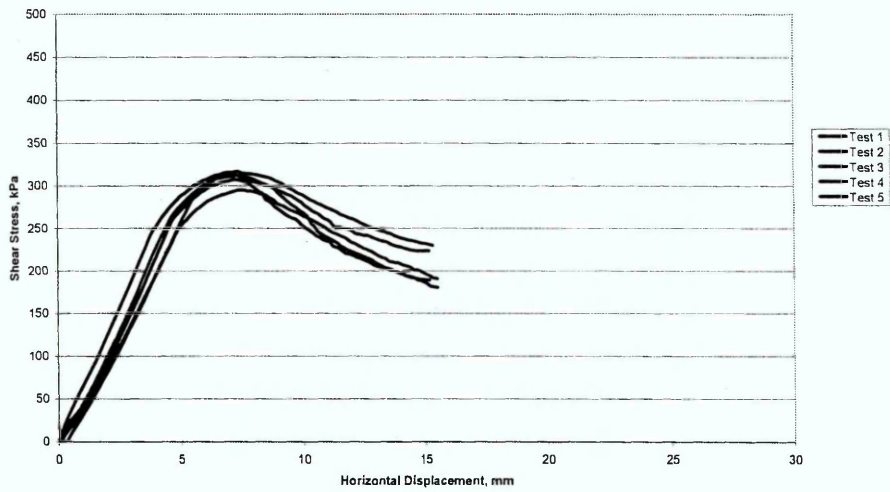


MATERIAL C

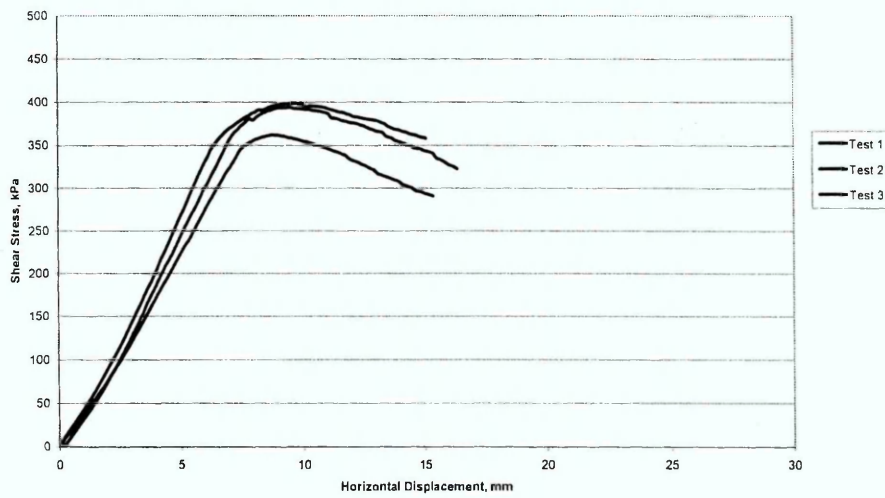
Shear Stress against Horizontal Displacement, Material C, SBT1, 95 kPa



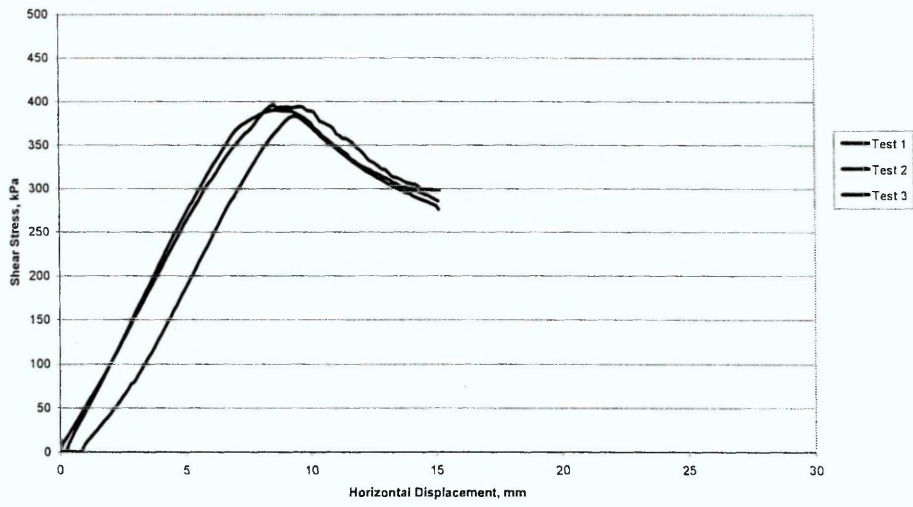
Shear Stress against Horizontal Displacement, Material C, SBT1, 143 kPa



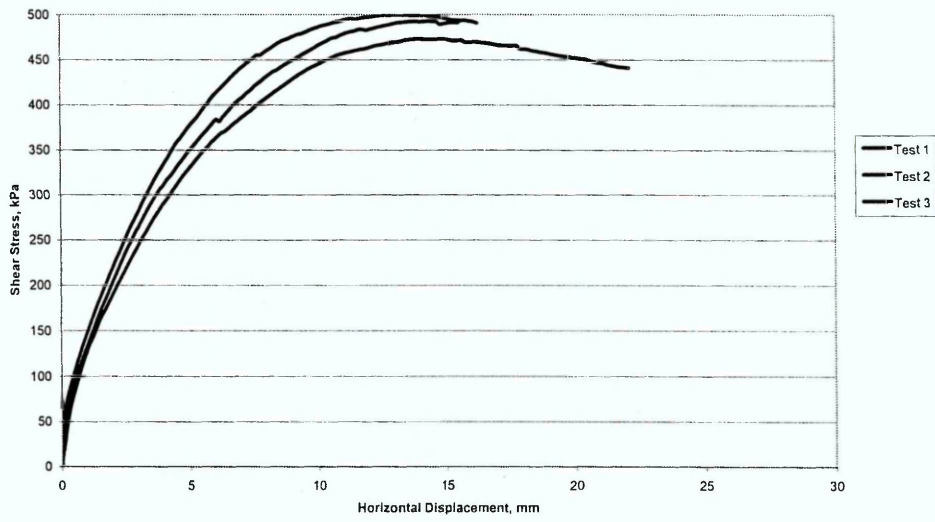
Shear Stress against Horizontal Displacement, Material C, SBT1, 190 kPa



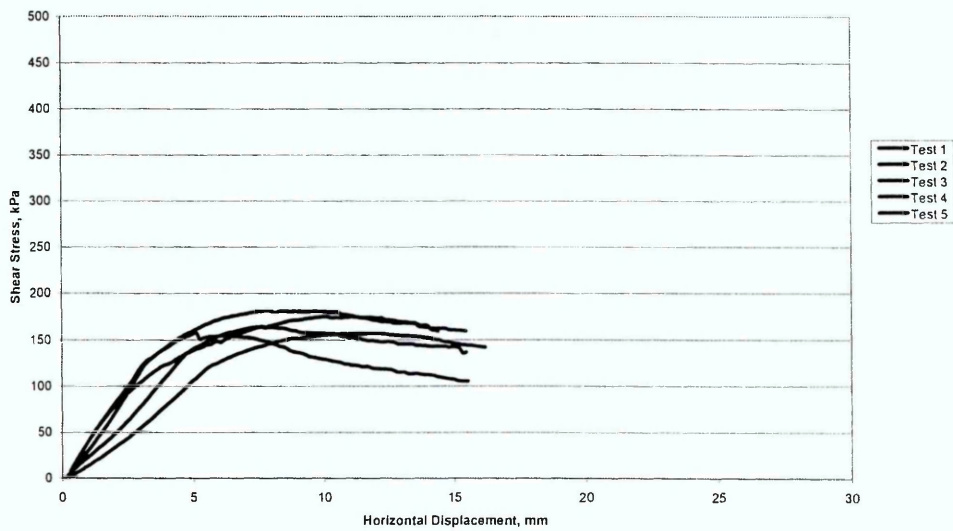
Shear Stress against Horizontal Displacement, Material C, SBT1, 238 kPa



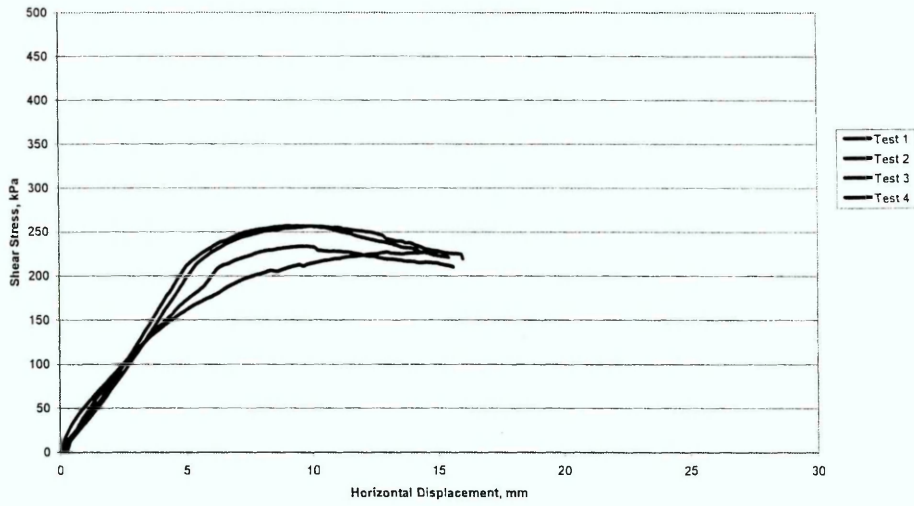
Shear Stress against Horizontal Displacement, Material C, SBT1, 317 kPa



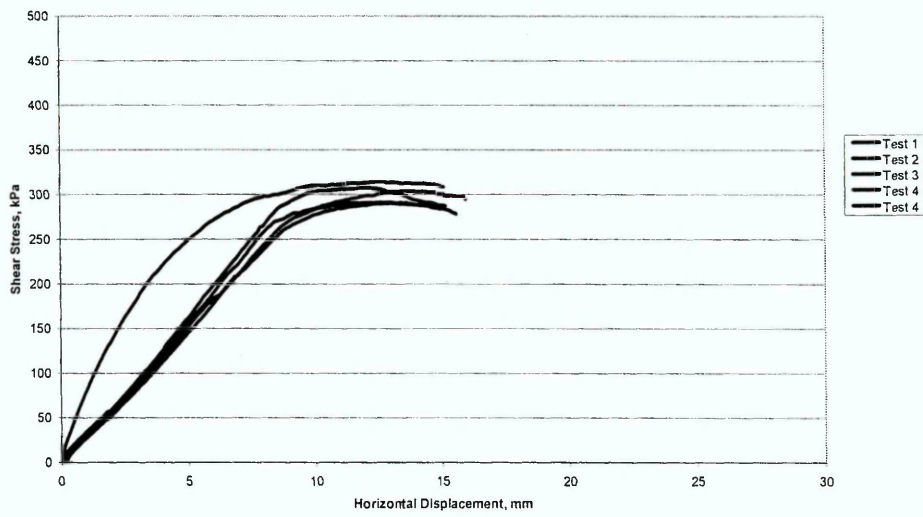
Shear Stress against Horizontal Displacement, Material C, SBT2, 95 kPa



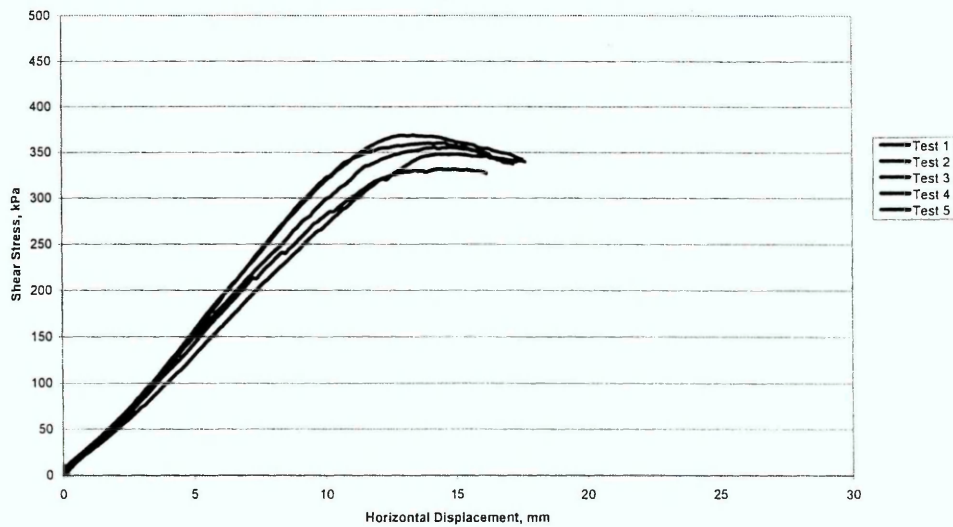
Shear Stress against Horizontal Displacement, Material C, SBT2, 143 kPa



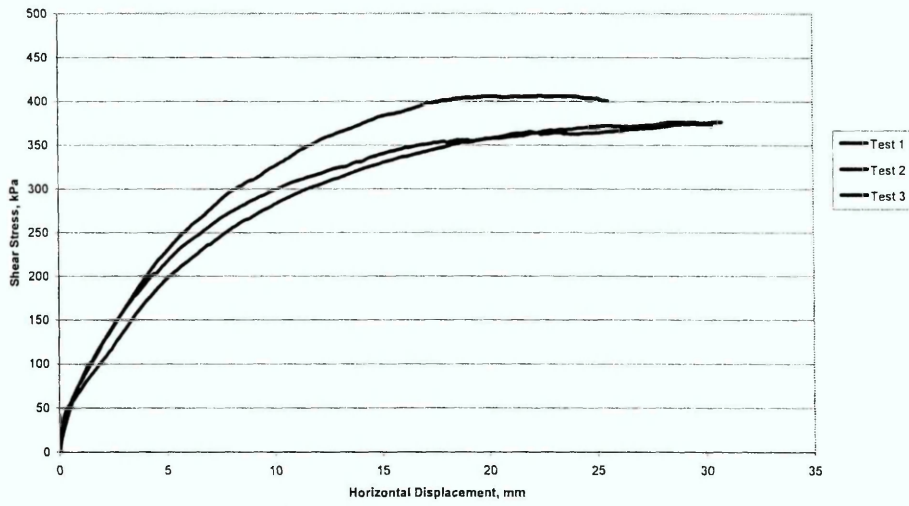
Shear Stress against Horizontal Displacement, Material C, SBT2, 190 kPa



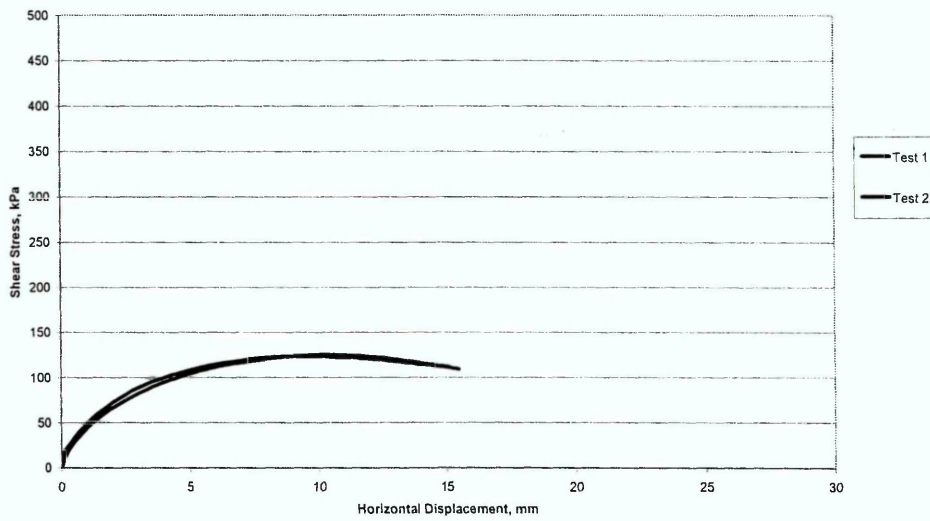
Shear Stress against Horizontal Displacement, Material C, SBT2, 238 kPa



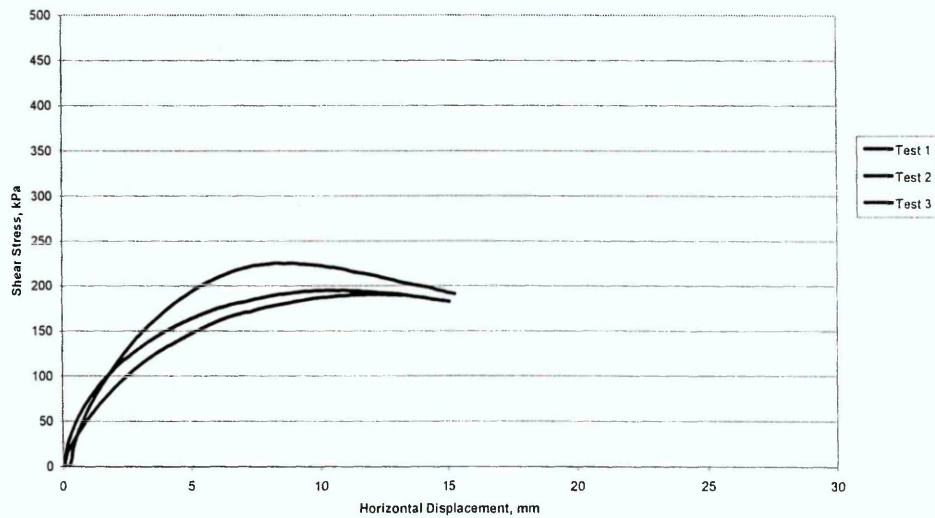
Shear Stress against Horizontal Displacement, Material C, SBT2, 317 kPa



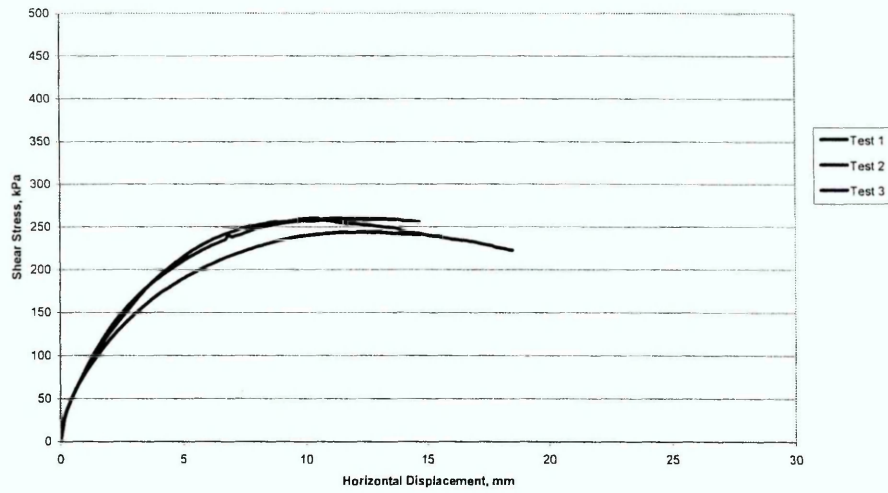
Shear Stress against Horizontal Displacement, Material C, SBT3, 95 kPa



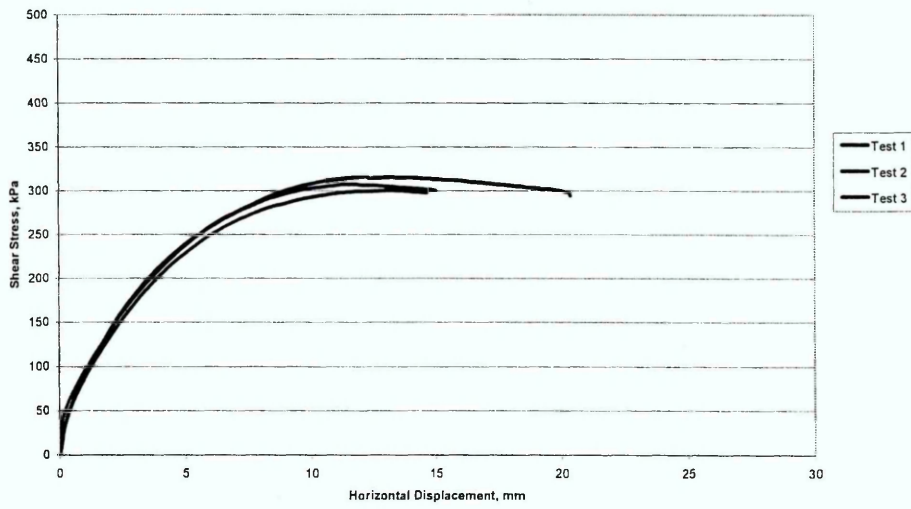
Shear Stress against Horizontal Displacement, Material C, SBT3, 143 kPa



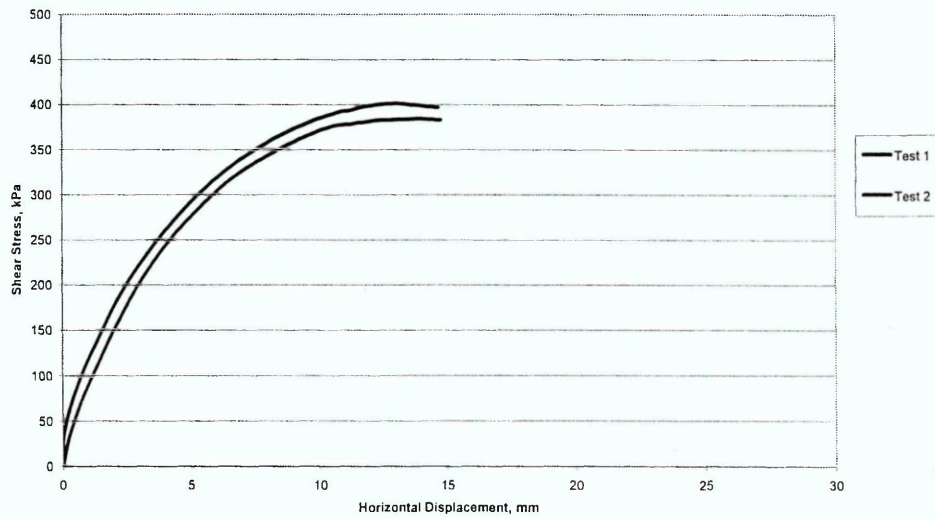
Shear Stress against Horizontal Displacement, Material C, SBT3, 190 kPa



Shear Stress against Horizontal Displacement, Material C, SBT3, 238 kPa



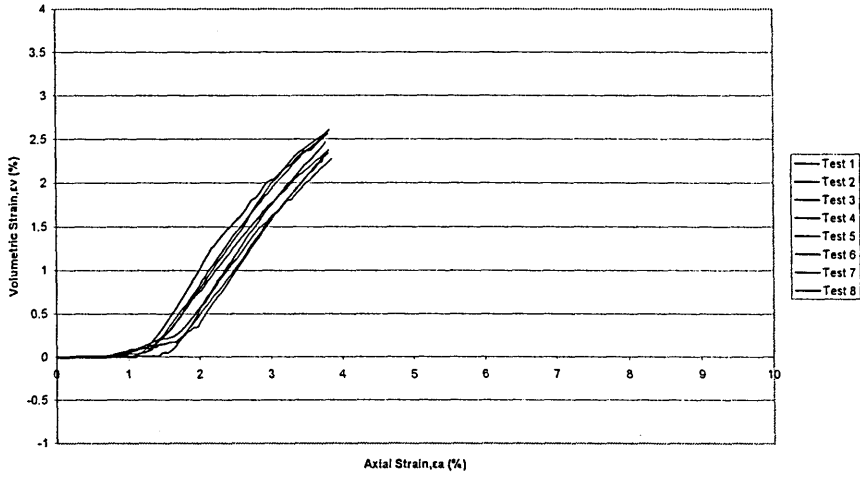
Shear Stress against Horizontal Displacement, Material C, SBT3, 317 kPa



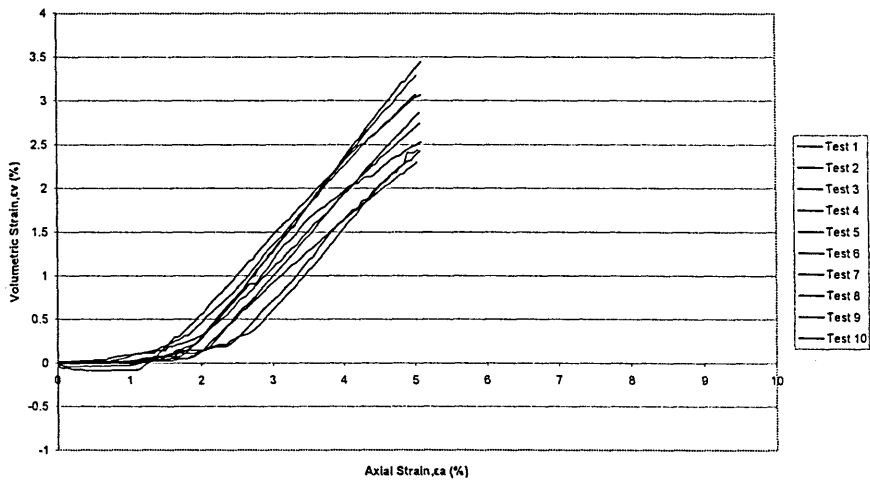
APPENDIX F

MATERIAL A

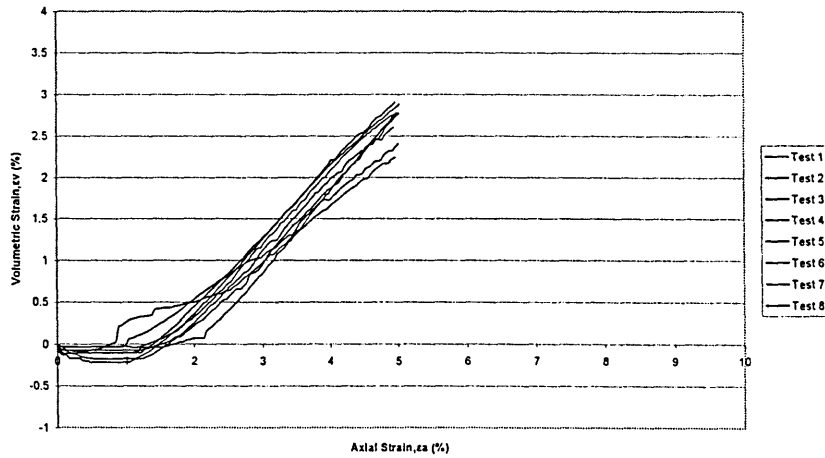
Volume Behaviour, Material A, SBT1, 95 kPa



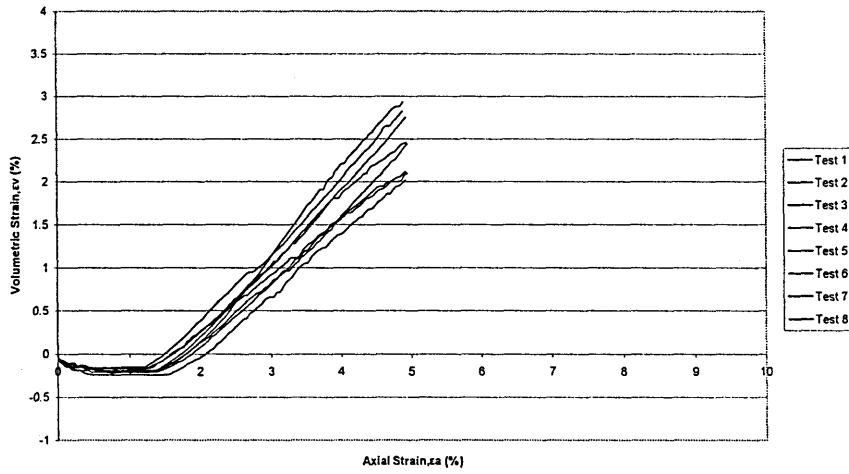
Volume Behaviour, Material A, SBT1, 143 kPa



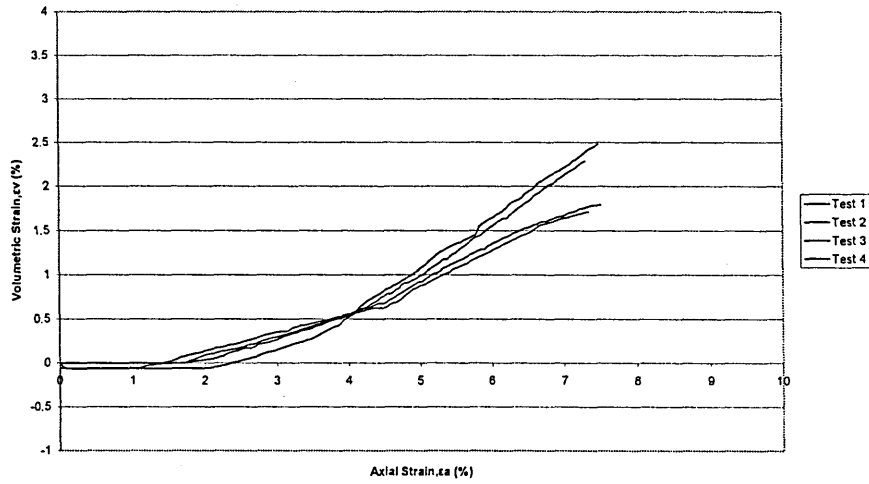
Volume Behaviour, Material A, SBT1, 190 kPa



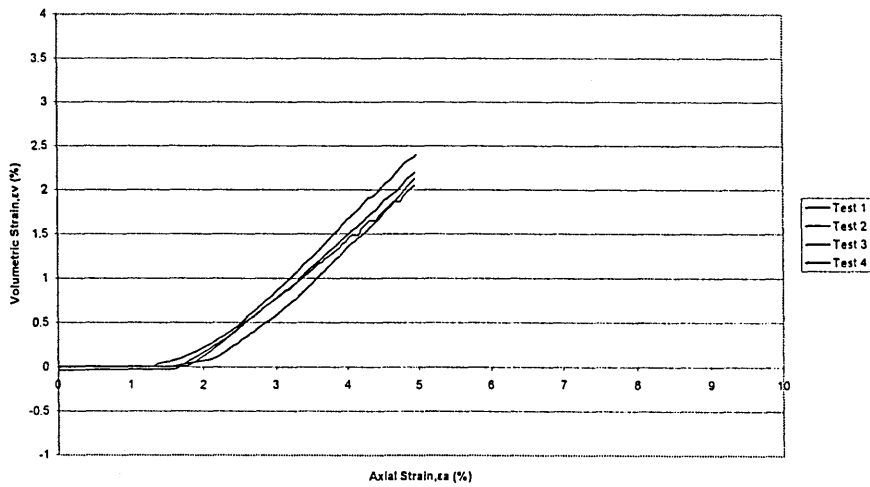
Volume Behaviour, Material A, SBT1, 238 kPa



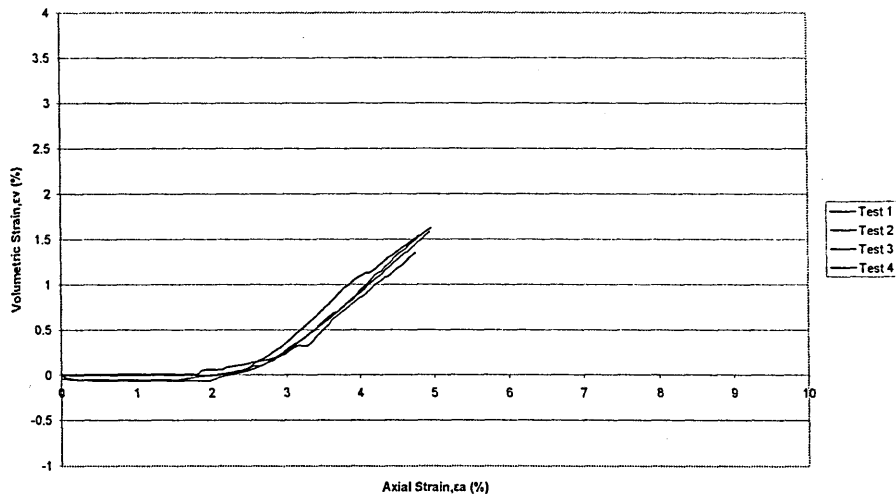
Volume Behaviour, Material A, SBT1, 317 kPa



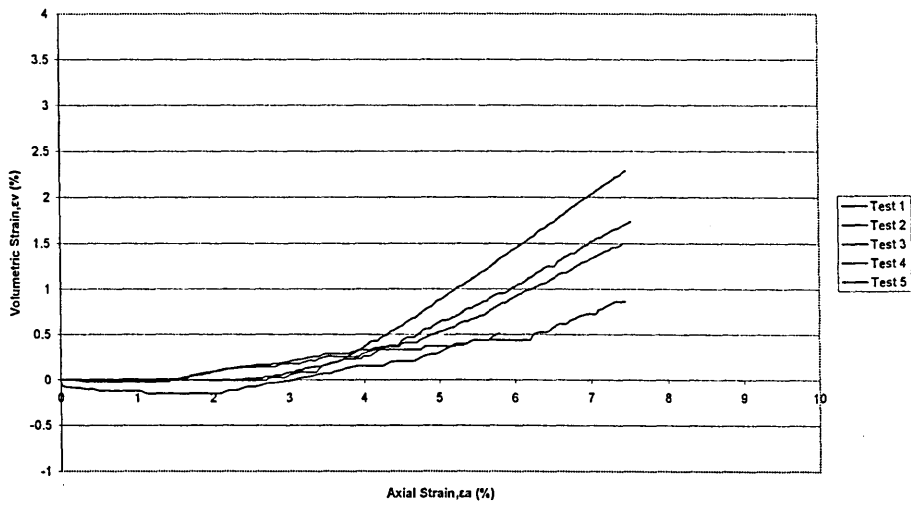
Volume Behaviour, Material A, SBT2, 95 kPa



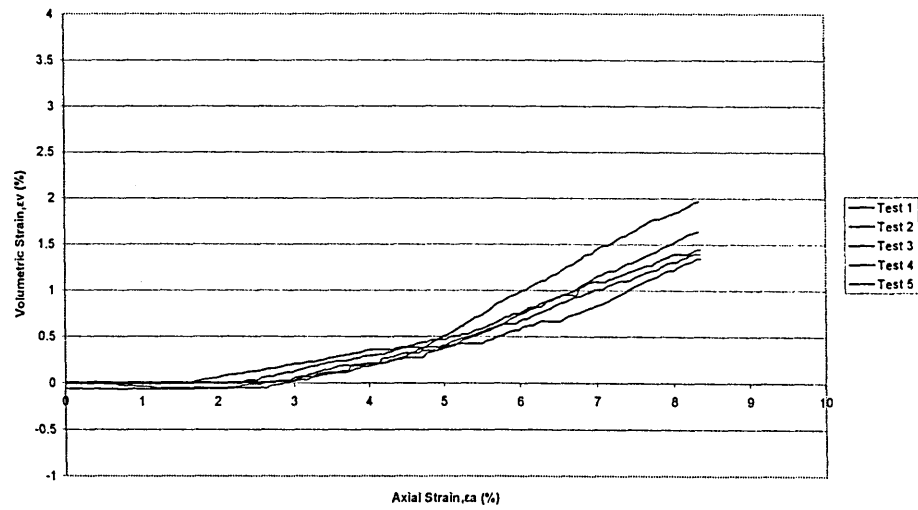
Volume Behaviour, Material A, SBT2, 143 kPa



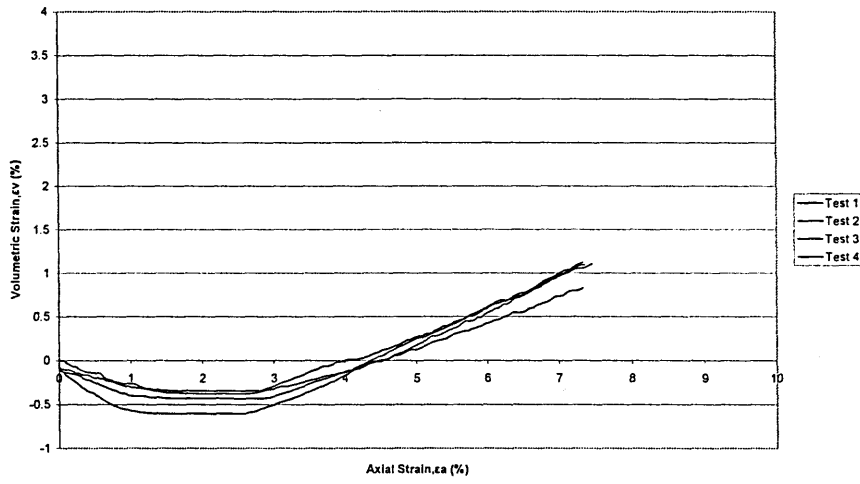
Volume Behaviour, Material A, SBT2, 190 kPa



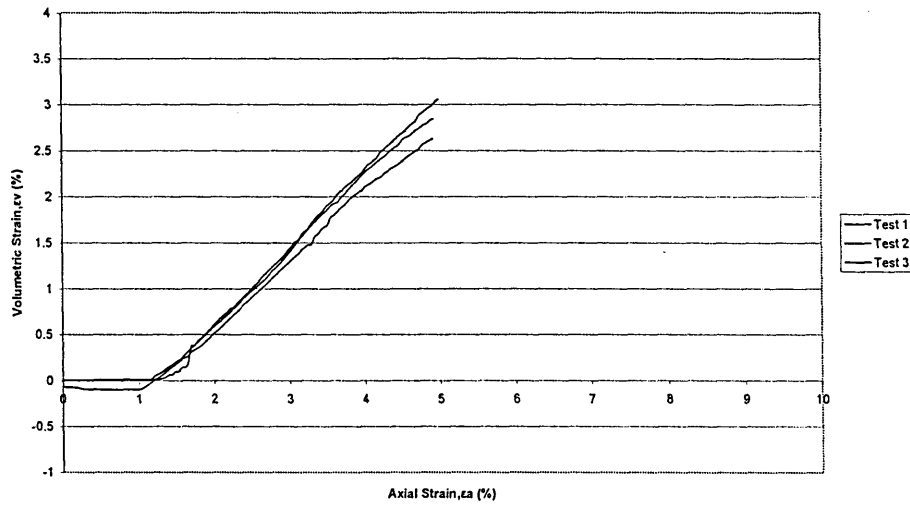
Volume Behaviour, Material A, SBT2, 238 kPa



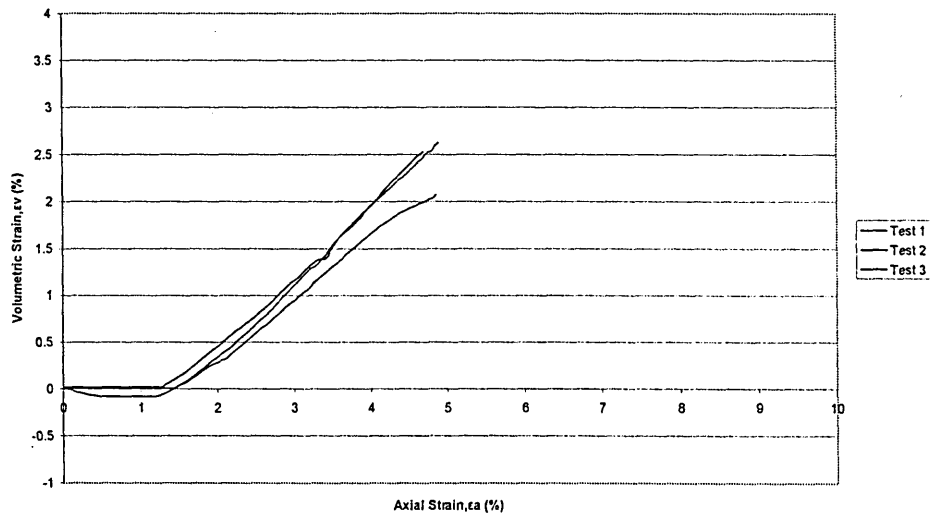
Volume Behaviour, Material A, SBT2, 238 kPa



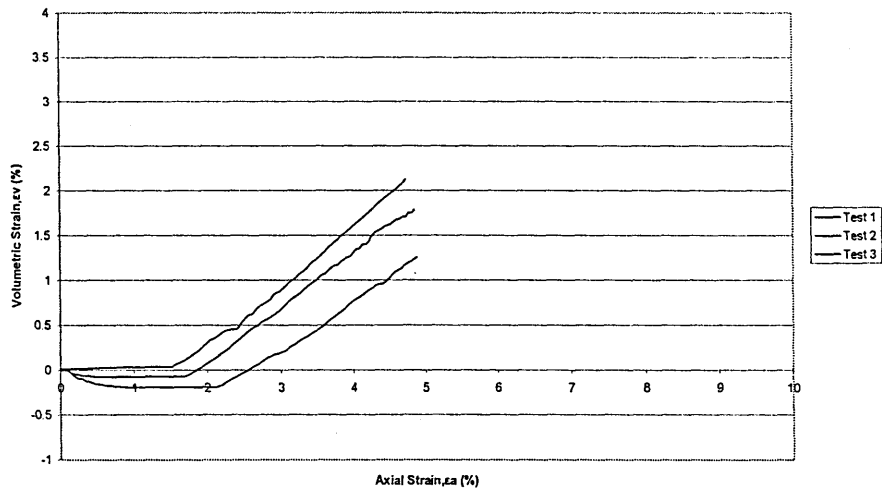
Volume Behaviour, Material A, SBT3, 95 kPa



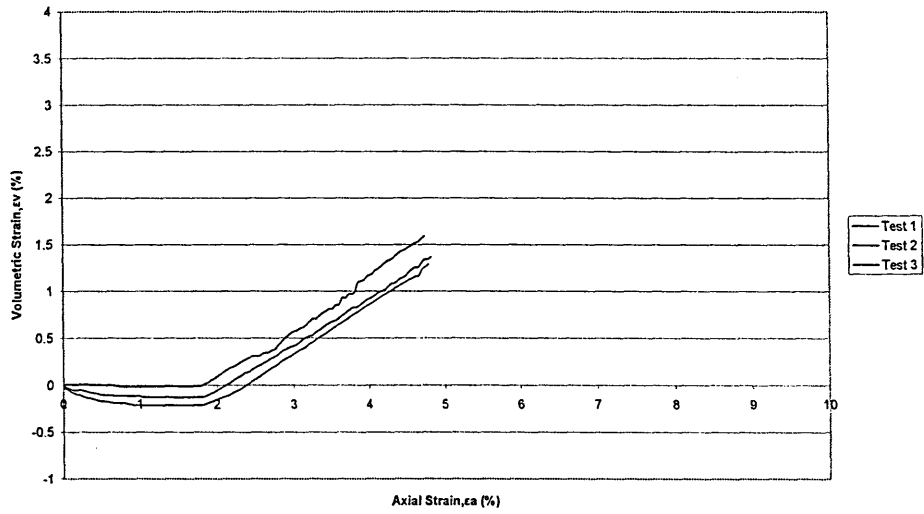
Volume Behaviour, Material A, SBT3, 143 kPa



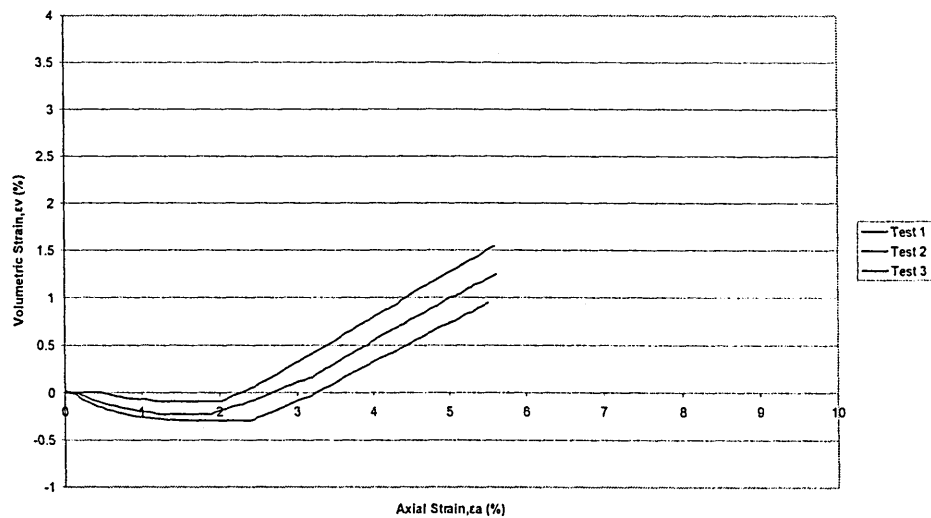
Volume Behaviour, Material A, SBT3, 190 kPa



Volume Behaviour, Material A, SBT3, 238 kPa

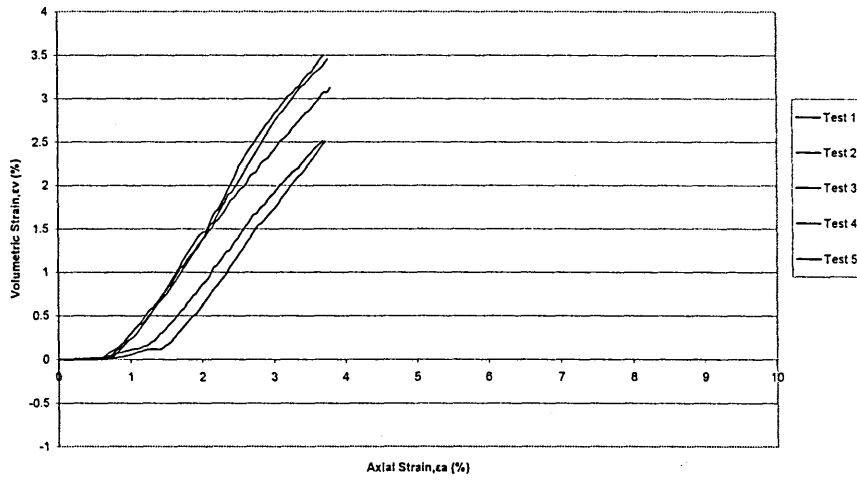


Volume Behaviour, Material A, SBT3, 317 kPa

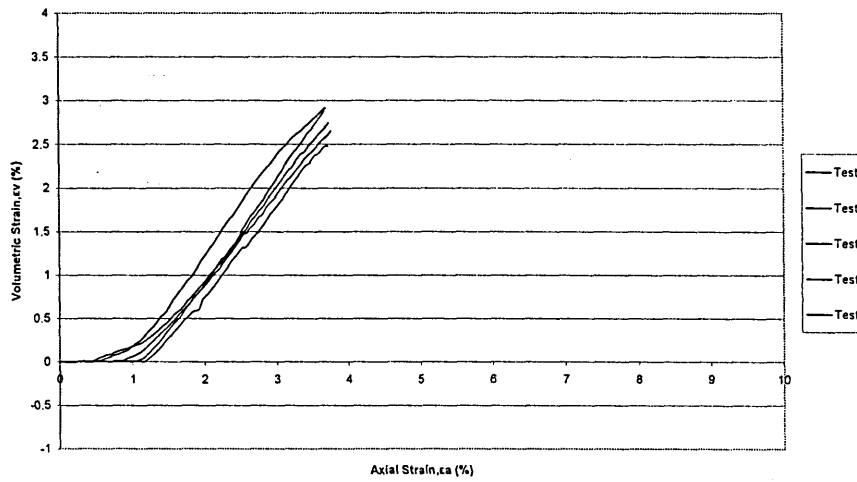


MATERIAL B

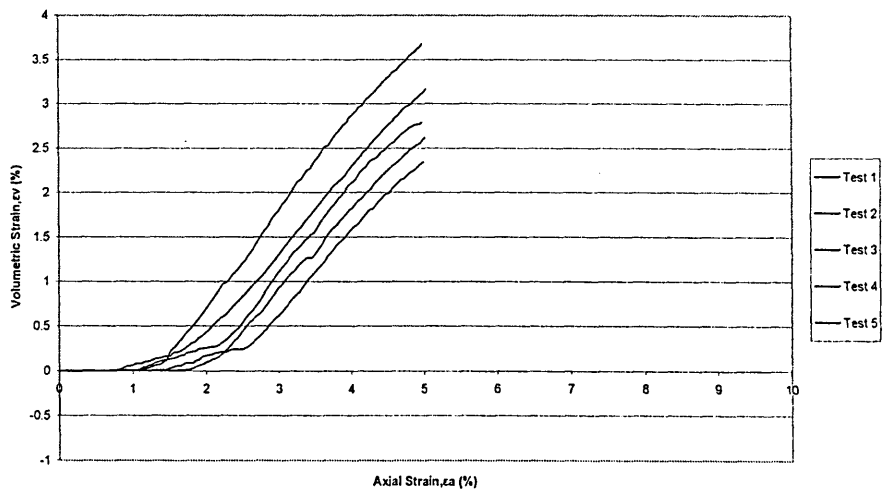
Volume Behaviour, Material B, SBT1, 95 kPa



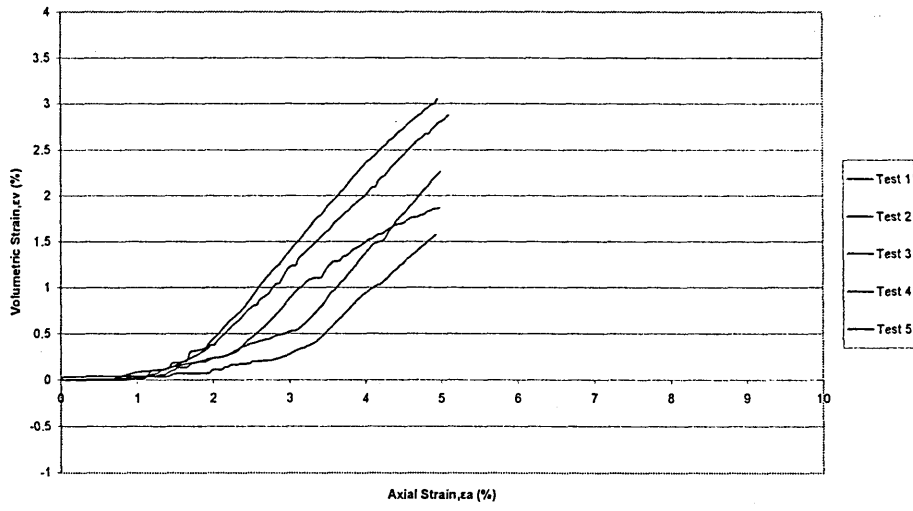
Volume Behaviour, Material B, SBT1, 143 kPa



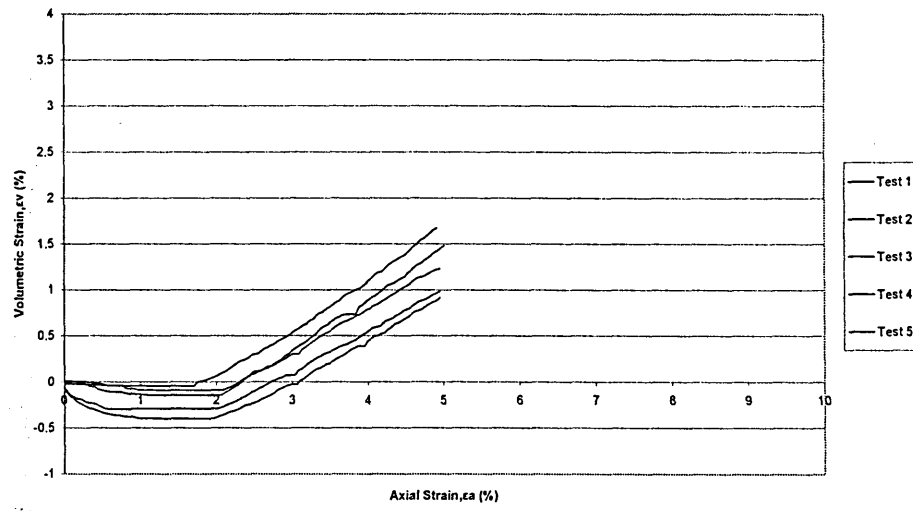
Volume Behaviour, Material B, SBT1, 190 kPa



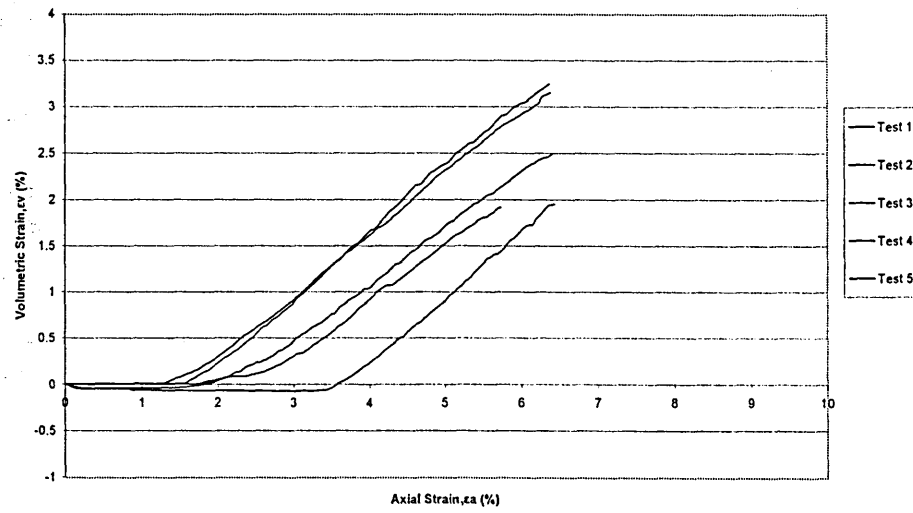
Volume Behaviour, Material B, SBT1, 238 kPa



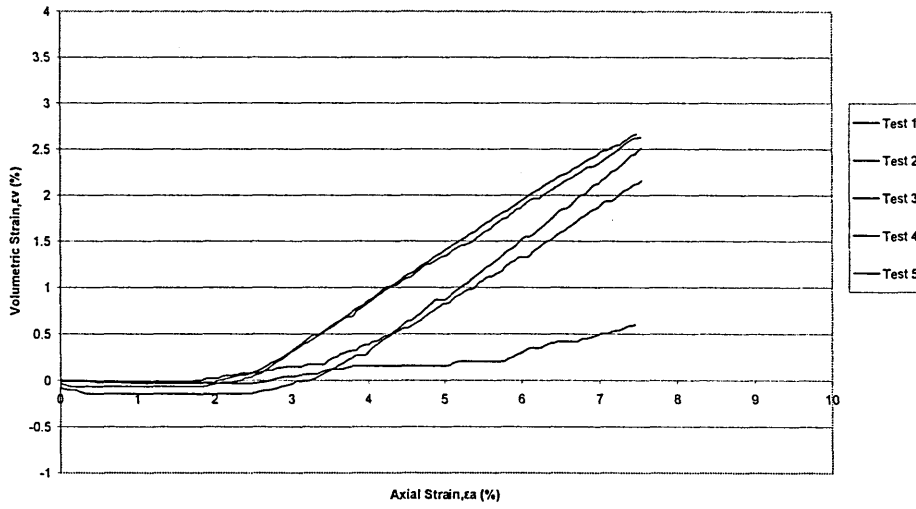
Volume Behaviour, Material B, SBT1, 317 kPa



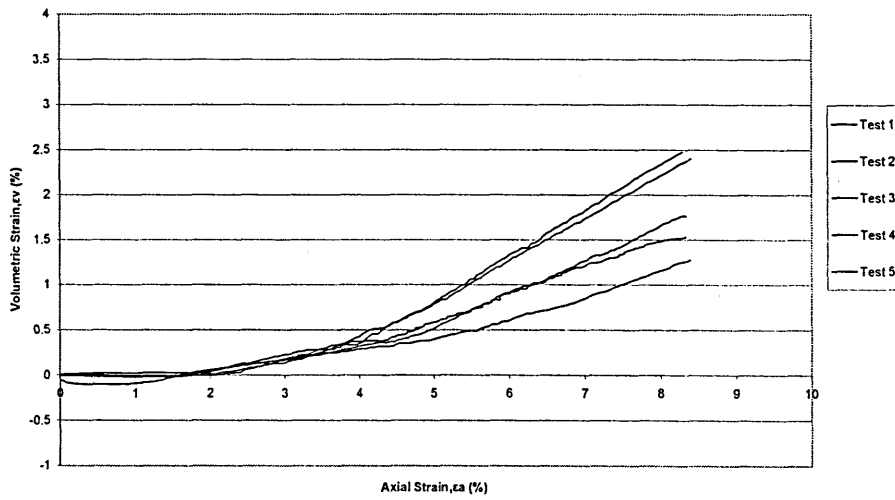
Volume Behaviour, Material B, SBT2, 95 kPa



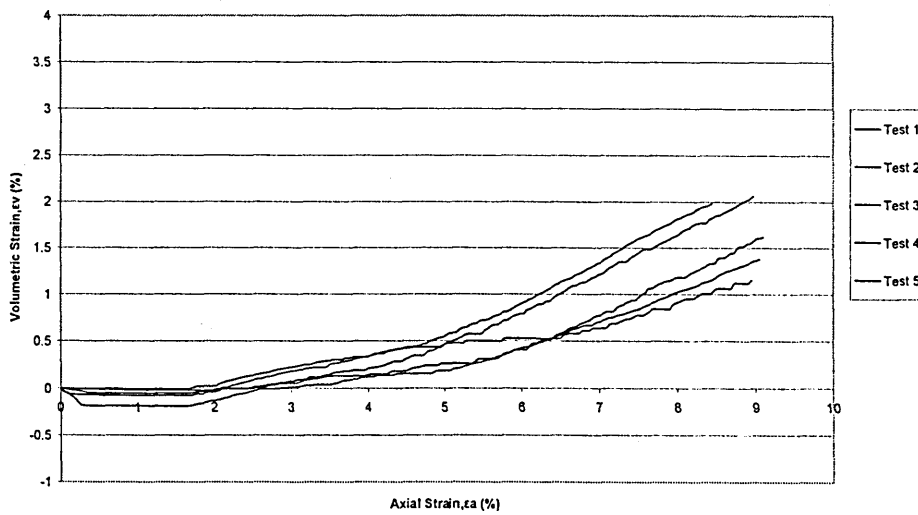
Volume Behaviour, Material B, SBT2, 143 kPa



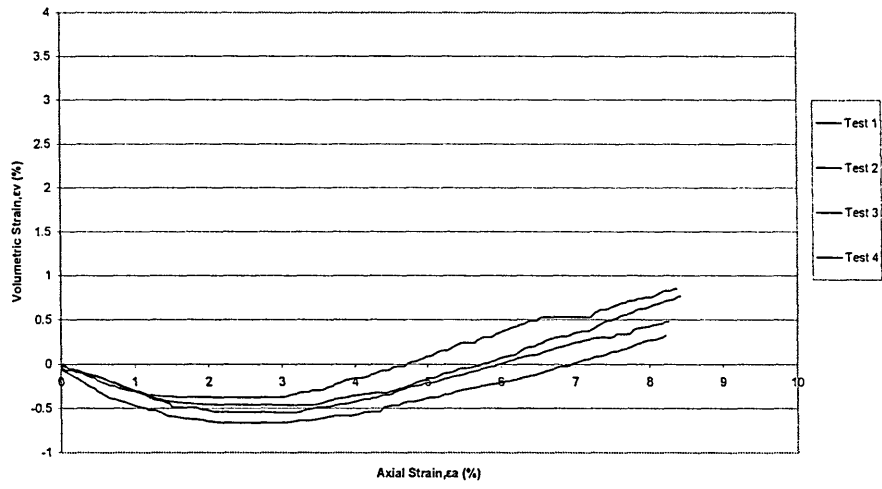
Volume Behaviour, Material B, SBT2, 190 kPa



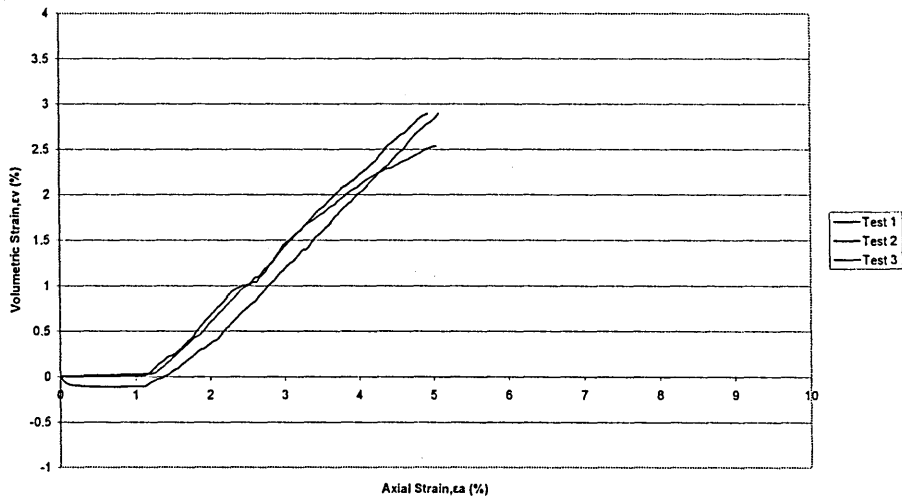
Volume Behaviour, Material B, SBT2, 238 kPa



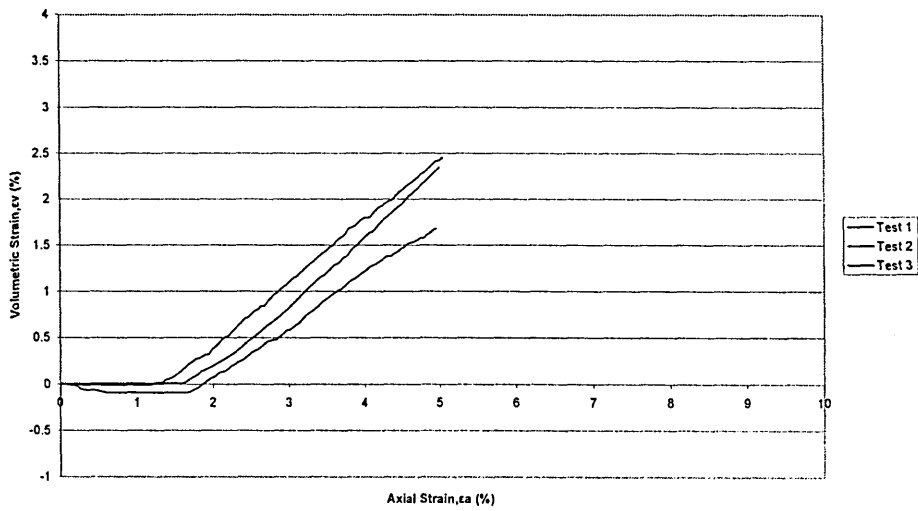
Volume Behaviour, Material B, SBT2, 317 kPa



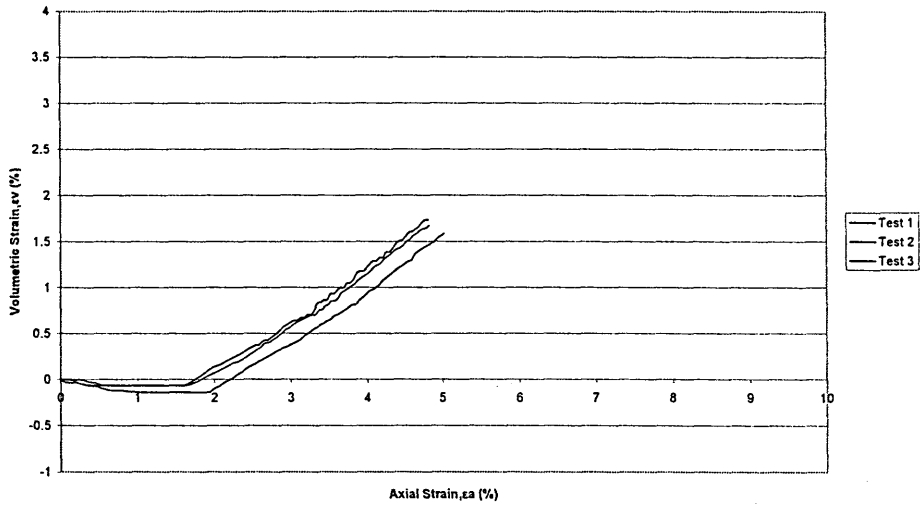
Volume Behaviour, Material B, SBT3, 95 kPa



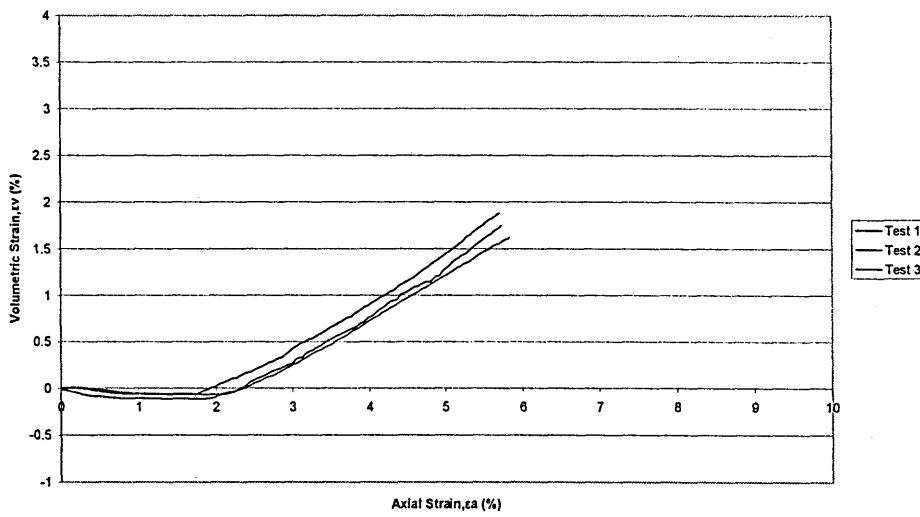
Volume Behaviour, Material B, SBT3, 143 kPa



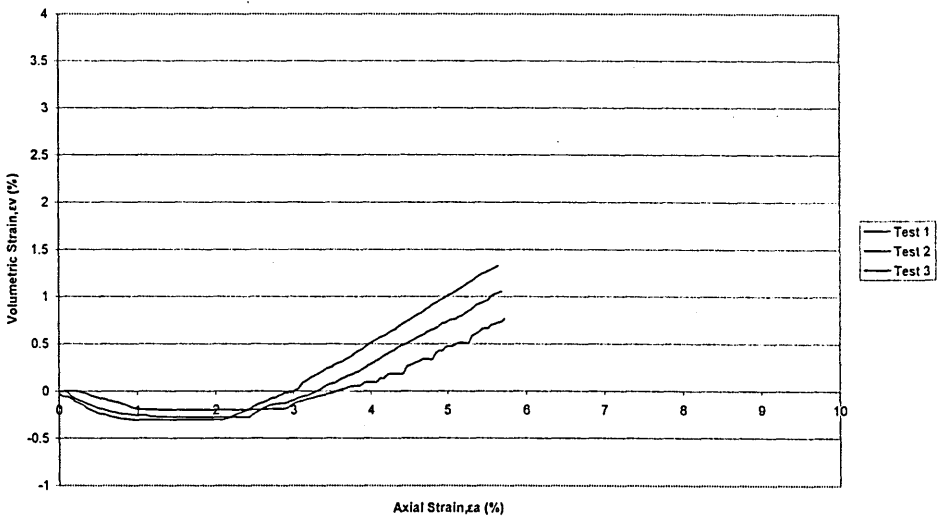
Volume Behaviour, Material B, SBT3, 190 kPa



Volume Behaviour, Material B, SBT3, 238 kPa

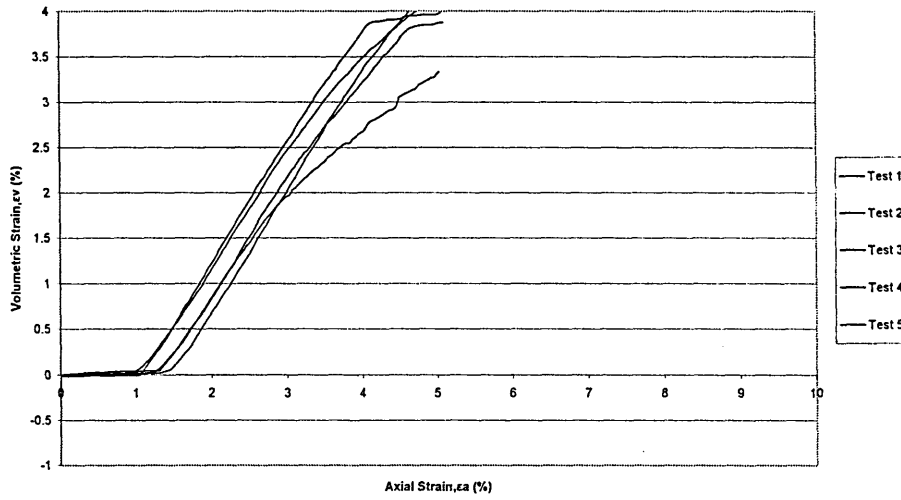


Volume Behaviour, Material B, SBT3, 317 kPa

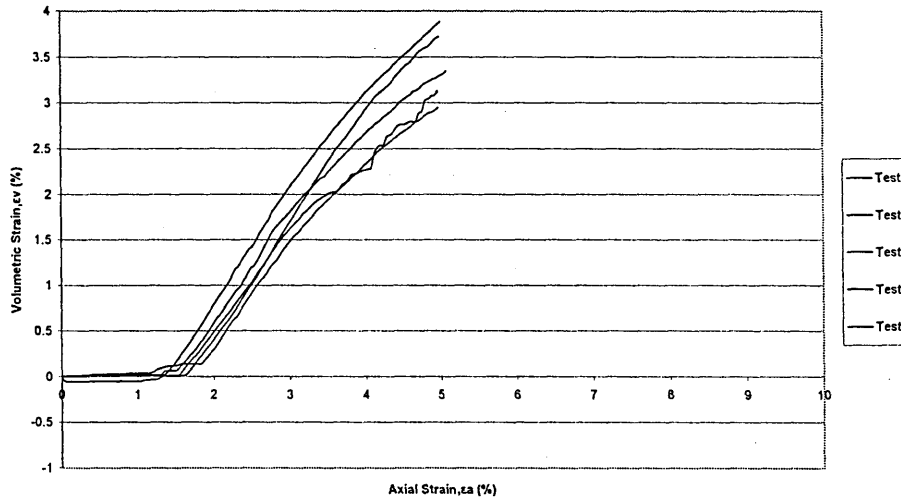


MATERIAL C

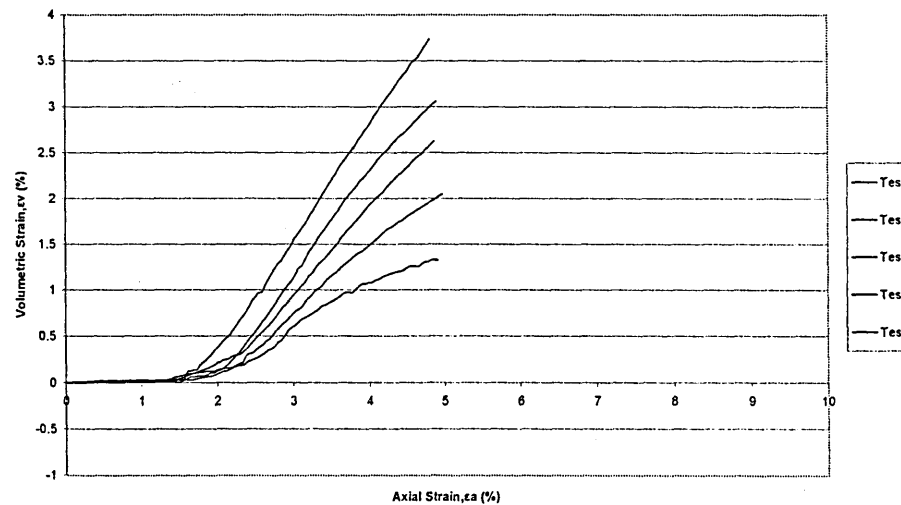
Volume Behaviour, Material C, SBT1, 95 kPa



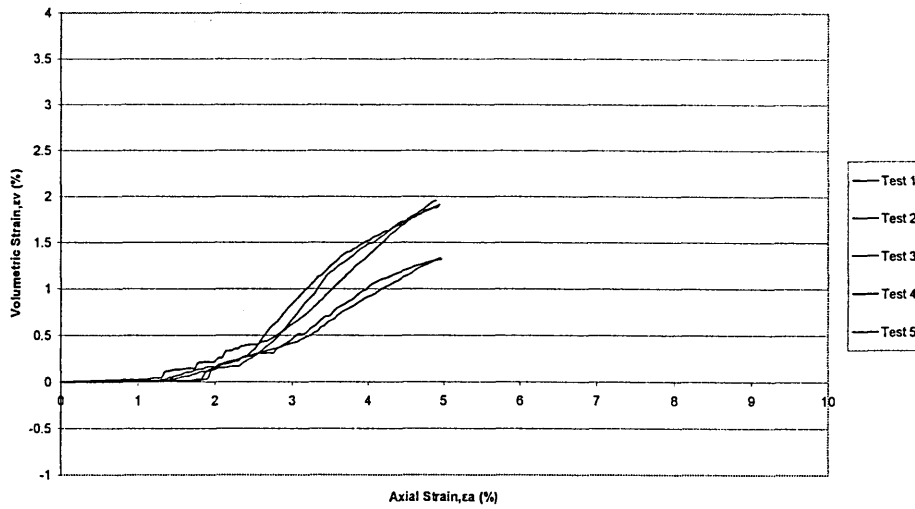
Volume Behaviour, Material C, SBT1, 143 kPa



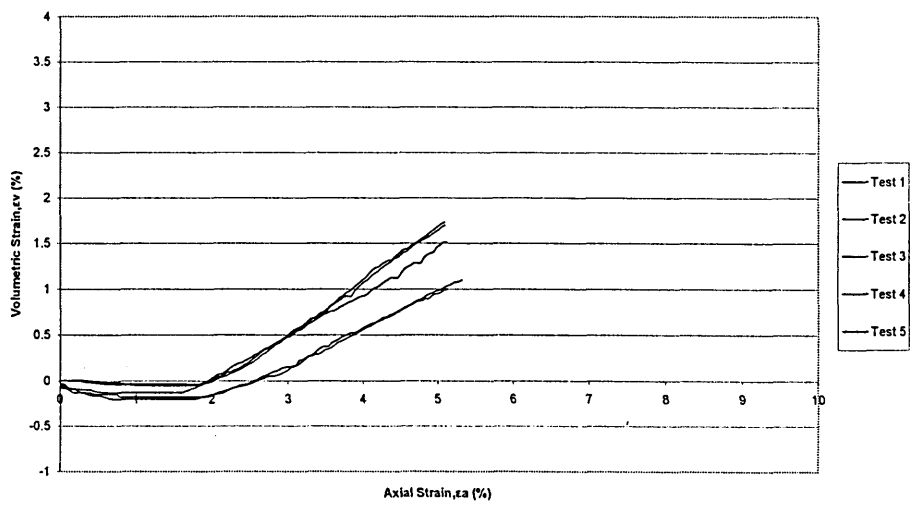
Volume Behaviour, Material C, SBT1, 190 kPa



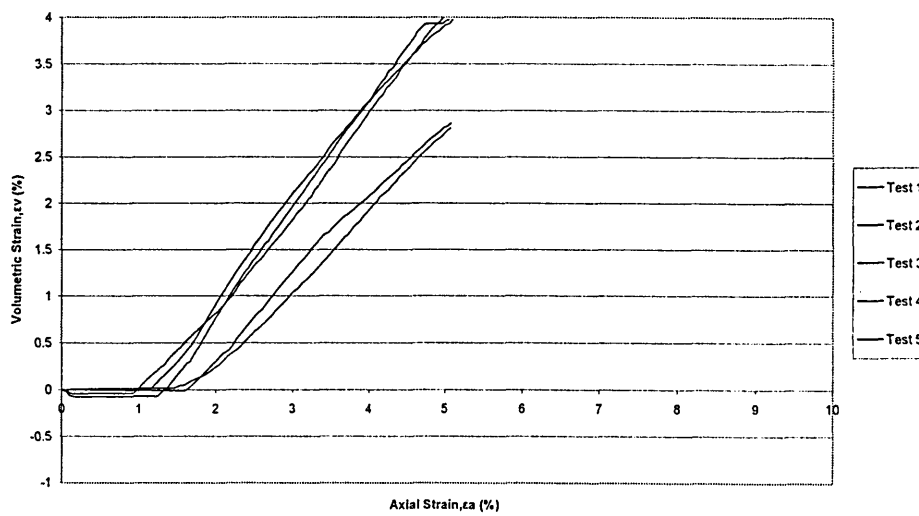
Volume Behaviour, Material C, SBT1, 238 kPa



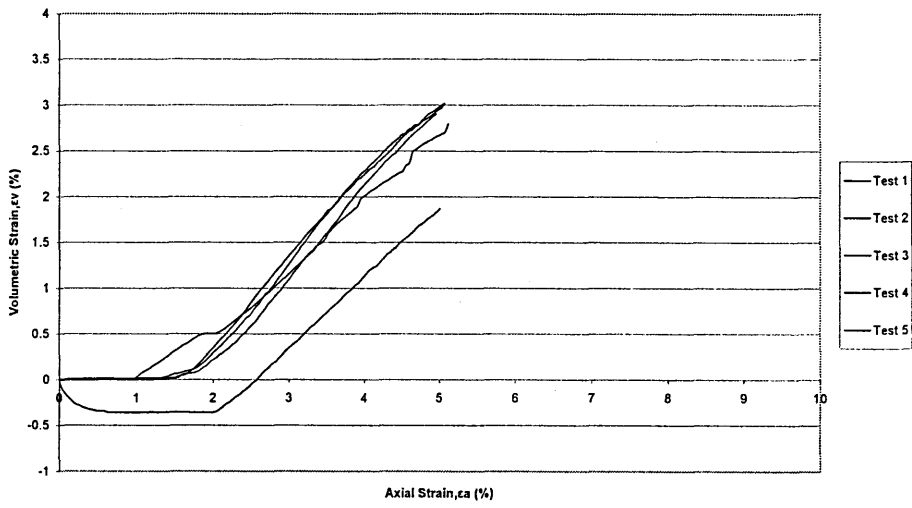
Volume Behaviour, Material C, SBT1, 317 kPa



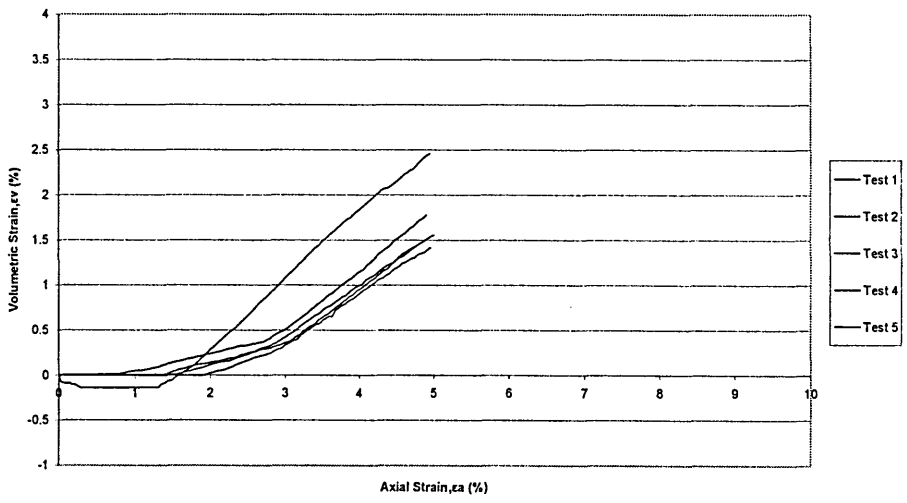
Volume Behaviour, Material C, SBT2, 95 kPa



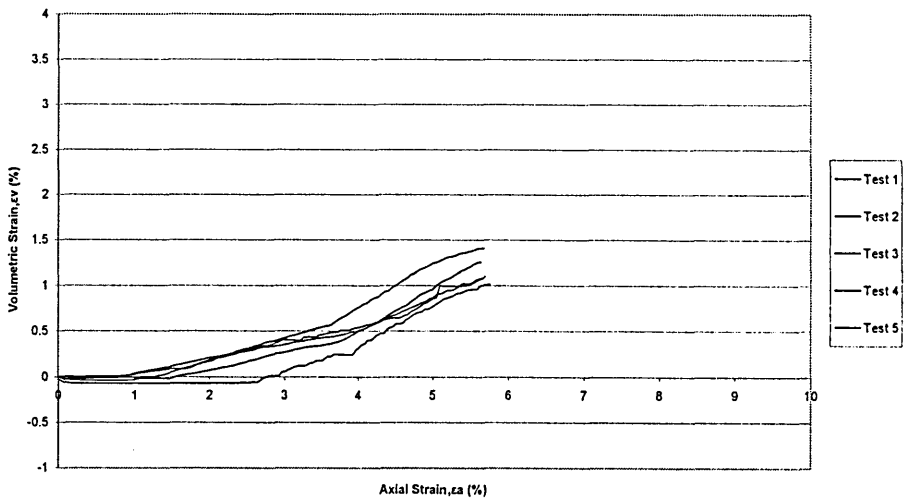
Volume Behaviour, Material C, SBT2, 143 kPa



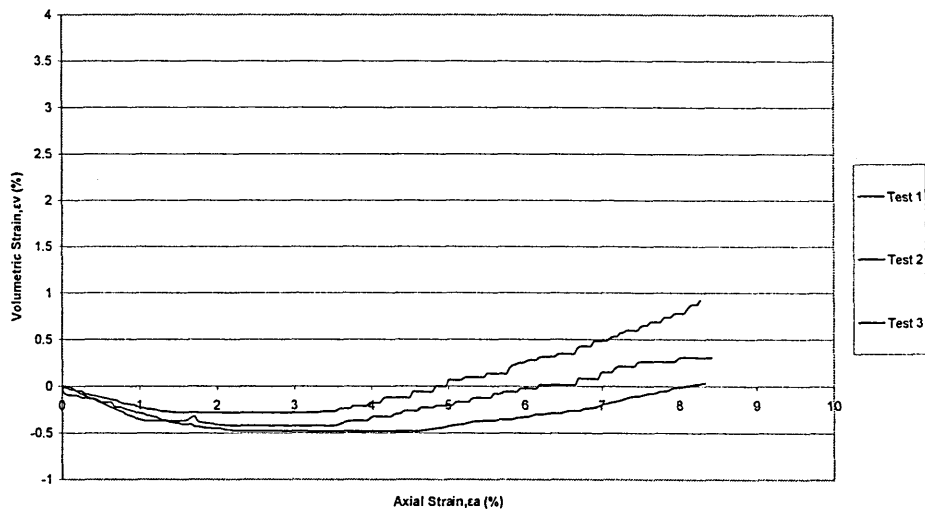
Volume Behaviour, Material C, SBT2, 190 kPa



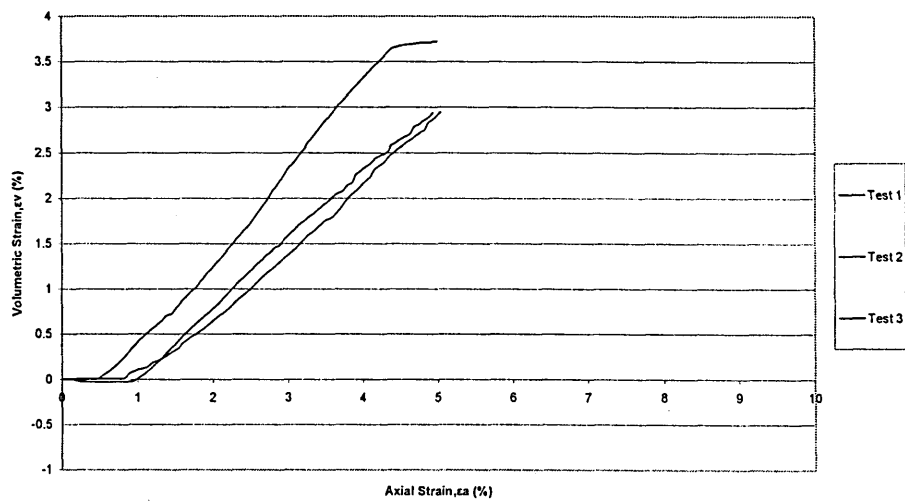
Volume Behaviour, Material C, SBT2, 238 kPa



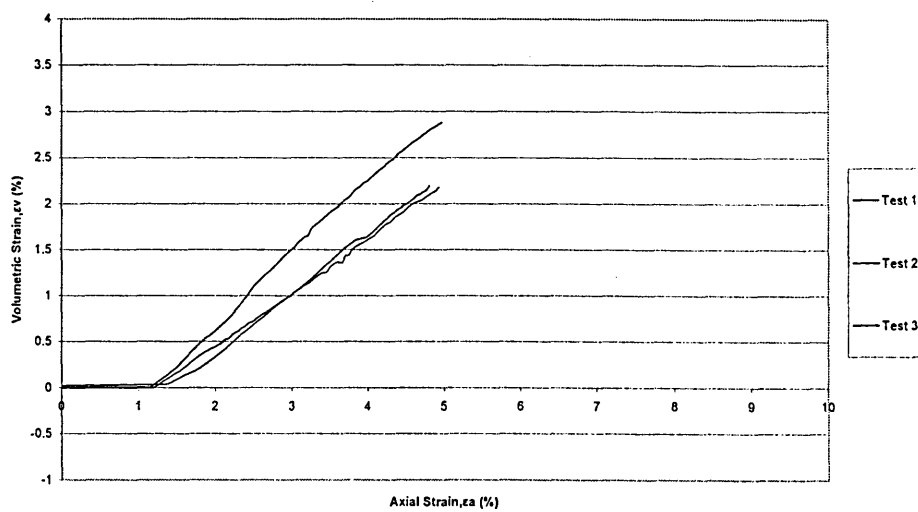
Volume Behaviour, Material C, SBT2, 317 kPa



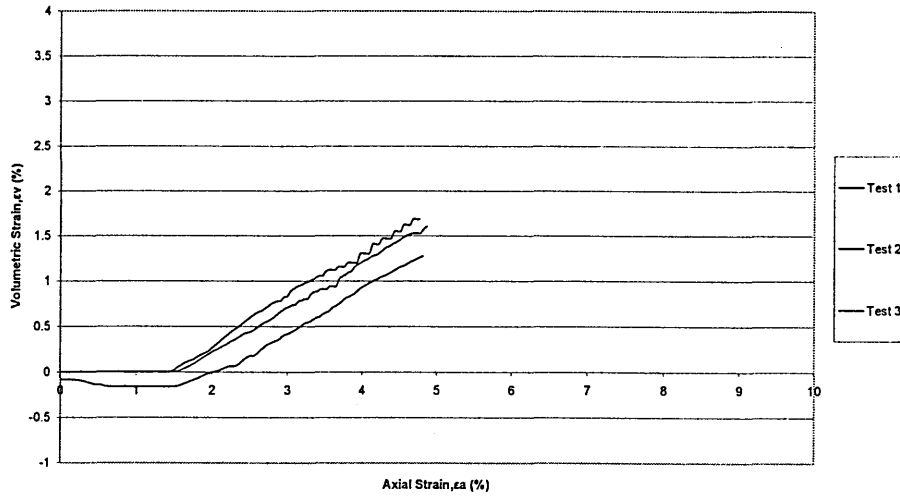
Volume Behaviour, Material C, SBT3, 85 kPa



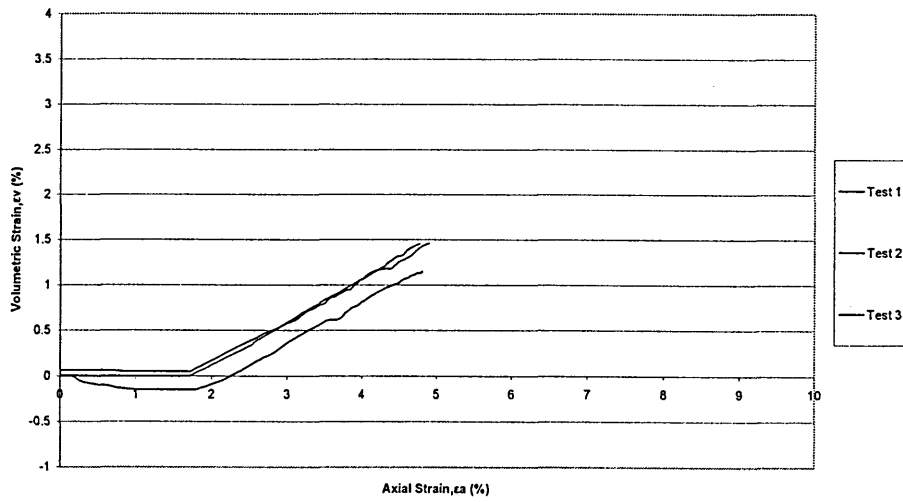
Volume Behaviour, Material C, SBT3, 143 kPa



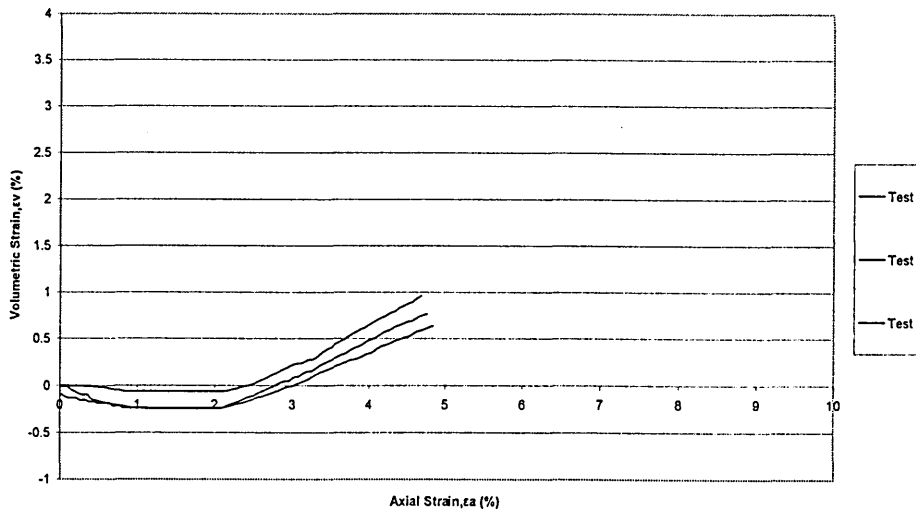
Volume Behaviour, Material C, SBT3, 190 kPa



Volume Behaviour, Material C, SBT3, 238 kPa



Volume Behaviour, Material C, SBT3, 317 kPa



Publications

I Chidioglou, A K Goodwin, P S Mangat & E A Laycock, Properties of Crushed Concrete and Bricks to be used for Geotechnical Applications, Eighth Young Geotechnical Engineering Symposium, Geotechnics Across Boundaries, 23 - 25 June 2004, Birmingham

I Chidioglou, A K Goodwin, P S Mangat & E A Laycock, Shear Behaviour of Crushed Concrete and Bricks, Sustainable Waste Management and Recycling: Challenges and Opportunities, International Conference, 14 - 15 September 2004, Kingston, UK

I Chidioglou, A K Goodwin & E A Laycock, Particle Shape of Crushed Concrete, Concrete International, Vol. 28 No 8, pp 50-55, August 2006

I Chidioglou, A K Goodwin, E, Laycock & F, O'Flaherty, Physical Properties of Demolition Waste Material, Institution of Civil Engineers Construction Materials Journal, Paper accepted for publication